A ROBUST ITERATIVE LEARNING CONTROL WITH NEURAL NETWORKS FOR ROBOT

Cheng Shao[1], Juan Nie[1], Furong Gao[2]

[1]Research Center of Information and Control
Dalian University of Technology, Dalian 116024, Liaoning, P.R. China
Email: cshao@dlut.edu.cn
[2]Department of Chemical Engineering, Hong Kong University of Science and Technology,
Clear Water Bay, Kowloon, Hong Kong

Abstract: Using identification of neural networks, a new robust iterative learning control algorithm is proposed in the paper. Combined with feedback control in real time, the neural network is employed to identify the nonlinear system online and to produce the feed-forward actions of iterative learning control algorithm to realize continuous trajectory tracking task for robot. Simulation results demonstrate that the algorithm can not only overcome uncertainties and external disturbances, but also meet the trajectory command with few iterative learning and network training, and thus possess better robustness and control performance.

Keywords: iterative learning control, neural network, system identification, disturbances rejection.

1. INTRODUCTION

Robot is a kind of high nonlinear, closely coupled and time-varying dynamic system, so that its exact dynamic model is difficultly established. In order to satisfy the requirement of high-precision motion control of robot, some of the literatures have proposed many new control methods, such as computed torque method, adaptive control method, varying-structured control method and iterative learning control method. Among these methods, iterative learning control has been aroused general interest. This scheme can utilize a prior knowledge regarding the controlled system, combining its output and desired signals, so as to make the controlled system yield the desired movement. Especially for high nonlinear and close coupled dynamical systems, meanwhile with high-precision requirement of position, like industrial robot and digital machine tool, iterative learning control has acquired some useful application results (Xie, Z.D et al., 2000) However, the complex industrial plant like robot not only possesses high nonlinear properties but also operates in an environment with external uncertainties in most cases. Therefore, it is more significant to investigate the robust learning control strategy for nonlinear system in the presence of uncertain disturbances.

Since neural network not only has the satisfactory capacity of approximating any nonlinear mapping but also can learn and adapt to the dynamical property of unknown system, neural network based control system has fairly strong adaptability and robustness (He, Y.B. and X.Z. Li, 2000). In resent years, neural network control considered as a new approach has been applied to robot control and obtained some research results. When introducing neural network to identify and control the nonlinear system, a double-neural network structure is to be used in most cases. One is to learn positive model of the controlled system as a identifying one itself, another is used to learn the inverse model as a controller. But the structure may lead to more parameters from controller to be adjusted, and stability and robustness of the closed loop system cannot be ensured. In (Li, M.Z. and F.L. Wang, 1998), on the basis of positive model identification of neural network, the control problem was converted to an optimizing one and then processed iterative solution. But it remains to be further studied to advance the precision of neural-identifying model and to select weight coefficients and step factors. A neural network controller with iterative learning algorithm is presented in (Wang, C.Q, 1998) incorporating feedback control actions, in order to overcome the uncertainties and load disturbances of model. The neural network based controller was to directly realize inverse-dynamic control, which means that the plant must be dynamically invertible, and thus the tracking precision lay on the precision of the inverse model. A case of existing uncertainties and parameter varieties was considered in (Ozaki T and Suzuki T, 1991) where two neural network controllers were employed to identify different parts of the model so as to compensate effects of uncertainties and parameter varieties. But this kind of neural network structure may induce many tuning parameters and need much more repetitive trials. Usually, there isn't

standard procedure to select the structure of neural network and effective algorithm; the training numbers over hundreds of neural network and the low convergence rate become one of the primary open problems. Simulation results in (Wang, C.Q, 1998) and (Ozaki T and Suzuki T, 1991) illustrated that the learning numbers and tracking error performance of iterative learning control based on neural network would be modified greatly.

This paper presents a new neural network based iterative learning control algorithm, which combines iterative learning control with neural network identification for the purpose of trajectory tracking control of robot. As neural network has the ability of self-learning, that utilizes the prior output data of uncertain system to estimate iteratively the system static state property to achieve ideal approaching precision for identification of positive model, a robust iterative learning control scheme on the basis of the better positive model is designed. The neural network is used to identify the positive model of the nonlinear system on iterative axis, which can give feed forward actions of iterative learning controller to reduce the effects of nonlinearities and model uncertainties. Meanwhile, the feedback actions of iterative learning controller make joint movement follow the desired trajectory on time axis by using the control parameters derived by the neural network. That is, after obtaining better approaching precision of network training for model identification iteratively trail by trail, the feed-forward actions of iterative learning control law of the next trail are constructed by the output signals of the neural network, and then integrated with feedback control to track the desired trajectory of robot in real time. The feedback control is introduced to compensate effects of both errors of identification and iterative learning, so the controlled system can get better robustness and control precision. As there exist many architectures of neural network, the paper uses the most common multi-layered neural network to identify the positive model. Simulation results indicate that the method is very effective to robotic systems with unknown external disturbances, and it can also acquire satisfying tracking performance by fewer numbers of network training and iterative learning processes.

2. MODEL IDENTIFICATION BASED ON NEURAL NETWORK

System identification is a basic and important work for the control system design. But identification of the complex system is a more difficult and challengeable issue. Robot is a kind of high nonlinear, close coupled and time-varying dynamical system, with the effects of model uncertainties and external disturbances, so it is difficult to establish its precise dynamical model. Owing to complicated mechanism of robot and many unknown uncertainties including measurement errors, the conventional methods of identification would not suit to high precision control of robot. While the nonlinear approximating property and the high parallel operation ability of neural

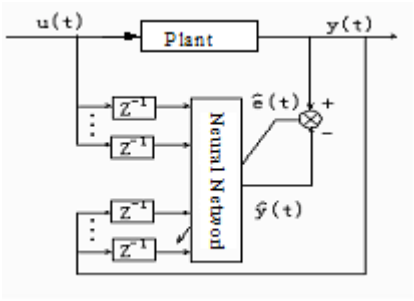

Fig.1. Architecture of the neural network based positive-model

network provide a valid way for identification of complex systems, especially for nonlinear system.

Using multi-layered static network to get the positive model of nonlinear system, the controlled plant can be considered as a "black-box", which means that it is unnecessary to analyze exactly the internal structure of unknown process or plant. As an approximate model of the actual system, if the neural network based model can give sufficiently small identification error, the output signals of the model can be considered as the output estimates of the actual plant. Therefore the following conventional MIMO nonlinear input-output discrete time plant is considered

$$y(t) = f(y(t-1), y(t-2), \cdots, y(t-n); \\ u(t-1), u(t-2), \cdots, u(t-m)) \quad (1)$$

where

$$u(t) = [u_1(t), u_2(t), \cdots, u_p(t)]^T \in R^p,$$

$$y(t) = [y_1(t), y_2(t), \cdots, y_q(t)]^T \in R^q$$

are the plant inputs and the plant outputs vectors of dimensions p and q, respectively, m, n are called as model orders and assumed to be known, and f is allowed as an unknown nonlinear input/output vector function of dimension q, *i.e.*

$$f(x) = [f_1(x), f_2(x), \cdots, f_q(x)]^T.$$

Eqn. (1) can be simplified as

$$y(t) = f(I(t-1)) \quad (2)$$

where

$$I(t-1) = [y(t-1)^T, \cdots, y(t-n)^T, \\ u(t-1)^T, \cdots, u(t-m)^T] \in R^{nq+mp}.$$

It is pointed out in (He, Y.B. and X.Z. Li, 2000) that a feed-forward neural network with simple hidden layer has the capability of approximating arbitrary nonlinear function if there are enough nodes on the hidden layer of the neural network. A neural network based positive model structure of the plant is illustrated in Fig.1, where the used neural network is a three-layered back propagation network showed in Fig.2. Then the neural network based identifying model can be described as follows

$$\hat{y}(t+1) = N(I(t), W) \quad (3)$$

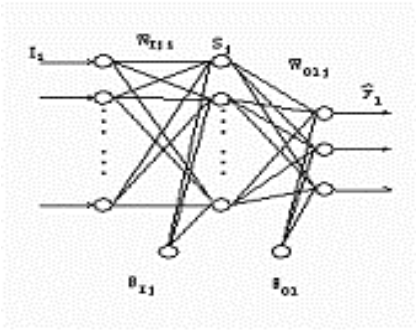

Fig.2. Architecture of the three-layered BP neural network

where W is the synaptic weights vector, N is the input/output mapping function of the neural network; $I(t) \in R^{nq+mp}$ represents the inputs of the neural network and $\hat{y}(t+1) \in R^q$ represents the neural network outputs composed of N_O output neurons. So the number of the output neurons of the neural network can be determined easily, *i.e.* $N_O = q$. In the architecture of the three-layered BP neural network showed in Fig.2, a nonlinear Sigmoid function in the hidden layer and a linear function in the output layer will be employed, and the outputs of the hidden layer and the output layer can be expressed as follows

$$S_j = f_s(net_j) = f_s(\sum_{i=1}^{N_I} W_{Iji} I_i + \theta_{Ij}), \quad j = 1,2,\cdots,N_H \tag{4}$$

$$\hat{y}_l = (\sum_{j=1}^{N_H} W_{Olj} S_j + \theta_{Ol}), \quad l = 1,2,\cdots,N_O \tag{5}$$

where $f_s(x) = \dfrac{1}{1+e^{-x}}$ is a sigmoid function, W_{Iji}, W_{Olj}, θ_{Ij}, θ_{Ol} are the connection weights and threshold values responding to the input layer to the hidden layer and the hidden layer to the output layer, respectively, I_i denotes the input of the input layer, net_j is the input of the hidden layer, S_j represents the output of the hidden layer, $\hat{y}$ is the outputs of the output layer, N_I, N_H, N_O represent the neuron number of the input, hidden and output layer, respectively. Define identification error of the neural network as

$$\begin{aligned} e_n(t+1) &= y(t+1) - \hat{y}(t+1) \\ &= f(I(t)) - N(I(t), W) \end{aligned} \tag{6}$$

When the neural network being trained sufficiently, the optimal weighting value W^* can be obtained and it holds that

$$\left\| f(I(t) - N(I(t), W^*) \right\| = \left\| e_n(t+1) \right\| \le \varepsilon, \quad \forall I(t) \in D \tag{7}$$

where ε is a sufficiently small positive constant standing for the given approximating precision, D is a strict compact set in R^{nq+mp}. However, in this paper the network training is integrated with iterative learning control. In the kth trial, minimize the following quadratic cost function to get an optimal weighting value W_k^* firstly by using all input-output data of this trial

$$J_k = \frac{1}{2} \sum_{t=0}^{T} [y_k(t) - \hat{y}_k(t)]^2, \quad k = 1,2,\cdots \tag{8}$$

where T is the period of the trials, $y_k(t)$ and $\hat{y}_k(t)$ represents the system outputs and the network outputs of the kth trial, respectively. To solve W_k^* from (8), the steepest descent algorithm is employed in the paper.

$$W_{r+1} = W_r - \beta \frac{\partial J}{\partial W_r} + \alpha \Delta W_{r-1}, r = 1,2,\cdots \tag{9}$$

where β is a learning rate and α is a momentum factor. The function of the momentum factor is to memorize the changing direction of connection weights in previous training procedure and restrain vibration of the system that may be produced called a smooth action. During the kth trial, the weight W_r can be modified recursively along optimal direction as the training number r increases, so one hopes that the identification error of model can be reduced gradually. When themodel satisfies the given approximating precision,the training process of (9) will be completed andthe final weight obtained from (9) will be set as W_k^*. Then using W_k^* calculates the network outputs defined by $\hat{y}_k^*(t)$ $(t \in [0,T])$ based on (4)and (5) for each trial that will be applied to construct the feed-forward actions of the k+1th iterative learning control law, and combined with feedback control in real time to produce the control inputs u_{k+1} that will be described in next section.

3. NEURAL NETWORKS BASED ITERATIVE LEARNING CONTROL FOR ROBOT

The dynamics equation of an n-degree-of –freedom robot can be described in the following

$$\begin{aligned} M(\theta(t))\ddot{\theta}(t) + V(\dot{\theta}(t), \theta(t)) \\ + G(\theta(t)) + T_a(t) = \tau(t) \end{aligned} \tag{10}$$

where $\theta(t) \in R^p$ is the vector of generalized joint position, $M(\theta(t)) \in R^{p \times p}$ is a symmetrical positive inertia matrix; $V(\dot{\theta}(t), \theta(t)) \in R^p$ is the vector representing centrifugal and Coriolis; $G(\theta(t)) \in R^p$ is the vector of gravitational term; $\tau(t) \in R^p$ is the vector of joint torques supplied by the actuators and $T_a(t) \in R^p$ is an unknown term arising from bounded disturbances. Due to the

uncertainties and external disturbances of the robotic dynamic model, it is impossible to get the exact value of generalized joint position. The paper coordinates a P-type iterative learning controller with identification model of neural network. Regarding the disturbances as a part of the system itself, the neural network is employed to identify the whole nonlinear system so as to make the outputs of network approach the actual outputs of the system infinitely. As an identified model of the controlled plant, if the model error ε is small enough, the outputs of neural network can be considered as the actual outputs of the controlled system, *i.e.* $y(t) \approx \hat{y}(t)$. In order to improve robustness of the controlled system and reduce the influence of nonlinear uncertainties and disturbances to control performance, a feed-forward compensation action is firstly introduced based on the iterative learning controller that may be either a conventional controller such as PID, PI, P-type controller or an intelligent controller like fuzzy controller and expert controller, but a simple PD-type controller is used in the paper. However an extension to other type of controllers is easily made. Suppose that u_{fb} is output of feedback controller and u_{ff} is the one of feed-forward controller based on the neural network identification. Then a compound control law $u(t)$ composed of u_{fb} and u_{ff} will be derived. The block diagram of architecture of control system is illustrated in Fig.3.

In the *k*th iterative learning control process, it can be known from the diagram that the control law of robot trajectory tracking is,

$$u^k(t) = u^k_{fb}(t) + u^k_{ff}(t) \tag{11}$$

where $u^k_{fb}(t) = k_p e^k_p(t) + k_d \dot{e}^k_p(t)$ is the feedback control action, k_p, k_d are the positive matrixes of position and velocity gains, respectively, $e^k_p(t) = y_d(t) - y^k_p(t)$, $y_d(t)$ is the desired trajectory of the system, $y^k_p(t)$ is the actual output including model uncertainties and external disturbances in the *k*th trial. But u_{ff} is obtained by

$$u^{k+1}_{ff}(t) = u^k_{ff}(t) + k_{ILC} e^k_n(t) \tag{12}$$

which is of the iterative learning controller, where k_{ILC} is the learning control gain matrix, $e^k_n(t) = y_d(t) - y^k_n(t)$, $y^k_n(t)$ is the output of neural network in the *k*th trial. To guarantee the convergence of iterative learning control algorithm (Pi, D.Y. and Y.X. Sun, 1999), the selection of k_{ILC} should satisfy

$$\rho(I - k_{ILC} D(0)) < 1 \tag{13}$$

where D is the close-loop transfer function matrix of the system, $\rho(\cdot)$ represents the corresponding spectrum radius.

For a two-degree-of-freedom robot, the orders *p* and *q* of the system are both 2, and maximum differential degree of its mathematical model is 2 also. The input signals of neural network are fed by vectors of the plant input signals and the desired trajectory signals with delay degrees 0,1 and 2. The neuron numbers of the input layer, hidden layer and output layer are $N_I = 12, N_H = 10$ and $N_O = 2$, respectively. The training algorithm of the network is described by (9). It is observed from next section that rather short learning time is needed in general.

In conclusion, the iterative learning control scheme proposed in this paper can be summarized as follows:

1) For $k = 0$, give an initial weight W^*_0 of W^*_k to produce $\hat{y}^k_n(t)$ $(t \in [0,T])$ based on (4) and (5), and only feedback control action is considered in (11).

2) For $k \geq 1$, use (9) to derive W^*_k and then (12) to calculate the feed forward action $u^k_{ff}(t)$.

Furthermore an iterative learning control law u_{k+1} resulting from (11) will be available. The process of iterative learning control is detached from neural network training. When the *k*th procedure of iterative learning control is completed, the neural network is

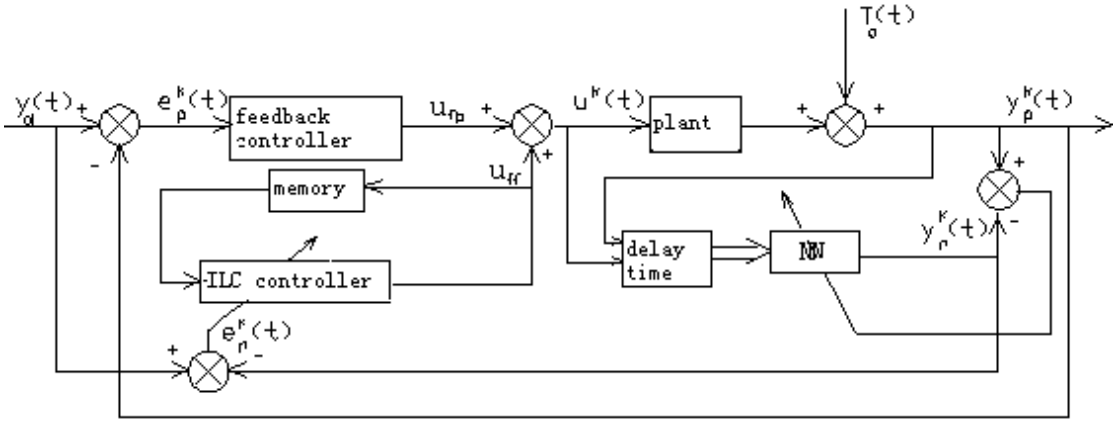

Fig.3. The block diagram of architecture of control system

then trained by (9) using all inputs and outputs in the *k*th trial.

4. SIMULATION AND ANALYSIS

The robot used in simulation is a two-degree-of-freedom SCARA-type one given in (Ozaki T, Suzuki T, 1991). The expression of each term in the robotic dynamic equation is shown as follows

$$M_{11} = m_1 K_1^2 + m_2 (L_1^2 + K_2^2 + 2L_1 K_2 \cos(\theta_2)) + I_1 + I_2$$

$$M_{12} = m_2 (K_2^2 + L_1 K_2 \cos(\theta_2)) + I_2$$

$$M_{21} = M_{12}$$

$$M_{22} = m_2 K_2^2 + I_2$$

$$V_1 = -m_2 L_1 K_2 \sin(\theta_2)(2\dot{\theta}_1 + \dot{\theta}_2)\dot{\theta}_2 + D_{m1}\dot{\theta}_1$$

$$V_2 = m_2 L_1 K_2 \sin(\theta_2)\dot{\theta}_1^2 + D_{m2}\dot{\theta}_2$$

$$G_1 = g((m_1 K_1 + m_2 L_1)\cos(\theta_1) + m_2 K_2 \cdot \cos(\theta_1 + \theta_2))$$

$$G_2 = g m_2 K_2 \cos(\theta_1 + \theta_2)$$

where the following physical parameters of the robot with two links are, arm length L_1=0.25m, L_2 =0.16m; link centers of gravity K_1 =0.2m, K_2 =0.14m; mass m_1 =9.5kg, m_2 =5.0kg; inertia $I_1 = 4.3\times10^{-3} kg\cdot m^2$, $I_2 = 6.1\times10^{-3} kg\cdot m^2$; motor damping coefficients $D_{m1} = 3.85\times10^{-3} N\cdot s\cdot m^{-1}$, $D_{m2} = 1.39\times10^{-3} N\cdot s\cdot m^{-1}$; gravitational acceleration $g = 9.81 m\cdot s^{-2}$.

The desired trajectories of two joints are $\theta_{1d} = -\frac{\pi}{2}\cos(\pi t/2.5), \theta_{2d} = \frac{\pi}{2}\sin(\pi t/2.5)$; the gain matrixes of the feedback controller are set at k_p =diag[300, 300], k_d = diag[20, 20]; the external disturbance was $T_a = [0.13\cos(\pi t/10 + 5), 0.23\sin(\pi t/10 + 4)]^T$; the gain matrix of learning controller is K_{ILC} =diag[100,100]; the connection weights of the neural network are randomly initialized between（-0.5,0.5）; the momentum factor is α =0.9, the learning rate is β =0.01. It takes about 5s for simulation, and the sampling period is 0.01s. The numbers of iterative learning and neural network training for one iterative learning procedure are both 20. As convergence of the BP network depends on the initial weights of its learning mode, we would reinitialize the connection weights at the outset of each learning trial. Fig.4 showed the tracking error of the manipulator with two joints, and (a)—(d) illustrate the error curves of the first, 7th,14th, and 20th iterative learning trial. At the 20th iterative learning control process, the index curve of training performance for the neural network identifying model was shown in Fig.5. It is easy to see from Fig.4(a)—(d) that the error curves of two joints possess clearly convergent trend as iterative learning times increase. At the 20th iterative learning control process, the error satisfied the requirement of better tracking precision. From Fig.5, it is clear that the performance criterion of the BP network training attain to 1e-6 level. Whereas the simulation results in (Wang, C.Q, 1998) presented that there existed certain error between the actual and desired trajectory of the joints when only feedback control was operated. At the 85th iterative learning control procedure, the square sum of tracking errors on two joints are 0.0059 and 0.064, respectively. As far as other kinds of external disturbances are concerned, such as a noise signal, an impulse at any time, simulations are also performed in the paper. The results show that the proposed scheme can also get rather good requirement of tracking precision.

5. CONCLUSION

The paper presents a method of iterative learning control combining with identifying model of neural network. The BP neural network is employed to identify the nonlinear system and to produce the feed-forward action of iterative learning control algorithm, and it is integrated with feedback control in real time to form the neural network based robust iterative learning control algorithm. The scheme

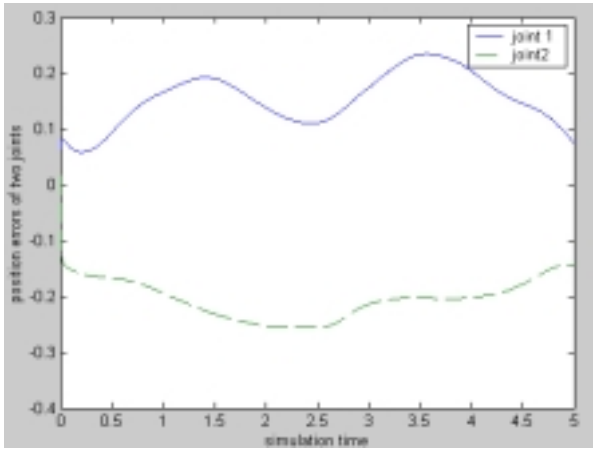

(a)

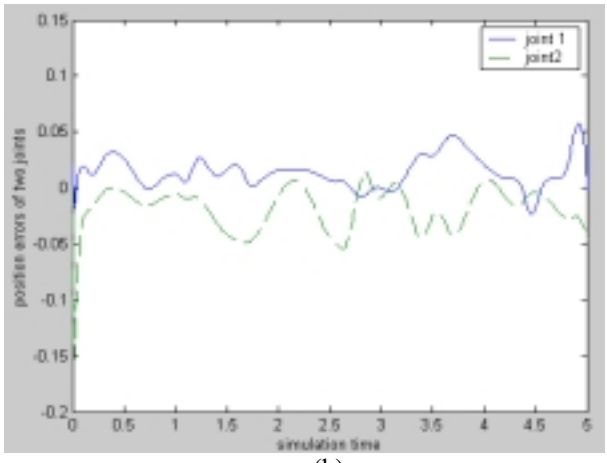

(b)

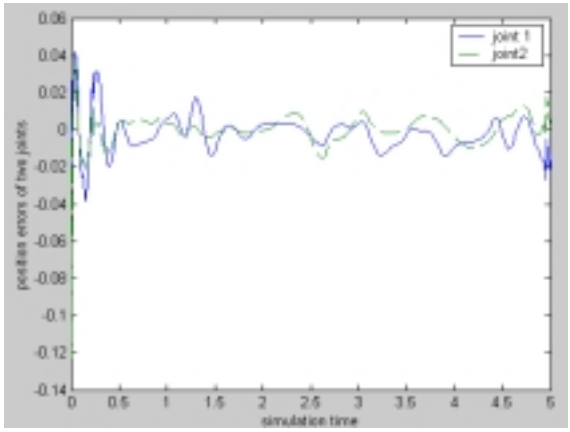

(c)

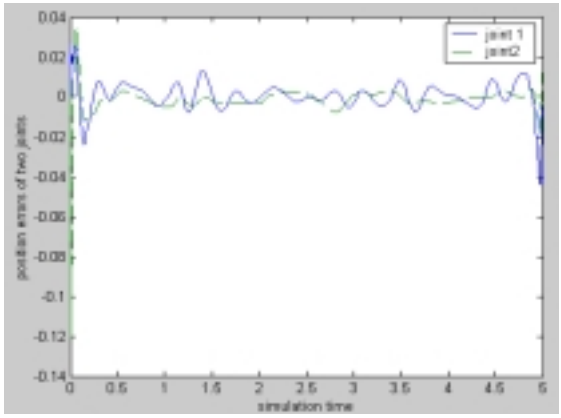

(d)

Fig.4. The tracking error curves of two joints:
(a) First trial; (b) 7th trial; (c) 14th trial; (d) 20th trial.;

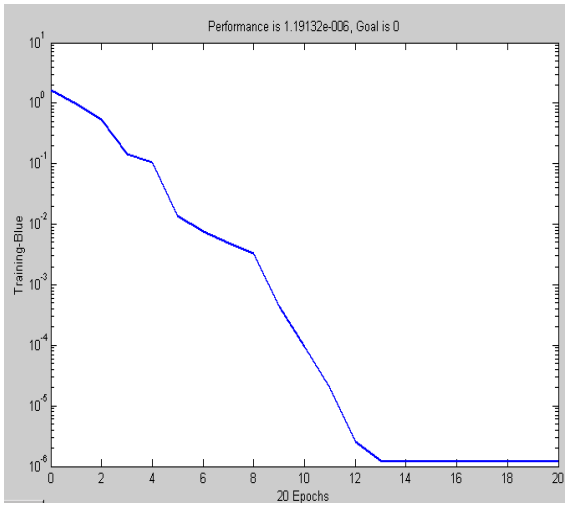

Fig.5. The performance index curve of the neural network identifying model

makes the robotic controller have the ability of self-learning and eliminate the influences of uncertainties and external disturbances of the dynamical model. Further analysis performed in the paper indicates that the control system can realize high-precision tracking to any trajectory on the condition that the identification precision of neural network is good enough. Moreover, the simulation investigation shows that the neural network based control strategy can be used better for the complex industrial processes.

6. ACKNOWLEDGEMENT

The authors would like to acknowledge the supports of Foundation for University Key Teacher by the Ministry of Education of China, the State Science and Technology Pursuit Plan Project of China (2001BA204B01), and the Hong Kong Research Grant Council (HK UST RIG95/96. EG03).

REFERENCES

Li, X.Z., L.K. Jian and Y. He (1997). Iterative Learning Control in Continual Trajectory Tracking of Nonlinear System. *Machine Tool and Hydraulic Pressure*, **5**, 22-23.

Li, M.Z. and F.L. Wang (1998). A Neural Network-Based Iterative Optimal Controller for Nonlinear Systems. *Journal of Northeastern University (Natural Science)*, **19(2)**, 191-194.

Wang, C.Q (1998). Iterative Learning Control for Robot Manipulators Using Neural Networks. *Journal of Nanjing University of Aeronautics & Astronautics*, **30(4)**, 395-399.

Ozaki T, Suzuki T (1991). Trajectory control of robotic manipulators using neural networks. *IEEE Trans on Industrial Electronics*, **38(3)**, 195-202.

He, Y.B. and X.Z. Li (2000). *Technology and Ap plications of Neural Network Control*, Science Publisher.

Xie, Z.D., S.L. Xie and Y.Q. Liu (2000). Development and Expectation for Learning Control Theory of Nonlinear System. *Control Theory and Application*, **17(1)**, 4-8.

Pi, D.Y. and Y.X. Sun (1999). The Convergence of Iterative Learning Control with Open-closed-loop P-type Scheme for Nonlinear Time-varying System. *Automatica*, **25(3)**, 351-354.

Shao, H.H (1997). *Advanced Control of Industrial Process*, ShangHai Jiaotong University Publisher.

ROBUST STABLE ADAPTIVE CONTROL OF UNCERTAIN BILINEAR PLANTS AND IT'S APPLICATION FOR DISTILLATION COLUMN

Cheng Shao†, Guangjun Luo†, and Furong Gao‡

†Research Center of Information and Control, Dalian University of Technology, Dalian, Liaoning, P.R. China

Email:cshao@dlut.edu.cn

‡ Department of Chemical Engineering, Hong Kong University of Science and Technology, Clear Water Bay, Kowloon, Hong Kong

Abstract: A robust adaptive control design is considered for a class of bilinear plants with unmodeled high-order dynamics and bounded disturbances. A basic optimal control law is first introduced by the generalized minimum variance control strategy, followed by a modification of introducing the modeling error estimate to the control law. Modified least-squares scheme with a relative dead zone is developed to form a novel robust adaptive controller. The resulting closed loop system is proven theoretically to have a zero average tracking error and robust stability. Furthermore, the simulation and an application in controlling of sensitive plate temperature of distillation column demonstrate the effectiveness of the algorithm.

Keywords: robust stability, adaptive control, bilinear system, unmodeled dynamics, distillation column.

1. INTRODUCTION

Attempts to invent, design and build systems capable of controlling unknown plants or adapting to unpredictable changes in the environment resulted in the emergence of adaptive control in the 1950s, and since then, adaptive control has been in the mainstream of control research and development with numerous papers and books published and successful applications every year (Åström 1983, Ljung and Söderstrom 1983, Goodwin and Sin 1984, Åström and Wittenmark 1995, Kanellakopoulos and Koktovic 1995, and the References therein). Significant contributions have been made with the stability establishment of adaptive control theory (Egardt 1979, Gawthrop 1980, Goodwin and Sin 1984, Middleton *et al.* 1988, 1989). They, however, have been limited to the ideal cases, such as linear plants of disturbance-free, random noises, etc. A stable adaptive control algorithm may not be necessarily robust stable (Egardt 1979, Rohrs *et al.* 1982), and the disturbances in an adaptive control system may be inherently related to the plant inputs and outputs (Krisselmeier and Anderson 1986). This led to the recent interest of the robust stability research for adaptive control systems. In the presence of nonlinear uncertainties, unmodeled dynamics and/or bounded disturbances, it has been shown that for the linear plants, robust stability can be ensured by combining the normalization, σ-modification and relative dead zone parameter estimation algorithms with the control strategies of minimum variance, generalized minimum variance or pole placement (Clarke and Gawthrop 1975, 1979, Gawthrop and Lim 1982, Middleton *et al*. 1988, 1989, Shao 1991, 1996). For the bilinear systems, adaptive control stability has been studied recently with bounded external disturbances (Sun and Rao 1999), but the robust stability has not been considered for the systems with the presence of unmodeled dynamics.

This paper examines the robust stable adaptive control problem of the bilinear system in the presence of unmodeled plant uncertainties and bounded disturbances. The considered plant is a class of high-order bilinear systems with unknown and perturbed parameters. By means of minimizing a generalized variance function, a basic control law is first derived and then modified by introducing model error feedback. A self-tuning controller is proposed by combining the control law with a modified least

squares parameter estimator with relative bilinear dead zone. With the proposed self-tuning controller, it is proven that robust stability for the bilinear system can be ensured with respect to the unmodeled high-order nonlinear dynamics and bounded disturbances, without any static state tracking error in an average sense.

Distillation column is a kind of important fraction equipment in chemistry industry. Due to the complex structure of the equipment and the different effects caused by the fluids, the whole system is of essential nonlinearity and of large delay. The control of distillation process is quite concerned with the products quality. In the control system designing for it, in order to satisfy the high quality demand, the sensitive plate temperature is usually selected as the controlled variable. Bilinear system can be used to model many industrial process. In this paper ,a plant of sensitive plate temperature modeled as bilinear system is presented and used as application model. Because of nonlinear characteristics of distillation column, it is naturally to develop robust nonlinear adaptive control algorisms to solve this problem. The experimental results suggested in the paper demonstrated the effectiveness of the proposed bilinear adaptive algorithm for control of distillation column also.

2. THE PLANT DESCRIPTION

Consider a class of bilinear plants with uncertain perturbation and bounded disturbances

$$y(t) = q^{-d} G_1 u(t) + q^{-d} G_2 y(t) u(t) + v(t) \tag{2.1a}$$

$$G_1 = \frac{B(1+\mu B')}{A(1+\mu A')} \tag{2.1b}$$

$$G_2 = \frac{C(1+\mu C')}{A(1+\mu A')} \tag{2.1c}$$

where y and u are the scalar output and input, respectively, v is a bounded output disturbance, $d \geq 1$ is the plant delay, A, A', B, B', C and C' are polynomials of delay operator q^{-1} of orders $n_A, n_{A'}, n_B, n_{B'}, n_C$ and $n_{C'}$, respectively, and $\mu \geq 0$ is a singular uncertain perturbation scalar, by which the unmodeled high-order dynamics will be brought. In fact from (2.1):

$$y(t) = \frac{B}{A} u(t-d) + \frac{C}{A} u(t-d) y(t-d) + \eta_P(t) \tag{2.2a}$$

$$\begin{aligned} \eta_P(t) = {} & \mu \frac{B(B'-A')}{A(1+\mu A')} u(t-d) \\ & + \mu \frac{C(C'-A')}{A(1+\mu A')} u(t-d) y(t-d) + v(t) \end{aligned} \tag{2.2b}$$

Consequently, a singular perturbation from $\mu > 0$ to $\mu = 0$ results in the reduced-order model

$$y(t) = \frac{B}{A} u(t-d) + \frac{C}{A} u(t-d) y(t-d) + v(t) \tag{2.3}$$

The designer is assumed to be given only the reduced-order model (2.3), without the knowledge of the coefficients of A, B and C. Therefore, the modeling errors $\eta_P(t)$ which includes the unmodeled high-order dynamics related to $u(t)$, $y(t)$ and their products, has to be considered in designing of adaptive controller and the robust stability of the resulting closed loop system must be ensured. Model representation of (2.3) has been effectively employed for modeling a combustion process with one input (flow of air) and one output (Oxygen content) in discrete time and many other industrial processes, such as nuclear fission, convective heat-transfer, and turbo-pump dynamics may be also effectively modeled by a bilinear system (Mohler 1991, Aganović and Gajić 1995). The analysis of the model is made with the following assumptions for the model polynomials A, B and C, in this paper.

Assumption 1: A is monic and coprime with B.

Assumption 2: n_A, n_B, n_C *and delay d are known.*

Remark 1: Assumption 1 implies that the reduced-model is controllable, the pole placement control design can, therefore, be applied to the processes that are unstable and/or non-minimum phase. Assumption 2 provides a necessary structure parameter frame for constructing a self-tuning controller.

3. A NOVEL SELF-TUNING CONTROLLER

Our objective is to design a self-tuning controller based on the reduced-order model, or the structural knowledge of A, B and C, so that the application of such a controller to the plant (2.1) results in a robust stable closed loop system tracking the desired output in the presence of the unmodeled dynamics and bounded disturbances.

Let P be an arbitrary monic polynomial in q^{-1} of order n_P. Introduce the polynomial identity

$$P = AF + q^{-d} G \tag{3.1}$$

where F and G are polynomials in q^{-1} of orders $n_F = d-1$ and $n_G = \max\{n_A - 1, n_P\}$, respectively, and F is monic also. Multiplying (2.2a) by AF gives

$$\begin{aligned} Py(t+d) = {} & Gy(t) + FBu(t) + FCu(t)y(t) \\ & + AF\eta_P(t+d) \end{aligned} \tag{3.2}$$

Define

$$\phi(t) = Py(t)$$

$$X^T(t) = (y(t), ..., y(t-n_G), u(t), ..., u(t-n_B-d+1), u(t)y(t), ..., u(t-n_C-d+1)y(t-n_C-d+1)) \quad (3.3)$$

$$\eta(t) = AF\,\eta_P(t) \quad (3.4)$$

Then a regression form of (3.2) can be given as follows

$$\phi(t+d) = \theta^T X(t) + \eta(t+d) \quad (3.5)$$

where θ is the parameter vector composed of the coefficients of *G*, *FB* and *FC*. It should be noted that though the plant is modeled linearly in θ, the nonlinearity exists in the multicity of measured inputs and outputs, and the high-order unmodeled dynamics $\eta(t)$. The following lemmas are given to establish a relative upper bound of $\eta(t)$.

Lemma 1: Let $D(q^{-1})$ be a polynomial in q^{-1} with finite order n_D. For arbitrary $\sigma \in (0,1)$ there exists $\mu_0 > 0$ such that $D_\mu(z^{-1}) = 1 + \mu D(z^{-1}) \neq 0$ for all $|z| > \sigma$ and $\mu \in [0, \mu_0]$, that is $D_\mu(q^{-1})$ is strictly *Hurwitz* uniformly in $\mu \in [0, \mu_0]$.

The proof is given in Shao (1996).

Lemma 2: There exist non-negative constants K_1 and K_2 independent of μ and μ_1 such that for all $\mu \in [0, \mu_1]$

$$|\eta(t)| \le \mu K_1 \{\max_{0\le\tau\le t} |y(\tau)| + \max_{0\le\tau\le t-d} |u(\tau)y(\tau)|\} + K_2 \quad (3.6)$$

Proof: Substituting (2.2*a*) into (2.2*b*) results in:

$$\eta_P(t) = \mu\frac{B'-A'}{1+\mu B'}y(t) + \mu\frac{C(C'-B')}{A(1+\mu B')}u(t-d)y(t-d) + \frac{1+\mu A'}{1+\mu B'}v(t) \quad (3.7)$$

The result follows from (3.7) and (3.4) by applying Lemma 1 to $B'_\mu = 1 + \mu B'$ and referring to the proof of Lemma 2 of Shao (1996).

To achieve a basic optimal control law, suppose that $\{\eta(t)\}$ is a white noise sequence, the generalized minimum variance control strategy of Clarke-Gawthrop type (Clarke and Gawthrop 1975, 1979) then may be employed by minimizing the following quadratic cost function with respect to *u*(*t*):

$$J = E\{P(y(t+d) - y^*(t+d)) + \tilde{Q}u(t)\}^2 \quad (3.8)$$

where *P* and $\tilde{Q}$ are constant weighting polynomials in q^{-1} with $\tilde{Q} = (1-q^{-1})Q$, and $y^*(t)$ is bounded desired output. It follows from (3.5) that

$$J = E\{(\theta^T X(t) - Py^*(t+d)) + \tilde{Q}u(t)\}^2 + D\eta \quad (3.9)$$

It is obvious that an optimal control law can be given by

$$\theta^T X(t) + \tilde{Q}u(t) = Py^*(t+d) \quad (3.10)$$

The preceding control law (3.10) is not suitable for our purpose, as $\eta(t)$ includes unmodeled dynamics. In fact for the self-tuning case, replacing θ in (3.10) with its estimate $\hat{\theta}(t)$ and then applying (3.10) to (3.5) one obtains

$$P(y(t+d) - y^*(t+d)) = (\theta - \hat{\theta}(t))^T X(t) - \tilde{Q}u(t) + \eta(t+d) \quad (3.11)$$

which means that due to the existence of $\eta(t)$ the tracking error $e(t) = y(t) - y^*(t)$ will not converge to zero even when the parameter estimates $\hat{\theta}(t)$ approach to their true values. To remove the effect of unmodeled dynamics, the control law (3.10) is modified by introducing an estimate of $\eta(t)$:

$$\hat{\eta}(t) = \phi(t) - \hat{\theta}(t)^T X(t-d) \quad (3.12)$$

which results in a novel self-tuning control law

$$\hat{\theta}(t)^T X(t) + \tilde{Q}u(t) = Py^*(t+d) - \hat{\eta}(t) \quad (3.13)$$

The parameter estimates are given by the modified least squares scheme with relative dead zone (Shao, 1996) by changing the parameter $\lambda(t)$ as follows:

$$\lambda(t) = \begin{cases} 0 & if\ |\varepsilon(t)| \le 2\beta[\mu^*(\max_{0\le\tau\le t}|y(\tau)| + \max_{0\le\tau\le t-d}|u(\tau)y(\tau)|) + 1] \\ \gamma & otherwise,\ \gamma \in [\sigma_0, 3(1-\sigma_0)/4] \\ & 0 < \sigma_0 < 3/7 \end{cases} \quad (3.14)$$

where β is positive user adjustable parameter with $\beta \ge \max\{K_1, K_2\}$ (see (3.6)), and $\{W(t)\}$ is a matrix sequence with arbitrary initial $W(-1) > 0$.

Remark 2: It can be shown that for a linear plant (*i.e.* *C* equals to zero in (2.1)) the quadratic cost function (3.8) is equivalent to the generalized minimum variance function of the Clarke-Gawthrop type (Clarke and Gawthrop 1975, 1979, Gawthrop 1980, Gathrop and Lim 1982, Shao 1996)

$$J = E\{[P(y(t+d) - y^*(t+d)]^2 + [\tilde{Q}u(t)]^2\} \quad (3.15)$$

And here choice of weighting polynomial $\tilde{Q}$ in the form of $\tilde{Q} = (1-q^{-1})Q$, to be seen in the sequel, will remove static state tracking error in an average sense.

Remark 3: It can be observed that a relative bilinear dead zone method is employed in this paper. Despite the appearance of the bilinear term in the control law, $u(t)$ is always solvable from (3.13) by choosing proper $\lambda(t)$ and/or α. The singularity problem in solving $u(t)$ from (3.13) can hence be avoided.

Remark 4: The condition $\beta \geq \max\{K_1, K_2\}$ is not crucial. In practice, one can start with a large initial value, and then reduce β when the closed-loop system approaches the steady state, to improve control accuracy.

The following assumption is made on P and $\widetilde{Q}$.

Assumption 3: The off-line choices of P and $\widetilde{Q}$ are such that

$$f(q^{-1}) = P(q^{-1})B(q^{-1}) + \widetilde{Q}(q^{-1})A(q^{-1}) \tag{3.16}$$

is stable, that is $f(z) \neq 0$, $|z| \leq 1$.

Remark 5: Assumption 3 is often made for linear control systems with the pole placement design. Here it is made, however, for the reduced-order model with the design consideration of the robust stable adaptive control of a bilinear system with unmodeld high-order dynamics. The linear part of the plant (2.2) may be unstable and/or non-minimum phase, without any further constraints on A and B.

The only assumption on the unmodeled dynamics is made as the following:

Assumption 4: A sufficiently small upper bound μ^* of μ is available. (*The meaning of 'sufficiently small' will be elaborated later.*)

Remark 6: This is a condition often used to construct relative dead zone adaptation algorithms for solving the linear robust adaptive control problems (Kreisslmeier and Andson 1986, Shao 1996). Extension has been made here to bilinear nonlinear systems with unmodeled high-order dynamics.

4. ROBUST STABILITY ANALYSIS

The following lemmas are given for the robust stability of the resulting closed loop system.

Lemma 3: If μ^* is sufficiently small such that $\mu^* \leq \mu_1$, the application of parameter estimation scheme (3.14) to (3.5) for all $\mu \in [0, \mu^*]$ has the following properties.

$$(1)\ \lim_{t\to\infty} \frac{\lambda(t)^{1/2}\varepsilon(t)}{[\alpha + X(t-d)^T W(t-2)X(t-d)]^{1/2}} = 0 \tag{4.1}$$

$$(2)\quad \left|[\hat{\theta}(t-1) - \hat{\theta}(t-d)]^T X(t-d)\right| \leq h(t)\|X(t-d)\|\ , \quad h(t) \to 0 \text{ as } t \to \infty \tag{4.2}$$

where $\|\cdot\|$ denotes the vector-Euclidean norm.

(3) $\hat{\theta}(t)$ is bounded.

The proof may be referred to that of Lemma 3 in Shao (1996), and is thus omitted here.

Lemma 4: The tracking error and the input dynamics satisfy

$$(PB + \widetilde{Q}A)e(t) = \widetilde{Q}Cy(t-d)u(t-d) + A\widetilde{Q}\eta_P(t) + B\Delta_d\varepsilon(t) + \delta_1(t) \tag{4.3}$$

$$(PB + \widetilde{Q}A)u(t-d) = -PCy(t-d)u(t-d) - AP\eta_P(t) + A\Delta_d\varepsilon(t) + \delta_2(t) \tag{4.4}$$

where $\Delta_d = 1 - q^{-d}$ and

$$\begin{aligned}\delta_1(t) &= B[\hat{\theta}(t-1) - \hat{\theta}(t-d)]^T X(t-d) \\ &\quad + B[\hat{\theta}(t-d) - \hat{\theta}(t-d-1)]^T X(t-2d) \\ &\quad - A\widetilde{Q}y^*(t)\end{aligned} \tag{4.5}$$

$$\begin{aligned}\delta_2(t) &= A[\hat{\theta}(t-1) - \hat{\theta}(t-d)]^T X(t-d) \\ &\quad + A[\hat{\theta}(t-d) - \hat{\theta}(t-d-1)]^T X(t-2d) \\ &\quad + APy^*(t)\end{aligned} \tag{4.6}$$

Proof: Using (3.13) and (3.14*d*) gives

$$\begin{aligned}P\epsilon(t) &= \phi(t) - \hat{\eta}(t-d) - \hat{\theta}(t-d)^T X(t-d) - \widetilde{Q}u(t-d) \\ &= \Delta_d\varepsilon(t) + [\hat{\theta}(t-1) - \hat{\theta}(t-d)]^T X(t-d) \\ &\quad + [\hat{\theta}(t-d) - \hat{\theta}(t-d-1)]^T X(t-2d) - \widetilde{Q}u(t-d)\end{aligned} \tag{4.7}$$

From (2.2*a*) one obtains

$$\begin{aligned}Ae(t) &= Bu(t-d) + Cu(t-d)y(t-d) \\ &\quad + A\eta_P(t) - Ay^*(t)\end{aligned} \tag{4.8}$$

A summation of (4.8) multiplied by $\widetilde{Q}$ and (4.7) multiplied by B results to (4.3) with $\delta_1(t)$ of (4.5). In the same fashion, a summation of (4.8) multiplied by P and (4.7) multiplied by -A leads to (4.4) with $\delta_2(t)$ of (4.6).

Lemma 5: Subject to Assumptions 1-4, there exist sufficiently small $\mu^* > 0$ and non-negative constants L_1', L_2' and L_3' that are independent of μ and polynomial C such that for all $\mu \in [0, \mu^*]$

$$\max_{0\le\tau\le t-d}|u(\tau)| \le L_1'(\mu_{\tilde{Q}}+\mu_P)\max_{0\le\tau\le t-d}|Cu(\tau)y(\tau)| + L_2'\max_{0\le\tau\le t}|\varepsilon(\tau)| + L_3' \quad (4.9)$$

$$\max_{0\le\tau\le t}|y(\tau)| \le L_1'(\mu_{\tilde{Q}}+\mu_P)\max_{0\le\tau\le t-d}|Cu(\tau)y(\tau)| + L_2'\max_{0\le\tau\le t}|\varepsilon(\tau)| + L_3' \quad (4.10)$$

where $\mu_{\tilde{Q}} = \sum_{i=0}^{n_{\tilde{Q}}}|\tilde{q}_i|$, $\mu_P = \sum_{i=0}^{n_P}|p_i|$, $\tilde{q}_i$ and p_i are coefficients of polynomials $\tilde{Q}$ and P, respectively.

The following assumption is further made on weighting polynomials P and $\tilde{Q}$ to ensure the resulting closed loop system with robust stability.

Assumption 5: The norms μ_P, $\mu_{\tilde{Q}}$ of P and $\tilde{Q}$, respectively, are relatively small.

Remark 7: Assumption 5 gives the specific requirement on the weighting polynomials P and $\tilde{Q}$ for the robust stabilization of bilinear systems, in addition to the general pole placement method.

Theorem 1: Subject to Assumptions 1-5, there exists sufficiently small $\mu^*>0$ such that the application of self-tuning control algorithm (3.14) to plant (2.1) ensures that

(1) The resulting closed loop system is globally robust stable in the sense that u and y are bounded for arbitrary bounded initial conditions and all $\mu \in [0, \mu^*]$

(2) The tracking error satisfies

$$\lim_{N\to\infty}\frac{1}{N}\sum_{t=0}^{N}e(t) = 0 \quad (4.11)$$

(3) In particular, if the disturbance v is constant (not necessarily equals to zero) and the reference signal y^* is fixed, then

$$\lim_{t\to\infty}[y(t) - y^*] = 0 \quad (4.12)$$

The proof is omitted here.

5. NUMERICAL SIMULATION

To demonstrate the effectiveness of the proposed adaptive control algorithm some numerical simulation results are given below.

EXAMPLE

Select
$A = 1 + q^{-1} + q^{-2}$, $B = 1$, $C = 1$; $A' = 1 + q^{-1}$, $B' = 1$, $C' = 1$. Then a bilinear system plant is given as below:

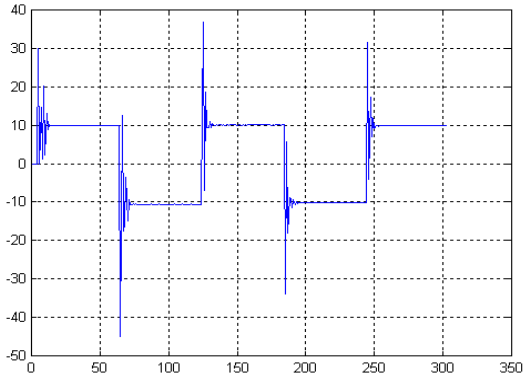

Fig.1 The plant output

$$y(k) = -y(k-1) - y(k-2) + u(k-2)*y(k-2) + u(k-2) - \mu*y(k-1)/(1+\mu) + (1+2\mu)/(1+\mu)*e(k)$$

$e(k)$ is a random gaussian distribution sequence with mean zero and variance 0.01; For designing controller:
$P = 6 + 5q^{-1} + q^{-2}$, Q=1, $\alpha = 1$, $\beta = 4$, $\gamma = 0.5$, $\mu = 0.01$, and the initial conditions:
$\hat{\theta}(0) = [-2, 0.4, 3, -0.01, 4, 0.3]$, $W(1) = aI > 0$, $(a = 0.8)$; As shown in figure 1, the controller worked well with the presence of unmodeled dynamics.

6. APPLICATION OF THE ALGORITHM

A certain loop in a industrial distillation column can be modeled as follows:

$$T(k+1) = 0.3848T(k) + 0.0767T(k)u(k) + 0.5*\sin(u(k-1)*y(k-1)) - 1.2663u(k) + e(k)$$

$T(k)$ (^oC) is the temperature of the sensitive plate, $u(k)$ $(kmol/h)$ is the charge in flow.

The sampling cycle T_s =1s. $e(k)$ is a random gaussian distribution sequence with mean zero and variance 0.01.The simulation result is shown in figure 2. From the results, it can be seen that the tracking error is zero and the tracking velocity is satisfactory. The robust adaptive control algorithm worked very well and improved the quality of the controlled system.

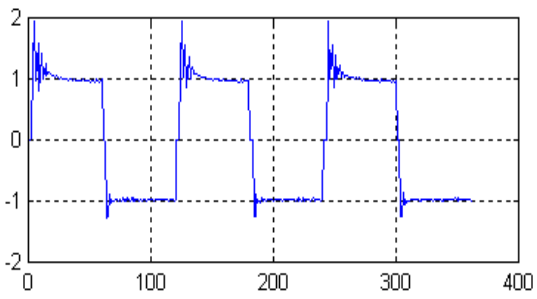

Fig.2 The plant output

7. CONCLUSIONS

A new self-tuning control algorithm has been developed in this paper for a class of bilinear systems with uncertain perturbation and bounded disturbances. The generalized minimum variance control strategy has been extended to suit our purpose together with a modified least squares estimation with relative nonlinear dead zone. The robust stability of the resulting closed loop system has been established with respect to unmodeled high-order dynamics related to the plant input and output, and to bounded disturbances. Simulation example and application for control of sensitive plate temperature of distillation column showed that the proposed algorithm is available for robust control of a class of nonlinear systems with uncertain disturbances and high degree unmodeled dynamics.

ACKNOWLEDGEMENT

The authors would like to acknowledge the supports of Foundation for University Key Teacher by the Ministry of Education of China, the State Science and Technology Pursuit Plan Project of China (2001BA204B01), and the Hong Kong Research Grant Council (HK UST RIG95/96. EG03).

REFERENCES

Åström, K. J., and Wittenmark, B. (1995). *Adaptive Control*. Addison-Wesley Publishing Company, Inc. Boston, MA, U.S.A.

Åström, K. J. (1983). Theory and applications of adaptive control-a survey. *Automatica*, **19**, 471.

Aganović, Z., and Gajić, Z. (1995). *Linear Optimal Control of Bilinear Systems*, Lecture Notes in Control and Information Sciences . Springer-Verlag, Berlin.

Clarke, D. W., and Gawthrop, P.J. (1975), Self-tuning controller. *Proceedings of the Institution of Electrical Engineers*, **122**, 929; (1979). Self-tuning control. *Ibid*., **126**, 633.

Egardt, B. (1979). *Stability of Adaptive Controllers*, Lecture Notes in Control and Information Sciences. Springer-Verlag, Berlin.

Gawthrop, P. J. (1980). On the stability and convergence of a self-tuning controller. *International Journal of Control*, **31**, 973.

Gawthrop, P. J., and Lim, K. W. (1982). Robustness of self-tuning controllers. *Proceedings of the Institution of Electrical Engineers*, Pt D, **129**, 21.

Goodwin, G. C., and Sin, K. S. (1984). *Adaptive Filtering Prediction and Control* . Prentice-Hall ,Englewood Cliffs, New Jersey, U.S.A..

Kreisselmeier, G. and Anderson, B. D. O. (1986). Robust model reference adaptive control. *IEEE Transactions on Automatic Control*, **31**, 127.Krstic, M.,

Kanellakopoulos, I., and Koktovic P. (1995). *Nonlinear and Adaptive Control Design.* John Wiley & Sons, Inc New York, U.S.A..

Ljung, L., and Söderstrom, T. (1983). *Theory and Practice of Recursive Identification.* MIT Press ,London, U.K..

Middleton, R. H., Goodwin, G. C., Hill, D. J. and Mayne, D. Q. (1988). Design issues in adaptive control. *IEEE Transactions on Automatic Control*, **33**, 50.

Middleton, R. H., Goodwin, G. C. and Wang, Y. (1989). On the robustness of adaptive controllers using relative deadzones. *Automatica*, **25**, 889.

Mohler, R.R. (1991). *Nonlinear Systems: Volume II, Applications to Bilinear Control* . Prentice-Hall, Englewood Cliffs, New Jersey, U.S.A..

Rohrs, C. E., Valavani, L., Athans, M., and Stein, G.(1982). Robustness of adaptive control algorithms in the presence of unmodeled dynamics,. *Proceedings of. 21st IEEE Conference on Decision and Control*, Orlando, FL. p.3.

Shao, C. (1991). Stable adaptive control system subject to bounded disturbances. *International Journal of Adaptive Control and Signal Processing*, **5**, 121.

Shao, C.(1996). On the robust stability of a Clarke-Gawthrop type of self-tuning controller. *International Journal of Control.* **64**, 721.

Sun, X. and Rao, M.(1999). Multivariable adaptive control of bilinear systems in the presence of bounded disturbances. *Preprints of 14th Triennial World Congress*, Beijing, P.R. China, **I**, 301.

COMBINED GAIN-SCHEDULING AND MULTIMODEL CONTROL OF A REACTIVE DISTILLATION COLUMN

Budi H. Bisowarno, Yu-Chu Tian, Moses O. Tadé

Department of Chemical Engineering,
Curtin University of Technology,
GPO Box U1987, Perth WA 6845, Australia

Abstract: Reactive distillation (RD) is a favourable alternative to conventional series of reaction-separation processes. Control of RD is challenging due to its integrated functionality and complex dynamics. Linear PID algorithm is not satisfactory and needs because of the need for adequate retuning over a wide range of operating conditions. Combined gain-scheduling and multimodel control scheme is proposed to handle the nonlinearities of the process. Simulation results show the superior performance of the proposed method to that of a standard PI control.

Keywords: reactive distillation, gain-scheduling, multimodel, switching, tuning.

1. INTRODUCTION

The RD column is gradually becoming an important unit operation in chemical process industry. It offers reduction in both investment as well as operational costs. Tight control of product composition and conversion is fundamental for an economically optimal operation. Unfortunately, both composition and conversion cannot be economically and reliably measured on-line and in real time. Moreover, the relationship between the product composition and the potential manipulated variable (eg. reboiler duty) may reveal multiplicity. Inferential control via stage temperatures, which have monotonic relationship with the manipulated variable, is commonly adopted.

Directionality of a chemical process means that a vector of inputs (eg. manipulated variables) is differently amplified according to its direction. It has been known to create considerable complex problem in control system design for multivariable processes such as in conventional distillation (Sågfors and Waller, 1995). Standard PID with fixed parameters is not satisfactory because of the need for adequate retuning over a wide range of operating conditions.

Inferential control of RD, which has directionality in the process gain, is investigated in this study. Limited number of reports has discussed control aspects of RD. Control strategies of batch RD (Sorensen and Skogestad, 1994) and its structure for optimisation (Wajge and Reklaitis, 1999) have been investigated. Recently, nonlinear control of batch RD has been proposed (Balasubramhanya and Doyle III, 2000). For continuous RD, a nonlinear input-output linearizing controller and nonlinear controller have been designed for ethylene glycol system (Kumar and Daoutidis, 1999). A robust PI control scheme has been proposed for the same system (Loperena et al., 2000). Linear and nonlinear control strategies have been applied for an ethyl acetate system (Vora and Daoutidis, 2001). A variety of control structures have also been explored for two product RD (Al-Arfaj and Luyben, 2000).

For ethyl tert-butyl ether (ETBE) RD, which is the focus of this study, general control considerations have been presented (Sneesby et al., 1997). Combined composition and conversion control have been discussed (Sneesby et al., 1999). Control performance of a variety of one-point control schemes has been compared (Bisowarno and Tadé, 2002). Pattern-based predictive control has recently been proposed for controlling the product composition (Tian et al., 2003). Effectiveness of control schemes has been compared for single and double-feed RD (Al-Arfaj and Luyben, 2002). Standard PI algorithms, which were employed for all cases, indicated more advanced controller is required to improve the control performance.

In this study, combined gain-scheduling and multimodel control will be implemented on one-point control of an ETBE RD. The models cover directionality of the process gain and a switching scheme will be employed to integrate them. Its performance will be compared to that of a standard PI controller.

2. REACTIVE DISTILLATION

A pilot scale packed RD column for ETBE production serves as an example for a typical single-feed two-products RD process. The column consists of 1 rectifying stage, 3 reactive stages, 4 stripping stages, a total condenser, and an electric partial reboiler, respectively, as shown in Figure 1. The feed is a mixture of isobutylene, ethanol, ETBE, and n-butane, resulting from a pre-reactor, which converts most of isobutylene to ETBE. Typical operating data including the operating range are summarised in Table 1. The primary and secondary manipulated variables are reboiler duty (Q_R) and reflux rate (L_R), respectively. LV control scheme, which outperforms other control schemes for this column (Bisowarno and Tadé, 2002), is employed.

Inferential control is adopted to control the ETBE purity. The relationship between the purity and the reboiler duty reveals input multiplicity phenomena as shown in Figure 2. Based on the sensitivity analysis, stage 7 temperature is found to be the most appropriate measured variable to infer the ETBE purity (Tian and Tadé, 2000). Figure 2 also shows the relationship between the stage 7 temperature and the reboiler duty. The nonlinear process gain ($\Delta T_7/\Delta Q_r$) is large around the nominal operating condition and becomes small outside this range.

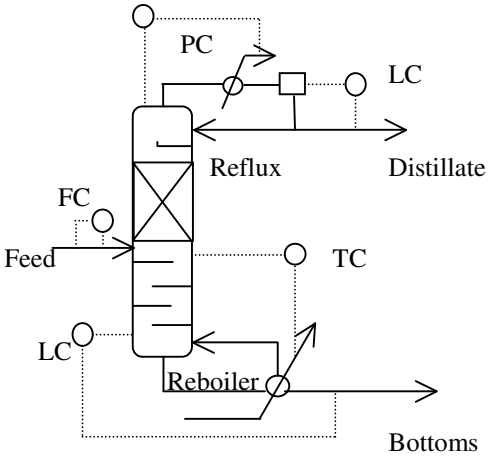

Fig. 1 ETBE Column with the controllers

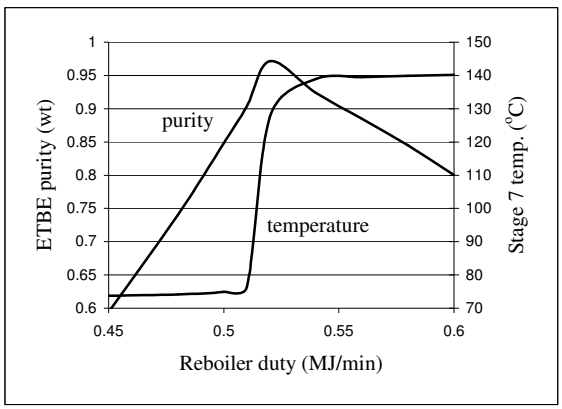

Fig.2 Stage 7 temp./purity vs. Q_R (L_R = 2.2 l/min)

Table 1 ETBE RD column characteristics and Inputs

Column Specifications:		
Nre/Nrx/Nst	3/3/5	
Feed stage	6	
Overhead pressure	950 kPa	
Feed Conditions:	Range	Nominal*
Temperature	30°C	30°C
Rate (l/min)	0.684-0.836	0.76
Comp. (mol)	70–80 mol% conversion in the pre-reactor	0.291 ETBE, 0.091 EtOH, 0.073 iBut, 0.545 nBut
Man. Variables:	Range	Nominal*
L_R (l/min)	2.0 – 2.4	2.2
Q_R (MJ/min)	0.4825-0.555	0.520

* Nominal (optimum) operating condition for designing the control system

3. CONTROL OBJECTIVES

The main objective of the control system is to keep the controlled stage 7 temperature close to the set-points despite the presence of disturbances. The most significant disturbances are changes in the feed flow rate and in the feed composition. The second objective is a sufficiently fast set-point tracking. These two objectives must be achieved for the entire operating range of the reactive distillation column.

4. CONTROL DESIGN METHOD

Adaptive control with multimodel was introduced in (Narendra and Balakrishnan, 1997). The basic idea is to choose the best model for the column from an a priori known set of models at every instant, and then apply the output of the corresponding controller to the column. Firstly, the process identification is performed by rapidly choosing the smallest error with respect to a criterion (switching). Unlike the previous work, the controller parameters are then adjusted using a parameter-adaptation algorithm in this study (gain-scheduling).

4.1 Multimodel

Although a single highly nonlinear and/or adaptive model may be used to represent the process dynamics, several simple fixed multimodels are employed. They are chosen to cope with nonlinear and time varying characteristics of each operating condition point. A proper switching scheme is needed to integrate the models. As a result, process identification and rapid control action can be satisfied.

Simplified input-output dynamic models of the manipulation and disturbance paths are identified

Table 2 Multimodels based on open-loop tests

L_R (l/min)	Q_R, min	Q_R, nom	Q_R, max
2.0	4709.5 / 238.4Ti s + 1	4679.5 / 78.5Ti s + 1	498 / 21 Ti s + 1
2.2	6442.75 / 197.4Ti s + 1	4675 / 73.2 Ti s + 1	493 / 23.2 Ti s + 1
2.4	960.5 / 122.4Ti s + 1	9043.5 / 126.1Ti s + 1	1472 / 54.9Ti s + 1
Disturbances at L_R = 2.2 l/min			
Feed rate		0.412 / 23.75Ti s + 1	
Feed comp.		0.163 / 6.75Ti s + 1	

around the optimum reboiler duty at constant reflux rate. Referring to Figure 2, three simplified models are derived to capture the nonlinearity of the process gain for each constant reflux rate. At each of the reboiler duty of 0.4825, 0.520, and 0.555 MJ/min, respectively, the models are derived at the reflux rate of 2.0, 2.2, and 2.4 l/min, respectively. The models of disturbance patch are derived at the optimum reboiler duty of 0.520 MJ/min. Table 2 shows the models formulated as first order transfer functions.

4.2 Switching scheme

The switching scheme involves firstly monitoring a performance index based on the identification error for each model and then switching to the model with smallest index. A small identification error leads to a small tracking error (Narendra and Balakrishnan, 1997). The performance index (IE) is formulated in equation 1,

$$IE = \alpha \varepsilon_i^2 + \beta \int \varepsilon^{-\lambda(t-\tau)} \varepsilon_i^2 \, dt, \; \alpha \geq 0 \text{ and } \beta > 0 \qquad (1)$$

where α and β are the weighting factors on the instantaneous measures and the long-term accuracy, respectively. These two free design parameters provide smooth transition between different process models. ε_i is the difference between the outputs of the model and the real plant.

4.3 Gain Scheduling

Gain scheduling is based on linear time-invariance of the process at a number of operating points. A linear controller is then designed for each operating point. Therefore, the parameters of the controller should be interpolated or scheduled (Rugh and Shamma, 2000). The controller gain is commonly scheduled due to the process nonlinearity with constant dynamics.

Switching between local linear controllers is a conventional way for gain scheduling. A function of a scheduling variable can also be employed to interpolate the gain. Measured ouput or set-point may be used as a scheduling variable (Bequette, 2000).

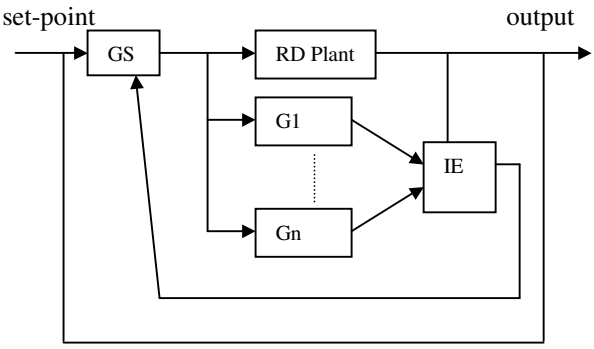

Fig. 3 Combined gain-scheduling and multimodel control scheme

In this study, the scheduling controller gain (Kc) is formulated in equation 2 (Ogunnaike and Ray, 1994),

$$Kc = \frac{Kco \, Kpo}{Kp} \qquad (2)$$

where Kco and Kpo are the reference values of the controller gain and process gains, respectively. The time varying process gain (Kp) is identified and computed on-line from the inferred variable and the manipulated variable.

The reference control parameters are tuned by using Abbas method (Abbas, 1997). This method relates the controller parameters to the characteristics of a first-order plus time delay model and the desired over-shoot of the closed loop system (Alexander and Trahan, 2001). For a PI controller, the controller parameters are formulated in equation 3,

$$Kc = \frac{T + \theta/2}{Kpo(\lambda + \theta)} \qquad (3a)$$

$$Ti = T + \theta/2 \qquad (3b)$$

where Kpo, T, and θ are the open-loop process gain, time constant, and time delay, respectively, and λ is the desired closed-loop time constant.

The general structure of the combined gain-scheduling and multimodel control scheme is shown in Figure 3. G1, Gn, GS, and IE are the simplified model 1, the simplified model n, the gain-scheduling controller, and the performance index, respectively.

5. CONTROL PERFORMANCE

The control performance of the proposed method is compared to that of a standard PI controller. The desired closed-loop time constant is chosen to be 5 min. Applying the Abbas method, the controller gain and time constant of the PI controller in the range of operating conditions are 0.00622 ^{o}C/(MJ/min) and

84.53 min, respectively. For the proposed method, the time constant is kept constant at 84.53 min while the controller gain is computed on-line as a function of the scheduling variable.

Figures 4 and 5 show the dynamic responses when the feed flow rates (F_f) increase or decrease steeply by using either standard PI or the proposed method, respectively. The Figure shows that the disturbance rejection of the proposed method is superior to the standard PI controller.

Figure 6 shows the dynamic response resulting from step change in the feed composition (F_c). The changes were represented by changes in the pre-reacted feed from 80 to 70 mol% of the isobutylene conversion. Figure 6 shows the proposed controller, which can tightly control the stage 7 temperature, does not keep the purity at the set-point value. This results from the model mismatch. Although more models can be employed to enhance the control performance, the intrinsic problem remains. This problem results from the difficulties to infer composition from VLE temperature measurements in multi-component mixture.

Figures 7 and 8 show the dynamic responses for step changes in the set-point value (T_7). The proposed method clearly has better set-point tracking as shown by shorter settling time.

The corresponding values of the integral absolute error (IAE) and integral of time-weighted absolute error (ITAE) criteria are shown in Table 3. The criteria confirm the previous analysis that the control performance can be improved by using the proposed method.

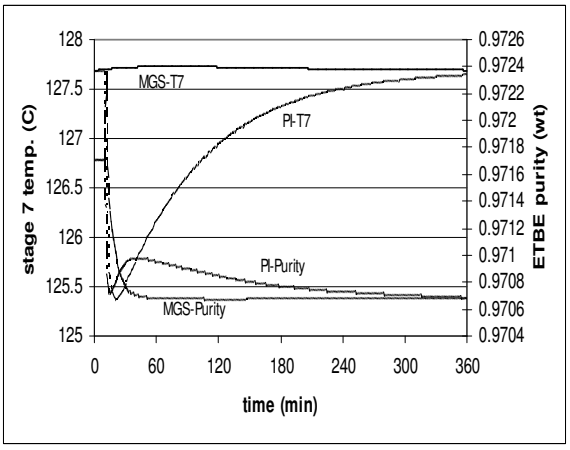

Fig. 4 Dynamic responses due to +10% Feed rate step change

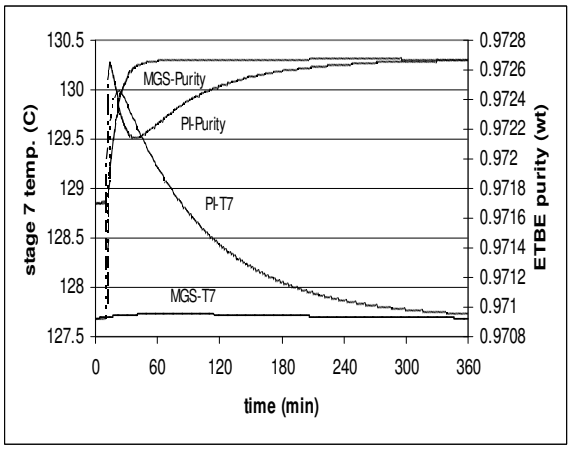

Fig. 5 Dynamic responses due to –10% Feed rate step change

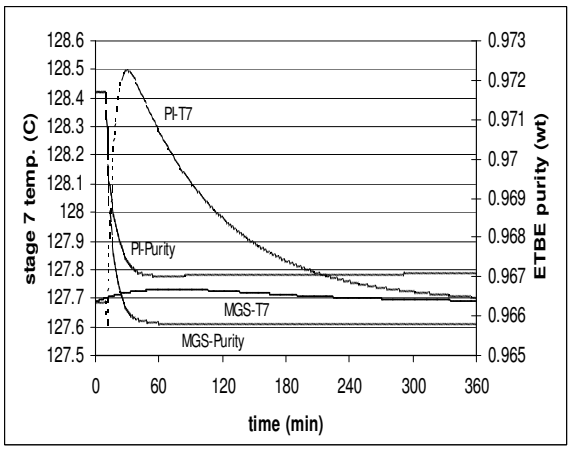

Fig. 6 Dynamic responses due to feed concentration step change

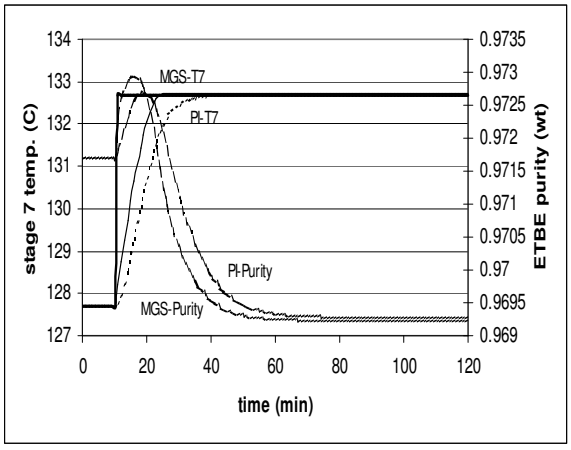

Fig. 7 Dynamic responses due to +5 set-point step change

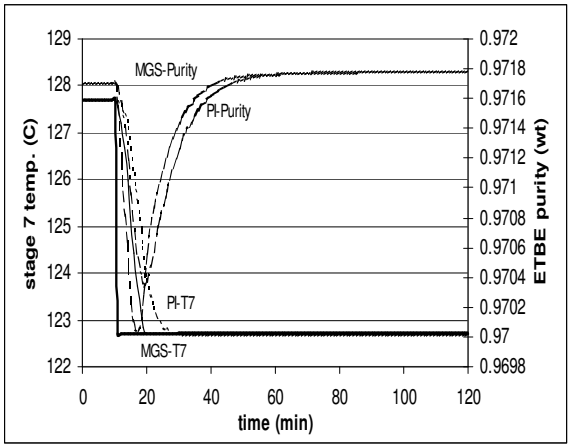

Fig. 8 Dynamic responses due to –5% set-point step change

Table 3 Comparison of IAE and ITAE indices

Magnitude	IAE		ITAE	
	PI	GS*	PI	GS*
+10% F_f	219	8.3	19990	1120
-10% F_f	218	8.3	19877	1113
80-70%conv. (F_c)	81	8.3	7741	1117
+5^{o}C T_7	19	4.1	389	288
-5^{o}C T_7	15	4.3	334	294

* The proposed method using gain-scheduling and multimodel control scheme

6. CONCLUSIONS

The combined gain-scheduling and multimodel control has been applied to a RD column for ETBE production having nonlinearity in the process gain. Several input-output first order models were derived. Gain-scheduling control was then implemented employing the multimodel for model identification and scheduling the controller gain. The proposed controller is superior to standard PI control with fixed parameters for RD columns. However, the effectiveness is reduced for feed composition disturbances. This work clearly demonstrates that nonlinear processes can be controlled successfully with a linear multimodel concept.

REFERENCES

Abbas, A. (1997). A new set of controller tuning relations. *ISA Transactions* **36**(3): 183-187.

Al-Arfaj, M. A. and W. L. Luyben (2000). Comparison of alternative control structures for two-product reactive distillation column. *Ind. Eng. Chem. Res.* **39**: 3298-3307.

Al-Arfaj, M. A. and W. L. Luyben (2002). Control Study of Ethyl *tert*-Butyl Ether Reactive Distillation. *Ind. Eng. Chem. Res.* **41**: 3784-3796.

Alexander, C. A. and R. E. Trahan (2001). A comparison of traditional and adaptive control strategies for systems with time delay. *ISA Transactions* **40**: 353-368.

Balasubramhanya, L. S. and F. J. Doyle III (2000). Nonlinear model-based control of a batch reactive distillation column. *J. Process Control* **10**: 209-218.

Bequette, B. W. (2000). Practical Approaches to Nonlinear Control: A Review of Process Application.

Bisowarno, B. H. and M. O. Tadé (2002). The Comparison of Disturbance Rejection Properties of One-Point Control Schemes for ETBE Reactive Distillation. *Chem. Eng. Comm.* **189**(1): 85-100.

Kumar, A. and P. Daoutidis (1999). Modeling, Analysis and Control of Ethylene Glycol Reactive Distillation Column. *AIChE Journal* **45**(1): 51-68.

Loperena, R. M., E. P. Cisneros, et al. (2000). A robust PI control configuration for a high-purity ethylene glycol reactive distillation column. *Chem. Eng. Sci.* **55**: 4925-4937.

Narendra, K. S. and J. Balakrishnan (1997). Adaptive Control Using Multiple Models. *IEEE Transactions on Automatic Control* **42**(2): 171-187.

Ogunnaike, B. and W. Ray (1994). *Process Dynamics, Modelling and Control*. Oxford, Oxford University Press.

Rugh, W. J. and J. S. Shamma (2000). A Survey of Research on Gain Scheduling. *Automatica*: 1401-1425.

Sågfors, M. F. and K. V. Waller (1995). Dynamic Low-Order Models for Capturing Directionality in Nonideal Distillation. *Ind. Eng. Chem. Res.* **34**: 2038-2050.

Sneesby, M. G., M. O. Tadé, et al. (1997). ETBE Synthesis via Reactive Distillation: 2. Dynamic Simulation and Control Aspects. *Ind. Eng. Chem. Res.* **36**: 1870-1881.

Sneesby, M. G., M. O. Tadé, et al. (1999). Two-Point Control of a Reactive Distillation Column for Composition and Conversion. *J. Process Control* **9**: 19-31.

Sorensen, S. and S. Skogestad (1994). Control strategies for reactive batch distillation. *J. Process Control* **4**: 205-217.

Tian, Y. C. and M. O. Tadé (2000). Inference of Conversion and Purity for ETBE Reactive Distillation. *Brazilian J. of Chem. Eng.* **17**(4-7): 617-625.

Tian, Y.-C., F. Zhao, et al. (2003). Pattern-based predictive control for ETBE reactive distillation. *J. Process Control* **13**(1): 57-67.

Vora, N. and P. Daoutidis (2001). Dynamic and Control of an Ethyl Acetate Reactive Distillation Column. *Ind. Eng. Chem. Res.* **40**: 833-846.

Wajge, R. M. and G. V. Reklaitis (1999). RBDOPT: a general-purpose object-oriented module for distributed campaign optimization of reactive batch distillation. *Chem. Eng. Journal* **75**: 57-68.

CONSTRUCTING TAKAGI-SUGENO FUZZY MODEL BASED ON MODIFIED FUZZY CLUSTERING ALGORITHM

Xing Zongyi, Jia Limin, Shi Tianyun, Qin Yong, Jiang Qiuhua

China Academy of Railway Science 100081 Beijing China

Abstract: Gath-Geva fuzzy clustering algorithm is a nonparallel fuzzy clustering algorithm and is not easy to get a suitable and interpretable fuzzy set. The outputs of the Takagi-Sugeno fuzzy model can influence the input space partition. Neglecting this influence increases the identification error. In this paper, a modified Gath-Geva fuzzy clustering algorithm is introduced to solve these problems. Together with weighted least square method, we construct Takagi-Sugeno model to identify non-linear system. The identification of the glass oven demonstrated the effectiveness of the proposed method.

Keywords: fuzzy clustering, Takagi-Sugeno model, fuzzy modeling

1. Introduction

Fuzzy modelling and identification techniques have become an active research area due to its successful application to non-linear complex systems, where traditional methods are difficult to apply because of lack of sufficient knowledge. Among the different fuzzy modelling techniques, the Takagi-Sugeno (TS) fuzzy model has attracted most attention.

The TS fuzzy model consists a set of if-then rules that have a special format with a polynomial function type consequent. The TS fuzzy model approach tries to decompose the input space into fuzzy subspace and then approximate the system in each subspace by a simple linear regression. Without the time-consuming and mathematically intractable defuzzification operation, the TS fuzzy model is the most popular candidate for fuzzy modelling.

There are two main issues in the process of constructing a TS fuzzy model. The first is how to determine the premise structure, and the second is how to estimate the parameters of the TS fuzzy model. Fuzzy clustering and least square method have proved to be suitable techniques to create TS fuzzy model.

Fuzzy clustering algorithms like the algorithm by Gustafson and Kessel (GK), Gath and Geva (GG), or the fuzzy C-means algorithm partition the input space into adequate subspaces and detect linear local substructures. Therefore, these algorithms are very suitable to construct TS fuzzy model from data. A modified Gath-Geva algorithm is proposed in this paper.

This work is supported by NSFC (60174051/F03) and ICTF (DZYFYY0204)

The paper is organized as follows. In section 2, we formulate the TS fuzzy model. A modified Gath-Geva fuzzy clustering (MGG) algorithm is described in section 3. Identification of glass oven is provided in section 4 to illustrate the effectiveness of the modified Gath-Geva algorithm. Finally, Section 5 constrains some conclusions.

2. Takagi-Sugeno Fuzzy Model

The Takagi-Sugeno Fuzzy Model was proposed by Takagi, Sugeno in an effort to develop a systematic approach to generating fuzzy rules from a given input-output data set. A typical fuzzy rule has the form:

$\boldsymbol{R_i}$: if x_1 is $A_{i,1}$ and and x_p is $A_{i,p}$ then y_i is $f_i(x)$

where

$$f_i(x) = a_{i,0} + a_{i,1}x_1 + \cdots + a_{i,p}x_p$$

in which i=1, ,k, $x_i(1 \leqslant i \leqslant c)$, are the input variables, y_i is the output variables, $A_{i,j}$, $(1 \leqslant j \leqslant p)$, are fuzzy sets defined on the universe of discourse of the input. $f_i(x)$ is usually a linear polynomial function in the input variables.

In the TS fuzzy model, each fuzzy rule describes a local linear model. All these local models combine to describe a non-linear complex system, which is difficult to find a global model.

The outputs of the TS fuzzy model is computed using the normalized fuzzy mean formula:

$$y(k) = \frac{\sum_{i=1}^{c} A_i(x) * f_i(x)}{\sum_{i=1}^{c} A_i(x)}$$

where A_i is the level of fulfilment of the ith rule:

$$A_i(x) = A_{i,1}(x_1) \times A_{i,2}(x_2) \times \cdots \times A_{i,p}(x_p)$$

in this paper, Gaussian membership functions are used to represent the fuzzy sets $A_{i,j}$:

$$A_{i,j}(x_j) = \exp(-\frac{1}{2}\frac{(x_j - v_{i,j})^2}{\sigma_{i,j}^2})$$

where $v_{i,j}$ represents the centre and $\sigma_{i,j}^2$ the variance of the Gaussian function.

3. Modified Gath-Geva fuzzy clustering algorithm

The algorithm by Gath and Geva is an extension of the Gustasfon-Kessel algorithm that also takes the size and the density of the clusters into account. Contrary to the GK algorithm, the GG algorithm does not restrict the cluster s volumes and the clusters can be directly described by univariate parametric membership functions. So lower approximation error and more relevant consequent parameters can be obtained than GK algorithm can.

The Gath-Geva fuzzy clustering algorithm can briefly described as follows:

1) Choose c the number of the clusters and the weighting exponent $m > 1$;
2) Generate the matrix U with the membership degrees μ_{ik} randomly. U must satisfy condition $\sum_{k=1}^{N} \mu_{i,k} = 1$.
3) Compute the centre of the clusters:

$$v_i^{(l)} = \frac{\sum_{k=1}^{N} (\mu_{i,k}^{(l-1)})^m z_k}{\sum_{k=1}^{N} (\mu_{i,k}^{(l-1)})^m}$$

4) Compute the fuzzy covariance matrices:

$$F_i^{(l)} = \frac{\sum_{k=1}^{N} \mu_{i,k}^{(l-1)} (z_k - v_i^{(l)})(z_k - v_i^{(l)})^T}{\sum_{k=1}^{N} \mu_{i,k}^{(l-1)}}$$

5) Compute the distance between the data z_k and the centre of the clusters v_i:

$$D_{i,k}^2(z_k, v_i) = \frac{(2\pi)^{\frac{n+1}{2}} \sqrt{\det(F_i)}}{\alpha_i} \exp(\frac{1}{2}(z_k - v_i^{(l)})^T F_i^{-1} (z_k - v_i^{(l)}))$$

with a prior probability α_i

$$\alpha_i = \frac{1}{N} \sum_{k=1}^{N} \mu_{i,k}$$

6) Update the partition matrix U of the membership degrees:

$$\mu_{i,k}^{(l)} = \frac{1}{\sum (D_{i,k}(z_k, v_i) / D_{j,k}(z_k, v_i))^{2/(m-1)}}$$

7) Stop if $\| U^{(l)} - U^{(l-1)} \| < \varepsilon$ else go to the step 3

Univariate membership functions can often be assigned linguistic labels. This makes fuzzy systems transparent, i.e. easy to read and interpret by humans. But it is difficult to specify meaningful labels for membership functions with high dimensional domains. So it is necessary to decompose multi-dimension membership functions to univariate membership functions. Projection method was often utilized.

The projections of ellipses or ellipsoids, which are the clusters of the Gath-Geva fuzzy clustering algorithm, are rectangles that contain the ellipses (see Fig.1). In this transformation process, the information about the clusters rotation and the scaling of the axes is lost, and thus decomposition error is made. To circumvent this problem, we propose a new Gath-Geva fuzzy clustering method.

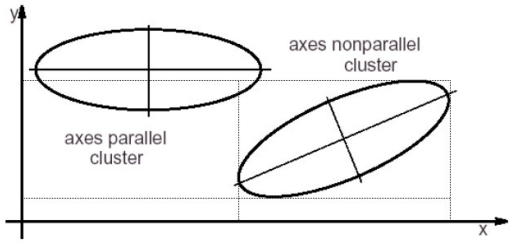

Fig.1 Axes parallel and nonparallel clusters

In Fig.1, the axes parallel cluster is illustrated. Obviously, axes parallel cluster has no rotation and thus reduce decomposition error. In Gath-Geva fuzzy clustering algorithm, if the covariance matrix is a diagonal matrix, only the axes are scaled and no rotation is performed.

For modification of the Gath-Geva algorithm, we assume the data are realization of p-dimensional normal distributions and each of these normal distributions is induced by p independent, one-dimension normal distribution.

The probability density function of the ith normal distribution is

$$g_i(x \mid \eta_i) = \frac{1}{(2\pi)^{p/2}} \cdot \frac{1}{\sqrt{\prod_{j=1}^{p} \sigma_j^{(i)}}} \cdot \exp(-\frac{1}{2} \sum_{j=1}^{p} \frac{(x_j - v_{i,j})^2}{\sigma_j^{(i)}})$$

where $\sigma_j^{(i)}$ is the jth element of the diagonal of the ith covariance A_i.

We introduce a fuzzification of the a posteriori probabilities in order to determine the parameter $\sigma_j^{(i)}$

$$p(\eta_i \mid x, y) = \coprod_{j=1}^{p} (p_i g_i(x_j))^{(u_{i,j})^m}$$

We determine the maximum likelihood estimator for the formula to obtain the estimation for the parameter:

$$\sigma_j^{(i)} = \frac{\sum_{k=1}^{N} \mu_{i,k} (x_{j,k} - v_{j,k})^2}{\sum_{k=1}^{N} \mu_{i,k}}$$

the distance between the data z_k and the centre of the clusters v_i is modified as:

$$D_{i,k}^2 = \prod_{j=1}^{q} \frac{\sqrt{2\pi\sigma_{i,j}}}{\alpha_i} \exp\left(\frac{1}{2}\frac{(x_{j,k} - v_{i,j})^2}{\sigma_{i,j}}\right)$$

Thus, we gain the axes parallel version of Gath-Geva fuzzy clustering algorithm with diagonal covariance matrix.

The outputs of the TS model can influence the input space partition. Neglecting this influence, the Gath-Geva fuzzy clustering algorithm misses some data in the output space, and cannot get the most optimized clusters. Fig.2 illustrates such circumstance for a two-input single-output system. The input variables, x_1 and x_2, are divided into clusters, S_1 and S_2. After identification, S_1 projects to S^1, and S_2 projects to S^2. The dots denote the outputs of the system and the lines denote the linear consequents of TS model. Obviously, some data leak out of the ellipsoids, and identification error increased.

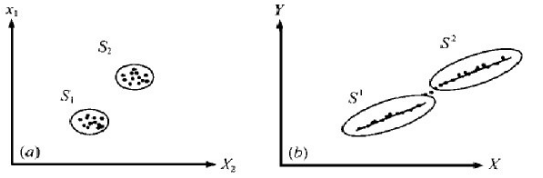

Fig.2 (a) input variables clustering (b) the actual outputs and the model outputs

To solve this problem, J.Abonyi introduce the error between actual output and model output, thus the formula of distance was modified as follow:

$$D_{i,k}^2 = \prod_{j=1}^{q} \frac{\sqrt{2\pi\sigma_{i,j}}}{\alpha_i} \exp\left(\frac{1}{2}\frac{(x_{j,k} - v_{i,j})^2}{\sigma_{i,j}}\right) \cdot \sqrt{2\pi\sigma_i} \exp\left(\frac{(y_k - f_i(x_k,\theta_i))^T (y_k - f_i(x_k,\theta_i))}{\sigma_i}\right)$$

The second part of the $D_{i,k}^2$ considers the influence mentioned above, and in this way the performance of the TS model is proved.

In this paper, the weighted least-squares estimator is used to estimate the consequent parameters of TS model.

$$\theta_i = (X_e^T \Phi_i X_e)^{-1} X_e^T \Phi_i y$$

where $Xe = [X\ 1]$ and X is the input matrix. Φ_i is a matrix having the membership degrees on its main diagonal. y is the output of the system.

From above, we give the modified Gath-Geva algorithm used to construct TS model.

The modified Gath-Geva fuzzy clustering algorithm can briefly described as follows:

1) Choose c the number of the clusters and the weighting exponent $m > 1$, choose the termination tolerance $\varepsilon > 0$
2) Generate the matrix U with the membership degrees μ_{ik} randomly. U must satisfy condition $\sum_{k=1}^{N} \mu_{i,k} = 1$.
3) Compute the centre of the clusters and Compute the standard deviations of the membership functions:

$$v_i^{(l)} = \frac{\sum_{k=1}^{N} (\mu_{i,k}^{(l-1)})^m z_k}{\sum_{k=1}^{N} (\mu_{i,k}^{(l-1)})^m}$$

$$\sigma_j^{(i)} = \frac{\sum_{k=1}^{N} \mu_{i,k} (x_{j,k} - v_{j,k})^2}{\sum_{k=1}^{N} \mu_{i,k}}$$

4) Compute the consequent parameters of TS models:

$$\theta_i = (X_e^T \Phi_i X_e)^{-1} X_e^T \Phi_i y$$

5) Compute the distance between the data z_k and the centre of the clusters v_i:

$$D_{i,k}^2 = \prod_{j=1}^{q} \frac{\sqrt{2\pi\sigma_{i,j}}}{\alpha_i} \exp\left(\frac{1}{2}\frac{(x_{j,k} - v_{i,j})^2}{\sigma_{i,j}}\right) \cdot \sqrt{2\pi\sigma_i} \exp\left(\frac{(y_k - f_i(x_k,\theta_i))^T (y_k - f_i(x_k,\theta_i))}{\sigma_i}\right)$$

with the a prior probability α_i

$$\alpha_i = \frac{1}{N} \sum_{k=1}^{N} \mu_{i,k}$$

6) Update the partition matrix U of the membership degrees:

$$\mu_{i,k}^{(l)} = \frac{1}{\sum \left(D_{i,k}(z_k, v_i) / D_{j,k}(z_k, v_i)\right)^{2/(m-1)}}$$

7) Stop if $\| U^{(l)} - U^{(l-1)} \| < \varepsilon$ else go to the step 3

4. Using modified Gath-Geva fuzzy clustering algorithm to construct TS model for glass oven

In this section, we will use the method mentioned above to construct Takagi-Sugeno model for glass oven. Other algorithms, including FMID and ANFIS, will also be used to identify the glass oven. The comparison of the result will prove the validity of the modified Gath-Geva fuzzy clustering algorithm.

The glass oven has 3 inputs (2 burners and 1 ventilator) and 6 outputs (temperature from sensors in a cross section of the furnace). The data have been pre-processed: detrending, peak shaving, delay estimates and normalization. The data set, including 1260 entries, is divided into a training subset and a test subset, each containing 600 samples. The number of clusters is 2.

The performance considered to evaluate the obtained model will be the root mean square error:

$$E = \frac{1}{P} \sum_{p=1}^{P} \sqrt{\frac{1}{N} \sum_{k=1}^{N} (y_k - \hat{y}_k)^2}$$

where P is the number of outputs and N is number of data, y_k is the actual output, and $\hat{y}_k$ if the model output.

Table 1 compares the performance of the model identified with these techniques, including FMID and ANFIS.

Table1. Comparison of the performance of the different algorithms

Method	Train data error	Test data error
MGG	0.8395	1.0732
FMID	0.8563	1.0489
ANFIS	0.7771	1.1403

The observation of this table indicates that modified Gath-Geva fuzzy clustering algorithm has slightly better performance than FMID in the training data set and slightly better performance than ANFIS in the test data set.

We explain the interpretability of the obtained TS fuzzy model of the 4th output as flows. For the number of clusters is two, there are also two rules.

R_1:

$$A_1 = \begin{bmatrix} 0.0309 & 0.0218 & 0.9892 \\ 1.0012 & 0.9924 & 0.0049 \end{bmatrix}$$

$$B_1 = [-0.2095 \quad 0.0620 \quad -1.9251 \quad 2.5638]$$

R_2:

$$A_2 = \begin{bmatrix} -0.0218 & -0.0099 & -1.0041 \\ 0.9960 & 1.0067 & 0.0071 \end{bmatrix}$$

$$B_2 = [-0.0413 \quad 0.0395 \quad -0.7477 \quad -1.4202]$$

The first row of A_i represents the centre v and the second row represents the variance σ^2 of the Gaussian function. B_i is the consequent parameters of the TS fuzzy model.

In Fig.3, we plot the curves of the actual outputs and the TS fuzzy model outputs of the 4th output of the glass oven. (a) is the result of training data and (b) is the result of test data.

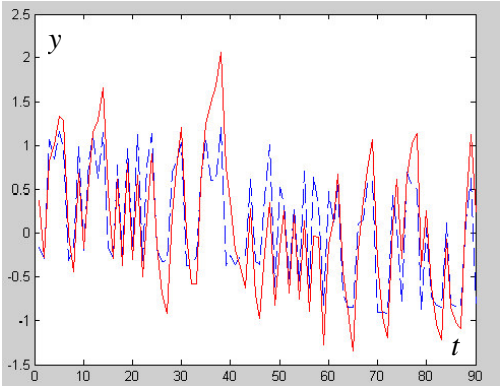

Fig.3 (a) the actual outputs (solid lines) and the TS model outputs (dotted lines) of the 4th outputs (training data, 90 samples).

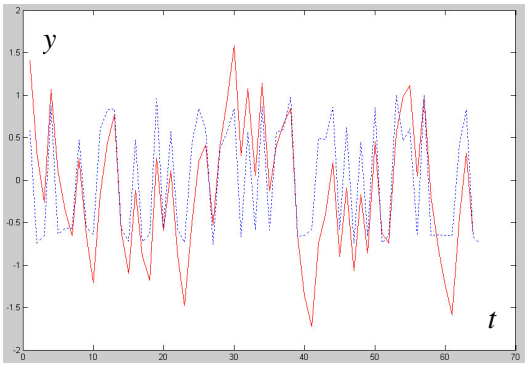

Fig.3 (b) the actual outputs (solid lines) and the TS model outputs (dotted lines) of the 4th output (test data, 65 samples).

This identification of the glass oven proves that the modified Gath-Geva fuzzy clustering algorithm can be used efficiently to construct Takagi-Sugeno fuzzy model.

5. Conclusions

We have proposed a modified Gath-Geva fuzzy clustering algorithm together with weighted least square method to create Takagi-Sugeno fuzzy model. Through minishing the projection error and considering the model outputs influence on input space partitions, we get interpretable and more accurate Takagi-Sugeno fuzzy model.

This method was used to identify the glass oven. The result proves that this method is sufficient to construct Takagi-Sugeno fuzzy model. We also compare other modelling methods, including FMID and ANFIS, with this method. The comparison shows its superiority.

REFERENCES

A.F. Gomez-Skarmeta (1999). About the use of fuzzy clustering techniques for fuzzy model identification *Fuzzy sets and systems* **106,**179-188.

Frank H?ppner and Frank Klawonn (1999). *Fuzzy Cluster Analysis*. John Wiley & Sons, LTD.

I.Gath and A.B. Geva (1989). Unsupervised optimal fuzzy clustering. *IEEE Transactions on Pattern Analysis and Machine Intelligence*. **11,** 773-781.

J.Abonyi and J.A Roubos. (2001). Compact TS-fuzzy models through clustering and OLS plus FIS model reduction. *FUZZ-IEEE. 2001*.

Jhy-shing Roger Jang (1997). *Neuro-Fuzzy and soft computing*. Prentice Hall

Tomohiro Takagi and Michio Sugeno (1985). Fuzzy identification of systems and it application to modeling and control. *IEEE Transactions on Systems, Man and Cybernetics*. **15,** 116-132.

Wang Hong-wei (2001). Improving fuzzy identifying method base on fuzzy clustering, *ACTA electronica sinica* . **29,** 436-438. (in Chinese).

NONLINEAR PREDICTIVE FUNCTIONAL CONTROL BASED ON ARTIFICIAL NEURAL NETWORK

Zhang Quanling, Xie Lei and Wang Shuqing

National Key Lab of Industrial Control Technology,
Zhejiang University, Hangzhou, 310027, P.R. China
E_mail: qlzhang@iipc.zju.edu.cn

Abstract: An Artificial Neural Network (ANN) is an adequate tool for modeling nonlinear systems and can be applied straightforward in the predictive functional control. New structure of ANN multi-step prediction that is different from cascade or parallel is presented, at the same time, the nonlinear predictive functional control using this ANN model has been developed in this paper. The useful of this control strategy is evaluated by applying it to a Continuous Stirred Tank Reactor (CSTR). The simulation results indicate that it is more effective than PID control.

Keywords: Artificial Neural Network, Nonlinear, Model Based Predictive Control, Predictive Functional Control

1. INTRODUCTION

Model Based Predictive Control (MBPC) refers to a class of algorithms that compute a sequence of manipulated variable in order to optimize the process performance. It is recognized as an efficient control strategy by the industrial control community. The first MBPC techniques were developed in 1970s. Model Predictive Heuristic Control (MPHC) based on finite impulse response has been successfully applied in PVC plant, a distillation column and power plant by Richalet, et al.(1978). Dynamic Matrix Control (DMC) based on finite step response was developed by Cutler, et al.(1980). Not only MPHC but also DMC belong to MBPC based on nonparametric model. In 1987, the Generalized Predictive Control (GPC) of Clarke, et al.(1987a,b) which absorbs the advantages of predictive control and adaptive control can turn the model parameter online. The Predictive Functional Control (PFC) which belongs to the third generation predictive control has been developed by Richalet, et al.(1988), which has been successfully used in the fast and accurate robot control.

Many processes are sufficiently nonlinear to preclude the successful application of linear model based predictive control technology. MBPC such as DMC and GPC developed initially for linear processes have been successfully extended to nonlinear processes by many researchers (Mutha, et al.(1998), Robit, et al.(1998)). Henson(1998) has published excellent technical reviews of Nonlinear Model Based Predictive Control (NMBPC). It has presented the current status of NMBPC technology, and meanwhile outlined myriads of directions for future research.

The purpose of this paper is to develop a Nonlinear Predictive Functional Control (NPFC) based on the Artificial Neural Network (ANN) model. The general principle of PFC is discussed in section 2. In section 3, the ANN model is developed. NPFC using ANN model is developed in section 4. Simulation results

are elucidated in section 5 and conclusion is described in section 6.

2. GENERAL PRINCIPLE OF PREDICTIVE FUNCTIONAL CONTROL

PFC belongs to the classical family of MBPC. It is essentially based on the following three principles of MBPC: predictive model, receding horizon optimization, modeling error compensation.

2.1 Predictive model

PFC uses a model to predict future output. The output of the model $y_m(k+i)$ can be divided into two main components: free response $y_l(k+i)$ and forced response $y_f(k+i)$.

Free response has nothing to do with future inputs and thus just depends on the actual model output.

The other component of the model output is forced response that depends on the set of future manipulated variables and has nothing to do with the actual model output. The structure of manipulated variables is the key to the control performance in PFC. The future manipulated variable are structured by a linear combination of functions defined forehead that we refer to as base functions. The future manipulated variables u(k+i) and forced response are given by:

$$u(k+i)=\sum_{n=1}^{N}\mu_n u_{bn}(i), i=1,2,...,H \quad (1)$$

$$y_f(k+i)=\sum_{n=1}^{N}\mu_n y_{bn}(i) \quad (2)$$

Where μ_n stands for coefficients, $u_{bn}(i)$ the nth base function at $t=iT_s$, $y_{bn}(i)$ is the advance output of the nth base function at $t=iT_s$ and T_s is the sampling period. The selection of the base functions depends on the nature of the set point and on the process. Often the polynomial base function set is used.

2.2 Receding Horizon Optimization

Various types of reference trajectories can be used. The most elementary reference trajectory is a first-order exponential trajectory. The reference trajectory $y_r(k+i)$ can be given by:

$$y_r(k+i)=c(k+i)-\lambda(c(k)-y_P(k)) \quad (3)$$

Where c is the set point, $\lambda = e^{(-Ts/Tr)}$ and T_r is the 95% response time of the reference trajectory, y_P is the process output.

The control objective of PFC is to minimize the sum of squared errors between the predicted output and the reference trajectory at all coincidence points. The objective function can be given by:

$$\min J_p=\sum_{i=H_1}^{H_2}(y_r(k+i)-\tilde{y}(k+i))^2 \quad (4)$$

$$\tilde{y}(k+i)=y_m(k+i)+e(k+i) \quad (5)$$

Where $\tilde{y}(k+i)$ is the predicted output at $t=(k+i)T_s$, $y_m(k+i)$ is the output of the model at $t=(k+i)T_s$, e(k+i) is the predicted errors, H_1, H_2 are coincidence horizon.

2.3 Modelling error compensation

The output of the predictive model and the process in general differ due to model mismatches, secondary input and disturbances which are not taken into account by the predictive model. There are several procedures to eliminate a permanent off-set by compensating the reference trajectory with the predicted errors between model and process output at each time instant of the coincidence horizon. The predicted errors can be given by:

$$e(k+i)=y_P(k)-y_m(k) \quad (6)$$

Where $y_P(k)$ is the process output at $t=kT_s$, $y_m(k)$ is the model output at $t=kT_s$.

3. ARTIFICIAL NEURAL NETWORK MODEL

PFC uses a model to predict future outputs. Any type of predictive model such as transfer function, state equations and ANN model can be used. NPFC requires the availability of a suitable nonlinear dynamic model of the process. The NPFC controller may be based on a fundamental model or a combination of the fundamental and empirical model. First, it is difficult for us to construct sufficiently accurate comprehensive mathematical process models. On the other hand, the potential disadvantage of the fundamental modeling approach is that the resulting dynamic model may be too complex to be useful for NPFC. In this work, ANN model is employed as the predictive model in PFC.

During the last decade, there has been an increasing trend in the industry towards the use of ANN. It has been proven that a feed forward ANN which is comprised of a great number of interconnected neurons can approximate any continuous function to any desired accuracy. This makes feed forward ANN very suited to deal with complex nonlinear. A feed forward layered ANN is employed as the model of NPFC.

The structure of ANN is shown in Fig 1. It consists of a layer of input neurons, a layer of output neurons, and two hidden layers. The transfer function f1(x) of the first hidden layer neuron is given by:

$$f1(x)=(e^{x}-e^{-x})/(e^{x}+e^{-x}) \quad (7)$$

The activate function f2(x) of the second hidden layer neuron is shown by:

$$f2(x)=1/(1+e^{-x}) \quad (8)$$

The transfer function f3(x) of the output hidden layer neuron is given by:

$$f3(x)=x \quad (9)$$

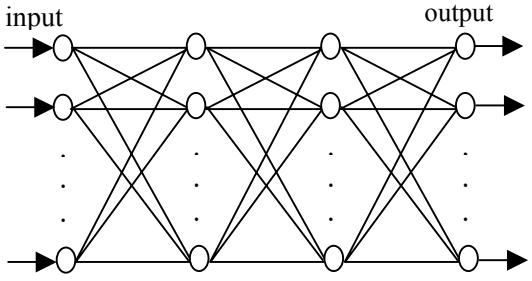

Fig. 1 Structure of ANN

The most important aspect of the ANN is learning the information about the system to be modeled. The most versatile learning algorithm for feed-forward layered network is back propagation (BP). Unfortunately, BP is very slow because it requires small learning rates for stable learning, on the other hand, it is possible for the network solution to become trapped in the local minimum. Levenberg_Marquardt(LM)(Matlab User's Guide, 1994) optimization algorithm is used in this investigation. This technique is more powerful than gradient descent, but requires more memory.

The L_M update rule is given by:

$$\triangle W=(J^{T}J+\mu I)^{-1}J^{T}E \quad (10)$$

Where J is the Jacobian matrix of derivation of each error to each weight, μ is a scalar, and e is an error vector. If the scalar μ is very large, the above expression approximates gradient, while if it is small the above expression becomes the Gauss-Newton method.

4. NONLINEAR PREDICTIVE FUNCTIONAL CONTROL

A NPFC strategy is developed in this section. The principle of the NPFC using ANN is shown in Fig. 2.

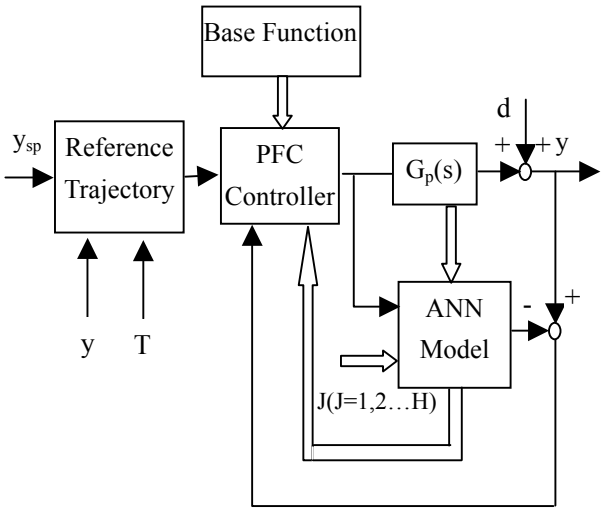

Fig. 2 Principle of the NPFC using ANN model

4.1 Artificial neural network model

Predictive model plays a key role in predictive functional control. It demands that certain precision must be attained, at the same time with multi-step prediction. Generally there are two kinds of structures which can fulfil multi-step prediction using ANN, one is cascade, the other is parallel. Cascade structure, in which the output of time k+1(y_m(k+1)) can be achieved from the data of time k, and next time y_m(k+1) as input to estimate the output of time k+2(y_m(k+2)), and so on. The benefit of this structure is that only one ANN model is needed. But there also exists the accumulation of prediction error in such a structure. Parallel structure needs many ANNs to predict, with each ANN for a specific step. The benefit of parallel is that the prediction error is comparatively small, but the disadvantage is that the calculation is heavy for there are so many ANNs to be trained. In this paper, a new structure for multi-step prediction is proposed. Only an ANN is needed in such a structure. In order to fulfil multi-step prediction, an additional input J(J=1,2,…H) is employed, which distinguishes the ANN outputs y_m(k+J). So the multi-step prediction is realized.

4.2 Nonlinear predictive functional control using artificial neural network model

The objective function of NPFC is similar to the other classical MBPC. With a certain optimization procedure we can determine a sequential manipulated variable that minimizes the objective function. The objective function of NPFC is given by equation 4. The method of Levenberg-Marquardt or Gauss-Newton which can be realized by MATLAB TOOLBOX is used as optimization algorithm.

The algorithm of NPFC can be summarized in the following steps:

1) Select the sample for training
2) Identify the ANN model with sample
3) Evaluate the extent of ANN model
4) Realize the NPFC strategy using ANN model and L_M optimization algorithm

① Calculate the error between the output of process y_p(k) and actual model output y_m(k)

② Calculate the actual model output y_m(k+i),i=1,2,…,H and the predictive output of the process $\tilde{y}(k+i)$

③ calculate for reference trajectory of y_r(k+i), i=1,2,…,H

④ calculate the sequence manipulated variable u(k+i) i=1,2,…,H using the method of L_M optimization algorithm.

⑤ Perform u(k) and go to ① at the next sample time.

5. SIMULATION

In order to evaluate the performance of the NPFC, a Continuous Stirred Tank Reactor (CSTR) is chosen as an application example.

5.1 Reactor

The dynamic equations describing the CSTR systems can be written as:

$$V\frac{dC_A}{dt} = F(C_{Af} - C_A) - Vk_0 e^{(-\frac{ET_r}{R_g})} C_A \tag{11}$$

$$V\rho C_p \frac{dT_r}{dt} = \rho C_p F(T_f - T_r) - V(-\Delta H)k_0 \exp(-\frac{ET_r}{R_g})C_A - UA_h(T_r - T_c) \tag{12}$$

The dynamic equations can be written in dimensionless from Venkateswarlu(1997) as:

$$\begin{aligned} \dot{x}_1 &= -x_1 + D_a(1-x_1)\exp(\frac{x_2}{1+x_2/\varphi}) \\ \dot{x}_2 &= -x_2 + B_h D_a(1-x_1)\exp(\frac{x_2}{1+x_2/\varphi}) + \beta(u-x_2) \\ y &= x_1 \end{aligned} \tag{13}$$

Where x_1 and x_2 are the dimensionless reactant concentration and temperature, respectively. The input u is the cooling jacket temperature. The physical parameters are chosen as:

$$D_a = 0.072,\ \Phi = 20.0,\ B_h = 8.0,\ \beta = 0.3 \qquad (14)$$

Here the task is to control the reactant concentration x_1, and the manipulated variable is the input u of the cooling water temperature.

5.2 Predictive model of artificial neural network

Given the $x_1(k)$, $x_2(k)$,u(k) at the $t=(k)T_s$ and J, the $x_1(k+J)$ at the $t=(k+J)T_s$ can be obtained. The number of neurons in the two hidden layers is 10, respectively. In order to evaluate the performance of the ANN model, 30 groups input data are created at random to compare the output of the ANN and process. The output of ANN model (+) and the output of the process (o) are shown in the Fig 3(a). The errors between the output of ANN model and process are shown in Fig 3(b). We can obtain that the accuracy of ANN model is enough for NPFC.

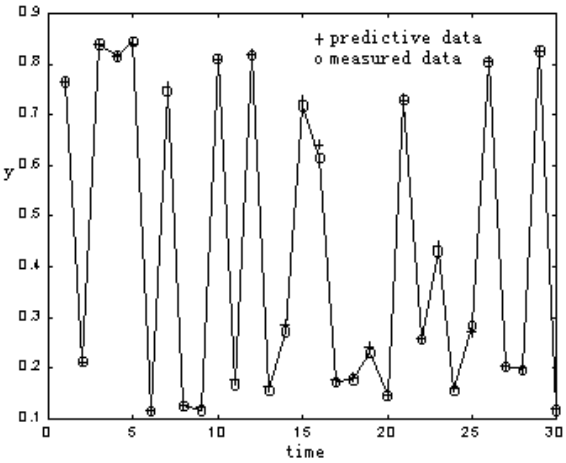

Fig. 3(a) Results of process output and ANN output

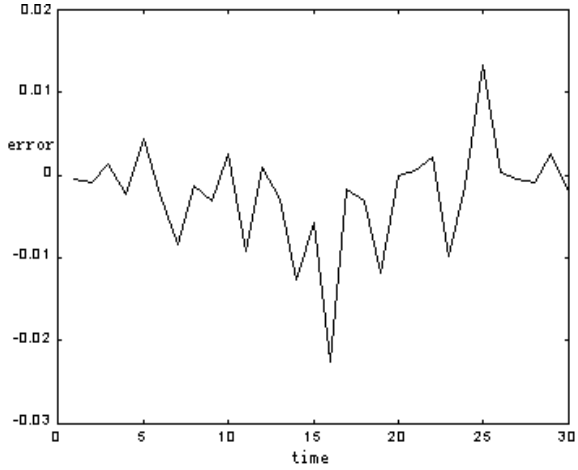

Fig. 3(b) Errors between process output and ANN output

5.3 Simulation of nonlinear predictive functional control and PID control for CSTR

Simulation studies are carried out in order to evaluate the performance of the NPFC, the results of PID are also presented as a reference. The parameters of PID are P=0.2, I=30 seconds and D=0. The NPFC selects one base function. The parameters of NPFC are given by H=5, Tr=10 seconds.

The setpoint of concentration is changed from x1=0.2 to x1=0.6 at t=20, at the same time, a step disturbance 0.1 has been applied to the system at t=200. The results of PID control are shown in the Fig 4(a). The manipulated variable of PID is shown in Fig 4(b). The results of NPFC are shown in the Fig 5(a). The manipulated variable of NPFC is shown in Fig 5(b).

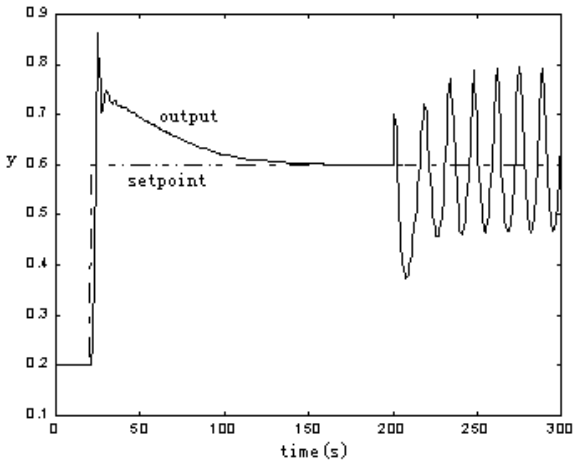

Fig. 4(a) Results of PID control

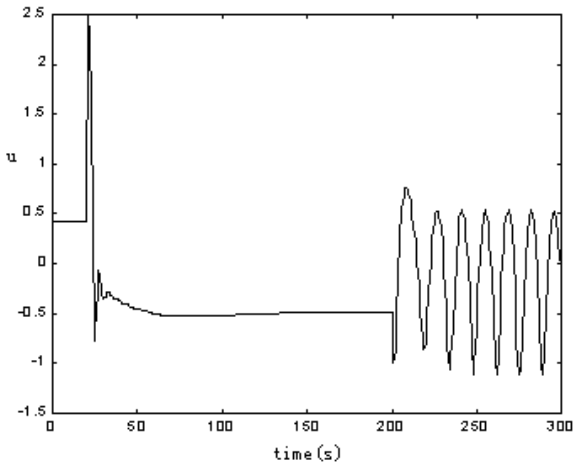

Fig. 4(b) Manipulated variable of PID control

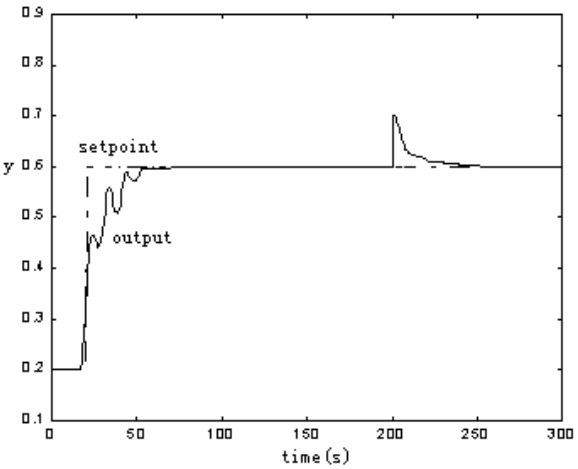

Fig. 5(a) Result of NPFC control

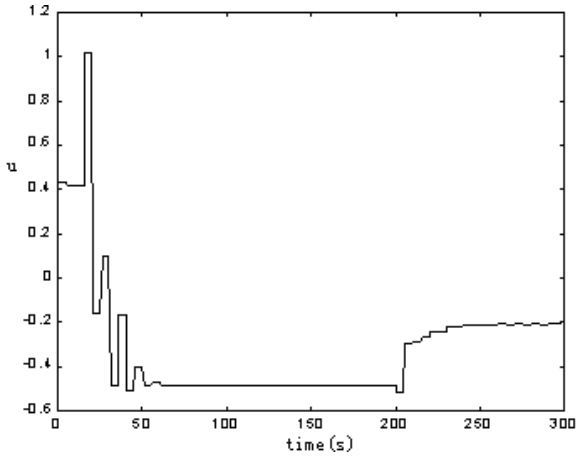

Fig. 5(b) Manipulated variable of NPFC control

As can be seen from the figure, PID control has fast response but has large overshoot. NPFC using ANN has slow response but no overshoot. Compared with PID control, NPFC can reject the disturbance more effectively.

6. CONCLUSION

An NPFC using ANN model strategy is presented for control of high-nonlinear system. The performance of this strategy is evaluated by applying it to a CSTR for controlling them at the desired state operating point. The results illustrate that the NPFC is more effective for control nonlinear system than PID control.

REFERENCES

Richalet J., Rault A., Testud J. L. and Papon J.(1978). Model predictive heuristic control: applications to industrial processes. *Automatica*, **14**, pp.413-428.

Cutler, C.R. and Ramaker, B.L.(1980). Dynamic matrix control-a computer control algorithm. *Proc. JACC*, San Francisco. WP5-B

Clarke, D.W., Mohtadi, C. and Tuffs, P.S.(1987a). Generalized predictive control-part 1. basic algorithm. *Automatica*, **23**, pp. 137-148.

Clarke, D.W., Mohtadi, C. and Tuffs, P.S.(1987b). Generalized predictive control-part 2. extensions and interpretations. *Automatica*, **23**, pp.149-160.

Richalet J., Doss S. A. A., Arber C., Kuntze H.B., Jacubasch A., Schill W.(1988). Predictive functional control: applications to fast and accurate robots. In: *Isermann R. ed. Automatic Control Tenth Triennial World Congress of IFAC V.4*, Oxford: Pergamon Press, pp.251-258.

Mutha, R. K., Cluett, W. R., and Penlidis, A.(1998). Modifying the prediction equation for nonlinear model-based predictive control. *Automatica*. **34**, pp1283-1287.

Rohit, S., Patwardhan, S., Lakshminarayanan, and Sirish L. Shah. (1998). Constrained nonlinear MPC using Hammerstein and Wiener models: PLS Framework. *AICHE,* **44**, pp.1611-1622.

Henson, M. A. (1998). Nonlinear model predictive control: current status and future directions, *Computers & Chemical Engineering*. **23**, pp187-202.

Neural Network Toolbox, Matlab User's Guide. (1994). *Math Works Inc.* pp.5-33,34.

Venkateswarlu, C.H. and Gangiah, K.(1997). Constrained generalized predictive control of unstable nonlinear proceses. *Trans IchemE*. **75**, Part A, pp.371-376.

COMPUTATIONAL INTELLIGENCE (CI) SELF-ADAPTIVE PID (CISAPID)

Mingzhong Yi Yong Qin LiMin Jia

Institute of Computing Technologies Head, Res. Centre for Intelligent Systems
CHINA ACADEMY OF RAILWAY SCIENCES

Abstract: A new method for Computational Intelligence (CI), CI formulated with Analytic Functions and Logics, is given, and a new PID controller - CISAPID is put forward. CISAPID take the strategy attempt to incarnate but not to realize or imitate the complex thinking and behaviour of human being. The constitution, principle and qualitative arguments tuning experience of CISAPID are analysed in detail. Simulation and practical application show that the performance of CISAPID is better than that of general PID.

Keywords: CI AI incarnate CISAPID PID

1. PREFACE

Computational Intelligence (CI) is a new chapter in Intelligence Theory[3]. The reason why the research of Artificial Intelligence (AI) did not achieve expected progression perhaps is that AI depend on excessively the advantage of computer - precise arithmetic and the fast calculation to imitate the complex thinking and action of human being[8]. But thinking and action of human being do not often depend on precise arithmetic and fast calculation, furthermore, the ability to abstract of human being plays, I think, the most important role in the intelligence of human being, but this ability is just what computer lacks extremely. So, an one-year old babe perhaps don't understand any arithmetic, and can't calculate at all, but some intelligence of his or hers is far more better than any current sophisticated computer. It is possible that the thinking mechanism of human being can hardly be cryptanalyzed completely, so, what machine can achieve or imitate is perhaps only fragmentary and dyshematopietic intelligence of human being forever, no matter what advanced machine can hardly reproduce entirely the complicated mechanism of the thinking of human being[7] [8].

But for practical application in engineering, it is enough to achieve our given purpose, to obtain a satisfactory but not optimal result, and the truly advanced theory, algorithm or method perhaps are those that are not complicated, sophisticated and optimal but practical, feasible, satisfactory, reliable and simple, thus, take a strategy attempt to incarnate but not to realize or imitate the complex thinking and behavior of human being is not only a remedy for computer's shortcoming, but also a practical, feasible and simple shortcut. So, in this paper, a new method for CI - CI formulated with Analytic Functions and Logics is given, Logics mentioned in this paper are expressed as "if … , then … " instructions of computer program, they are enough to incarnate logical relation for practical project, it is no need to resort to more complex method.

2. COMBINE CI WITH PID

Today, the most popular controller is still PID controller, even in developed country - Japan, the rate of utilization of PID controller reached 84.5%[10].

But general PID has many intrinsic shortcomings. In order to improve the performance of general PID , many scholars had done a lot of research. So, how to combine Computational Intelligence with widely used general PID is very significative in theory and in practice. So, in this paper, a new PID controller-CISAPID is put forward.

In our practical project for engineering, this controller seems not highly depend on the precise model of controlled object (we could not find the precise model), but make use of some Analytic Functions and Logics to regulate arguments of PID real-timely according to the feedback information, to incarnate some intelligence of human being to a certain degree in a practical, flexible, simple way, and to incarnate knowledge, experience and rules of experts and skilled operators, thus, it has some characteristics of Fuzzy Control and Expert Control. But it is not confined to the patterns of Fuzzy Control and Expert System, because fuzzy rule table is not intuitionistic, and is not convenient to establish, furthermore, we don't want to make the control system too complex. In practical project, the more simple a system is, the more practical, feasible, reliable and robust it often is. So, if it is able to achieve the same satisfactory efficiency, the control system should be simple as best as possible, thus, not only the control efficiency is improved, but also the hardware cost and the developing cycle are reduced markedly, thus this system is advanced in fact. According to the viewpoint of James C. Bezdek, CI is based on the data provided by operator, but traditional AI is on so-called "knowledge". He defined the CI system as follows: When a system only treats with the data from bottom, and possess the part for pattern recognition, and don't make use of knowledge in the sense of AI, then, this system can be viewed as a CI system. Such a system would have characteristics as follows: has the adaptability of compute; has the tolerance of compute error; close to the speed that human handling problem; close to the error rate of human being[3]. So, we can also think in the same way: If a controller treats with the data from

bottom only based on Logics and Analytic Functions abstracted from experience, rules and knowledge of experts and operators, and possess the part for pattern recognition, and don't make use of knowledge in the sense of AI, then this controller can also be viewed as a CI controller. So, CISAPID can also be viewed as a controller based on CI.

3. CISAPID

For typical standard negative feedback control system, general PID controller can be expressed as:

$$u=K_p(e+\frac{1}{T_i}\int e\,dt+T_d\frac{de}{dt}) \quad (1)$$

The CI Self-adaptive PID Controller (CISAPID) can be formulated as follows[6] [5]:

$$u=(1-k\_u)*(Kp\_e*e+Ki\_e*\int e\,dt+Kd\_e\_de*\frac{de}{dt}+Kd\_dde*\frac{d^2e}{dt^2})+k\_u*u_0 \quad (2)$$

$$Kp\_e=Kp0\_e+Kp1\_e*(1-\exp(-Kp\_s*W\_Kp\_e*(e-p*s)^2)) \quad (3)$$

$$Ki\_e=Ki0\_e+Ki1\_e*\exp(-W\_Ki\_e*e^2) \quad (4)$$

$$Kd\_e\_de=Kd\_e+Kd\_de \quad (5)$$

$$Kd\_e=Kd0\_e+Kd1\_e*\exp(-Kd\_s*W\_Kd\_e*(e-p*s)^2) \quad (6)$$

$$Kd\_de=Kd0\_de+Kd1\_de*\exp(-W\_Kd\_de*(de)^2) \quad (7)$$

$$Kd\_dde=Kd0\_dde+Kd1\_dde*\exp(-W\_Kd\_dde*(d^2e)^2) \quad (8)$$

$$u_0=(u\_0+u\_1*u\_power+u\_2*(u\_power)^2+...+u\_n*(u\_power)^n+...)/(1+u\_power+(u\_power)^2+...+(u\_power)^n+...) \quad (9)$$

e=setting value-actual value, error *e*. *Kp_e*, *Ki_e*, *Kd_e* indicate that these arguments are related to *e*. *Kd_de* indicate that the argument is related to *de*, the first-order differential of *e*; *Kd_e_de* indicate that the argument is related to *e* and *de*; *Kd_dde* indicate that the argument is related to d^2e, the second-order differential of *e*; So as to the rest. If arguments except *Kp0_e*, *Ki0_e*, *Kd0_e* are all 0, then, CISAPID turn itself back to general PID. The reasons why we construct Analytic Functions as above and more detailed information about arguments tuning, please refer to my master's degree thesis. The tuning method of *Kp0_e*, *Ki0_e*, *Kd0_e* can refer to the tuning method of general PID based on object model or dynamic response curve[1], such as Ziegler Nichols - frequency response method[9], CohenCoon - response curve method[2],integral squared error - ISE[4] and so on. Because physical meaning of the other arguments are explicit, simple, and regular, so, it is not very difficult to determine them by off-line simulation or resort to experience and by means of trial-and-error method. Further more, what needed to tune are their initial arguments, the running arguments are self-adjust online and real-timely based on the initial arguments according the situation on-site. Even if you did not tune these arguments very well, or the controlled object and other factors had already changed, the control efficiency would not decline greatly (but the burden of executing mechanism would perhaps increase), thus, the self-adaptability and robust of this controller are good.

3.1 The proportional action of CISAPID

$$Kp\_e=Kp0\_e+Kp1\_e*(1-\exp(-Kp\_s*W\_Kp\_e*(e-p*s)^2)) \quad (3)$$

Kp_e is similar to a reversed double peak gaussian function, the larger the *W_Kp_e* is, the more sharp the curve is, the value of *W_Kp_e* should ensure that system would respond enough proportional action within a wide range, so the value of *W_Kp_e* should be minor; *p* is a sign variable, when $e<0$, $p=-1$; when $e\geqslant 0$, $p=+1$. $s\geqslant 0$ is an offset; *Kp_s* is related to offset *s*, and is a coefficient to adjust *W_Kp_e*, when $|e|\geqslant s$, $Kp\_s=1$, when $|e|<s$, it is allowed $Kp\_s\neq 1$. Because of offset *s*, the minimum value of *Kp_e* is not at the point of $e=0$, but at the point of $e=+s$ or $-s$. If system is not very stable, and the requirement for accuracy and rapidity are not high when system is near to the equilibrium point, then, *Kp_s* should be nearly equal to 0, thus, when $|e|<s$, *Kp_e* would hardly increase with the reduction of $|e|$, and seems to be a constant, and this is beneficial to system stability.

Analytic Function of formula (3) in fact incarnated knowledge, rules and experience of experts and operators, and approximately incarnated the fuzzy rules as follows:

if $|e|$ is "extreme big", **then** proportional action *Kp_e* should be "very big";

if $|e|$ is "very big", **then** proportional action *Kp_e* should be "comparatively big";

if $|e|$ is "comparatively big", **then** proportional action *Kp_e* should be "not big and not small";

if $|e|$ is "a bit big" (namely, $|e|$ is a little bigger than *s*), **then** proportional action *Kp_e* should be "comparatively small";

if $|e|$ is "not big and not small" (namely, $|e|=s$), **then** proportional action *Kp_e* should be "minimum";

if $|e|$ is "comparatively small" (namely, $|e|$ is a little smaller than *s*), **then** proportional action *Kp_e* should be "comparatively small";

if $|e|$ is "very small" (namely, $|e|$ is approaching to 0 or $|e|=0$), **then** proportional action *Kp_e* should be "not big and not small";

3.2 The integral action of CISAPID

$$Ki\_e=Ki0\_e+Ki1\_e*\exp(-W\_Ki\_e*e^2) \quad (4)$$

Ki_e is a gaussian function related to error *e*. The value of *W_Ki_e* should cause system respond integral action only within narrow ranges (error is very small). When error *e* becomes a little big, integral action should be near to 0 in order to carry out the isolation of integral action and to avoid integral saturation. So the value of *W_Ki_e* should be a little larger, then the curve of *Ki_e* would be very

sharp. *Ki0_e* should be far less than *Ki1_e* to help to realize the isolation of integral.

Analytic Function of formula (4) in fact incarnated knowledge, rules and experience of experts and operators, and approximately incarnated the fuzzy rules as follows:

if |*e*| is "extreme big", **then** integral action *Ki_e* should be "extreme small";

if |*e*| is "very big", **then** integral action *Ki_e* should be "extreme small";

if |*e*| is "comparatively big", **then** integral action *Ki_e* should be "very small";

if |*e*| is "a bit big" (namely, |*e*| is a little bigger than *s*), **then** integral action *Ki_e* should be "very small";

if |*e*| is "not big and not small", **then** integral action *Ki_e* should be "comparatively small";

if |*e*| is "comparatively small", **then** integral action *Ki_e* should be "a bit small";

if |*e*| is "very small" (namely, |*e*| is approaching to 0 or |*e*|=0), **then** integral action *Ki_e* should be "not big and not small";

3.3 The differential action of CISAPID

$$Kd\_e\_de=Kd\_e+Kd\_de \quad (5)$$

$$Kd\_e=Kd0\_e+Kd1\_e*exp(-Kd\_s*W\_Kd\_e*(e-p*s)^2) \quad (6)$$

$$Kd\_de=Kd0\_de+Kd1\_de*exp(-W\_Kd\_de*(de)^2) \quad (7)$$

$$Kd\_dde=Kd0\_dde+Kd1\_dde*exp(-W\_Kd\_dde*(d^2e)^2) \quad (8)$$

Kd_e is a double peak gaussian function. *p* is a sign variable, when $e<0$, $p=-1$;when $e\geqslant 0$, $p=+1$. $s\geqslant 0$ is an offset, and is not the same value as that of formula (3); *Kd_s* is related to *s*, and is a coefficient to adjust *W_Kd_e*, when $|e|\geqslant s$, $Kd\_s=1$, when $|e|<s$, it is allowed that $Kd\_s\neq 1$. For the reason of simple, you can assign $Kd\_s=1$. But if disturbance is severe, then, you should assign $Kd\_s>1$, then, when |*e*| is approaching to *0*, differential action *Kd_e* can reduce more quickly, thus, system would not be very sensitive to disturbance.

Analytic Function of formula (6) in fact incarnated knowledge, rules and experience of experts and operator, incarnated approximately the fuzzy rules as follows:

if |*e*| is "extreme big", **then** differential action *Kd_e* should be "extreme small";

if |*e*| is "very big", **then** differential action *Kd_e* should be "extreme small";

if |*e*| is "comparatively big", **then** differential action *Kd_e* should be "comparatively small";

if |*e*| is "a bit big" (namely, |*e*| is a little bigger than *s*), **then** differential action *Kd_e* should be "not big and not small";

if |*e*| is "not big and not small" (namely, |*e*|=*s*), **then** differential action *Kd_e* should be "maximum";

if |*e*| is "comparatively small" (namely, |*e*| is a little smaller than *s*), **then** differential action *Kd_e* should be "comparatively big";

if |*e*| is "very small" (namely, |*e*| is approaching to 0 or |*e*|=0), **then** differential action *Kd_e* should be "not big and not small";

Kd_de and *Kd_dde* are help to control more ahead when controlled object is of very great inertia and hysteresis such as furnace temperature control system. If the inertia and hysteresis are not very great, or if filtering for *de* and *dde* are not very satisfactory, then *Kd_de* and *Kd_dde* are not necessary. Knowledge, rules, experience of experts and operators and the fuzzy rules incarnated by the Analytic Functions of formula (7)(8) are similar to those of (3), the main deffrence is that the curve of *Ki_e* should be very sharp.

From above, we can see that CISAPID is not only a controller of proportional action, integral action and differential action, it is actually related to the first-order and second-order differential of error *e*, the ability that it can control ahead according to the error tendency is very strong, so, engineering application of this thesis is kiln temperature control system with very great inertia and hysteresis.

3.4 Dynamical Weighting Average Algorithm with selection

It is also important to make use of u_0. When adjust system on-site, because of the intrinsic shortcoming of general PID and complexity of control system, you can only compromise among stability, rapidity, accuracy and anti-disturbance. System would often oscillate even if you make great effort to tune the arguments of PID. The purpose of u_0 is just to turn this disadvantage into advantage.

It can be observed, the oscillation of output *u* is often symmetrical about "a specific value", so, the oscillation in fact provide some important information: this "a specific value" is probably close to so-called "setting value" or "right value", so, if we can properly figure out this "a specific value" and let it be u_0, and add this u_0 to output *u*, then, it is equivalent to give a reference point to output *u* (if $k\_u=0.5$), and it also seems to calculate output *u* based on "setting value" or "right value", thus, it is possible that output *u* would probably be just right, and thus system would eliminate oscillate very soon of its own accord. the calculation of u_0 is as follows:

$$u_0=(u\_0+u\_1*u\_power+u\_2*(u\_power)^2+...+u\_n*(u\_power)^n+...)/(1+u\_power+(u\_power)^2+...+(u\_power)^n+...) \quad (9)$$

u_0, *u_1*, *u_2*, ... , *u_n*, ... represent the value of output *u* at current moment, previous one moment, previous two moment, … , previous *n* moment, … , This is in fact the Dynamical Weighting Average of output *u* at each moment. The selection of weight coefficient *u_power* is very important, if we make $u\_power=0.9847$, then, *u_300* would have little effect on u_0, because *u_300* is multiplied a coefficient $u\_power^{300}=0.9847^{300}=0.009799<0.01=1\%$. So, the nearer *u_i* approach to current moment, the more effects it has on u_0; the further *u_i* is away from current moment, the less effects it has on u_0. This Dynamical Weighting Average Algorithm is coincide with practical situation, the u_0 that figured out as above mainly reflect current working information, but also reflect previous working information to certain extent, thus, this u_0 is quite possible to close to so-called "setting value" or "right value". Further more, we can also multiply a coefficient *u_power_i* before corresponding *u_i*.

*u_power_i=Ku0_e/(Ku0_e+Ku1_e)+Ku1_e/(Ku0_e +Ku1_e)*exp(-W_Ku_e*(e_i)^2)* (10)

Assign biggish value to *W_Ku_e*, and make *Ku0_e* far too less than *Ku1_e*, thus curve *u_power_i* is very sharp, only when *e_i* is very little, then *u_power_i* would approach to 1, otherwise, *u_power_i* is always very little, thus, those *u_i* that correspond to biggish *e_i* are filtered off, however, those *u_i* that correspond to minor *e_i* are selected. So, algorithm of formula (9) change into the algorithm of formula (10) with selection, and better efficiency would be get.

Of course, what mentioned above are only close to, not equal to so-called "setting value" or "right value", but for practical project in engineering, it is enough to incarnate the idea of "closing to"; If k_u=0, then output u of CISAPID would not relate to u_0. If "setting value input" of system is a constant, then k_u could be greater than 0.5, or even near to 1. In fact, The Analytic Functions of formula (9) and (10) incarnate the ideal of "stabilizing by force" and "Sampling and Statistical Learning", and computer is always in a state of self-studying and self-perfecting, the more it has learned, the more it become "clever" [8]. Statistical Learning has solid theoretical basis, and is drove fully by objective data, so, playing an important role in CI. Basal model, strategy and algorithm related to the design of Statistical Learning perhaps is a direction needed our efforts in future.

Practical running of the algorithms mentioned above shows: With u_0, CISAPID can shorten control time notably if input is step signal, can come into stable-state and close to "setting value" or "right value" more quickly, and can keep stable-state for a comparatively longer time. But, if system is simple and is very stable, then, it is not necessary to make use of this algorithm;If system is tracking system and the requirement for rapidity is high, it is also not appropriate to make use of this algorithm.

4. SIMULATION[6]

Typical object $G(S)=\frac{e^{-5s}}{(60s+1)(50s+1)}$ is taken as controlled object to carry out simulation. As to such second-order object with great inertia, great hysteresis in practical project, what is the most important may be stability and rapidity but not accuracy or control time (is allowed to correspond to 5% (or >5%) error range). There are four criterion for performance comparison during simulation: 1.Integral Squared Error (ISE), (let $J=\int e^2 dt$); 2. Rise time (defined as the time needed that system rise from zero to 90% steady-state value); 3.Average value of $|e|$; 4.Overshoot;

ISE and Rise time are main criterions. Arguments of General PID (perhaps had been optimized in reference [6]) are as follows: Kp=5, Ki=0.025, Kd=90; Arguments of CISAPID (only satisfactory but not optimized) are as follows: Kp0_e=4.999, Kp1_e=217, W_Kp_e=100, p_s=0.085, Kp_s=0.0002119, Ki0_e=0.015, Ki1_e=0.1, W_Ki_e=100, Kd0_e=90, Kd1_e=100, W_Kd_e=100, d_s=0.2, Kd_s=2

4.1 Performance comparison

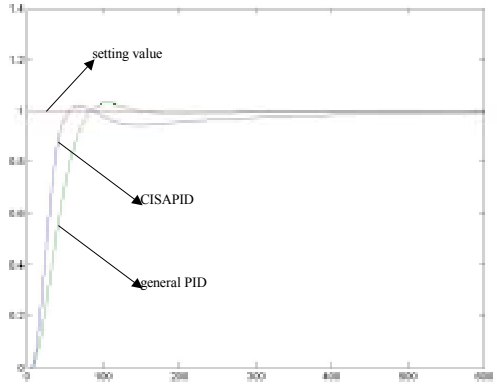

Fig.1 Comparison between CISAPID and general PID for ideal case

When the case is ideal, and there are no disturbance and non-linear parts, the performance of general PID is very well, but it is still inferior to that of CISAPID. General PID: ISE is 29.29, average value of |e| is 0.07128, rise time is 66 seconds, overshoot is 3.014%; CISAPID: ISE is 21.15, enhancement is 27.79%, average value of |e| is 0.06706, enhancement is 5.92%, rise time is 42 seconds, enhancement is 36.364%, overshoot is 2.319%, enhancement is 23.06%;

If controlled object changed greatly, for instantce, hysteresis changed to 8 seconds, pole points changed to 1/110 and 1/100, simulating curves are as follows:

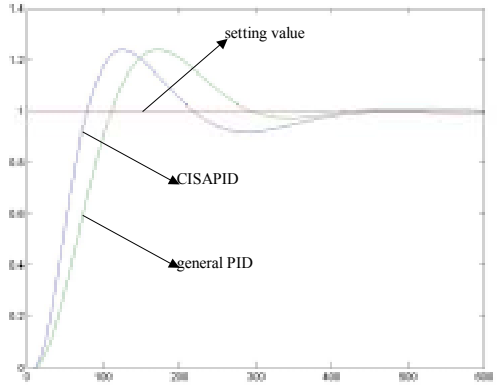

Fig.2 Comparison between CISAPID and general PID if controlled object had changed

Compare with Fig.1: general PID: ISE is 55.38, 55.38-29.29=26.09, average value of |e| is 0.1581, 0.1581-0.07128=0.08682, rise time is 100 seconds, 100-66=34, overshoot is 23.91%, 23.91%-3.014%=20.896%; CISAPID: ISE is 41.56, 41.56-21.15=20.41<26.09, average value of |e| is 0.1316, 0.1316-0.06706=0.06454<0.08682, rise time is 71 seconds, 71-42=29<34, overshoot is 23.88%, 23.88%-2.319%=21.561%>20.896%;

From above we know that the performance of general PID and CISAPID are both worsen when controlled

object changed, but the worse of CISAPID are less than those of general PID except overshoot.

4.2 Comparison for Anti-disturbance

We could suppose that disturbance is a sinusoidal input of which the amplitude is 0.2 and the frequency is 0.0314 radian / second (cycle is 200 seconds), then, simulating curves are as follows:

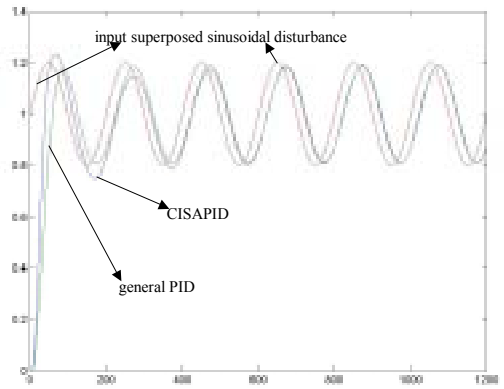

Fig.3 Comparison between CISAPID and general PID if disturbance is sinusoidal

It can be known from the Fig.: general PID: ISE is 46.38, average value of |e| is 0.1207, rise time is 65 seconds, overshoot is 19.38%; CISAPID: ISE is 34.94, enhancement is 24.67%, average value of |e| is 0.1065, enhancement is 11.765%, rise time is 44 seconds, enhancement is 32.31%, overshoot is 24.28%, enhancement is - 25.28%; When input is changing, the requirement for rapidity is main to make system follow the change of input quickly enough, it is allowed that overshoot increased a bit. It also can be known from the Fig.: the output of CISAPID and general PID are both lag behind input, but, after system become stable, the lag of CISAPID is less about 1 second than that of general PID.

If load (y_d) decreased 0.2 suddenly at t=400, and increased y_d=0.2 suddenly at t=700, and setting value of input increased 0.2 suddenly at t=1000, then, simulating curves are as follows:

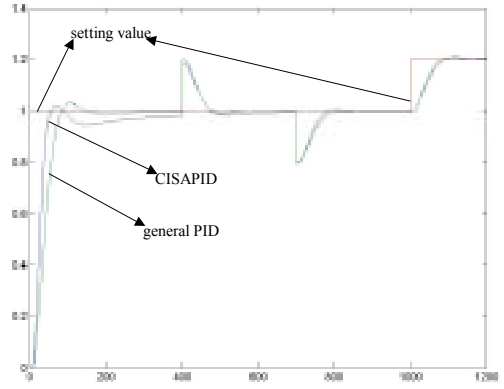

Fig.4 Comparison between CISAPID and general PID if load changed suddenly and disturbance is a step input

It can be known from the Fig.: general PID: ISE is 32.74, average value of |e| is 0.05612, rise time is 66 seconds, overshoot is 3.014%; CISAPID: ISE is 24.63, enhancement is 24.77%, average value of |e| is 0.05451, enhancement is 2.87%, rise time is 42 seconds, enhancement is 36.364%, overshoot is 2.319%, enhancement is 23.06%.

4.3 Comparison for non-minimum phase

Add a non-minimum phase part on the base of previous controlled object, then, transfer function is

G(S)= $\dfrac{e^{-5s}(1-s)}{(60s+1)(50s+1)}$ instead, simulating curves are as follows:

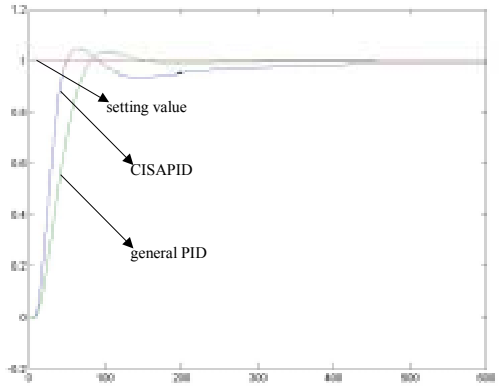

Fig.5 Comparison between CISAPID and general PID if there is a non-minimum phase part

It can be known from the Fig.: general PID: ISE is 29.91, average value of |e| is 0.07195, rise time is 66 seconds, overshoot is 3.48%; CISAPID: ISE is 21.95, enhancement is 26.613%, average value of |e| is 0.06958, enhancement is 3.294%, rise time is 41 seconds, enhancement is 37.88%, overshoot is 4.735%, enhancement is - 36.06%, this is because rise time reduced greatly, rapidity improved greatly, so, overshoot increased a bit more;On the whole, if there is a non-minimum phase part, performance of CISAPID is still better than that of general PID greatly (main criterion ISE improved 21.95%,rapidity(rise time) improved 37.88%).

5. CONCLUSION

The constitution, principle and qualitative arguments tuning experience of an ameliorative PID controller-Computational Intelligence Self-Adaptive PID Controller (CISAPID) has analysed in detail, and the ability for anti-disturbance, robustness, adaptability and the performance for non-minimum phase system of CISAPID are also discussed. Contrastive simulation between CISAPID and general PID showed that the efficiency of CISAPID is better than that of general PID, and practical application in engineering (High Temperature tunnel kiln in TEGAOTE special kiln Corporation, Sansui, GuangDong Province) also showed that the performance of CISAPID is practical, feasible, satisfactory, reliable but simple, better than that of general PID

5.1 Innovative ideas of CISAPID

Here, we should first thank QingChang Zhong, JianYing Xie, Hui Li, please refer to reference [6] for

specific details, they bring gaussian function into PID and put forward a new PID controller- Variable Arguments PID (VAPID). But, the constitution of proportional gain function and differential gain function of VAPID are all have something to be improved, and they were probably not aware of : If this idea improved appropriately, it is in fact a new idea for CI with Analytic Functions and Logics at which computer is good. Then, this new idea only process bottom data, and possess the part for pattern recognition (by means of Analytic Functions and Logics), and don't make use of knowledge in the sense of AI, but can incarnate knowledge, rules and experience of experts or operators and can perform Fuzzy Logic Control and Expert Control to a certain extent, thus, this system is a CI system in fact. So-called innovative ideas in this thesis are listed simply as follows, please refer to my master's degree for more details, and we urgently welcome precious critical advice.

1) A new idea - incarnate Computational Intelligence with analytic functions and Logics
2) Particular structure of CISAPID
3) Proportional action of CISAPID
4) Differential action of CISAPID: (1) Based on e; (2) Based on de; (3) Based on d^2e
5) Dynamical Weighting Average Algorithm with selection of CISAPID

5.2 The problems to be improved for CISAPID

There are many arguments of CISAPID, it is a little inconvenient to tune so many arguments, and we have not yet find perfect tuning method in theory, all these are to be improved in future.

As to so many arguments that to be tuned and optimized, resort to Neural Network, Genetic and Evolutive Algorithms maybe good ideas.

Sampling and Statistical Learning, and the basal model, strategy and algorithm related to the design of Statistical Learning perhaps is a direction needed our efforts in future.

At last, it is needed to point out: The reasons why we attempt to incarnate but not to realize or imitate are mainly as follows: 1) It is easy to incarnate, but it is difficult to realize or imitate. 2) Algorithms are comparatively concise, feasible, ingenious, but they are enough to achieve given target for practical application in engineering.

But all these are still only the execution but not the creation of intelligence of human being, in the long run, research for CI should probably aim at the purpose of creating intelligence.

REFERENCES

[1] A A Rovira, P W Murrill, C L Smith. Tuning Controllers for Set-Point Change Instruments and Control Systems, 1969,42(12)

[2] Cohen G N, Coon G A. Theoretical Considerations of Retarded Control. Trans. ASME, 1953,75:287

[3] FuChun Sun, ZengQi Sun Technique on Computational Intelligence (in chinese)

[4] Lopez A M et al. Controller Tuning Relationships Based on Integral Performance Criteria. Instrumentation Technology.1967, 14:57

[5] MingZhong Yi Arguments Self-learning PID Control system with Prediction of BP-NN based on PCC Transactions of 14TH Conference of Control and Decision 2002.5: 484～492(in chinese)

[6] QingChang Zhong,JianYing Xie,Hui Li PID controller with Variable Arguments (in chinese) 《Information and Control》Vol.28 No.4 1999

[7] Unscramble Intelligence Computation in 21th Century the third International Conference on Computation in 21 Century Microsoft Research China (in chinese)

[8] Unscramble Intelligence Computation of Microsoft the third International Conference on Computation in 21 Century(in chinese)

[9] Ziegler J G,Nichols N B. Optimum Settings for Automatic Controllers.Trans. ASME, 1942,64:759

[10]森, 重政, PID オートチェニクコニトロテの動向, 計測と制御 1990, 29(8): 29～34

Robust Stability Analysis for Descriptor Systems with State Delay and Parameter Uncertainty ‡

Shengyuan Xu * **James Lam** * **Chengwu Yang** †

Abstract: This paper considers the problem of robust stability analysis for continuous descriptor systems with state delay and structured uncertainties. A computationally simple approach to test stability of descriptor delay systems is proposed. Based on this, we developed a sufficient condition which guarantees that the perturbed descriptor delay system under consideration is regular, impulse-free and stable for all admissible uncertainties. An example is provided to demonstrate the application of the proposed approach.

Keywords: Continuous descriptor systems, robust stability, time-delay systems, uncertain systems.

1. Introduction

In the past years, much attention has been addressed to the study of stability analysis and controller design for time-delay systems since time delays are often the main causes for instability and poor performance of systems and encountered in various engineering systems such as chemical processes, long transmission lines in pneumatic systems, and so on [8] . When parameter uncertainty appears in a delay system, the problem of robust stability as well as robust stabilization has been dealt with and various approaches have been proposed [5, 16] .

On the other hand, it is known that descriptor systems provide a more natural description of dynamical systems than state-space systems and have attracted much interest in recent years. Descriptor systems are also referred to as singular systems, implicit systems, generalized state-space systems, differential-algebraic systems or semi-state systems [4] . Applications of such systems can be found in dynamic models of chemical systems [2, 11] , mechanical engineering [9] , and other areas. There have been many research works on extending existing theories and results based on state-space systems to descriptor systems [4, 14] . Recently, there has been a growing interest in the study of robust stability analysis and robust control for descriptor systems [6, 7, 15, 21] . In [6] and [7] , upper bounds on structured perturbations ensuring robust stability for uncertain continuous and discrete descriptor systems were given, respectively. For descriptor systems with unstructured uncertainties, [20] and [22] studied the robust stability problem by extending the concept of "*quadratic stability*" for state-space systems, and some sufficient conditions for robust stability were obtained. Similar results for discrete-time descriptor systems were reported in [21] . Very recently, discrete descriptor systems with time delays as well as parametric uncertainties were studied in [18] , where both robust stability and robust D-stability results were presented. For continuous descriptor delay systems with unstructured uncertainties, sufficient conditions for both robust stability and robust stabilization were given in [19] . It is worth pointing out that when dealing with the robust stability problem for descriptor delay systems, similar to delay-free case [6, 7] , not only stability robustness, but also regularity and impulse immunity (for continuous descriptor systems) and causality (for discrete descriptor systems) should be considered simultaneously [18, 19] , while for state-space delay systems the latter two issues do not arise. For continuous descriptor delay systems, although robust stability results for unstructured uncertainties were obtained in [19] , when structured uncertainties appear, no results on robust stability are available in the literature, this issue is still open.

In this paper, we deal with the problem of robust stability for continuous descriptor systems with state delay and structured uncertainties. The purpose is to develope conditions such that the perturbed descriptor delay system under consideration is regular, impulse-free and stable for all admissible uncertainties. We first present a computationally simple stability condition for descriptor delay systems without parameter uncertainties. Then, by this and some properties of modulus matrix, a robust stability condition is proposed, which can be viewed as an extension of existing results on robust stability for descriptor systems without delay. Finally, an example is given to demonstrate the effectiveness of the proposed approach.

Notation. Throughout this paper, for matrices X, $Y \in \mathbb{R}^{n\times n}$, the notation $X \geq Y$ means that $X_{ij} \geq Y_{ij}$, i, $j = 1, 2, \ldots, n$, where X_{ij}, Y_{ij} $(i, j = 1, 2, \ldots, n)$, are elements of X and Y, respectively. I is the identity matrix with appropriate dimension. The superscript "T" represents the transpose. $\mathbb{C}^+$ is the closed right-half plane. $\|x(t)\|$ denotes the Euclidean norm of vector x. $\rho(M)$ refers to spectral radius of matrix M and $|M|_m$ is the modulus matrix of M. Matrices, if not explicitly stated, are assumed to have compatible dimensions.

* Department of Mechanical Engineering, University of Hong Kong, Pokfulam Road, Hong Kong.

† 810 Division, School of Power Engineering, Nanjing University of Science and Technology, Nanjing, 210094, P.R. China.

‡ This work is supported by RGC HKU 7103/01P.

2. Preliminaries and Problem Formulation

Consider the following linear continuous descriptor system with parameter uncertainties and state delay:

$$\begin{aligned}(\Sigma): \quad E\dot{x}(t) &= (A+\Delta A)x(t) \\ &\quad +(A_d+\Delta A_d)x(t-\tau) \quad (1)\\ x(t) &= \phi(t),\ t\in(-\tau,0] \quad (2)\end{aligned}$$

where $x(t)\in\mathbb{R}^n$ is the state, $u(t)\in\mathbb{R}^m$ is the control input. The matrix $E\in\mathbb{R}^{n\times n}$ may be descriptor, we shall assume that rank $E=r\leq n$. A and A_d are known real constant matrices with appropriate dimensions. $\tau>0$ is a constant time delay of the system, $\phi(t)$ is the compatible continuous vector valued initial condition. ΔA and ΔA_d are time-invariant parameter uncertainties and are assumed to have the following properties [7, 13] :

$$|\Delta A|_m\leq M_A,\ |\Delta A_d|_m\leq M_d \quad (3)$$

where M_A and M_d are constant matrices whose elements are all nonnegative. The constant matrices M_A and M_d represent the highly structured information for the additive perturbation matrices ΔA and ΔA_d. The parameter uncertainties ΔA and ΔA_d are said to be admissible if (3) holds.

The nominal descriptor delay system of (1) can be written as:

$$E\dot{x}(t)=Ax(t)+A_dx(t-\tau). \quad (4)$$

Definition 1 [4, 14]

(I) The pair (E,A) is said to be regular if $\det(sE-A)$ is not identically zero.

(II) The pair (E,A) is said to be impulse-free if $\deg(\det(sE-A))=\operatorname{rank}E$.

(III) The pair (E,A) is said to be stable if all of its finite eigenvalues are in the open left-half plane.

The descriptor delay system (4) may have an impulsive solution, however, the regularity and the absence of impulses of the pair (E,A) ensure the existence and uniqueness of an impulse-free solution to this system, which is shown in the following lemma.

Proposition 1 [19] *Suppose the pair (E,A) is regular and impulse free, then the solution to (4) exists and is impulse-free and unique on $(0,\infty)$.*

In view of this, we introduce the following definition for descriptor delay system (4).

Definition 2 [19]

(I) The descriptor delay system (4) is said to be regular and impulse-free if the pair (E,A) is regular and impulse free.

(II) The descriptor delay system (4) is said to be stable if for any $\varepsilon>0$ there exists a scalar $\delta(\varepsilon)>0$ such that, for any compatible initial conditions $\phi(t)$ satisfying $\sup_{-\tau\leq t\leq 0}\|\phi(t)\|\leq\delta(\varepsilon)$, the solution $x(t)$ of system (4) satisfies $\|x(t)\|\leq\varepsilon$. Furthermore,

$$x(t)\to 0,\ t\to\infty$$

The purpose of this paper is to develop robust α-stability conditions for descriptor delay systems. To this end, it is worth pointing out that the regularity, impulse immunity as well as stability robustness should be considered simultaneously when dealing with the problem of robust stability analysis for uncertain descriptor delay systems [19] , which is similar to the robust stability analysis for uncertain descriptor systems without delay [6, 7] .

3. Main Results

In this section, a computationally simple robust stability condition for descriptor delay systems will be developed. We first present the following lemma which will play a key role in the derivation of our main results.

Lemma 1 *Suppose the pair (E,A) is regular, impulse-free and stable, then the descriptor delay system (4) is regular, impulse-free and stable if*

$$\rho\left[(sE-A)^{-1}A_d\right]<1,\quad\forall\ s\in\mathbb{C}^+. \quad (5)$$

Proof. From the Definition 2, the regularity and impulse immunity of the pair (E,A) implies that the descriptor delay system (4) is regular, impulse-free. To show the stability of system (4), we first note that from [4] the regularity and impulse immunity of the pair (E,A) guarantees that there exist two invertible matrices P and Q such that

$$PEQ=\begin{bmatrix}I&0\\0&0\end{bmatrix},\ PAQ=\begin{bmatrix}A_1&0\\0&I\end{bmatrix} \quad (6)$$

where $A_1\in\mathbb{R}^{r\times r}$. Since the pair (E,A) is stable, we have that $sI-A_1$ is invertible for all $s\in\mathbb{C}^+$, which implies that $(sE-A)^{-1}$ is well defined for all $s\in\mathbb{C}^+$. Now, write

$$PA_dQ=\begin{bmatrix}A_{d1}&A_{d2}\\A_{d3}&A_{d4}\end{bmatrix} \quad (7)$$

compatibly with (6). Noting

$$\lim_{s\to\infty}(sE-A)^{-1}A_d=Q\begin{bmatrix}0&0\\-A_{d3}&-A_{d4}\end{bmatrix}Q^{-1}. \quad (8)$$

This together with (5) implies that

$$\rho(A_{d4})<1. \quad (9)$$

Now set $\xi(t)=Qx(t)$ and decompose

$$\xi(t)=\begin{bmatrix}\xi_1(t)^T&\xi_2(t)^T\end{bmatrix}^T$$

where $\xi_1(t)\in\mathbb{R}^r$ and $\xi_2(t)\in\mathbb{R}^{n-r}$. Then, noting (6) and (7), system (4) can be transformed to

$$\begin{aligned}\dot{\xi}_1(t) &= A_1\xi_1(t)+A_{d1}\xi_1(t-h)+A_{d2}\xi_2(t-h)\\ \xi_2(t) &= -A_{d3}\xi_1(t-h)-A_{d4}\xi_2(t-h).\end{aligned}$$

On the other hand, considering (5), it is easy to see

$$\det\left[I-(sE-A)^{-1}A_de^{-s\tau}\right]\neq 0,\quad \forall\ s\in\mathbb{C}^+.$$

Using this and noting $\det(sE-A)\neq 0$ for all $s\in\mathbb{C}^+$, we have

$$\begin{aligned}&\det\left(sE-A-A_de^{-s\tau}\right)\\ &=\det(sE-A)\det\left[I-(sE-A)^{-1}A_de^{-s\tau}\right]\neq 0,\forall\ s\in\mathbb{C}^+.\end{aligned}\tag{10}$$

That is,

$$\det\begin{bmatrix} sI-A_1-A_{d1}e^{-s\tau} & -A_{d2}e^{-s\tau}\\ -A_{d3}e^{-s\tau} & -I-A_{d4}e^{-s\tau}\end{bmatrix}\neq 0,\quad \forall\ s\in\mathbb{C}^+.$$

From this and (9) and along the same lines as in the proof of Theorems A and B (page 384) in [10] we can show that

$$\xi_1(t)\to 0,\ \xi_2(t)\to 0, t\to\infty.$$

This implies

$$x(t)\to 0,\ t\to\infty.$$

Therefore, the descriptor delay system (4) is stable. □

The following lemmas will be used in the proof of our main results.

Lemma 2 [7, 17] *For any $n\times n$ matrices X, Y and Z with $|X|_m\leq Z$, we have*

(a) $|XY|_m\leq |X|_m|Y|_m\leq Z|Y|_m$
(b) $|X+Y|_m\leq |X|_m+|Y|_m\leq Z+|Y|_m$
(c) $\rho(X)\leq\rho(|X|_m)\leq\rho(Z)$
(d) $\rho(XY)\leq\rho(|X|_m|Y|_m)\leq\rho(Z|Y|_m)$
(e) $\rho(X+Y)\leq\rho(|X+Y|_m)\leq\rho(|X|_m+|Y|_m)\leq\rho(Z+|Y|_m)$.

Lemma 3 [12] *For any $n\times n$ matrices X, if $\rho(X)<1$, then $\det(I-X)\neq 0$.*

Lemma 4 [1] *A regular pair (E,A) is impulse-free if and only if $(sE-A)^{-1}$ is proper.*

Lemma 5 [3] *Let $M(s)$ be a square rational matrix and be decomposed uniquely as $M(s)=M_p(s)+M_{sp}(s)$, where $M_p(s)$ is a polynomial matrix and $M_{sp}(s)$ is a strictly proper rational matrix. Then $M^{-1}(s)$ is proper if and only if $M_p^{-1}(s)$ exists and is proper.*

Suppose the pair (E,A) is regular, impulse-free and stable, then we can write

$$(sE-A)^{-1}=G(s)+H\tag{11}$$

where $G(s)$ is a strictly proper rational matrix which is analytic in right-half s-plane and H is a constant matrix.

Lemma 6 [6] *If the pair (E,A) is regular, impulse-free and stable, then*

$$\left|(sE-A)^{-1}\right|_m\leq L+|H|_m\tag{12}$$

where

$$L=\int_0^\infty |G(t)|_m\,dt.\tag{13}$$

and $G(t)$ is the impulse response of $G(s)$ which is given in (11).

Now we are in a position to present the robust stability result for uncertain discrete descriptor delay systems.

Theorem 1 *Suppose the pair (E,A) is regular, impulse-free and stable, then the uncertain descriptor delay system (Σ) is still regular, impulse-free and stable for all admissible uncertainties ΔA and ΔA_d if*

$$\rho\left[(L+|H|_m)M_A\right]+\rho\left[(L+|H|_m)(|A_d|_m+M_d)\right]<1\tag{14}$$

where H and L are given in (11) and (13), respectively.

Proof. From (14), it is easy to show that

$$\rho\left[(L+|H|_m)M_A\right]<1.\tag{15}$$

Then, by Lemma 2 and (11) we have

$$\begin{aligned}\rho\left[(sE-A)^{-1}\Delta A\right] &\leq \rho\left[\left|(sE-A)^{-1}\Delta A\right|_m\right]\\ &\leq \rho\left[\left|(sE-A)^{-1}\right|_m|\Delta A|_m\right]\\ &\leq \rho\left[(L+|H|_m)M_A\right]<1\end{aligned}\tag{16}$$

for all $s\in\mathbb{C}^+$. Therefore, it follows from Lemma 3 that

$$\det\left[I-(sE-A)^{-1}\Delta A\right]\neq 0,\quad \forall\ s\in\mathbb{C}^+.$$

Thus, $\forall\ s\in\mathbb{C}^+$,

$$\begin{aligned}&\det(sE-A-\Delta A)\\ =\ &\det(sE-A)\det\left[I-(sE-A)^{-1}\Delta A\right]\neq 0.\end{aligned}$$

This implies that the pair $(E,A+\Delta A)$ is regular for all admissible uncertainties. Next, we shall show that, for all admissible uncertainties, the pair $(E,A+\Delta A)$ is impulse-free. Applying Lemma 2 and noting (15), it can be seen that

$$\begin{aligned}\rho(H\Delta A) &\leq \rho(|H\Delta A|_m)\leq\rho(|H|_m M_A)\\ &\leq \rho\left[(L+|H|_m)M_A\right]<1.\end{aligned}$$

By Lemma 3, we have that $I-H\Delta A$ is invertible. Now, considering (11) we can write

$$\begin{aligned}&[sE-(A+\Delta A)]^{-1}\\ =\ &\left[I-(sE-A)^{-1}\Delta A\right]^{-1}(sE-A)^{-1}\\ =\ &\left[(I-H\Delta A)-G(s)\Delta A\right]^{-1}(sE-A)^{-1}.\end{aligned}\tag{17}$$

Taking into account $G(s)\Delta A$ is strictly proper and $I-H\Delta A$ is invertible, it then follows from Lemma 5 that $[(I-H\Delta A)-G(s)\Delta A]^{-1}$ is proper. Noting this and recalling that $(sE-A)^{-1}$ is proper, we have that

$$[sE-(A+\Delta A)]^{-1}$$

is proper too. Therefore, it follows from Lemma 4 that the pair $(E,A+\Delta A)$ is impulse-free. This together with the regularity of the pair $(E,A+\Delta A)$ implies that the uncertain descriptor delay system (Σ) is regular and impulse-free for all admissible uncertainties..

On the other hand, by Theorem 9.8.3 in [12] , it follows from (16) that for all $s \in \mathbb{C}^+$ we can write

$$\begin{aligned}\left[I-(sE-A)^{-1}\Delta A\right]^{-1} &= I+(sE-A)^{-1}\Delta A \\ &\quad +\left[(sE-A)^{-1}\Delta A\right]^2+\cdots.\end{aligned}$$

Using this and (15), we have

$$\begin{aligned}&\rho\left[\left|\left(I-(sE-A)^{-1}\Delta A\right)^{-1}\right|_m\right] \\ \le\ &\rho\Big[I+\left|(sE-A)^{-1}\Delta A\right|_m \\ &+\left|\left[(sE-A)^{-1}\Delta A\right]^2\right|_m+\cdots\Big] \\ \le\ &\rho\Big[I+\left|(sE-A)^{-1}\right|_m|\Delta A|_m \\ &+\left[\left|(sE-A)^{-1}\right|_m|\Delta A|_m\right]^2+\cdots\Big] \\ \le\ &1+\rho\left[\left(L+|H|_m\right)M_A\right] \\ &+\rho\left(\left[\left(L+|H|_m\right)M_A\right]^2\right)+\cdots \\ =\ &1/\left(1-\rho\left[\left(L+|H|_m\right)M_A\right]\right).\end{aligned}$$

Hence,

$$\begin{aligned}&\rho\left[(sE-(A+\Delta A))^{-1}(A_d+\Delta A_d)\right] \\ =\ &\rho\left[\left(I-(sE-A)^{-1}\Delta A\right)^{-1}(sE-A)^{-1}(A_d+\Delta A_d)\right] \\ \le\ &\rho\Big[\left|\left(I-(sE-A)^{-1}\Delta A\right)^{-1}\right|_m\left|(sE-A)^{-1}\right|_m \\ &\times|(A_d+\Delta A_d)|_m\Big] \\ \le\ &\rho\left[\left|\left(I-(sE-A)^{-1}\Delta A\right)^{-1}\right|_m\right] \\ &\times\rho\left[\left|(sE-A)^{-1}\right|_m|(A_d+\Delta A_d)|_m\right] \\ \le\ &\frac{\rho\left[\left(L+|H|_m\right)\left(|A_d|_m+M_d\right)\right]}{1-\rho\left[\left(L+|H|_m\right)M_A\right]}. \qquad (18)\end{aligned}$$

From (14), it can be easily shown that

$$\frac{\rho\left[\left(L+|H|_m\right)\left(|A_d|_m+M_d\right)\right]}{1-\rho\left[\left(L+|H|_m\right)M_A\right]}<1.$$

This together with (18) gives

$$\rho\left[(sE-(A+\Delta A))^{-1}(A_d+\Delta A_d)\right]<1. \qquad (19)$$

By recalling the pair $(E, A+\Delta A)$ is regular and impulse-free, noting (19) and using Lemma 1, we have the uncertain descriptor delay system (Σ) regular, impulse-free and stable for all admissible uncertainties. □

Remark 1 *Theorem 1 provides a simple method to test whether the uncertain descriptor delay system (Σ) is regular, impulse-free and stable for all admissible uncertainties under the assumption that the pair (E, A) is regular, impulse-free and stable. Note that in order to use Theorem 1, the computation of the matrices L and H is necessary. A simple method proposed in* [6] *can be resorted to and the matrices L and H can thus be easily computed.*

Remark 2 *In the case when $A_d = 0$ and $M_d = 0$, that is, the time-delay system (Σ) reduces to a descriptor system without delay, it is easy to verify that Theorem 1 coincides with Theorem 2.7 in* [6] *, therefore, Theorem 1 can be viewed as an extension of existing results on robust stability for descriptor systems with delay-free to descriptor delay systems.*

4. Example

Consider the uncertain continuous descriptor delay system (Σ) with parameters as follows:

$$E = \begin{bmatrix} 0 & -1 & 0 & 0 \\ 1 & -1 & 0 & 1 \\ 0 & 0 & 0 & 0 \\ 0.5 & -0.5 & 0 & 0.5 \end{bmatrix},$$

$$A = \begin{bmatrix} 0 & 6 & 0 & 0 \\ -5 & 5.5 & 0 & -5 \\ 0 & 1 & 0 & -2 \\ -2.5 & 2.75 & 1 & -2.5 \end{bmatrix},$$

$$A_d = \begin{bmatrix} 0 & -0.6 & 0.1 & 0 \\ -0.4 & -0.1 & 0.2 & 0 \\ 0 & 0.1 & -0.1 & 0.2 \\ 0.1 & -0.1 & 0 & -0.5 \end{bmatrix}$$

$$M_A = \begin{bmatrix} 0.1 & 0.1 & 0.1 & 0 \\ 0.1 & 0.1 & 0 & 0.2 \\ 0 & 0.1 & 0.1 & 0.1 \\ 0.1 & 0 & 0.2 & 0.1 \end{bmatrix},$$

$$M_d = \begin{bmatrix} 0.1 & 0.2 & 0.1 & 0.1 \\ 0.1 & 0 & 0.1 & 0.1 \\ 0.1 & 0.3 & 0 & 0.1 \\ 0.2 & 0 & 0.1 & 0 \end{bmatrix}.$$

The time delay is $\tau = 2$. It can be verified that there exist two invertible matrices

$$U = \left[\begin{array}{c} U_a \\ \hline U_b \end{array}\right] = \left[\begin{array}{cccc} -1 & 0 & 0 & 0 \\ 0.5 & -1 & 0 & 0 \\ \hline 0 & 0.5 & 0 & -1 \\ 0 & 0 & -1 & 0 \end{array}\right]$$

$$V = \left[\begin{array}{c|c} V_a & V_b \end{array}\right] = \left[\begin{array}{cc|cc} 0 & -1 & 0 & -0.5 \\ 1 & 0 & 0 & 0 \\ 0 & 0 & -1 & 0 \\ 0.5 & 0 & 0 & 0.5 \end{array}\right]$$

such that

$$UEV = \left[\begin{array}{c|c} I & 0 \\ \hline 0 & 0 \end{array}\right] = \left[\begin{array}{cc|cc} 1 & 0 & 0 & 0 \\ 0 & 1 & 0 & 0 \\ \hline 0 & 0 & 0 & 0 \\ 0 & 0 & 0 & 0 \end{array}\right],$$

$$UAV = \left[\begin{array}{c|c} A_1 & 0 \\ \hline 0 & I \end{array}\right] = \left[\begin{array}{cc|cc} -6 & 0 & 0 & 0 \\ 0 & -5 & 0 & 0 \\ \hline 0 & 0 & 1 & 0 \\ 0 & 0 & 0 & 1 \end{array}\right].$$

Therefore, the pair (E, A) is regular, impulse-free. Now using the method in [7] , we obtain

$$\begin{aligned} L &= \int_0^\infty |G(t)|_m \, dt = \int_0^\infty \left|V_a e^{A_1 t} U_a\right|_m dt \\ &= \begin{bmatrix} 0.1 & 0.2 & 0 & 0 \\ 0.1667 & 0 & 0 & 0 \\ 0 & 0 & 0 & 0 \\ 0.0833 & 0 & 0 & 0 \end{bmatrix} \end{aligned}$$

$$|H|_m = |V_b U_b|_m = \begin{bmatrix} 0 & 0 & 0.5 & 0 \\ 0 & 0 & 0 & 0 \\ 0 & 0.5 & 0 & 1 \\ 0 & 0 & 0.5 & 0 \end{bmatrix}.$$

Then, we can calculate

$$\begin{aligned} \rho\left[\left(L + |H|_m\right) M_A\right] &= 0.3043 \\ \rho\left[\left(L + |H|_m\right) \left(|A_d|_m + M_d\right)\right] &= 0.6315 \end{aligned}$$

and

$$\begin{aligned} &\rho\left[\left(L + |H|_m\right) M_A\right] + \rho\left[\left(L + |H|_m\right) \left(|A_d|_m + M_d\right)\right] \\ = \; & 0.9358 < 1. \end{aligned}$$

Hence, from Theorem 1 it is seen that the uncertain descriptor delay system under consideration is regular, impulse-free and stable for all admissible uncertainties.

5. Conclusions

In this paper, the problem of robust stability analysis for continuous descriptor systems with state delay and structured uncertainties has been studied. A sufficient condition ensuring regularity, impulse immunity and stability for the perturbed descriptor delay system has been presented. The proposed approach is computationally simple to use. An example has been provided to demonstrate the effectiveness of the proposed approach.

References

[1] D. J. Bender and A. J. Laub. The linear-quadratic optimal regulator for descriptor systems. *IEEE Trans. Automat. Control*, 32:672–687, 1987.

[2] G. D. Byrne and P. R. Ponzi. Differential-algebraic systems, their applications and solutions. *Comput. Chem. Engng.*, 12:377–382, 1988.

[3] C.-T. Chen. *Linear System Theory and Design*. New York: Holt Rinehart and Winston, 1984.

[4] L. Dai. *Singular Control Systems*. Berlin: Springer-Verlag, 1989.

[5] S. H. Esfahani, S. O. R. Moheimani, and I. R. Petersen. LMI approach suboptimal quadratic guaranteed cost control for uncertain time-delay systems. *IEE Proc. Control Theory Appl.*, 145:491–498, 1998.

[6] C.-H. Fang and F.-R. Chang. Analysis of stability robustness for generalized state-space systems with structured perturbations. *Systems Control Lett.*, 21:109–114, 1993.

[7] C.-H. Fang, L. Lee, and F.-R. Chang. Robust control analysis and design for discrete-time singular systems. *Automatica*, 30:1741–1750, 1994.

[8] J. K. Hale. *Theory of Functional Differential Equations*. New York: Springer-Verlag, 1977.

[9] H. Hemami and B. F. Wyman. Modeling and control of constrained dynamic systems with application to biped locomotion in the frontal plane. *IEEE Trans. Automat. Control*, 38:355–360, 1979.

[10] P. Janssens, J. Mawhin, and N. Rouche. *Équations Différentielles et Fonctionnelles Non Linéaires*. Paris: Hermann, 1973.

[11] A. Kumar. *Control of Nonlinear Differential Algebraic Equation Systems: with Application to Chemical Processes*. Boca Raton: Chapman and Hall/CRC, 1999.

[12] P. Lancaster and M. Tismenetsky. *The Theory of Matrices*. 2nd edition. New York: Academic Press, 1985.

[13] C. H. Lee, T. H. S. Li, and F. C. Kung. D-stability analysis for discrete systems with a time delay. *Systems Control Lett.*, 19:213–219, 1992.

[14] F. L. Lewis. A survey of linear singular systems. *Circuits, Syst. Signal Processing*, 5:3–36, 1986.

[15] C. Lin, J. L. Wang, G.-H. Yang, and J. Lam. Robust stabilization via state feedback for descriptor systems with uncertainties in the derivative matrix. *Int. J. Control*, 73:407–415, 2000.

[16] M. S. Mahmoud and N. F. Al-Muthairi. Quadratic stabilization of continuous time systems with state-delay and norm-bounded time-varying uncertainties. *IEEE Trans. Automat. Control*, 39:2135–2139, 1994.

[17] J. M. Ortega and W. C. Rheinboldt. *Iterative Solution of Non-Linear Equation in Several Variables*. New York: Academic, 1970.

[18] S. Xu, J. Lam, and L. Zhang. Robust D-stability analysis for uncertain discrete singular systems with state delay. *IEEE Trans. Circuits Syst. I*, 49:551–555, 2002.

[19] S. Xu, P. Van Dooren, R. Stefan, and J. Lam. Robust stability and stabilization for singular systems with state delay and parameter uncertainty. *IEEE Trans. Automat. Control*, 47:1122–1128, 2002.

[20] S. Xu and C. Yang. An algebraic approach to the robust stability analysis and robust stabilization of uncertain singular systems. *Int. J. Systems Sci.*, 31:55–61, 2000.

[21] S. Xu, C. Yang, Y. Niu, and J. Lam. Robust stabilization for uncertain discrete singular systems. *Automatica*, 37:769–774, 2001.

[22] K. Yasuda and F. Noso. Decentralized quadratic stabilization of interconnected descriptor systems. In *Proc. 35th IEEE Conf. Decision and Control*, pages 4264–4269, Kobe, Japan, 1996.

Zone Model Predictive Control Algorithm Using Soft Constraint Method

Xu Zuhua Zhao Jun Qian JiXin*

Institute of Systems Engineering, Zhejiang University, Hangzhou,310027,China

Abstract: A zone model predictive control algorithm is proposed and developed through the soft constraint method. The estimation of zone violation is avoided; as a consequence the selection of the approximate setpoint when the control variable violates its zone constraint is skipped. To further improve control performance, zone trajectory method is proposed and a parameter is provided to trade off the response performance and model accuracy. The effective performance is proved by the simulation results. The stability of the algorithm is also analyzed.

Keywords: Model Predictive Control; Zone Control; Soft Constraint; Stability Analysis

1. INTRODUCTION

Although in industrial control applications, the controlled variable usually has a specific set point. It is common that many of the controlled variables have range limits rather than set point. This kind of process variable is treated as zone variable in most industrial MPC controller such as RMPCT, DMCPlus and HIECON, which all provide zone and setpoint options for CVs to meet industrial need (Richalet, *et al*., 1978; Qin and Badgwell, 1997; Morari and Lee, 1999).

Zone control is also necessary for over-specified processes, whose process model can be cast at steady state by the following form (Muske and Rawlings, 1993)

$$\begin{bmatrix} y_1 \\ \vdots \\ y_s \end{bmatrix} = \begin{bmatrix} a_{11} & \cdots & a_{1r} \\ \vdots & & \vdots \\ a_{s1} & \cdots & a_{sr} \end{bmatrix} \begin{bmatrix} u_1 \\ \vdots \\ u_r \end{bmatrix} + \begin{bmatrix} d_1 \\ \vdots \\ d_s \end{bmatrix} \qquad (1)$$

where a_{ij} is steady gain ， d_i is disturbance. When the number of outputs exceeds the number of inputs, all the set points cannot be met at the same time. If one of the set points is changed into a zone specification, the outputs specifications are relaxed slightly. The probability that the process will meet all of its specifications increases. Moreover, because the output's change within zone is ignored, the need to coordinate the movement of inputs is largely eliminated, which decreases its sensitivity to model mismatch and improves its robust performance, especially for the process whose outputs and inputs variables are interacted with each other strongly.

*Address correspondence to this author
E-mail: xuzh@iipc.zju.edu.cn.

In conventional dynamic model control, zone control cannot be solved directly. But the receding optimization formulation of model predictive control provides the possibility to realize zone control. Zhou (2001) used setpoint approximation method to implement zone control, but the limit was that it still needed estimation of zone violation concomitant with the selection of the approximate setpoint value.

In this paper, a zone model predictive control algorithm using the soft constraint method is proposed to achieve better control performance and to avoid the mentioned problem. To further improve control performance, zone trajectory method is proposed which provides a tuning parameter to trade off the response performance and model accuracy. The stability of the algorithm is analyzed finally.

2. ZONE CONTROL ALGORITHM

Consider a stable multi-input multi-output system represented by the following model (Garcia, *et al*., 1989)

$$y(k+j|k) = \sum_{i=1}^{N-1} H_i \Delta u(k+j-i) + H_N u(k+j-N) + d(k+j|k)$$

$$d(k+j|k) = d(k|k) = y(k) - \sum_{i=1}^{N-1} H_i \Delta u(k-i) - H_N u(k-N) \qquad (2)$$

$$H_i = \begin{bmatrix} a_{11}(i) & \cdots & a_{1r}(i) \\ \vdots & & \vdots \\ a_{s1}(i) & \cdots & a_{sr}(i) \end{bmatrix}$$

where

$y(k+j|k)$=Predicted output vector at time $k+j$

$y(k)$=Actual output vector at time k

$u(k)$=Actual input vector at time k

$d(k+j|k)$=Predicted disturbance vector at time $k+j$

N = model horizon length
r = number of inputs
s = number of outputs

For setpoint control, the optimization problem at every sampling time is solved (Cutler and Ramaker, 1979; Garcia and Prett, 1986; Garcia, *et al*., 1989): Find the a optimal sequence of M future manipulated variable moves $\Delta u(k),\cdots,\Delta u(k+M-1)$ so that the prediction of the manipulated variables and controlled outputs satisfy the criteria which minimizes the sum of squared deviations of the predicted CV values from a time varying reference trajectory over P future time steps. The formulation of optimization problem is:

$$\min_{\Delta u(k),\cdots\Delta u(k+M-1)} J_k = \sum_{j=1}^{P} \left\| y(k+j|k) - w(k+j|k) \right\|_Q^2 + \sum_{j=0}^{M-1} \left\| \Delta u(k+j) \right\|_S^2 \quad (3)$$

$$s.t. \quad u^- \le u(k+j) \le u^+$$
$$\Delta u^- \le \Delta u(k+j) \le \Delta u^+, \ \forall j = 1, M$$

where
$w(k+j|k)$=reference trajectory value at time $k+j$

A zone region is defined by the minimum and maximum values of a controlled variable's desired range of values. One way to simply implement zone control is to use setpoint approximation method: when the CV is predicted to lie within its zone, its weight coefficient of matrix Q is set to zero so the controller will ignore it; when the CV is predicted to violate its zone limits, its weight is non-zero and a point within zone is defined as the approximate setpoint and is chose to drive the output back into the zone. The simple way to estimation the zone violation of output is by examining the initial predictive value of outputs.

Even though the initial predictive value of outputs meets its zone limits, some of output predictive value still may violate its limits when correcting other outputs error during calculating the optimal inputs moves sequences. The controller will transiently move the output farther outside its zone limit, because the controller ignores the output's error when the predictive initial value of outputs lie within its zone. The solution of set point approximation method is generally sub-optimal. Moreover, the selection of the approximate setpoint when the control variable violates its zone constraint lacks rigorous analysis rules, because distinct response performance can be achieved by selecting different approximate setpoint values.

For zone control, the deviation between the output predictive value and zone limits $[\ y_c^-\ \ y_c^+\ ]$ is defined as

$$e(k+j|k) = \begin{cases} y(k+j|k) - y_c^+, \text{if } y(k+j|k) \ge y_c^+ \\ y_c^- - y(k+j|k), \text{ if } y(k+j|k) \le y^- \\ 0, \text{ if } y(k+j|k) \le y_c^+ \text{ and } y(k+j|k) \ge y_c^- \end{cases} \quad (4)$$

The optimization problem of zone control can be formulated as

$$\min_{\Delta u(k),\cdots\Delta u(k+M-1)} J_k = \sum_{j=1}^{P} \left\| e(k+j|k) \right\|_Q^2 + \sum_{j=0}^{M-1} \left\| \Delta u(k+j) \right\|_S^2$$
$$s.t \quad u^- \le u(k+j) \le u^+$$
$$\Delta u^- \le \Delta u(k+j) \le \Delta u^+, \ \forall j = 1, M \quad (5)$$

Apparently, $e(k+j|k)$ is the optimal value $\varepsilon^*(k+j|k)$ of following optimization problem

$$\min_{\varepsilon(k+j|k)} \varepsilon(k+j|k)$$
$$s.t \quad y_c^- - \varepsilon(k+j|k) \le y(k+j|k) \le y_c^+ + \varepsilon(k+j|k)$$
$$\varepsilon(k+j|k) \ge 0$$

Therefore, optimization problem (5) can be further transformed as

$$\min_{\substack{\Delta u(k),\cdots,\Delta u(k+M-1) \\ \varepsilon(k+1|k),\cdots,\varepsilon(k+P|k)}} J_k = \sum_{j=1}^{P} \left\| \varepsilon(k+j|k) \right\|_Q^2 + \sum_{j=0}^{M-1} \left\| \Delta u(k+j) \right\|_S^2$$
$$s.t \quad u^- \le u(k+j) \le u^+ \quad (6)$$
$$\Delta u^- \le \Delta u(k+j) \le \Delta u^+, \ \forall j = 1, M$$
$$y_c^- - \varepsilon(k+j|k) \le y(k+j|k) \le y_c^+ + \varepsilon(k+j|k)$$
$$\varepsilon(k+j|k) \ge 0, \ \forall j = 1, P$$

In the above problem formulation, the zone limits is treated as soft constraints by adding a slack variable. At the same time the slack variables are also included in the objective function to be minimized.

Soft Constraints are used to prevent the controller from introducing transient errors by defining soft constraints on the controlled outputs at intervals from the current interval to predictive horizon. When the controlled variable has a set point instead of a zone region, both the upper and lower limits of the zone are set equal to the set point.Through soft constraint method, the estimation on the zone violation is avoided; as a consequence the selection of the approximate setpoint when the control variable violates its zone constraint is skipped.

In order to drive the outputs back into its zone region more slowly to avoid overshoot consequently, zone trajectory is introduced for each controlled output as follows

$$\min_{\substack{\Delta u(k),\cdots,\Delta u(k+M-1) \\ \varepsilon(k+1|k),\cdots,\varepsilon(k+P|k)}} J_k = \sum_{j=1}^{P} \left\| \varepsilon(k+j|k) \right\|_Q^2 + \sum_{j=0}^{M-1} \left\| \Delta u(k+j) \right\|_S^2$$
$$s.t \quad u^- \le u(k+j) \le u^+$$
$$\Delta u^- \le \Delta u(k+j) \le \Delta u^+ \quad (7)$$
$$y_r^-(k+j) - \varepsilon(k+j|k) \le y(k+j|k) \le y_r^+(k+j) + \varepsilon(k+j|k)$$

where $y_r^-(k+j)$ $y_r^+(k+j)$ is determined as follows:

If $y(k)$ within $[\ y_c^-\ \ y_c^+\ ]$, then

$$y_r^-(k+j) = y_c^- \text{ and } y_r^+(k+j) = y_c^+$$

If $y(k) \ge y_c^+$, then

$$y_r^-(k+j) = y_c^- \text{ and}$$
$$y_r^+(k+j) = \alpha^j y(k) + (1-\alpha^j) y_c^+$$

If $y(k) \le y_c^-$, then

$$y_r^+(k+j) = y_c^+ \text{ and}$$
$$y_r^-(k+j) = \alpha^j y(k) + (1-\alpha^j) y_c^-$$

where α is the time constant, which is determined

by the trade-offs that inherently exist between speed of response and model accuracy or inputs movement. A smaller value gives faster response and consequently large MV movement, which requires a more accurate model for stable control. A larger value, on the contrary gives slower response with smaller MV movement and works well with a less accurate model.

The controller is obliged to keep the CV within the constraints defined by the zone trajectory, but it is allowed to follow any figure within these constraints. The sensitivity to model error is decreased and the robustness is improved

3. STABILITY ANALYSIS

Alex Zheng and Manfred Morari(1995) analyzed the closed-loop stability for constrained MPC with setpoint control. Zone Control also has the similar property when using soft constraint method.

Assume:

a) There is no model mismatch
b) Predictive horizon is infinite
c) Steady-state gain matrix of the model has full row rank.

then the closed-loop system is asymptotically stable if and only if the optimization problem (7) is feasible at the first sampling time.

Proof:

If the optimization problem is not feasible, then the controller is not defined.

At sampling time k, the optimal solution is

$$\Delta u^*(k+i|k), i=0,\cdots,m-1$$
$$\varepsilon^*(k+i|k), i=1,\cdots,\infty$$

At sampling time k+1,the solution (18) is a feasible solution but may not be the optimal solution.

$$\Delta u(k+i|k+1)=\Delta u^*(k+i|k), i=1,\cdots,m-1$$
$$\Delta u(k+m|k+1)=0$$
$$\varepsilon(k+i|k+1)=\varepsilon^*(k+i|k), i=2,\cdots,\infty$$

Define $\Delta u_k=\Delta u^*(k|k)$ $\varepsilon_k=\varepsilon^*(k+1|k)$

The above feasible control input yields:

$$J^*_{k+1}\le J_{k+1}=J^*_k-\varepsilon_k{}^T Q\varepsilon_k-\Delta u_k{}^T S\Delta u_k$$
$$J^*_{k+1}\le J^*_k-\varepsilon_k{}^T Q\varepsilon_k-\Delta u_k{}^T S\Delta u_k$$

Therefore, the sequence $\{J^*_k\}$ is non-increasing, its low boundary is zero. Consequently, the sequence $\{J^*_k\}$ converges. So

$$\lim_{k\to\infty}\left(\varepsilon_k{}^T Q\varepsilon_k+\Delta u_k{}^T S\Delta u_k\right)$$
$$\le\lim_{k\to\infty}\left(J^*_k\right)-\lim_{k\to\infty}\left(J^*_{k+1}\right)=0$$

This together with Q、$S>0$ implies that $\varepsilon_k\to 0$ and $\Delta u_k\to 0$ as $k\to\infty$. Since the steady-state gain matrix of the model is bounded, $y(k)$ approaches the steady-state value asymptotically.

4. SIMULATION

(1) Consider the two-input three-output system:

$$G(s)=\begin{bmatrix}\frac{1.77e^{-28s}}{60s+1} & \frac{5.88e^{-27s}}{50s+1}\\ \frac{5.72e^{-14s}}{60s+1} & \frac{6.9e^{-15s}}{40s+1}\\ \frac{4.42}{44s+1} & \frac{7.2}{19s+1}\end{bmatrix}$$

with the following input constraints

$$-0.5\le u_1,u_2\le 0.5 \qquad |\Delta u_1|,|\Delta u_2|\le 0.03$$

and the following initial conditions

$$y_1=y_2=y_3=0 \qquad u_1=u_2=0$$

Choose T=5s,N=100,M=4,P=30,Q=I,S=I,α= 0.95

If all of the controlled outputs have set points

$$y_1=0.59 \quad y_2=0.64 \quad y_3=0.67$$

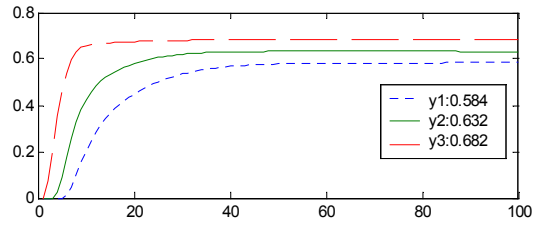

Fig. 1. Responses of setpoint control

Because the degree of freedom is insufficient, it is physically impossible to keep all output at setpoint or within range. When the set point for y_3 is replaced by zone limit$[0.65 \quad 0.7]$, all output specification would be met.

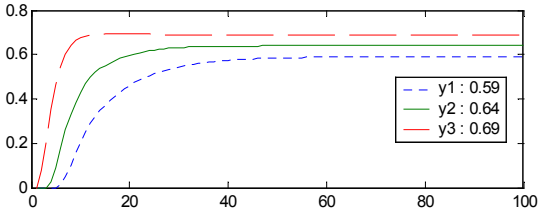

Fig.2. Responses of zone Control

(2) Consider the system:

$$G(s)=\begin{bmatrix}\frac{1.77e^{-28s}}{60s+1} & \frac{5.88e^{-27s}}{50s+1} & \frac{4.05e^{-27s}}{50s+1}\\ \frac{5.72e^{-14s}}{60s+1} & \frac{6.9e^{-15s}}{40s+1} & \frac{5.39e^{-18s}}{50s+1}\\ \frac{4.42e^{-22s}}{44s+1} & \frac{7.2}{19s+1} & \frac{4.38e^{-20s}}{33s+1}\end{bmatrix}$$

with the following input constraints

$$-1\le u_1,u_2,u_3\le 1 \qquad |\Delta u_1|,|\Delta u_2|,|\Delta u_3|\le 0.03$$

and the following output regulatory objective

$$y_1=0.2 \qquad -0.5\le y_2,y_3\le 0.5$$

and the following initial conditions

$$y_1=y_2=y_3=0 \qquad u_1=u_2=u_3=0$$

Choose T=5,N=100,M=4,P=30,Q=I,S=I,α= 0.95

When using set point approximation, the result is shown as follows:

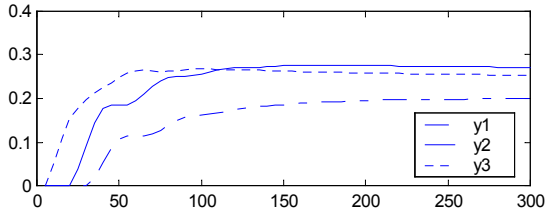

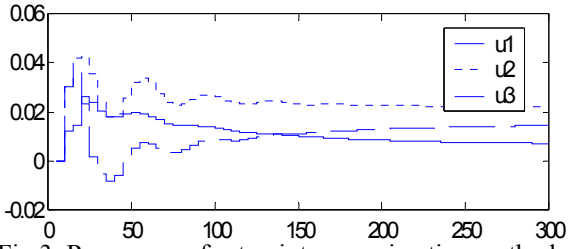

Fig.3. Responses of set point approximation method

When using soft constraint method, the result is shown as follows:

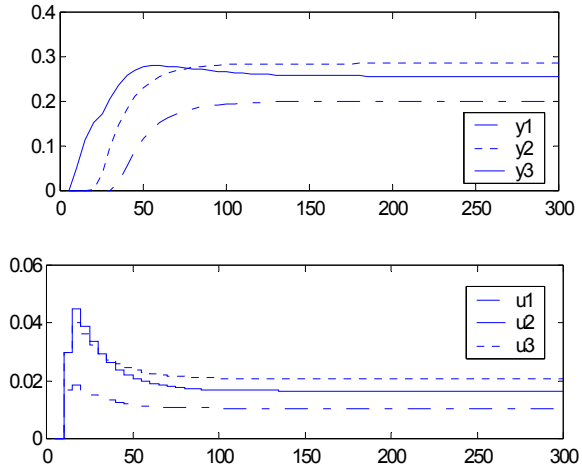

Fig. 4. Responses of soft constraint method

From the simulation result, the soft constraint method prevent the controller from moving a CV farther outside zone while correcting other CV errors by defining constraints on the CVs that are imposed at intervals from the current interval out to the predictive horizon. In setpoint approximation method, the controller will ignore the CV when the CV is predicted to be within its zone, so its performance is worse than that with soft constraint method.

5. CONCLUSION

Estimating the violation of zone output limits in the setpoint approximation method is simply through examining its output predictive initial value, but it can not always keep zone output in its zone limit while correcting other outputs errors. Using the soft constraint method, zone specification is directly imposed as constraints in optimization formulation, while correcting other CV errors, it will not violate zone output limits, but its computing burden is larger than the setpoint approximation method. The tuning parameter provided by zone trajectory method enables a flexible way to achieve better performance and reach a tradeoff between performance and model accuracy.

REFERENCES

Zheng, A. and Morari, M. (1995). Stability of model predictive control with mixed constraints. *IEEE Trans. Aut Control*, 40(10),pp.1818-1823.

Cutler, C.R. and B.L.Ramaker (1979). Dynamic matrix control – a computer algorithm .*In AIChE 86th National Meeting*,Houston,TX,

Gracia, C.E.,and A.M.Morshedi(1986).Quadratic programming solution of dynamic matrix control (QDMC). *Chem.Eng.Commun*.,46,pp.73-87

Gracia, C.E.,D.M.Prett, M.Morari(1989). Model predictive control: theory and practice-a survey. *Automatica*,25(3),pp.335-348

Gracia, C.E.and D.M.Prett (1986). Advances in industrial model predictive control. *CPCIII*, pp.249-294, Cache and Elsevier, Amsterdam.

Richalet,J., J.Rault, J.L.Testutud, J.Papon(1978). Model predictive heuristic control: applications to industrial processes. *Automatica*, 14(5), pp. 413-428

Muske, K R. and J. B. Rawlings (1993). Model predictive control with linear models. *AIChE* J., 39(2), pp.262-287

Morari, M. and J.H. Lee (1999). Model predictive control: past, present and future. *Comp. Chem. Eng.*, 23,pp.667-682

Qin, S.J.and T. A.Badgwell(1997). An overview of industrial predictive control technology. In (J.C.Kantor, C.E.Garcia, B.Carnahan, editors), *Chemical Process Control-V,* 232-256, AICHE.

Zhou, Lifang, and JiXin, Qian, (2002). Study on predictive control algorithm for horizon control. In *Proceedings of the 4th World Congress on Intelligent Control and Automation*, pp. 717-721

EVALUATION METHOD AND WORKBENCH FOR APC STRATEGIES

G. Reinig, B. Mahn, M. Boll

Ruhr University of Bochum, Faculty of Mechanical Engineering,
Chair of Control Engineering
BASF AG, Ludwigshafen Dept. WLF/AM

Abstract: The large number of various advanced control strategies (e.g. Model Predictive Control, Neural Networks or Fuzzy Control) and the lack of a practically usable selection methodology make it very difficult to choose an appropriate strategy for a given plant. In order to support the selection of proper control strategies and products a set of relevant evaluation criteria is developed. A flexible and expandable test environment (workbench) is created aiming at a controller evaluation considering these criteria. The evaluation approach and workbench are demonstrated for PID based and commercial Model Predictive Controllers at some typical process units and plants.

Keywords: Advanced Process Control, Model Predictive Control, Evaluation, Simulation

1. INTRODUCTION

In the last decade, in the area of process control more sophisticated control strategies have been developed (e.g. Model Predictive Control, Neural Networks or Fuzzy Control). With the number of advanced control algorithms increasing a sound selection of the control strategy and product became a challenging task.

The main objective of this project was to develop a methodology and tools to evaluate / compare different control approaches from the viewpoint of industrial application.

To obtain practical relevance all important aspects of the controller application should be considered. Therefore the standard criteria describing the controlled variable performance (i.e. set point and disturbance responses, IAE, ISE) are extended by such practical issues as:

- Engineering and operational aspects
- Robustness and integrity
- Ability to explicitly consider constraints.

Based on literature (Harris, 1996; Joshi, 1997; Le Page, 1998; Schuler, 1998; Seborg, 1999), interviews of control engineers and personal experience a criteria catalogue was accomplished (details in section 4.).

A set of answers to all the criteria is thought as valued guideline for the selection of most appropriate control strategies or products. Considering the diversity of all the criteria, the processes, the enterprises and the control tasks no attempt is undertaken to provide a single selection, instead the user is supported in his multiobjective decision.

The initial idea of the project was to create only exemplary evaluations of important control strategies for typical process units which should represent entire classes of equipment and to obtain generic evaluations. However, a retrospective result is the usefulness of the proposed approach for any specific process assumed its detailed dynamic model is available.

While some of the criteria can be evaluated using documentation / literature others need

measurements in a real plant or - as chosen in this project - in a suitable simulation environment.
This simulation environment (referred to as Workbench) is the platform for the detailed dynamic process simulation, for the basic control functions, and can be connected to commercial Advanced Control Algorithms. It is utilized to "experimentally" obtain the controller design models as well as to implement and evaluate the controllers.
To achieve an industrially relevant assessment of the above mentioned criteria a commercial distributed control system (DCS) is used and representative commercial advanced controller software packages can be included. The emulated controller of the DCS performs the basic controls of the simulated units or plants, and provides the interface between the emulated DCS controllers and the advanced controller (Figure 1). In addition it provides the function blocks for some conventional advanced control strategies (e.g. PID based, and decoupling control).

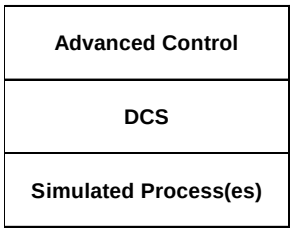

Fig. 1 Workbench Structure

2. TECHNICAL REQUIREMENTS FOR THE WORKBENCH

A complete controller evaluation is not possible in a sole offline-simulation environment such as Matlab/Simulink since the actual commercial control products are available only as self-contained applications without source code. This and the intended use of the workbench lead to the following demands:

- evaluation of strategies and products
- evaluation of commercial and user programmed controller
- fast simulation
- high reproducibility
- availability of appropriate interfaces
- implementation on heterogeneous distributed computers / DCS systems
- assessment of engineering effort
- flexible choice of controller or process models, respectively.

The selected workbench structure is depicted in figure 2 and contains the following levels:
APC-Strategies / Products: Commercial as well as user-specified APC-strategies, which are relevant for the process industry and hence will be assessed.
Distributed Control System (DCS): The DCS is utilized as Operator-Station, data transfer unit and watchdog. In addition, PID-controllers can be realized in the DCS. The control units (process connected devices) can be emulated on the PC.

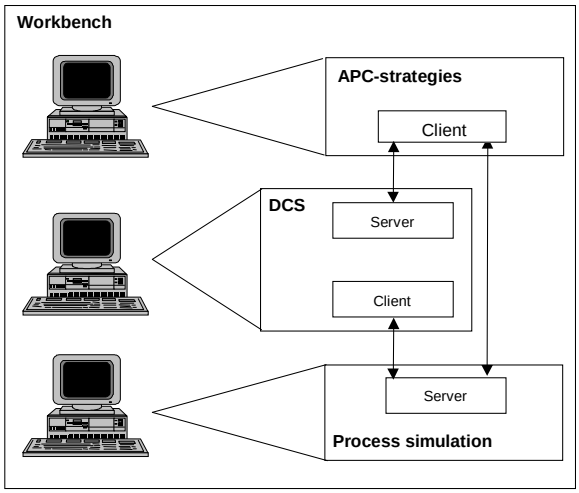

Fig.2 Client-Server-Concept of the Workbench

Process simulation: The existing plant is replaced by a dynamic typically non-linear, first principles process model. The demand of a flexible and easily usable workbench requires a well-defined connection from the APC to the simulation process via the DCS (Figure 2). The desired flexibility and short training period to get familiar with the workbench is attained by using Microsoft Windows NT operating system which provides several (industrial) standard interfaces like Dynamic Data Exchange (DDE) and OLE for process control (OPC). Because of the performance advantage of the OPC versus the DDE and its popularity in process automation the OPC-interface is selected as standard interface in the workbench.
Most of the actual APC products provide an OPC-interface, therefore they can easily be implemented in the workbench. However, the products of the simulation level (i.e. MatLab or Gproms) do not provide this interface as standard feature. Therefore several simulation products were extended with the OPC interface. OPC is based on the Client-Server-Concept, and the APC-strategies usually provide the OPC-Client functionality only. Thus the selected DCS needs to have an OPC Server and an OPC Client in order to accomplish the depicted connections. The OPC code of WinTECH Software Design was used to add these functions to Matlab/Simulink and stand-alone simulations (WinTECH, 2001). The different workbench levels can be implemented on a single PC or two / three PCs communicating via TCP/IP.
Due to the real time character of some workbench components (e.g. DCS, MPC) their calculations are normally triggered by the computer's real time clocks. The interactions of the process model and the controller must be synchronized. The achievement of a significant acceleration of the simulation time compared with real time (up to the factor of 100 on standard PC) was a challenge and at the same time a prerequisite to cope with the many simulations necessary for the evaluation. One simple option is to "shrink" the controller's time scale by the ratio "necessary computation time for

integrating the model about a given real time interval / real time interval". Another option is using the "external trigger" mode of the APC-strategies. In this mode (often hidden for end user) the controller calculations can be triggered by an external program.

3. PROCESS MODELLS AND CONTROLLERS IMPLEMENTED

The four process models used in the workbench hitherto are:

- A Binary distillation column: A simple distillation process, enabling initial experience in controller implementation and evaluation
- A Distillation Operator Training simulator: A detailed rigorous dynamic plant model which can be used not only for normal operation but also for the simulation of start-up, shut down transients and several process / equipment malfunctions.
- A Divided Wall Column (DWC): A DWC can efficiently be used for the separation of three products. Since a dynamic model was developed for a DWC pilot plant the evaluation approach could be accomplished on the model and on the pilot plant. This provided the opportunity to validate the simulation based evaluation approach by real process data.
- The Tennessee Eastman process: A complex academically well acknowledged control benchmark process

All models contain unit operations relevant and typical for process industry. With the exception of the first model they all comprise not only the main equipment components but also the auxiliary ones, e.g. separators, pumps heat exchangers.

The commercial DCS and controllers which were offered to participate at the evaluation are:

- DCS PlantScape, Honeywell
- RMPCT, Honeywell
- DMC, Aspen
- INCA, Ipcos
- 3dMPC, ABB .

4. APPLICATION OF THE EVALUATION CRITERIA

The evaluation approach is divided into five groups containing qualitative or numerical ratings. The tables 1 to 5 list the criteria concerning:

- identification and tuning
- implementation of the controller
- control performance
- control system robustness and integrity
- usability

The application of the evaluation criteria is exemplarily demonstrated here for the binary distillation column.

The binary distillation column (Figure 3) comprises 41 stages and separates a binary mixture. The model is based on the following assumptions:

- Constant relative volatility
- Constant hold-up
- Perfect level control.

The model of the distillation column considers the material balance and the phase equilibrium on each stage.

As both the bottom and the top condenser levels are assumed as perfectly controlled, the remaining manipulated variables reflux flow and heating steam flow are utilized to adjust the concentrations of the light component x_T and x_B.

The control objective is to ensure tight control of x_T and x_B during operating point transition and in the presence of disturbances (feed flow and composition changes).

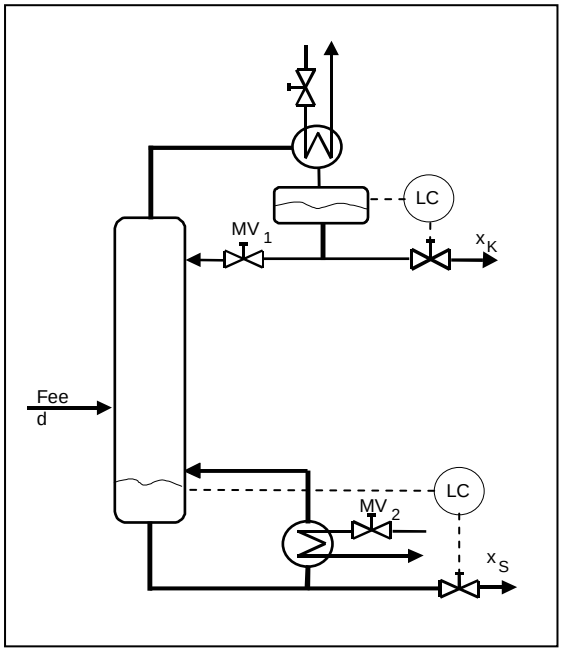

Fig.3 Distillation column

The model of the column is a non-linear Multi Input Multi Output (MIMO) system. Although the process has only two manipulated and two controlled variables, it represents some typical features of distillation units.

The comparative evaluation study includes the following controllers:

- Decentralized PID controller
- PID controller with steady state decoupling
- Commercial Linear model predictive controllers (MPC #1, MPC #2).

Both PID based control structures are implemented on the DCS, the MPCs are installed on top of the DCS.

The evaluation method comprises the assessment of the controller design steps and of the controller performance:

- Controller design:

- Identification to obtain the controller design model (e.g. step tests at the rigorous model)
- Tuning of the controller
- Offline simulation using the design model

- Implementation of the controller on the non-linear simulation model of the plant.
- Investigation of controller performance
  - Controlled variable performance
  - Stability
- Applicability

Example:
The first step of the controller design is the model identification to obtain a design model (figure 4).

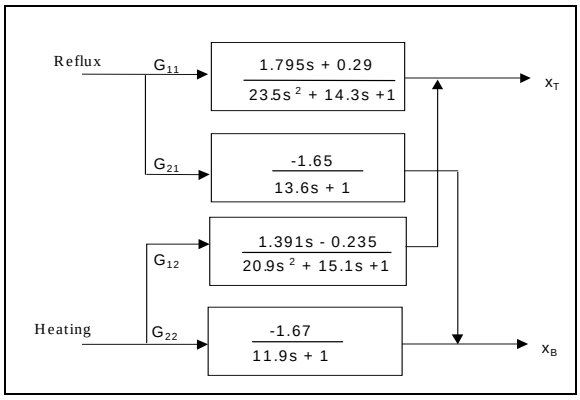

Fig.4 Linear model of the column

At the next step the controllers are to be configured and tuned. To achieve an equal performance specification for all controllers, the tuning parameters are adjusted to obtain the same closed loop settling time (figure 5) with minimum manipulated variables activity.
This indirect "unification" was necessary because the optimisation criteria of the commercial MPCs differ widely and are not documented in detail.

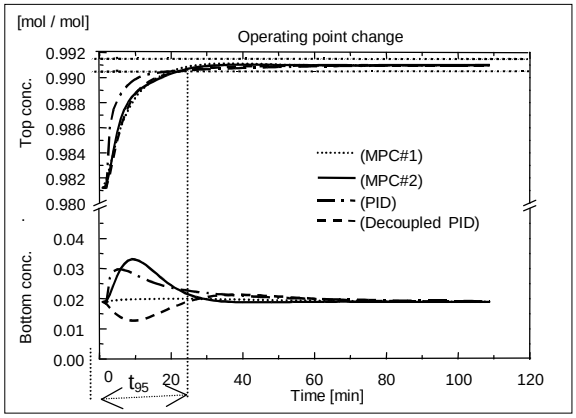

Fig. 5 Closed loop settling time t_{95} specification (linear model)

For the PID controllers the IMC tuning was applied whereby the two λ were determined by a non-linear optimisation according to the above objective.
The evaluation criteria concerning identification are shown in (table 1).

After being tuned the controllers can be implemented and used to control the non-linear simulation process. The assessment of the implementation procedure is given in table 2.
The controlled variable performance can be evaluated analysing figure 6.

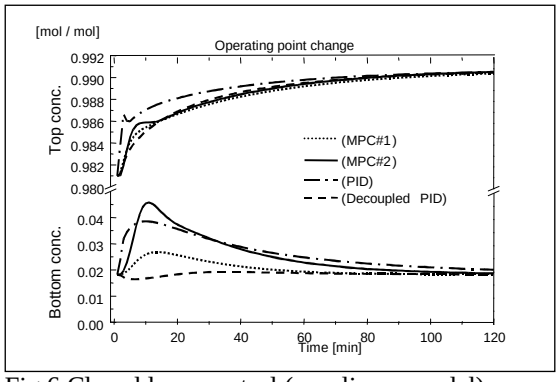

Fig.6 Closed loop control (non-linear model)

It shows the transients of the non-linear plant with the different controllers for a given change of the operating point (x_T).
Further quantitative evaluation criteria values are given in table 3 to assess the controlled variable performance.
As analytical considerations of the stability margins are hardly possible many of the considered controllers they are determined here by an empirical simulation approach. To do this gain or dead time blocks are placed between model outputs and controller inputs. Either the gain or the dead time is increased until the closed loop stability threshold is reached. The obtained gain and delay represent some kind of of the phase and gain margins. The robustness is considered as criteria in the table 4 below, see also (Subawalla, 1996; Le Page, 1998).
Last but not least some features describing the practical usability are investigated (table 5).
From these evaluation criteria it gets evident that the selection of a control strategy and product for a given plant type and control objective is a multi-objective task. However, the proposed criteria give a clear guideline, which allows to give the choice a reasonable foundation. Besides the proposed evaluation criteria, the final decision is also influenced by "external" and partially soft factors as companies policy.
For the given simple binary distillation with relatively "control-friendly" steady state and dynamic behaviour and no explicit constraints on controlled and manipulated variables the best choice is obviously a pair of PID controllers with steady state decoupling.
Similar investigations were performed also for the other processes mentioned above and for an additional commercial MPC. The evaluation results are published in (Mahn, 2003).

5. SUMMARY

The proposed approach to evaluate control strategies and products (incl. their tools) in a close-to-reality simulation environment has been tested on several processes from a relatively simple binary distillation column up to the difficult to control Tennessee Eastman Challenge benchmark process. The approach was successfully validated applying the evaluation criteria for both a real pilot plant DWC with DCS and for a simulated DWC in the workbench.

Until now PID based control structures and several linear MPC controllers were analysed.

The major findings for the time being are:

- The evaluation of advanced control strategies using a simulation environment and rigorous models of typical units is feasible (and affordable).
- While the evaluation results of the workbench regarding the controllers inspire confidence the assessment methods / tools seems to be less significant due to the variety of disturbances and operating limitations in real plant experiments.
- Practically relevant evaluations comprise more than just controlled variable performance only.
- The evaluation results can be significantly biased / influenced by the evaluator's experience. This issue is worsened due to the lack of good product manuals / documentation.
- The maturity of the evaluated APC products regarding the engineering by external users is still low.
- Besides the use as evaluation tool the developed workbench turned out to be a useful medium to acquaint oneself with the identification / design and operation of control products and to try out control system designs.

Tab. 1 Criteria concerning identification and tuning

Criteria group	Criteria	PID	PID with decoupling	MPC #1	MPC #2
Identification	Identification tool available	No[1]	No[1]	Yes	Yes
Tuning	Model accuracy	Normal	Normal	Normal	High
	Number of tuning parameters	1[2]	1[2]	1	5 (many)
	Tuning rules available	Yes	Yes	Yes	No
	Off Line simulation possible	No	No	Yes	Yes
	Adaptation of parameters possible	Yes	Yes	No	No
	PV transformation possible	Yes	Yes	Yes	Yes

[1] several identification tools available [2] due to IMC-tuning

Tab. 2 Criteria concerning the implementation of the controller

		DCS			
Criteria group	Criteria	PID	PID with decoupling	MPC #1	MPC #2
Implementation	Transfer of tuning parameters from offline to online possible	No	No	No	Yes
	Minimal execution period	50 ms	50 ms	5 sec	5 sec
	Connection controller to DCS	Browser	Browser	Manual	Manual
	Special requirements for the tags	No	No	Yes	Yes

Tab. 3 Criteria concerning the control variable performance

		DCS			
Criteria group	Criteria	PID	PID with decoupling	MPC #1	MPC #2
Controller Performance	$J_{11} = [\ \Sigma e(x_T)^2 \mid \Sigma \Delta u_1^2\ ]$ $J_{22} = [\ \Sigma e(x_B)^2 \mid \Sigma \Delta u_2^2\ ]$ $RPI = \frac{J_{ij}(Actual\ Controller)}{J_{ij}(Dec.PID\ Controller)}$	Top conc. [1 | 1] [1 | 1] Bottom conc. [1 | 1] [1 | 1]	Top conc. [2.0 | 0.5] [0.005 | 1.0] Bottom conc. [0.2 | 0.9] [2.1 | 0.32]	Top conc. [2.0 | 0.3] [0.1 | 0.6] Bottom conc. [0.8 | 0.1] [2.3 | 0.06]	Top conc. [1.9 | 0.2] [1.0 | 0.5] Bottom conc. [0.8 | 0.06] [2.3 | 0.02]

e = set point-controlled variable Δu =manipulated variable J = controller performance criteria

Tab. 4 Criteria concerning the control system robustness

		DCS			
Criteria group	Criteria	PID	PID with decoupling	MPC #1	MPC #2
Stability margin*	Robust design possible	Yes	Yes	No	No
	$RRI_{KP} = \frac{\Delta KP}{\Delta KP_{PID}}$ (1)	$RPI_{KP}(x_T)=1$ $RPI_{KP}(x_B)=1$	$RPI_{KP}(x_T)=18$ $RPI_{KP}(x_B)=4$	$RPI_{KP}(x_T)=3.0$ $RPI_{KP}(x_B)=1.2$	$RPI_{KP}(x_T)=3.0$ $RPI_{KP}(x_B)=1.5$
	$RRI_{TP} = \frac{\Delta TP}{\Delta TP_{PID}}$ (2)	$RPI_{TP}(x_T)=1$ $RPI_{TP}(x_B)=1$	$RPI_{TP}(x_T)=4.5$ $RPI_{TP}(x_B)=1.2$	$RPI_{TP}(x_T)=5.0$ $RPI_{TP}(x_B)=2.4$	$RPI_{TP}(x_T)=5.0$ $RPI_{TP}(x_B)=3.2$

(*): Used as measure of the control system robustness

(1): ΔKP is the minimal change of the process gain, which induces unstable operation for the controller.

(2): ΔTP is the minimal change of the process dead time, which induces unstable operation of the system.

ΔKP_{PID}, ΔKT_{PID} are the values of the stability thresholds of the PID controllers used as reference.

Tab. 5 Criteria concerning the usability

		DCS			
Group of criteria	Criteria	PID	PID with decoupling	MPC #1	MPC #2
Usability	Separately usable subsystems supported	Yes	No	Yes	Yes
	Anti-reset windup supported	Yes	No	Yes	Yes
	User interface available / customized possible	Yes / Yes	Yes / Yes	Yes / No	Yes / No
	Quality of human-machine-interface (poor, normal, excellent)	Normal	Normal	Normal	Poor
	Quality of user guide (poor, normal, excellent)	Normal	Normal	Poor	Poor

ACKNOWLEDGEMENT

The project is based on the budget of the federal state Nordrhein-Westfalen and sponsored by the process engineering company Krupp-Uhde and supported by the control / software companies Aspen Tech, ABB, Honeywell, Invensys and IPCOS.

REFERENCES

Bequette, B. W. (1998): *Process Dynamics Modelling, Analysis and Simulation*, Prentice Hall PTR, ISBN 0-13-206889-3

Downs, J.J.; Vogel, E.F. (1993): A plant-wide industrial process control problem, *Chemical Engng.* vol.17, no.3, pp. 245-255

Furata K. et al. (1999): Control Benchmark Study for Process Industry Control Engineers. *Proceedings of the 14th IFAC World Congress*, ISBN 0080432484

Harris, T.J.; Boudreau, F.; MacGregor, J.F. (1996): Performance Assessment of Multivariable Feedback Controllers. Automatica, vol. 32 no. 11, pp. 1505-1518

Joshi, N.V.; Murugan, P.; Rhinehart, R.R. (1997): Experimental comparison of control strategies. *Control Eng. Practice*, vol.5, no. 7, pp. 885-896

Le Page, G.P.; Tade, M.O.; Stone, R.J. (1998): Comparative evaluation of advanced process control techniques for alumina flash calciners, J. Proc. Cont., vol.8, no.4, pp. 287-298

Mahn, B., Reinig, G. (2000): An Approach to Evaluation of Advanced Control Strategies for the Process Industry. *IFAC Symposium CACSD2000*, 11—13 Sept. 2000, Salford, UK

Rickers, N.L.: http://depts.washington.edu/control

Schuler, H.; Holl, P. (1998): Erfolgreiche Anwendungen gehobener Prozessführungsstrategien. *ATP*, vol.40, no. 2 pp. 37-41

Schultz, M.A. et al. (2002): Reduce Costs with Dividing-Wall Columns . *www.cepmagazine.org*, May 2002

Seborg, D.E. (1999): A Perspective on Advanced Strategies for Process Control. Highlights of ECC'99; Springer Verlag pp. 102-134

Subawalla, H.; Paruchuri, V.P. et al. (1996): Comparison of Model-Based and Conventional Control: A Summary of Experimental Results. *Ind. Eng. Chem. Res.* vol.35, no.10, pp. 3547-3559

WinTECH, (2001): http://www.win-tech.com/html/opcstk.htm

Contact address:
gunter.reinig@ruhr-uni-bochum.de

NON-FRAGILE PID STABILIZING CONTROLLER ON SECOND-ORDER SYSTEMS WITH TIME DELAY

Jian-ming Xu Li Yu

College of Information Engineering, Zhejiang University of Technology, Hangzhou 310032, China
Email: lyu@hzcnc.com

Abstract: Based on an extension of the Hermite-Biehler Theorem to the quasipolynomial stability problem, this paper studies the problem of stabilizing a second-order plant with dead time via a PID controller. The region in PID parameters space for the closed-loop stability is given. For a feasible proportional gain (k_p), the region of all the admissible integral gains (k_i) and derivative gains (k_d) is a convex polygon. The PID controller design is formulated as a convex optimization problem of load disturbance rejection with constraints on stability and non-fragility, which can be solved by using existing linear programming techniques. *Copyright © 2003 IFAC*

Key words: PID control; stability; non-fragile; quasipolynomial; linear programming

1. INTRODUCTION

In today's process industry it is still PID controllers that are the most frequently used controllers. Estimates indicate that more than 90% of all controllers used are of the PID type. The main reason is its relatively simple structure, which can be easily understood and implemented in practice (Åström & Hägglund, 1995). In order to satisfy the increasing requirements for control systems performance, knowing all stabilizing PID controllers and using this information in controller design can be extremely useful. To this extent, Ho, Datta, and Bhattacharyya (1996) obtained a characterization of all stabilizing gains using a generalized Hermite-Biehler Theorem. They (1997a,b) have then extended this result to characterize stabilizing PID controllers. Recently, Silva et al (2001) solved the problem of stabilizing a first-order plant with time delay via a PI controller. On the other hand, in practice, controllers do have a certain degree of errors due to finite word length in any digital systems, the imprecise inherent in analog systems and need for additional tuning of parameters in the final controller implementation. It is shown that relatively small perturbations in controller parameters could even destabilize the close-loop system (Kell and Bhattacharyya 1997, Dorato 1998). This brings a new issue: how to design a controller for a given plant such that the controller is insensitive to some amount of errors with respect to its parameters, i.e., the controller is non-fragile.

In this paper, the problem of designing a non- fragile PID controller is studied for a class of second-order systems with time delay. First the region in PID parameters space for the closed-loop stability is derived based on a suitable extension of the Hermite-Biehler Theorem. Then the primary goal of the design problem is to achieve good disturbance rejection, which in mathematical terms corresponds to minimizing the integrated error. According to Åström *et al*. (1998), this is equivalent to maximizing the integral gain k_i for a step change in the load disturbance. Finally the PID controller design is to maximize the integral gain k_i with constraints on stability and non-fragility.

This paper is organized as follows. In Section 2, some preliminary results due to Pontryagin and others are presented for the stability of systems with time delay. These results are used in Section 3 to study the stabilization problem via a PID controller. The procedure for determining the PID parameters is presented in Section 4. The simulation and experiment examples are given in Section 5 and Section 6 to demonstrate the usefulness of the proposed results.

2. PROBLEM STATEMENT AND PRELIMINARY RESULTS

Consider the feedback control system shown in Fig.1,

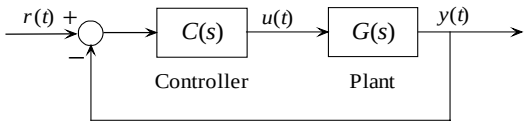

Fig.1. Feedback control system.

where the transfer function $G(s)$ and the PID controller $C(s)$ are in the form of

$$G(s) = \frac{k}{as^2 + bs + 1} e^{-Ls} \tag{1}$$

$$C(s) = \frac{k_d s^2 + k_p s + k_i}{s} \tag{2}$$

where k, a, b, L are known, k_d, k_p, k_i are the PID

parameters.

When the time delay L of the plant model is zero, the characteristic equation of the closed-loop system is given by

$$\delta(s) = as^3 + (b + kk_d)s^2 + (1 + kk_p)s + kk_i \ . \quad (3)$$

It can be concluded from the Routh-Hurwitz stability criterion that the closed-loop system is stable if

$$a > 0, \quad b + kk_d > 0,$$
$$k_p > \frac{ak_i}{b + kk_d} - \frac{1}{k}, \quad kk_i > 0. \quad (4)$$

or

$$a < 0, \quad b + kk_d < 0,$$
$$k_p < \frac{ak_i}{b + kk_d} - \frac{1}{k}, \quad kk_i < 0. \quad (5)$$

When the delay of the model is nonzero, the closed-loop characteristic equation of the system is given by

$$\delta(s) = k(k_d s^2 + k_p s + k_i)e^{-Ls} + s(as^2 + bs + 1) \quad (6)$$

that includes an exponent term. So the region of parameters k_d, k_p, k_i can't be determined directly by Routh-Hurwitz stability criterion for closed-loop stability. To overcome the difficulty, a new method is put forward based on the Hermite-Biehler Theorem and its extension.

Consider the closed-loop characteristic equation of the system with time delay

$$\delta(s) = d(s) + e^{-sT_1}n_1(s) + \cdots + e^{-sT_m}n_m(s) \quad (7)$$

where $d(s), n_i(s)$ $(i = 1,2,\cdots,m)$ are polynomials with real coefficients. The characteristic equations of this form are known as quasipolynomials. To study the stability of certain classes of quasiplynomials, we first introduce the extension of the Hermite-Biehler Theorem, which was developed by Bhattacharyya et al (1995). In (7), assuming

A1. $\deg[d(s)] = n$ and $\deg[n_i(s)] < n$, for $i = 1,2,\cdots,m$;

A2. $0 < T_1 < T_2 < \cdots < T_m$.

Instead of (7), we consider

$$\delta^*(s) = e^{sT_m}\delta(s)$$
$$= e^{sT_m}d(s) + e^{s(T_m - T_1)}n_1(s) + e^{s(T_m - T_2)}n_2(s) + \cdots + n_m(s) \quad (8)$$

Since e^{sT_m} does not have any finite zeros, the Hurwitz stability of $\delta(s)$ is equivalent to that of $\delta^*(s)$. The following Lemma presents a necessary and sufficient condition for the Hurwitz stability of $\delta(s)$.

Lemma 1. (**Extended Hermite-Biehler Theorem**) Let $\delta^*(s)$ be given by (8), and write

$$\delta^*(j\omega) = \delta_r(\omega) + j\delta_i(\omega)$$

where $\delta_r(\omega)$ and $\delta_i(\omega)$ represent, respectively, the real and imaginary parts of $\delta^*(j\omega)$. Under assumptions (A1) and (A2), $\delta^*(s)$ is Hurwitz stable if and only if

(1) $\delta_r(\omega)$ and $\delta_i(\omega)$ have only single real roots and these interlace;

(2) $\delta_i'(\omega_0)\delta_r(\omega_0) - \delta_i(\omega_0)\delta_r'(\omega_0) > 0$, for some ω_0 in $(-\infty, \infty)$.

where $\delta_r'(\omega)$ and $\delta_i'(\omega)$ denote the first derivative with respect to ω of $\delta_r(\omega)$ and $\delta_i(\omega)$, respectively.

A crucial step in applying the above theorem to check stability is to ensure first that $\delta_r(\omega)$ and $\delta_i(\omega)$ have only real roots. Such a property can be ensured by using the following result (Bellman & Cooke, 1963).

Lemma 2. Let M and N denote the highest powers of s and e^s, respectively, in $\delta^*(j\omega)$, and η be an appropriate constant such that the coefficients of terms of highest degree in $\delta_r(\omega)$ and $\delta_i(\omega)$ do not vanish at $\omega = \eta$. Then for the equations $\delta_r(\omega) = 0$ or $\delta_i(\omega) = 0$ to have only real roots, it is necessary and sufficient that in the interval $\omega \in [-2l\pi + \eta, 2l\pi + \eta]$ $\delta_r(\omega)$ or $\delta_i(\omega)$ has exactly $4lN + M$ real roots starting with a sufficiently large number l.

3. STABILIZATION USING A PID CONTROLLER

In this section, a stabilizing region in PID parameters space is given based on the extended Hermite-Biehler Theorem. Obviously, the equation (6) satisfies the assumptions (A1) and (A2). A quasipolynomial is constructed as follows:

$$\delta^*(s) = e^{Ls}\delta(s)$$
$$= k(k_d s^2 + k_p s + k_i) + s(as^2 + bs + 1)e^{Ls}$$

Substituting $s = j\omega$ in the above yields

$$\delta^*(j\omega) = \delta_r(\omega) + j\delta_i(\omega).$$

where

$$\delta_i(\omega) = \omega[kk_p - (a\omega^2 - 1)\cos(L\omega) - b\omega\sin(L\omega)];$$
$$\delta_r(\omega) = kk_i - kk_d\omega^2 + \omega(a\omega^2 - 1)\sin(L\omega) - b\omega^2\cos(L\omega).$$

The controller parameter k_p only affects the imaginary part of $\delta^*(j\omega)$. Whereas k_i and k_d affect the real part $\delta^*(j\omega)$. Let $z = L\omega$, then

$$\delta_r(z) = k\left[k_i - k_d\frac{z^2}{L^2} - h(z)\right] \quad (9)$$

$$\delta_i(z) = \frac{z}{L}\left[kk_p - \left(a\frac{z^2}{L^2} - 1\right)\cos(z) - b\frac{z}{L}\sin(z)\right] \quad (10)$$

where

$$h(z) = \frac{z}{kL}\left[b\frac{z}{L}\cos(z) - \left(a\frac{z^2}{L^2} - 1\right)\sin(z)\right]. \quad (11)$$

A general assumption on $k > 0, a > 0, b > 0, L > 0$ is suitable for a second-order model with time delay. The following theorem gives a stabilizing region in PID parameters space.

Theorem 1. Under the assumption on $k>0,\ a>0,\ b>0$ and $L>0$, the closed-loop system with transfer function $G(s)$ as in (1) is stable if and only if

$$k_p \in (\max(-1/k, k_{plow}), k_{pup});$$

$$k_i>0,\ \ k_d>-\frac{b}{k},\ \ k_p>\frac{ak_i}{b+kk_d}-\frac{1}{k};$$

$$k_i-k_d\frac{z_1^2}{L^2}<h_1,\ \dots,\ \ k_i-k_d\frac{z_{e-2}^2}{L^2}<h_{e-2};$$

$$k_i-k_d\frac{z_2^2}{L^2}>h_2,\ \dots,\ \ k_i-k_d\frac{z_{f-2}^2}{L^2}>h_{f-2}. \qquad (12)$$

Where

(1). k_{plow} and k_{pup} denote the upper bound of all minimum values and lower bound of all maximum values, respectively, for

$$k_p(z)=\frac{1}{k}\left[\left(a\frac{z^2}{L^2}-1\right)\cos(z)+\frac{b}{L}z\sin(z)\right];$$

(2). $z_j>0\ (j=1,2,3,\cdots)$ denote the roots of $\delta_i(z)$ associated with a given parameter k_p;

(3). When j is an odd number, k_{dj} denote k_d in the joints of $k_i-k_d(z_j^2/L^2)=h_j$ and $k_i=0$. Then e is the minimum odd number satisfying $k_{de}<k_{d1}$;

(4). When j is an even number, k_{dj} denotes k_d in the joints of $k_i-k_d(z_j^2/L^2)=h_j$ and $k_i-k_d(z_1^2/L^2)=h_1$. Then f is the minimum even number satisfying $k_{df}>k_{d2}$.

(5).Where

$$h_j=h(z_j)=\frac{z_j}{kL}\left[b\frac{z_j}{L}\cos(z_j)-\left(a\frac{z_j^2}{L^2}-1\right)\sin(z_j)\right].$$

Proof:

Step 1: Check the condition 2 of Lemma 1. Let $\omega_0=z_0=0$, thus

$$\delta_i'(z_0)\delta_r(z_0)-\delta_i(z_0)\delta_r'(z_0)=kk_i(kk_p+1)/L.$$

From the above assumption and (4), then $\delta_i'(z_0)\delta_r(z_0)-\delta_i(z_0)\delta_r'(z_0)>0$ if $k_i>0$ and $k_p>-1/k$.

Step 2: Check the condition 1 of Lemma 1. From (10) the roots of the imaginary part can be computed, i.e.,

$$\delta_i(z)=\frac{z}{L}\left[kk_p-\left(a\frac{z^2}{L^2}-1\right)\cos(z)-b\frac{z}{L}\sin(z)\right]=0.$$

The solution are $z=0$ and

$$k_p=\frac{1}{k}\left[\left(a\frac{z^2}{L^2}-1\right)\cos(z)+\frac{b}{L}z\sin(z)\right]. \qquad (13)$$

For $j=1,2,3,\cdots$; the derivatives of k_p versus z

$$k_p'\left[\left(j-\frac{1}{2}\right)\pi\right]=\frac{1}{k}\left[(-1)^j\left(a\frac{(2j-1)^2\pi^2}{4L^2}-1\right)+(-1)^{j-1}\frac{b}{L}\right], \qquad (14)$$

$$k_p'(j\pi)=(-1)^j\frac{j}{k}\left(\frac{2a}{L^2}+\frac{b}{L}\right)\pi. \qquad (15)$$

From (14), (15) and the assumption on $k>0, a>0, b>0, L>0$, it can be seen that k_p is strictly monotonously increasing in $(2j-1)\pi$, while it is strictly monotonously decreasing in $2j\pi$. This means that k_p versus z depicted by (13) is oscillatory and nonconvergent, and its oscillatory period is gradually to tend towards 2π. The curve of k_p versus z depicted by (13) is shown in figure 2, where *A*, *B*, *C* and *D* represent extremums of the curve, respectively.

Now check if $\delta_i(z)$ has only real roots using Lemma 2. Substituting $s_1=Ls$ in the expression for $\delta^*(s)$, it can be seen that for the new quasi-polynomial in s_1, $M=3$ and $N=1$. Select $\eta=\pi/4$ to satisfied the requirements that $\sin(\eta)\neq 0$ and $\cos(\eta)\neq 0$. Now from Figs 2(a) and 2(b), it is seen that for a given $k_p^*\in(-1/k, k_{pa})$, $\delta_i(z)$ has four real roots in the interval $[0, 2\pi-\pi/4]=[0, 7\pi/4]$, including a root at $z=0$. Since $\delta_i(z)$ is an even function of z, it follows that in the interval $[-7\pi/4, 7\pi/4]$, $\delta_i(z)$ will have seven roots, whereas $\delta_i(z)$ has no root in the interval $[7\pi/4, 9\pi/4]$. Thus, $\delta_i(z)$ has $4N+M=7$ real roots in the interval $[-2\pi+\pi/4, 2\pi+\pi/4]$. Moreover, it is clear that $\delta_i(z)$ has two real roots in each of the intervals $[2l\pi+\pi/4, 2(l+1)\pi+\pi/4]$ and $[-2(l+1)\pi+\pi/4, -2l\pi+\pi/4]$ for $l=1,2,\cdots$. Hence, it follows that $\delta_i(z)$ has exactly $4lN+M$ real roots in $[-2l\pi+\pi/4, 2l\pi+\pi/4]$ starting from $l=1$ for any given $k_p^*\in(-1/k, k_{pa})$. At the same time, starting from $l=2$, $\delta_i(z)$ has $4lN+M$ real roots in the interval $[-2l\pi+\pi/4, 2l\pi+\pi/4]$ for any given $[-2l\pi+\pi/4, 2l\pi+\pi/4]$ shown in Fig.2(c); while in Fig. 2(d), starting from $l=3$, $\delta_i(z)$ has $4lN+M$ real roots in the interval $[-2l\pi+\pi/4, 2l\pi+\pi/4]$. Hence from Lemma 2, it can be concluded that $\delta_i(z)$ has $4lN+M$ roots in the interval $[-2l\pi+\pi/4, 2l\pi+\pi/4]$ starting from a large enough value of *l*, for $k_p\in(\max(-1/k, k_{plow}), k_{pup})$.

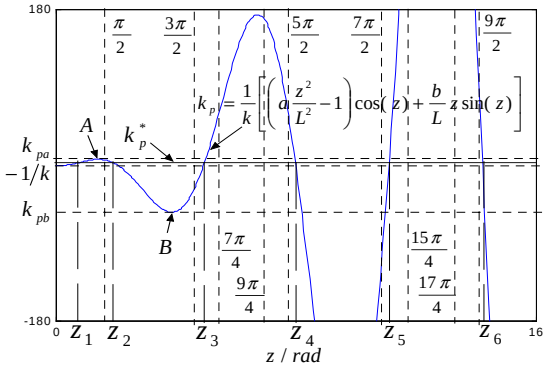

(a) for $a\frac{\pi^2}{4L^2}-1>\frac{b}{L}$

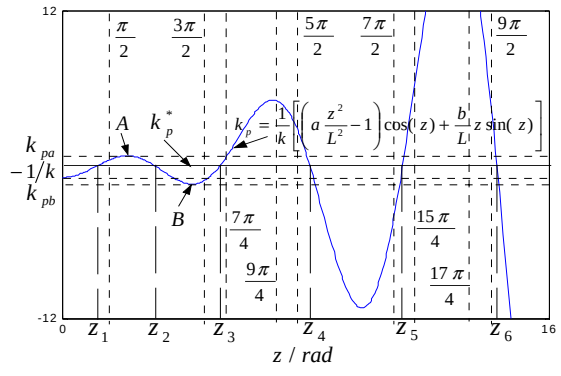

(b) for $a\frac{\pi^2}{4L^2}-1<\frac{b}{L}<a\frac{9\pi^2}{4L^2}-1$

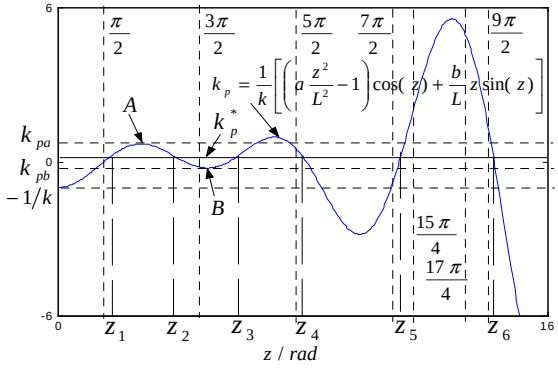

(c) for $a\frac{9\pi^2}{4L^2}-1<\frac{b}{L}<a\frac{25\pi^2}{4L^2}-1$

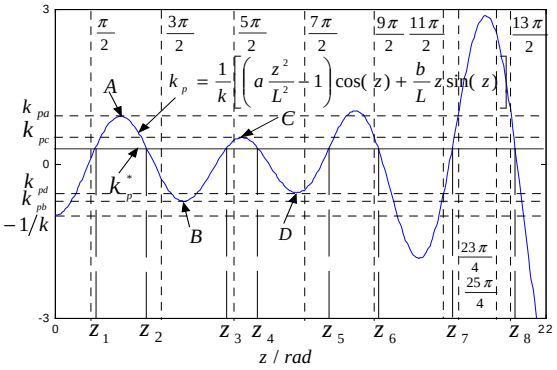

(d) for $a\frac{25\pi^2}{4L^2}-1<\frac{b}{L}<a\frac{49\pi^2}{4L^2}-1$

Fig.2. The curve of k_p versus z by equation (13)

Let z_j denote roots of $\delta_i(z)$, then interlacing of the roots of $\delta_i(z)$ and $\delta_r(z)$ is equivalent to $\delta_r(z_0)>0$ (since $k_i>0$ as derived in step 1), $\delta_r(z_1)<0$, $\delta_r(z_2)>0$, $\delta_r(z_3)<0$, $\delta_r(z_4)>0$, and so on. Using this fact and (9), (11) it is obtained

$$\begin{aligned}
&\delta_r(z_0)>0 \quad \Rightarrow \quad k_i>0\\
&\delta_r(z_1)<0 \quad \Rightarrow \quad k_i-k_d\left(z_1^2/L^2\right)<h_1\\
&\delta_r(z_2)>0 \quad \Rightarrow \quad k_i-k_d\left(z_2^2/L^2\right)>h_2\\
&\delta_r(z_3)<0 \quad \Rightarrow \quad k_i-k_d\left(z_3^2/L^2\right)<h_3\\
&\delta_r(z_4)>0 \quad \Rightarrow \quad k_i-k_d\left(z_4^2/L^2\right)>h_4\\
&\qquad\vdots
\end{aligned} \tag{16}$$

where $h_j=h(z_j)$ for $j=1,2,3,\ldots$.

Eq. (16) should be simplified since it includes infinite inequalities. As shown in Fig.2, z_j is approaching $(j-3/2)\pi$ as j increases.

For odd number j, $\lim_{j\to\infty}\cos(z_j)=0$ and $\lim_{j\to\infty}\sin(z_j)=-1$. Let k_{dj} denotes k_d in joints of $k_i-k_d\left(z_j^2/L^2\right)=h_j$ and $k_i=0$. Then

$$k_{dj}=-\frac{L^2h_j}{z_j^{\,2}}=-\frac{L}{k}\left[\frac{b}{L}\cos(z_j)-\left(a\frac{z_j}{L^2}-\frac{1}{z_j}\right)\sin(z_j)\right].$$

Using this fact, if $k_{de}<k_{d1}$ (e is an odd number), then $k_{dj}<k_{d1}$ when $j>e$.

For even number j, we have $\lim_{j\to\infty}\cos(z_j)=0$ and $\lim_{j\to\infty}\sin(z_j)=1$. Let k_{dj} denotes k_d in joints of $k_i-k_d\left(z_j^2/L^2\right)=h_j$ and $k_i-k_d\left(z_1^2/L^2\right)=h_1$. Then

$$\begin{aligned}
k_{dj}&=L^2\frac{h_1-h_j}{z_j^2-z_1^2}\\
&=\frac{\dfrac{L^2h_1}{z_j^2}+\dfrac{L}{k}\left[\left(a\dfrac{z_j}{L^2}-\dfrac{1}{z_j}\right)\sin(z_j)-\dfrac{b}{L}\cos(z_j)\right]}{1-\left(z_1^2/z_j^2\right)}
\end{aligned}$$

where $z_j\neq 0$.

Using this fact, if $k_{df}>k_{d2}$ (f is an even number), then $k_{dj}>k_{d2}$ when $j>f$.

In a word, for a controlled plant $G(s)$ described by (1), the closed-loop system is stable if and only if (12) is satisfied. □

4. PID CONTROLLER DESIGN

Using Theorem 1, a region in (k_i,k_d), which is a convex polygon, can be determined to stabilize a second-order system with time delay for a feasible k_p. By linear programming, the extremum can be computed in this region with maximum k_i, which is also a vertex of this convex polygon. Thus the closed-loop system will possibly be unstable if there are small perturbations in controller parameters, i.e., this controller is fragile. In order to overcome the drawback problem, a non-fragile PID controller will be presented. It is given by solving the following optimization problem

$$\begin{aligned}
&\text{Maximize} \quad k_i\\
&\text{subject to}\\
&k_p\in\left(\max\left(-1/k,k_{plow}\right)+d\ ,\ k_{pup}-d\right);\\
&k_i-r>0,\quad k_d-r>-b/k\ ,\\
&k_i+r\sqrt{1+(1+kk_p)^2/a^2}-k_d(1+kk_p)/a<b(1+kk_p)/ak\ ,\\
&k_i+r\sqrt{1+(z_1/L)^4}-k_d(z_1/L)^2<h_1\ ,\\
&\qquad\vdots
\end{aligned}$$

$$k_i + r\sqrt{1+(z_{e-2}/L)^4} - k_d(z_{e-2}/L)^2 < h_{e-2},$$
$$k_i - r\sqrt{1+(z_2/L)^4} - k_d(z_2/L)^2 > h_2,$$
$$\vdots$$
$$k_i - r\sqrt{1+(z_{f-2}/L)^4} - k_d(z_{f-2}/L)^2 > h_{f-2}. \qquad (17)$$

Where d denotes an acceptable perturbation size of k_p. r denotes an acceptable perturbation size of k_i and k_d, also is the distance between both borders of the (k_i, k_d) regions given by (12) and (17), for a feasible k_p. Both regions are two similar convex polygons each other. As a result, the closed-loop system will be guaranteed to be stable as long as perturbations in the controller parameters are smaller than r and d.

5. SIMULATION EXAMPLE

Consider a high-order and heavily oscillatory process

$$G(s) = \frac{1}{(s^2+s+1)(s+2)^2}e^{-0.1s}.$$

Its second-order model (Wang, 1999) is given by

$$\hat{G}(s) = \frac{0.222}{1.256s^2+1.101s+1}e^{-0.837s}.$$

With the proposed PID controller design procedure, $k_{plow} = -4.5045$, $k_{pup} = 10.0995$, then when $d = r = 4$, the PID controller designed is

$$C(s) = 4.4485 + \frac{5.107}{s} + 8.3013s.$$

Wang's method (1999) gives rise to

$$C'(s) = 1.503 + \frac{1.366}{s} + 1.715s.$$

The closed–loop performances of the proposed PID controller (solid line) and Wang's PID controller (dot line) are shown in Fig.3, where a step load disturbance is introduced to at $t = 30$ sec. Both controllers parameters k_p, k_i and k_d in Fig. 3(a) are not perturbed, and in Fig. 3(b)-(d) are perturbed, i. e., they are deviated $-1.5, 1.5, 1.5$ in Fig. 3(b), $1.5, -1.366, 1.5$ in Fig. 3(c), $1.5, 1.5, -1.5$ in Fig. 3(d) from their design values, respectively. It can be seen from the results of simulation that the proposed method is superior to Wang's method in the rejection of load disturbances and non-fragility.

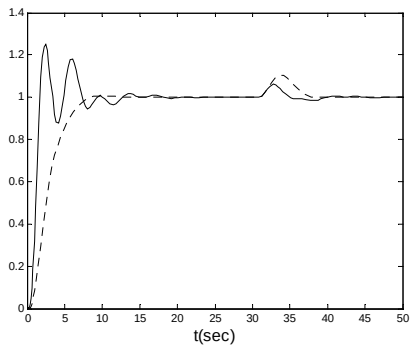

(a)

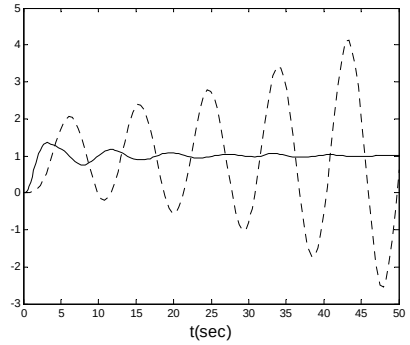

(b)

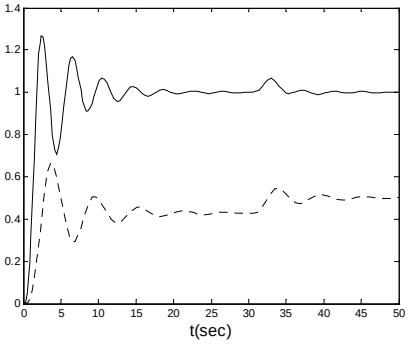

(c)

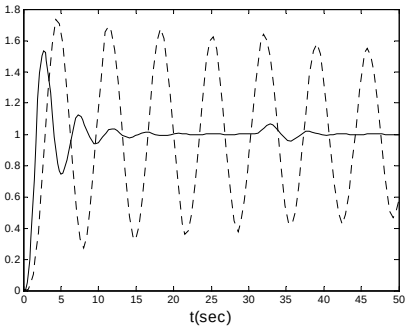

(d)

Fig 3. Step responses of the process

6. EXPERIMENT EXAMPLE

The above approach of PID controller design will be tested on a water level control plant with three tanks. The plant is described as

$$G(s) = \frac{1.39}{3136s^2+137.6s+1}e^{-30s}.$$

With the proposed PID controller design procedure for this model, $k_{plow} = -0.7194$, $k_{pup} = 3.89$, then when $r = 0.05$, the PID controller designed is

$$C(s) = 2.738 + \frac{0.0513}{s} + 125.6s.$$

Åström's method (1984) gives

$$C'(s) = 2.09 + \frac{0.012}{s} + 92s.$$

The step responses with the above two PID controllers: the proposed PID (up) and Åström's PID (down) are shown in Fig.4, a step load disturbance is introduced to at $t = 900$ sec. There is a higher overshoot in the step responses with the proposed method , but it is superior to Åström's method in the rejection of load disturbances.

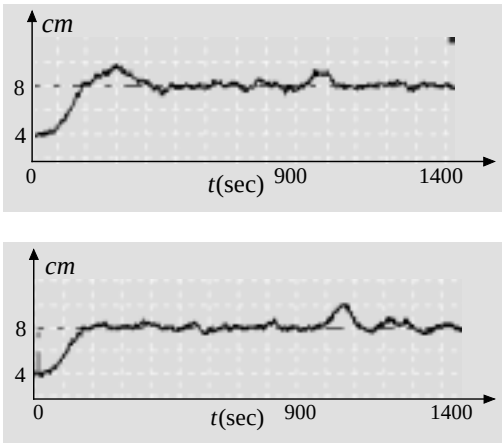

Fig 4. Step responses of the water level control plant

The acceptable perturbation size (as $r = 0.0513$) of the proposed PID parameters is larger than that (as $r = 0.012$) of Åström's PID parameters. For instance, when the integral gains (k_i) of both controllers are deviated -0.045 and -0.01 from their design values, respectively, the step responses with the proposed PID (up) and Åström's PID (down) are shown in Fig.5. It is obvious that the proposed controller can tolerate a larger perturbation extent compare with Åström's controller.

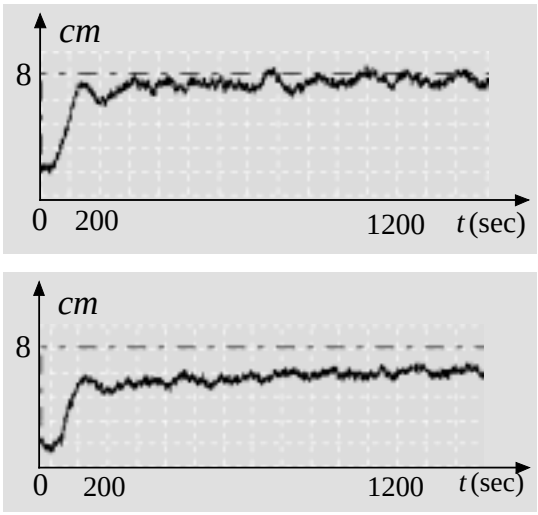

Fig 5. Step responses of the process for k_i is deviated from the its design value

7. CONCLUSIONS

Based on an extension of the Hermite-Biehler Theorem to the quasipolynomial stability problem, a characterization of the complete set of stabilizing PID controller have been obtained for a given second-order plant with dead time. This result opens up the possibility of designing PID controller to optimize a given performance criteria. The main reason to optimize the load disturbance response instead of the set point response is that load disturbances are more likely to change during operation compared to set points, which are usually kept fixed. A good set point tracking can be achieved by using the feed forward term of two degrees of freedom PID controller (Panagopoulos, 1999). The non-fragile PID controller can tolerate a larger parameter perturbation extent. Consistent and satisfactory responses are obtained as shown in simulation and experiment example results.

ACKNOWLEDGEMENTS

This work was supported by the National Natural Science Foundation of China under Grant 60274034.

REFERENCES

Åström, K.J., & Hägglund, T. (1984). Automatic tuning of simple regulators with specifications on phase and amplitude margins. *Automatica*, 20(5): 645-651.

Åström, K.J., & Hägglund, T. (1995). *PID Controllers: Theory, Design and tuning*. Research Triangle Park: Instrument Society of America.

Åström, K.J., Panangopoulos, H., & Hägglund, T. (1998). Design of PI Controllers based on Non-Convex Optimization. *Automatica*, 34(5): 585-601.

Bellman, R., & Cooke, K.L. (1963). *Differential-difference equations*. London: Academic Press Inc.

Bhattacharyya, S. P., Chapellat, H., & Keel, L. H. (1995). *Robust control*: *The parametric approach.* Englewood Cliffs, NJ: Prentice-Hall.

Dorato, P. (1998). Non-fragile controller design, an overview, In *Proceedings of the Amer. Contr. Conf.*, Philadephia, Pennsylvania : 2829-2831.

Ho, M.T., Datta, A., & Bhattacharyya, S. P. (1996). A new approach to feedback stabilization. In *Conf. on decision control,*, December, Kobe, Japan : 4643-4648.

Ho, M.T., Datta, A., & Bhattacharyya, S. P. (1997a). A linear programming characterization of all stabilizing PID controllers. In *Proceedings of the Amer. Contr. Conf.*, June, Albuquerque, NM: 3922-3928.

Ho, M.T., Datta, A. & Bhattacharyya, S. P. (1997b). Control system design using low order controllers: Constant gain, PI and PID. In *Proceedings of the Amer. Contr. Conf.*, June, Albuquerque, NM: 571-578.

Keel, L.H., & Bhattacharyya, S. P. (1997). Robust, fragile, or optimal ? *IEEE Trans. on Automatic Control*, *42*(8): 1098-1105.

Panagopoulos, H., Åström, K. J., & Hägglund, T. (1999). Design of PID Controllers based on Constrained Optimization. In *Proceedings of the Amer. Contr. Conf.*, San Diego, California.

Silva, G. J., Datta, A., & Bhattacharyya, S. P. (2001). PI stabilization of first-order systems with time delay. *Automatica*, 37(12): 2025-2031.

Wang, Q.G., Lee, T. H., Fung, H.W., & Bi, Q. (1999). PID Tuning for Improved Performance. *IEEE Trans. on control systems technology*, 7(4): 457-465.

A METHOD OF CONTROLLING UNSTABLE, NON-MINIMUM-PHASE, NONLINEAR PROCESSES

Chanin Panjapornpon* **Masoud Soroush** *,[1]
Warren D. Seider **

* *Department of Chemical Engineering, Drexel University, Philadelphia, PA 19104, U.S.A.*
** *Department of Chemical Engineering, University of Pennsylvania, Philadelphia, PA 19104, U.S.A.*

Abstract: A method of controlling general nonlinear processes is presented. It is applicable to stable and unstable processes, whether non-minimum- or minimum-phase. The control system includes a nonlinear state feedback and a reduced-order nonlinear state observer. The state feedback induces an approximately linear response. The application and performance of the control method are shown by implementing it on a chemical reactor with multiple steady states. The control system is used to operate the reactor at one of the steady states, which is unstable and non-minimum-phase. The simulation results show that the closed-loop system is globally asymptotically stable.

Keywords: nonlinear control; unstable systems; feedback linearization; non-minimum-phase systems; model-based control

1. INTRODUCTION

During the past 20 years, many advances have been made in nonlinear model-based control, mainly in the frameworks of model-predictive and differential-geometric control. In model-predictive control, the controller action is the solution to a constrained optimization problem that is solved on-line. In contrast, differential-geometric control is a direct synthesis approach in which the controller is derived by requesting a desired closed-loop response in the absence of input constraints. In other words, model-predictive control involves numerical model inversion, while differential-geometric control involves analytical model inversion. In model-predictive control, non-minimum-phase behavior is handled simply by increasing prediction horizons, but in differential geometric control, special treatment is needed.

Differential-geometric controllers were initially developed for unconstrained, minimum-phase (MP) processes. During the past two decades, these controllers were extended to unconstrained, non-minimum-phase (NMP), nonlinear processes. The resulting controllers include those developed by (Kravaris and Daoutidis, 1990; Isidori and Byrnes, 1990; Isidori and Astolfi, 1992; Wright and Kravaris, 1992; van der Schaft, 1992; Isidori, 1995; Chen and Paden, 1996; Devasia et al., 1996; Doyle III et al., 1996; McLain et al., 1996; Hunt and Meyer, 1997; Niemiec and Kravaris, 1998; Kravaris et al., 1998; Devasia, 1999). Most of these controllers are applicable only to single-input single-output, NMP processes. Although controllers of Niemiec and Kravaris (1998), Isidori and Byrnes (1990),

[1] Corresponding author. masoud.soroush@coe.drexel.edu
[2] The authors gratefully acknowledge financial support from the National Science Foundation

Isidori and Astolfi (1992), van der Schaft (1992), Chen and Paden (1996), Hunt and Meyer (1997), Devasia et al., (1996), Devasia (1999), and Isidori (1995) are applicable to multi-input multi-output (MIMO), NMP processes, either sets of partial differential equations must be solved (Isidori and Byrnes, 1990; Isidori and Astolfi, 1992; van der Schaft, 1992), or the controllers are applicable to a very limited class of processes (Chen and Paden, 1996; Hunt and Meyer, 1997; Devasia et al., 1996; Devasia, 1999; Isidori, 1995). Recently a differential-geometric control law was developed by Kanter et al. (2002) for stable, nonlinear processes with input constraints and deadtimes, whether the delay-free part of the process is non-minimum- or minimum-phase. This control law cannot be used to operate a process at an unstable operating point.

This paper presents a control method that is applicable to stable or unstable nonlinear processes, whether minimum- or non-minimum-phase. The control system includes a nonlinear state feedback and a reduced-order nonlinear state observer. The state feedback induces an approximately linear response. The application and performance of the control method are shown by implementing it on a chemical reactor with multiple steady states.

This paper is organized as follows. The scope of the study and some mathematical preliminaries are given in Section 2. Section 3 presents the nonlinear feedback control method. The application and performance of the control method are illustrated by numerical simulation of a chemical reactor with multiple steady states in Section 4.

2. SCOPE AND MATHEMATICAL PRELIMINARIES

Consider the general class of multivariable processes with a mathematical model in the form:

$$\left.\begin{aligned} \frac{dx}{dt} &= f(x,u), \quad x(0)=x_0 \\ y &= h(x) \end{aligned}\right\} \tag{1}$$

where $x = [x_1 \cdots x_n]^T \in \Re^n$ is the vector of state variables, $u = [u_1 \cdots u_m]^T \in \Re^m$ is the vector of manipulated inputs, $y = [y_1 \cdots y_m]^T \in \Re^m$ is the vector of controlled outputs, $f(x,x) = [f_1(x,u) \cdots f_n(x,u)]^T$ and $h(x) = [h_1(x) \cdots h_m(x)]^T$ are smooth. The relative order (degree) of a state x_i, is denoted by r_i, where r_i is the smallest integer for which $\partial[d^{r_i}x_i/dt^{r_i}]/\partial u \neq 0$.

For a given setpoint value, y_{sp}, the corresponing steady state values of the state variables and manipulated inputs satisfy:

$$\begin{aligned} 0 &= f(x_{ss}, u_{ss}) \\ y_{sp} &= h(x_{ss}) \end{aligned}$$

These relations are used to describe the dependence of a nominal steady state, x_{ss_N}, on the setpoint: $x_{ss_N} = F(y_{sp})$.

Let $H(x) = x$ and define the following notation:

$$\begin{aligned} H_i^1(x) &= \frac{dx_i}{dt} \\ &\vdots \\ H_i^{r_i-1}(x) &= \frac{d^{r_i-1}x_i}{dt^{r_i-1}} \\ H_i^{r_i}(x,u) &= \frac{d^{r_i}x_i}{dt^{r_i}} \\ H_i^{r_i+1}(x,u^{(0)},u^{(1)}) &= \frac{d^{r_i+1}x_i}{dt^{r_i+1}} \\ &\vdots \\ H_i^{p_i}(x,u^{(0)},u^{(1)},\ldots,u^{(p_i-r_i)}) &= \frac{d^{p_i}x_i}{dt^{p_i}} \end{aligned} \tag{2}$$

where $p_i \geq r_i$ and $u^{(\ell)} = d^\ell u/dt^\ell$.

3. NONLINEAR CONTROL METHOD

A state feedback that induces approximately linear responses to the state variables, is first derived. A reduced-order state observer is then designed to reconstruct unmeasured state variables from the output measurements. To add intgeral action to the state feedback-state observer system, a dynamic system is finally added.

3.1 State Feedback Design

Let us request a linear response of the following form for each of the state variable:

$$\begin{aligned} (\epsilon_1 D+1)^{p_1}x_1 &= x_{ss_{N_1}} \\ &\vdots \\ (\epsilon_n D+1)^{p_n}x_n &= x_{ss_{N_n}} \end{aligned} \tag{3}$$

where $D = d/dt$, and $\epsilon_1, \cdots, \epsilon_n$ are positive constants that set the speed of the state responses. The state responses in (3) can be obtained only when $n = m$. However, since in many processes $m < n$ (there are more state variables than manipulated inputs), the state responses in (3) cannot be achieved. We relax the request for the linear responses by trying to obtain state responses that are as close as possible to the the linear ones described by (3). To this end, we solve the following moving-horizon optimization problem:

$$\min_{u(t)} \sum_{i=1}^{m} w_i \, ||x_{d_i}(\tau) - \hat{x}_i(\tau)||^2_{q_i,[t,\, t+T_{h_i}]} \tag{4}$$

subject to:

$$u^{(\ell)}(t) = 0, \quad \ell > 1,$$

where t represents the present time, and $\hat{x}_i(\tau)$ and $x_{d_i}(\tau)$ are predicted values of the state variable x_i and the desired (reference) trajectory of the state variable, respectivey. $||x_i(\tau)||_{q_i,[t,\, t+T_{h_i}]}$ denotes the q_i-function norm of the scalar function $x_i(\tau)$ over the finite time interval $[t, t+T_{h_i}]$ with $T_{h_i} > 0$:

$$||x_i(\tau)||_{q_i,[t,t+T_{h_i}]} = \left[\int_t^{t+T_{h_i}} |x_i(\tau)|^{q_i} d\tau\right]^{\frac{1}{q_i}}, \; q_i \geq 1$$

and $w_1, \cdots, w_m$ are adjustable positive scalar weights whose values are set according to the relative importance of the state variables: the higher the value of w_i, the smaller the mismatch between x_{d_i} and x_i.

3.1.1. Output Prediction Equation The future value of the ith state variable over the time interval $[t, t+T_{h_i}]$ is predicted using a truncated Taylor series:

$$\begin{aligned}\hat{x}_i(\tau) = x_i(t) + \frac{dx_i(t)}{dt}[\tau - t] + \cdots + \\ \frac{d^{p_i}x_i(t)}{dt^{p_i}}\frac{[\tau - t]^{p_i}}{p_i!}, \;\; i = 1, \cdots, m\end{aligned} \tag{5}$$

where

$$\begin{aligned} x_i(t) &= H_i(x(t)) \\ \frac{dx_i(t)}{dt} &= H_i^1(x(t)) \\ &\vdots \\ \frac{d^{r_i-1}x_i(t)}{dt^{r_i-1}} &= H_i^{r_i-1}(x(t)) \\ \frac{d^{r_i}x_i(t)}{dt^{r_i}} &= H_i^{r_i}(x(t), u^{(0)}(t)) \\ &\vdots \\ \frac{d^{p_i}x_i(t)}{dt^{p_i}} &= H_i^{p_i}(x(t), u^0(t), \cdots, u^{(p_i-r_i)}(t)) \end{aligned}$$

3.1.2. Reference Trajectory The reference trajectory of the ith state variable, x_{d_i}, describes the path that the ith state variable, x_i, is forced to follow at time t. The reference trajectory is trackable when the following conditions are satisfied:

$$\begin{aligned} x_{d_i}(t) &= x_i(t) = H_i(x(t)) \\ \frac{dx_{d_i}(t)}{dt} &= \frac{dx_i(t)}{dt} = H_i^1(x(t)) \\ &\vdots \\ \frac{d^{r_i-1}x_{d_i}(t)}{dt^{r_i-1}} &= \frac{d^{r_i-1}x_i(t)}{dt^{r_i-1}} = H_i^{r_i-1}x(t)). \end{aligned}$$

Furthermore, every reference trajectory, x_{d_i}, should take its corresponding state variable, x_i, to its set-point value, $x_{ss_{N_i}}$, as $t \to \infty$. A class of reference trajectories that has these properties is described by

$$\begin{bmatrix} (\epsilon_1 D + 1)^{p_1} x_{d_1}(\tau) \\ \vdots \\ (\epsilon_m D + 1)^{p_m} x_{d_m}(\tau) \end{bmatrix} = x_{ss_N}$$

subject to the "initial" conditions:

$$\begin{aligned} x_{d_i}(t) &= H_i(x(t)) \\ &\vdots \\ \frac{d^{r_i-1}x_{d_i}(t)}{dt^{r_i-1}} &= H_i^{r_i-1}(x(t)) \\ \frac{d^{r_i}x_{d_i}(t)}{dt^{r_i}} &= H_i^{r_i}(x(t), u^{(0)}(t)) \\ & \qquad\qquad i = 1, \cdots, m \\ &\vdots \\ \frac{d^{p_i-1}x_{d_i}(t)}{dt^{p_i-1}} &= H_i^{p_i-1}(x(t), u^{(0)}(t), \cdots, u^{(p_i-1-r_i)}(t)) \end{aligned}$$

A series solution for the reference trajectory, x_{d_i}, has the following form:

$$\begin{aligned} \hat{x}_{d_i}(\tau) = H_i(x(t)) + \sum_{\ell=1}^{r_i-1} H_i^\ell(x(t))\frac{[\tau - t]^\ell}{\ell!} \\ + \sum_{\ell=r_i}^{p_i-1} H_i^\ell(x(t), u^{(0)}(t), \cdots, u^{(\ell-r_i)}(t))\frac{[\tau - t]^\ell}{\ell!} \\ + \left[\frac{x_{ss_{N_i}} - H_i(x(t)) - \sum_{\ell=1}^{r_i-1}\epsilon_i^\ell \binom{p_i}{\ell} H_i^\ell(x(t))}{\epsilon_i^{p_i}}\right. \\ \left. - \frac{\sum_{\ell=r_i}^{p_i-1}\epsilon_i^\ell \binom{p_i}{\ell} H_i^\ell(x(t), u^{(0)}(t), \cdots, u^{(\ell-r_i)}(t))}{\epsilon_i^{p_i}}\right] \\ \times \frac{[\tau - t]^{p_i}}{p_i!} + \text{higher order terms} \end{aligned} \tag{6}$$

3.1.3. State Feedback For a process in the from of (1), by using the series forms of the output prediction and reference trajectory equations in (5) and (6), the optimization problem in Eq.4 is:

$$\min_u \sum_{i=1}^{m} w_i \left[\frac{x_{ss_{N_i}} - H_i(x) - \sum_{\ell=1}^{r_i-1} \epsilon_i^\ell \binom{p_i}{\ell} H_i^\ell(x)}{\epsilon_i^{p_i}} - \frac{\sum_{\ell=r_i}^{p_i} \epsilon_i^\ell \binom{p_i}{\ell} H_i^\ell(x, u, 0, \cdots, 0)}{\epsilon_i^{p_i}} \right]^2 \times \left\| \frac{[\tau - t]^{p_i}}{p_i!} \right\|^2_{q_i, [t,\ t+T_{h_i}]} \tag{7}$$

In the case that $n = m$, the performance index in (4) takes the value of zero and thus, the linear closed-loop state responses of (3) are achieved.

The preceding state feedback is represented in a compact form by:

$$u = \Psi(x, x_{ss_N}) \tag{8}$$

3.2 Reduced-Order State Observer

In general, measurements of all state variables are not available. In such cases, estimates of the unmeasured state variables can be obtained from the output measurements. Here, we use a reduced-order nonlinear state observer to reconstruct the unmeasured state variables. The details and properties of this estimator can be found in (Soroush, 1997).

For a nonlinear process in the form of (1), the non-redundancy of the controlled outputs ensures the existence of a locally invertible state transformation of the form

$$\begin{bmatrix} \eta \\ y \end{bmatrix} = \mathcal{T}(x) = \begin{bmatrix} Px \\ h(x) \end{bmatrix}$$

where $\eta = [\eta_1, \cdots, \eta_{n-q}]^T$, and P is a constant $(n-q) \times n$ matrix which for the sake of simplicity, is chosen such that (i) each row of P has only one nonzero term equal to one, and (ii) locally

$$rank \left\{ \frac{\partial}{\partial x} \begin{bmatrix} Px \\ h(x) \end{bmatrix} \right\} = n$$

The new variables $\eta_1, \cdots, \eta_{n-q}$ are simply $(n-q)$ state variables of the original model of (1), which satisfy the preceding rank condition, and thus the state transformation $[\eta\ y]^T = \mathcal{T}(x)$ is at least locally invertible. In many cases such as the process example considered in this article, the measurable outputs are some of the state variables. In such cases, the state transformation is linear and globally invertible.

The system of (1), in terms of the new state variables $\eta_1, \cdots, \eta_{n-q}, y$, takes the form

$$\begin{cases} \dot{\eta} = F_\eta(\eta, y, u) \\ \dot{y} = F_y(\eta, y, u) \end{cases} \tag{9}$$

where

$$F_\eta(\eta, y, u) = Pf\left[\mathcal{T}^{-1}(\eta, y), u\right];$$

$$F_y(\eta, y, u) = \left.\frac{\partial h(x)}{\partial x}\right|_{x=\mathcal{T}^{-1}(\eta,y)} f\left[\mathcal{T}^{-1}(\eta, y), u\right]$$

One can then design a closed-loop, reduced-order observer of the form:

$$\begin{aligned} \dot{z} &= F_\eta(z + Ly, y, u) - LF_y(z + Ly, y, u) \\ \hat{x} &= T^{-1}(z + Ly, y) \end{aligned} \tag{10}$$

where the constant $[(n-q) \times q]$ matrix L is the observer gain. The observer gain should be set such that the observer error dynamics are asymptotically stable (Soroush, 1997).

3.3 Integral Action

To ensure offset-free response of the closed-loop system in the presence of constant disturbances and model errors, the final control system should have integral action. The integral action can be added by using the dynamic system:

$$\begin{aligned} (\epsilon_1 D + 1)^{p_1} \xi_1 &= \phi_1(x, u) \\ &\vdots \\ (\epsilon_n D + 1)^{p_n} \xi_n &= \phi_n(x, u) \end{aligned} \tag{11}$$

where

$$\phi_i(x, u) = \sum_{\ell=0}^{r_i-1} \epsilon_i^\ell \binom{p_i}{\ell} H_i^\ell(x) + \sum_{\ell=r_i}^{p_i-1} \epsilon_i^\ell \binom{p_i}{\ell} H_i^\ell(x, u^{(0)}, \cdots, u^{(\ell-r_i)}), \quad i = 1, \cdots, m$$

3.4 Control System

Combing the equations in (8), (10) and (11) leads to the following control system that has intgeral action:

$$\begin{aligned} \dot{z} &= F_\eta(z + Ly, y, u) - LF_y(z + Ly, y, u) \\ \hat{x} &= T^{-1}(z + Ly, y) \\ (\epsilon_1 D + 1)^{p_1} \xi_1 &= \phi_1(x, u) \\ &\vdots \\ (\epsilon_n D + 1)^{p_n} \xi_n &= \phi_n(x, u) \\ v &= F(y_{sp}) - \hat{x} + \xi \\ u &= \Psi(\hat{x}, v) \end{aligned} \tag{12}$$

The control system parameters $\epsilon_1, \cdots, \epsilon_n$ set the speed of the closed-loop state responses; the smaller the value ϵ_i, the faster the x_i response. The parameters $p_1, \cdots, p_n$ should be chosen such that $p_1 = r_1, \cdots, p_n = r_n$ when the process is minimum-phase, and $p_1 > r_1, \cdots, p_n > r_n$ when the process is non-minimum-phase.

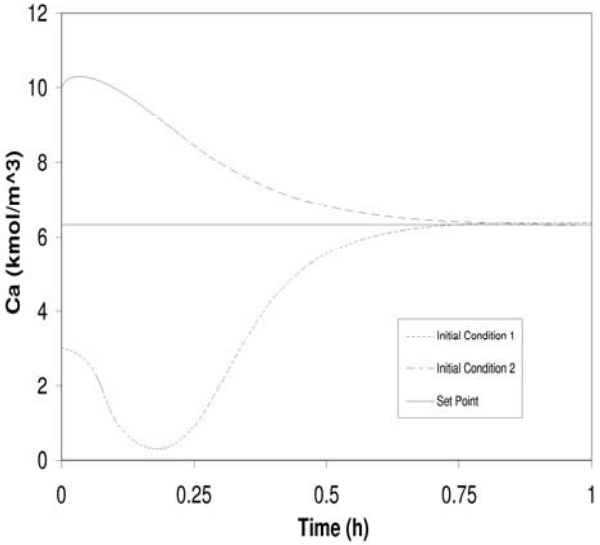

Fig. 1. Closed-loop response of the reactant outlet concentration for different initial conditions.

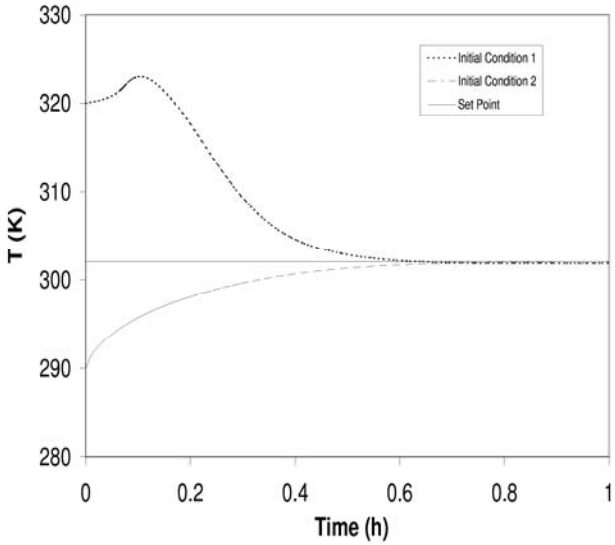

Fig. 2. Closed-loop response of the outlet stream temperature corresponding to Figure 1.

4. APPLICATION TO A CHEMICAL REACTOR

Consider a constant-volume, non-isothermal, continuous-stirred-tank reactor, in which the reaction $A \rightarrow B$ takes place in liquid phase. The reactor dynamics are represented by the following model:

$$\begin{aligned} \frac{dC_A}{dt} &= -kC_A + (C_{A_i} - C_A)u/V \\ \frac{dT}{dt} &= \gamma kC_A + (T_i - T)u/V + q \\ y &= T \end{aligned} \tag{13}$$

where $k = 5.0 \times 10^8 \exp(-8100/T)\ \ s^{-1}$, $\gamma = 3.9\ m^3\ K\ kmol^{-1}$, $q = -2.519 \times 10^{-2}\ K.s^{-1}$, $C_{A_i} = 12\ kmol\ m^{-3}$, $T_i = 300\ K$, and $V = 0.1\ m^3$.

The control method of (13) is applied to the reactor, and the resulting controller is used to operate the reactor at the unstable, non-minimum-phase steady state ($6.319\ kmol.m^{-3}$, $302.0\ K$). The following controller parameter values are used: $\epsilon_1 = 360\ s$, $\epsilon_2 = 360\ s$, $p1 = 2$, $p_2 = 2$, and $L = 0.5$

For the two sets of initial conditions, $[C_A(0),\ T(0)]$= [3.0, 320] and [10.0, 290], the peformance of the controller is shown in Figures 1–3. As can be seen from these figures, the controller is capable of operating the process at the desired steady state, regardless of the initial conditions of the process.

NOTATION

A= Reactant
B = Product
C_{A_i} = Inlet concentration of the reactant, $kmol\ m^{-3}$.
C_A= Outlet concentration of the reactant, $kmol\ m^{-3}$.
D = Differential operator, $D = d/dt$.
k = Reaction rate constant, s^{-1}.
m= Number of manipulated inputs and controlled outputs.
n = Process order.
r_i = Relative order of state variable x_i.
t = Time, s.
T = Reactor outlet temperature, K.
T_i = Reactor inlet temperature, K.
u = Process input vector.
V = Reactor volume, m^3.
x = Vector of state variables.
y = Vector of controlled outputs.
y_{sp} = Vector of set-points.

Greek

$\epsilon_1, \cdots, \epsilon_n$ = adjustable parameters of controller.
$\xi_1, \cdots, \xi_n$ = State variables of the controller.
γ = Reactor model parameter, $K\ m^3\ kmol^{-1}$.

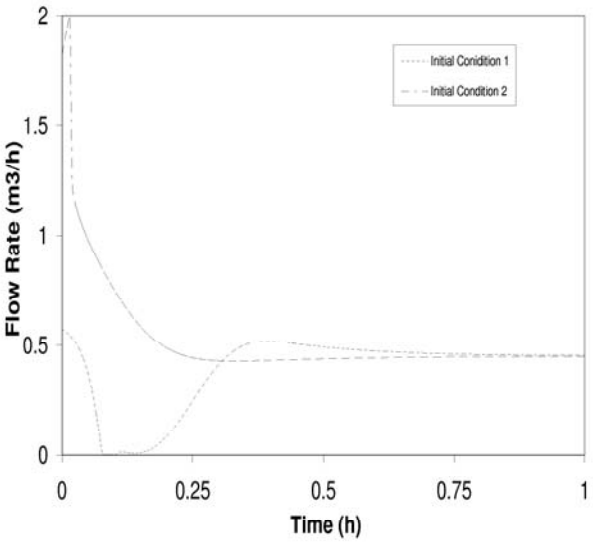

Fig. 3. Manipulated input profiles corresponding to Figures 2 and 3.

REFERENCES

Chen, D., and B. Paden, "Stable Inversion of Nonlinear Non-minimum-phase Systems," *International J. Contr.*, **64**, 81 (1996).

Chen, H., and F. Allgower, "A Quasi-infinite Horizon Nonlinear Model Predictive Control Scheme with Guaranteed Stability," *Automatica*, **34**, 1205 (1998).

Devasia, S., "Approximated Stable Inversion for Nonlinear Systems with Nonhyperbolic Internal Dynamics," *IEEE Trans. on Automatic Contr.*, **44**, 1419 (1999).

Devasia, S., D. Chen, and B. Paden, "Nonlinear Inversion-based Output Tracking," *IEEE Trans. on Automatic Contr.*, **41**, 930 (1996).

De Nicolao, G., L. Magni, and R. Scattolini, "Stabilizing Receding-Horizon Control of Nonlinear Time-Varying Systems," *IEEE Trans. on Automatic Control*, **43**, 1030 (1998).

Doyle III, F. J., F. Allgöwer, and M. Morari, "A Normal Form Approach to Approximate Input-Output Linearization for Maximum Phase Nonlinear SISO Systems," *IEEE Transactions on Automatic Control*, **41**, 305 (1996).

Hunt, L. R., and G. Meyer, "Stable Inversion for Nonlinear Systems," *Automatica*, **33**, 1549 (1997).

Isidori, A., *Nonlinear Control Systems*; Springer-Verlag; New York (1995).

Isidori, A., and A. Astolfi, "Disturbance Attenuation and H_∞ Control via Measurement Feedback in Nonlinear Systems," *IEEE Trans. on Automatic Contr.*, **37**, 1283 (1992).

Isidori, A., and C. I. Byrnes, "Output Regulation of Nonlinear Systems," *IEEE Trans. on Automatic Contr.*, **35**, 131 (1990).

Kanter, J. M., M. Soroush, and W. D. Seider, "Nonlinear Controller Design for Input-Constrained, Multivariable Processes," *I&EC Research*, in press (2002).

Kravaris, C., and P. Daoutidis, "Nonlinear State Feedback Control of Second-Order Nonminimum Phase Nonlinear Systems," *Comp. Chem. Eng.*, **14**, 439 (1990).

Kravaris, C., M. Niemiec, and R. Berber, and C. B. Brosilow, "Nonlinear Model-based Control of Nonminimum-phase Processes," In *Nonlinear Model Based Process Control*, R. Berber and C. Kravaris, Eds.; Kluwer, Dordrecht (1998).

McLain, R. B., M. J. Kurtz, M. A. Henson, and F. J. Doyle III, "Habituating Control for Nonsquare Nonlinear Processes," *Ind. & Eng. Chem. Research*, **35**, 4067 (1996).

Niemiec, M., and C. Kravaris, "Controller Synthesis For Multivariable Nonlinear Nonminimum-phase Processes," *Proceedings of ACC*, Philadelphia, PA, 2076-2080 (1998).

Soroush, M., "Nonlinear State-Observer Design with Application to Reactors," *Chem. Eng. Sci.*, **52(3)**, 387–404 (1997).

Soroush, M., and S. Valluri, "Optimal Directionality Compensation in Processes with Input Saturation Non-linearities," *Int. J. Control*, **72**, 1555-1564 (1999).

van der Schaft, A. J., "L_2 Gain Analysis of Nonlinear Systems and Nonlinear State Feedback H_∞ Control," *IEEE Trans. on Automatic Contr.*, **37**, 770 (1992).

Wright, R. A., and C. Kravaris, "Non-Minimum-Phase Compensation for Nonlinear Processes," *AIChE J.*, **38**, 26 (1992).

DESIGN OF A SLIDING MODE CONTROL SYSTEM BASED ON AN IDENTIFIED SOPDT MODEL

Chyi-Tsong Chen* **and Shih-Tien Peng**

Department of Chemical Engineering
Feng Chia University
Taichung 407, Taiwan

Abstract: Based on an identified SOPDT model, a designed optimal sliding surface and the use of a delay-ahead predictor, a novel and systematic sliding mode control system design methodology is proposed for the regulation of chemical processes. The convergence property of the closed-loop system is guaranteed theoretically through satisfying a sliding condition and the control system performance is examined with some typical chemical processes. Besides, with the concept of delay equivalent, a simple technique is presented such that the proposed sliding mode control scheme can be utilized directly to handle with the regulation control of non-minimum phase processes.

Keywords: sliding mode control, predictor, optimal sliding surface, non-minimum phase, SOPDT model.

1. INTRODUCTION

Due to its simplicity and the capability of representing the process dynamics more accurately than a first-order plus dead-time (FOPDT) model, the second-order plus dead-time (SOPDT) model is widely adopted for process modeling and is then enhanced for controller design. Up to date, many identification methods for estimating the SOPDT model parameters have been proposed in the literature, and based on SOPDT model various controller design methodologies have been presented (Hwang, 1993; Sung et al., 1996; Jahanmiri and Fallahi, 1997; Wang et al., 2001). Based on a single closed-loop test, Hwang (1993) presented an adaptive pole design method for PID controllers. Sung et al. (1996) presented a relay feedback test with combining a P controller to identify a SOPDT model, and then an automatic tuning rule for PID controller was proposed for on-line application. With an alternative identification method for SOPDT model, Jahanmiri snd Fallahi (1997) conveyed the concept of Internal Model Control (IMC) to improve the performance of a PID controller. Wang et al. (2001) proposed a simple closed-loop identification method for SOPDT and based on the model a PID auto-tuning strategy is applied.

In general, for on-line control the identification of a SOPDT model is usually accomplished in a single test by using either a closed-loop or open-loop identification method and thereafter the identified model is directly used for the tuning of a linear controller, such as PID-type controllers. This kind of approach is simple and straightforward. However, if uncertainties exist in the identification phase, an inaccurate SOPDT model may give rise to a poorly designed linear controller and therefore may lead to unsatisfactory control performance. The performance degradation is mainly due to that the uncertainties in a process are usually not explicitly considered when applying the identification-then-tune methods.

Recently, there is increasing interest in the development of robust control system for processes having uncertainties. The sliding mode control strategy appears to be one of the most promising model-based approaches to the control of uncertain processes. To account for system's input-delay, Camacho et al. (1999) and Camacho and Smith (2000) proposed the synthesis of a sliding mode controller based on an FOPDT model. Their approaches resulted in a fixed structure controller with a set of tuning equations being formulated as a function of the model's characteristic parameters. Hu et al., (2000) adopted linear matrix inequality technique and a sliding mode control method to handle a class of uncertain time-delay systems. Based on the Lyapunov theorem, Chou and Cheng (2001) proposed an adaptive variable structure control strategy to stabilize a class of perturbed time-varying delay systems. Their method does not require the upper bound of perturbations and the performance of the system can be obtained by pre-specifying a set of suitable eigenvalues. Although these approaches have potential to deal with uncertainties and state delay, they do not consider the compensation for input-delay as a whole. For the issue of dealing with input-delay, Kojima et al. (1994) explored the H_∞ stabilization problem of uncertain input-delay systems. More recently, Roh and Oh (1999; 2000) investigated the feasibility of the sliding surface with

*Author to whom all correspondence should be addressed. Tel: +886-4-24517250 ext. 3691;
Fax: +886-4-24510890; E-mail: ctchen@fcu.edu.tw

including a predictor to compensate for the input delay of the system.

In this paper, we propose a simple and novel sliding mode control system for the regulation of chemical processes. Based on an identified SOPDT model, a delay-ahead predictor is developed for state estimation and a correction term from the measured process output is incorporated to enhance the prediction accuracy of the process states. With the help of state predictor and a designed optimal sliding surface, a sliding mode controller that is able to account for model uncertainties can be easily constructed and implemented. The robust stability as well as the system behavior of the closed-loop system is analyzed through guaranteeing the sliding condition. Besides, in this paper the presented scheme is further extended to one that is able to deal with the process having inverse response. The effectiveness and applicability of the proposed scheme is tested with some typical processes, including an underdamped process with long dead-time, an overdamped high order process and a non-minimum phase one. The performance comparisons with some existing SOPDT-based techniques are also included for evaluation.

The remainder of this paper is organized as follows. In the next section, the predictor design, sliding mode controller design methodology as well as the optimal sliding surface design has been presented. Besides, for extension to non-minimum phase process, a simple strategy is introduced. The subsequent section performs extensive simulations to demonstrate and verify the proposed scheme. Finally conclusion remarks are made.

2. A SLIDING MODE CONTROL TECHNIQUE

In this section, we devote to develop a sliding mode control scheme for the regulation of chemical processes. In essence, the sliding mode control is a kind of model-based scheme, and the SOPDT model is the most widely used process model especially for the underdamped process and the high-order process which has the same multiple poles. Therefore, in what follows we shall present a systematic sliding mode controller design methodology based on an identified SOPDT model.

2.1 Predictor design based on an identified SOPDT model.

Consider an identified, stable SOPDT model as follows:

$$\widetilde{G}(s) = \frac{b_1}{s^2 + a_2 s + a_1} e^{-\theta s} \tag{1}$$

In order to deal with the input delay and hence facilitate the design of a sliding mode control system, we shall first discuss the development of a delay-ahead predictor based on the SOPDT model. To proceed, we convert the above model into an equivalent state space model as

$$\dot{\widetilde{x}}_1(t) = \widetilde{x}_2(t) \tag{2a}$$

$$\dot{\widetilde{x}}_2(t) = -a_1\widetilde{x}_1(t) - a_2\widetilde{x}_2(t) + b_1 u(t-\theta) \tag{2b}$$

$$\widetilde{y}(t) = \widetilde{x}_1(t) \tag{2c}$$

where $\widetilde{x}_1$ and $\widetilde{x}_2$ are the states, and $\widetilde{y}$ and u are, respectively, the model output and control input. By removing the time-delay from the above model, we can construct a delay-ahead prediction model as

$$\dot{x}_1^*(t) = x_2^*(t) \tag{3a}$$

$$\dot{x}_2^*(t) = -a_1 x_1^*(t) - a_2 x_2^*(t) + b_1 u(t) \tag{3b}$$

$$y^*(t) = x_1^*(t) \tag{3c}$$

In order to improve the accuracy of the state prediction, especially in the face with modelling errors and unmeasured disturbance, the following correction from the measured process output can be used for practical implementation

$$\hat{x}_1(t+\theta|t) = x_1^*(t) + y(t) - \widetilde{x}_1(t) \tag{4a}$$

and

$$\hat{x}_2(t+\theta|t) = x_2^*(t) \tag{4b}$$

where $y(t)$ is the actual process output and $\hat{x}_1(t+\theta|t)$ is the predicted output at time $t+\theta$ based on the information available at time t. By the comparison of Eqs. (2) and (3), it follows that $x^*(t) = \widetilde{x}(t+\theta)$ if the predictor is initialized as $x^*(0) = \widetilde{x}(\theta)$. This initialization can be achieved at steady state because in this case $\widetilde{x}(\theta) = \widetilde{x}(0)$. Hence, in the absence of plant/model mismatch the prediction model yields the plant state one time delay ahead, i.e. $\hat{x}(t+\theta|t) = \widetilde{x}(t+\theta)$. The presented prediction model, which is delay free, can facilitate the design of a sliding controller for SOPDT model.

2.2 Sliding mode controller design.

Having characterized the prediction model, we shall discuss in this subsection the design of a delay-ahead sliding mode controller. To account for model uncertainties in the controller design, we consider the following uncertain model

$$\dot{x}_1^*(t) = x_2^*(t) \tag{5a}$$

$$\dot{x}_2^*(t) = -(a_1 + \Delta a_1)x_1^*(t) - (a_2 + \Delta a_2)x_2^*(t) + (b_1 + \Delta b_1)u(t) \tag{5b}$$

where Δa_1, Δa_2 and Δb_1 are the variations of model parameters. To begin with, we rewrite the uncertain model as

$$\dot{x}_1^*(t) = x_2^*(t) \tag{6a}$$

$$\dot{x}_2^*(t) = -a_1 x_1^*(t) - a_2 x_2^*(t) + b_1 u(t) + h(\mathbf{x}^*, t) \tag{6b}$$

where

$$h(\mathbf{x}^*, t) = -\Delta a_1 x_1^*(t) - \Delta a_2 x_2^*(t) + \Delta b_1 u(t) \tag{7}$$

is the term containing the uncertainties. Let the hard constraint of the control input be

$$|u(t)| \le \bar{u} \tag{8}$$

and therefore the upper bound function, $h_{\max}(\cdot)$, of $h(\cdot)$ can be estimated as

$$\left|h(\mathbf{x}^*,t)\right| \le h_{\max}(\mathbf{x}^*,t) \tag{9}$$

where

$$h_{\max}(\mathbf{x}^*,t) = \sup\left|\Delta a_1 x_1^*(t)\right| + \sup\left|\Delta a_2 x_2^*(t)\right| + \max\left|\Delta b_1\right|\bar{u} \tag{10}$$

Next, let's choose a sliding function as follows:

$$\delta = c_1 x_1^*(t) + c_2 x_2^*(t) \tag{11}$$

The following theorem presents a sliding mode controller for the considered uncertain model.

Theorem 1: The following control law

$$\begin{aligned} u(t) = {} & b_1^{-1}[a_1 x_1^*(t) + (a_2 - c_2^{-1}c_1)x_2^*(t)] \\ & -(b_1 c_2)^{-1}(\alpha + \bar{h}(\mathbf{x}^*,t))\text{sign}(\delta) \end{aligned} \tag{12}$$

admit the uncertain system of (5) to satisfy the sliding condition of $\frac{1}{2}\frac{\mathrm{d}}{\mathrm{d}t}\delta^2 \le -\alpha|\delta|$, where α is the pre-specified positive constant regarding to the system performance and $\bar{h}(\mathbf{x}^*,t) = |c_2| h_{\max}(\mathbf{x}^*,t)$

Proof: See Appendix A.

The fundamental idea behind the use of the zero level set of the auxiliary output, denoted by $\Sigma = \{\mathbf{x}^* | \delta = 0\}$, as a sliding surface (switching manifold) is to force the controlled motion to adopt Σ as an integrated manifold. When the system trajectory is outside the manifold, the strategy forces the states toward the design sliding surface. Upon reaching Σ fast switching takes place in the immediate vicinity of Σ, which tries to keep the trajectory constrained to Σ. To eliminate the undesirable switching (chattering phenomena) of the manipulated variable, it is practical to replace the sign function in (12) by a saturation function, $\text{sat}(\delta/\beta)$, which is defined by

$$\text{sat}(\delta/\beta) = \begin{cases} \delta/\beta, & \text{if} \quad |\delta/\beta| < 1 \\ \text{sign}(\delta/\beta), & \text{if} \quad |\delta/\beta| \ge 1 \end{cases} \tag{13}$$

where $\beta > 0$ represents the boundary layer thickness. Here, it should be noted that the selection of the sliding function may affect the control performance since it is involved in the controller. In general, the selection of β represents the trade-off between the high performance and the extent of the chattering attenuation. To achieve optimal performance, we discuss in the following subsection the design of an optimal sliding function for practical application.

2.3 Optimal sliding function design.

Let's introduce a performance index as follows:

$$J = \int_{t_s}^{t} \mathbf{x}^*(t)\,\mathbf{Q}\,\mathbf{x}^*(t)\mathrm{d}t \tag{14}$$

where $\mathbf{x}^*(t) \equiv [x_1^*(t) \quad x_2^*(t)]^T$, t_s is the beginning time of the sliding motion, and $\mathbf{Q} = \begin{bmatrix} q_{11} & q_{12} \\ q_{21} & q_{22} \end{bmatrix}$ is a positive define, symmetric matrix, i.e. $q_{12} = q_{21}$ and $q_{11}q_{22} - q_{12}^2 > 0$. Also, let an auxiliary variable, v, be given by

$$v = x_2^*(t) + \frac{q_{12}}{q_{22}} x_1^*(t) \tag{15}$$

The performance function can thus be rewritten as

$$J = \int_{t_s}^{t} (q_{11}^* x_1^{*2}(t) + q_{22} v^2(t))\mathrm{d}t \tag{16}$$

where $q_{11}^* = q_{11} - q_{12}^2/q_{22}$. Then, with the definition of v, and from Eq. (15), we have

$$\dot{x}_1^*(t) = a_1^* x_1^*(t) + v \tag{17}$$

where $a_1^* = -q_{12}/q_{22}$. The optimal control law for the above dynamic equation with the performance index of (16) is given by (Sage and White, 1977)

$$v = -\frac{p}{q_{22}} x_1^*(t) \tag{18}$$

where p is the positive root of the quadratic polynomial $p^2 - 2a_1^* q_{22} p - q_{22} q_{11}^* = 0$, i.e. $p = -q_{12} + \sqrt{q_{11}q_{22}}$. By inserting Eq. (15) into the above optimal solution, we can conclude that a set of optimal sliding coefficients, c_1 and c_2, are given by $c_1 = \sqrt{q_{11}q_{22}}$ and $c_2 = q_{22}$.

2.4 Practical implementation.

With the output correction of Eq. (4), the control law of (12) can be implemented with the replacement of $\mathbf{x}^*(t)$ by $\hat{\mathbf{x}}(t+\theta\,|\,t)$. Thus, for practical implementation the control law is formulated as

$$\begin{aligned} u(t) = {} & b_1^{-1}[a_1 \hat{x}_1(t+\theta\,|\,t) + (a_2 - c_2^{-1}c_1)\hat{x}_2(t+\theta\,|\,t)] \\ & -(b_1 c_2)^{-1}(\alpha + \bar{h}(\hat{\mathbf{x}}(t+\theta\,|\,t),t))\text{sign}(\hat{\delta}) \end{aligned} \tag{19}$$

where the sliding function $\hat{\delta}$ is given by

$$\hat{\delta} = c_1 \hat{x}_1(t+\theta\,|\,t) + c_2 \hat{x}_2(t+\theta\,|\,t) \tag{20}$$

The schematic diagram of the proposed sliding mode control system is depicted in Fig. 1.

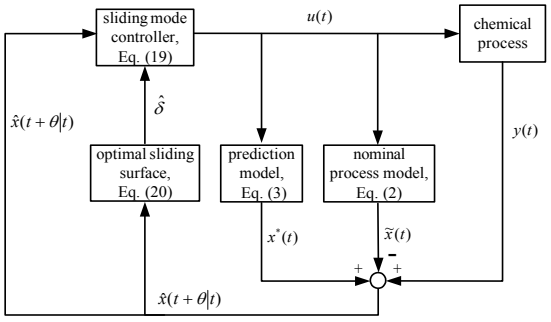

Fig. 1. A schematic diagram of the sliding mode control system.

2.5 Extension to non-minimum phase processes.

If the process has inverse response, we can identify the process as a SOPDT model with a right-half-plane (RHP) zero. For example, we can apply the

identification method of Park et al. (1998) to give a model of the form

$$\widetilde{G}(s) = \frac{-b_2 s + b_1}{s^2 + a_2 s + a_1} e^{-\theta s} \tag{21}$$

Then, by using the equivalent time-delay concept of Sung and Lee (1996)

$$\exp(-\theta_{\text{equivalent}} s) \cong 1 - \theta_{\text{equivalent}} s \tag{22}$$

the above non-minimum phase model can be transformed to a standard SOPDT model as

$$\overline{G}(s) = \frac{b_1}{s^2 + a_2 s + a_1} e^{-(\theta + \frac{b_2}{b_1}) s} \tag{23}$$

Therefore, based on the above equivalent SOPDT model, the proposed sliding mode control scheme can applied directly to non-minimum phase processes.

3. SIMULATION STUDIES

To verify the effectiveness and applicability of the proposed approach, we apply it to some typical chemical processes, including an underdamped process with long dead time, an overdamped high order process and a non-minimum phase system. The performance comparisons with the SOPDT model-based techniques of Sung et al. (1996) and Jahanmiri and Fallahi (1997) are included for evaluation. For the later simulation studies, we assume that the hard input constraint is $|u(t)| \le 1$, i.e., $\overline{u} = 1$. Also, the parameters of the sliding mode controller are set to be $\alpha = 0.1$ and $\beta = 0.4$. To demonstrate the ability of output regulation by the proposed approach, we further assume that the system outputs are perturbed to move away from their steady states with the magnitude of +1.0 initially in the Examples 3.1 and 3.2, and -0.2 in the Example 3.3.

Example 3.1 Underdamped second-order with long deadtime process.

$$G_p(s) = \frac{1}{9s^2 + 2.4s + 1} e^{-5s} \tag{24}$$

To apply the proposed scheme, we first convey a system identification technique to this system. With the closed-loop identification technique of Park et al. (1998), the SOPDT model parameters are given by $a_1 = 0.1111$, $a_2 = 0.2667$, $b_1 = 0.1111$ and $\theta = 5$. For sliding mode controller design, we assume that each of these model parameters has 25% variations from its estimated values. Also, let $\mathbf{Q} = \begin{bmatrix} 0.03 & 0 \\ 0 & 2 \end{bmatrix}$, then we arrive at a set of optimal sliding coefficients as $c_1 = 0.2449$ and $c_2 = 2$. Having previous information for design, one can easily implemented a sliding mode control system for this process. Fig. 2 depicts the output regulation results and the produced control input. The performance of the proposed scheme with arbitrary sliding coefficients is also included for comparison. From this figure, it is shown clearly that the proposed scheme provides a smoother and faster control performance as compared with the ISE optimal PID (Sung et al., 1996) and an IMC-PID scheme (Jahanmiri and Fallahi, 1997). The design of an optimal sliding surface for the sliding controller apparently results in a better performance than the arbitrary one does. Also observed is that the IMC-PID scheme of Jahanmiri and Fallahi (1997) produces more vigorous control input which violates the hard constraints and therefore results in a more oscillatory system output. On the contrary, there is no violation of the input hard constraint by applying the proposed technique since the input range can be pre-considered in the design stage. To verify the ability of handling with process uncertainties, we assume that the identified model remains unchanged, while the dynamics of the actual plant vary to $G_p(s) = \frac{1}{11s^2 + 2s + 1} e^{-6s}$. Fig. 3 depicts the system performance in the face with this plant/model mismatch. The simulation results show clearly that the proposed scheme is still very robust in response to the plant uncertainties, while the IMC-PID leads to undesirable oscillation.

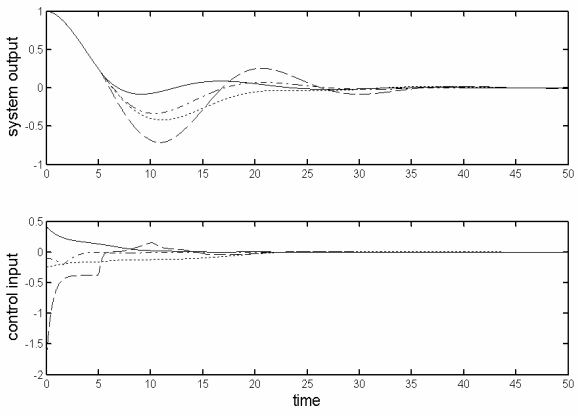

Fig. 2. Closed-loop system performance of Example 3.1. ——— the proposed approach with an optimal sliding surface; -·-·-·- the proposed approach with arbitrary sliding coefficients ($c_1 = 1$ and $c_2 = 2$) ; --------Jahanmiri and Fallahi (1997); ·····Sung et al. (1996).

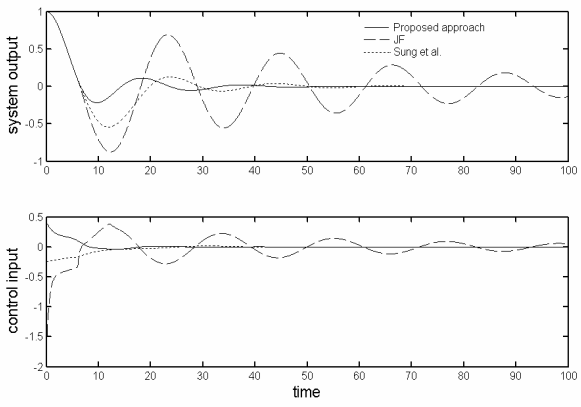

Fig. 3. Closed-loop system performance of Example 3.1 in the face with plant/model mismatch.

Example 3.2 High-order with deadtime process.

$$G_p(s) = \frac{1}{s^5 + 5s^4 + 10s^3 + 10s^2 + 5s + 1} e^{-2s} \qquad (25)$$

By using the technique of Park et al. (1998) to this process, the SOPDT model parameters are identified as $a_1 = 0.2291$, $a_2 = 0.8465$, $b_1 = 0.2291$ and $\theta = 3.3$. Similarly, we consider 25% parameter variations in the design of the sliding controller. Let $\mathbf{Q} = \begin{bmatrix} 0.3 & 0 \\ 0 & 1.2 \end{bmatrix}$ for this process, we have the optimal sliding coefficients of $c_1 = 0.6$ and $c_2 = 1.2$. From Fig. 4, it is also observed that the closed-loop control performance by the proposed approach is smoother than both the methods of Sung et al. (1996) and Jahanmiri and Fallahi (1997). To evaluate the ability of handling process uncertainties, we further assume that the process dynamics change to

$$G_p(s) = \frac{1}{s^5 + 3s^4 + 12s^3 + 9s^2 + 6s + 1} e^{-2.5s} \qquad (26)$$

but the identified model remains unchanged. The simulation results shown in Fig. 5 again corroborate the effectiveness and robustness of the proposed scheme in the face with uncertainties.

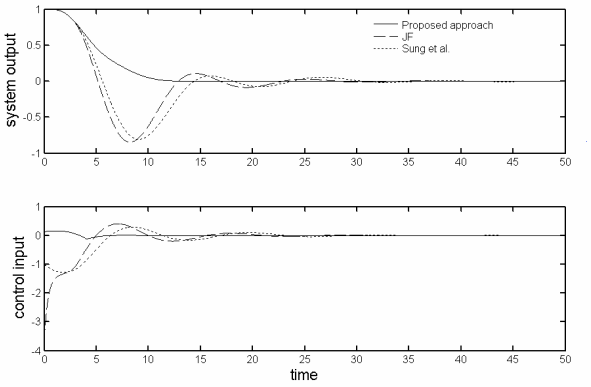

Fig. 4. Closed-loop system performance of Example 3.2.

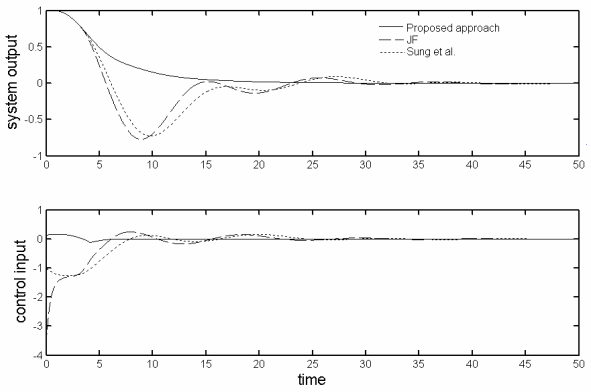

Fig. 5. Closed-loop system performance of Example 3.2 in the face with plant/model mismatch.

Example 3.3 Non-minimum phase process.

$$G_p(s) = \frac{-s + 0.5}{s^4 + 5s^3 + 8.75s^2 + 6.25s + 1.5} e^{-2s} \qquad (27)$$

To apply the proposed scheme to this non-minimum phase process, we first identify the process model as in the form of Eq. (21). By applying the identification technique of Park et al. (1998), we have the model parameters as $a_1 = 0.4417$, $a_2 = 1.2915$, $b_1 = 0.1473$, $b_2 = 0.2249$ and $\theta = 2.5387$. Therefore an equivalent SOPDT model can be given by

$$\overline{G}_p(s) = \frac{0.1473}{s^2 + 1.2915\,s + 0.4417} e^{-4.0655s} \qquad (28)$$

Now, by considering 25% parameter variations and choosing $\mathbf{Q} = \begin{bmatrix} 1.5 & 0 \\ 0 & 1.2 \end{bmatrix}$, we can construct a sliding mode control system for this non-minimum phase system. From Fig. 6, it is evident that the proposed scheme rapidly forces the system output back to its set-point. In contrast, both the approaches of Sung et al. (1996) and Jahanmiri and Fallahi (1997) results in serious oscillation in the process output as well as the produced control input. For the case that the process dynamics vary to

$$G_p(s) = \frac{-1.2s + 0.5}{s^4 + 6s^3 + 7.5s^2 + 5.5s + 1.5} e^{-2.5s} \qquad (29)$$

the simulation results shown in Fig. 7 reveal that the proposed control strategy still gives to robust system performance, while both the linear techniques of Sung et al. (1996) and Jahanmiri and Fallahi (1997) become quite unstable by the influence of this significant plant/model mismatch.

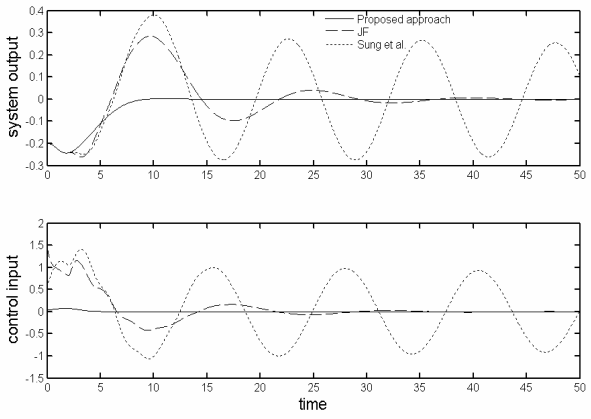

Fig. 6. Closed-loop system performance of Example 3.3.

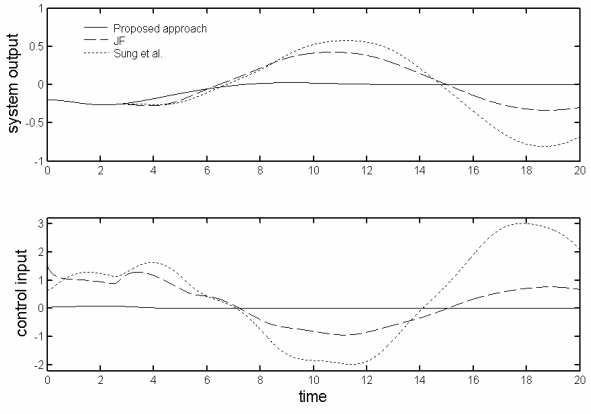

Fig. 7. Closed-loop system performance of Example 3.3 in the face with plant/model mismatch.

4. CONCLUSIONS

This paper has presented a systematic and novel model-based control system for the regulation of chemical processes. Based on an identified SOPDT model, a delay-ahead predictor and a designed optimal sliding surface, a sliding mode control scheme has been developed. The stability of the closed-loop system as well as the control performance is guaranteed with satisfying a sliding condition. Besides, with the concept of delay equivalent, the presented scheme can be easily extended to deal with the regulation problem of processes having inverse response. The effectiveness and applicability of the proposed sliding mode control technique has been tested with some typical plants. Moreover, performance comparisons with some existing SOPDT-based techniques are included for further evaluation. Extensive simulation results reveal that the proposed sliding mode control scheme appears to be a simple, robust and powerful approach to the regulation control of chemical processes.

Acknowledgement --- This paper was supported by the National Science Council of Taiwan (ROC) under Grant NSC90-2214-E-035-008.

Appendix A: Proof of the sliding condition

By taking time derivative of the sliding function (11) and inserting the control law of (12), we have

$$\begin{aligned}\dot{\delta} &= c_1\dot{x}_1^*(t) + c_2\dot{x}_2^*(t)\\ &= c_1x_2^*(t) + c_2\{-a_1x_1^*(t) - a_2x_2^*(t) + b_1[b_1^{-1}(a_1x_1^*(t)\\ &\quad + (a_2 - c_2^{-1}c_1)x_2^*(t)) - (b_1c_2)^{-1}(\alpha + \bar{h}(\mathbf{x}^*,t))\text{sign}(\delta)]\\ &\quad + h(\mathbf{x}^*,t)\}\\ &= -(\alpha + \bar{h}(\mathbf{x}^*,t))\text{sign}(\delta) + c_2h(\mathbf{x}^*,t)\end{aligned} \tag{A1}$$

Further, by checking

$$\begin{aligned}\frac{1}{2}\frac{\mathrm{d}}{\mathrm{d}t}\delta^2 &= \delta\cdot\dot{\delta} = -\alpha|\delta| - \bar{h}(\mathbf{x}^*,t)|\delta| + \delta c_2h(\mathbf{x}^*,t)\\ &= -\alpha|\delta| - \bar{h}(\mathbf{x}^*,t)|\delta|\left(1 - \frac{\delta c_2h(\mathbf{x}^*,t)}{|\delta|\bar{h}(\mathbf{x}^*,t)}\right)\\ &= -\alpha|\delta| - \bar{h}(\mathbf{x}^*,t)|\delta|\left(1 - \frac{\delta c_2h(\mathbf{x}^*,t)}{|\delta||c_2|h_{\max}(\mathbf{x}^*,t)}\right)\\ &\le -\alpha|\delta|\end{aligned} \tag{A2}$$

it is shown obviously that the sliding condition is satisfied.

REFERENCES

Chou, C.H. and C.C. Cheng (2001). Design of adaptive variable structure controllers for perturbed time-varying state delay systems. *Journal of the Franklin Institute*, ***338***, pp. 35-46.

Camacho, O., R. Rojas and W. Garcia (1999). Variable structure control applied to chemical processes with inverse response. *ISA Transactions*, ***38***, pp. 55-72.

Camacho, O. and C.A. Smith (2000). Sliding mode control: an approach to regulate nonlinear chemical processes. *ISA Transactions*, ***39***, pp. 205-218.

Hu, J., J. Chu and H. Su (2000). SMVSC for a class of time-delay uncertain systems with mismatching uncertainties. *IEE Proc.-Control Theory Appl.*, ***147***, pp. 687-693.

Hwang, S.H. (1993). Adaptive dominant pole design of PID controllers based on a single closed-loop test. *Chem. Engng Commun.*, ***124***, pp. 131-152.

Jahanmiri, A. and H.R. Fallahi (1997). New methods for process identification and design of feedback controller. *Trans IChemE*, ***75***, pp. 519-522.

Kojima, A., K. Uchida, E. Shimemura and S. Ishijima (1994). Robust stabilization of a system with delayed in control. *IEEE Transactions on Automatic Control*, ***39***, pp. 1694-1698.

Park, J.H., H. I1 Park and I.B. Lee (1998). Closed-loop on-line process identification using a proportional controller. *Chemical Engineering Science*, ***53***, pp. 1713-1724.

Roh, Y.H. and J.H. Oh (1999). Robust stabilization of uncertain input-delay systems by sliding mode control with delay compensation. *Automatica*, ***35***, pp. 1861-1865.

Roh, Y.H. and J.H. Oh (2000). Sliding mode control with uncertainty adaptation for uncertain input-delay systems. *Int. J. Control*, ***73***, pp.1255-1260.

Sage, A.P. and C.C. White (1985). *Optimum systems control* (2nd Ed). Prentice-Hall, Englewood Cliffs, New Jersey.

Sung, S.W. and I.B. Lee (1996). Limitations and countermeasures of PID controllers. *Ind. Engng Chem. Res.*, ***35***, pp. 2596-2610.

Sung, S.W., J. O, I.B. Lee, J. Lee and S.H. Yi (1996). Automatic tuning of PID controller using second-order plus time delay model. *Journal of Chemical Engineering of Japan*, ***29***, pp. 990-999.

Wang, Q.G., Y. Zhang and X. Guo (2001). Robust closed-loop identification with application to auto-tuning. *Journal of Process Control*, ***11***, pp. 519-530.

NONLINEAR MIMO ADAPTIVE PREDICTIVE CONTROL BASED ON WAVELET NETWORK MODEL[1]

Dexian Huang, Yuhong Wang and Yihui Jin

Department Automation , Tsinghua University, Beijing, 100084, China

ABSTRACT: A MIMO nonlinear adaptive predictive control strategy is presented in which the wavelet neural network based on a set of orthogonal wavelet functions is adopted. A nonlinear mapping from the network-input space to the wavelons output space in the hidden layer is performed firstly. Then, the output layer uses a linear structure. Its weight coefficients can be estimated by a linear least-squares estimation method. The excellent statistic properties of the weight parameter estimation can be obtained. Based on developed recursive algorithm, a MIMO nonlinear adaptive predictive control strategy is implemented. A simulated MIMO nonlinear process example shows that the control scheme is effective. *Copyright © 2002 IFAC*

Keywords: Non-linear MIMO adaptive control, predictive control, wavelet, neural network.

1. INTRODUCTION[1]

During the past twenty years, model-predictive control algorithms (MPC), based on linear process models, have been widely studied and applied in the chemical process industries. However, many processes are highly non-linear, uncertain and MPC algorithms based on linear process models may result in poor control performance and as a result, MPC techniques have recently been extended to these processes during the last decade(Keerthi,1990, Proll, 1994). However, generic nonlinear models is difficult to get and apply. Neural networks hold the promise of solving the problems. Feed forward neural networks provide a connectionist model that performs a mapping from an input space to an output space. Such networks can approximate any non-linear functions to an arbitrary accuracy. However, some network training problems, such as undesirable local minimum, of multi-layer perceptrons preclude their wide applications to on-line nonlinear system identification in adaptive control.

Wavelet is a powerful tool for function approximation (Daubechies, 1988). Under some mild conditions, the universal approximation of wavelet networks is guaranteed (Zhang ,1995). Based on a set of orthogonal wavelet functions, a least-squares learning algorithm is adopted to train the wavelet network in contrast to the non-linear gradient optimization used in standard feed forward networks (Bakshi and Stephanopoulos, 1993). In addition, wavelet neural networks have advantages in their structure, which is easy to specify in model identification. SISO first-order and high order non-linear dynamic processes have been successfully identified by wavelet neural networks and SISO non-linear predictive controllers have been realized. The control performances superior to a standard PID controller were achieved (Huang, 1997, 1999).

In this paper, a nonlinear adaptive predictive control strategy based orthogonal wavelet network model is presented. Based on a set of orthogonal wavelet functions, wavelet neural network performs a nonlinear mapping from the network-input space to the wavelons output space in hidden layer firstly. Since almost all dynamic processes in the chemical industries are lowpass systems, they can be approximated only by scale function terms $\sum_n \langle f, \varphi_{M,n} \rangle \varphi_{M,n}(x)$ at any accuracy. Therefore, we only use scale function in wavelons. This will simplifies wavelet network and decreases network size in online training obviously. Then, the output layer adopts linear structure. Its weight coefficients, i.e. $\langle f, \varphi_{M,n} \rangle$, can be estimated by a linear least-squares estimation algorithm.

Because the solid theory basis and special structure of wavelet neural network, the wavelet neural network holds the advantages superior to other neural network. First, its network structure is easy to specify based on its theory analysis and intuition. Secondly, network training do not rely on stochastic gradient type techniques such as the “back propagation” and can avoids the problem of poor convergence or undesirable local minimum, which is more serious for other neural networks when training data is contaminated seriously by noise.

The excellent statistic properties of the weight parameters of wavelet network as linear least-squares estimation algorithm in system identification can be proved. In intuition, it can been seen that the wavelet network is a ideal lowpass filter which passes true

[1] The project is supported by National High Tech R&D Project(NO. 863/CIMSAA413130) of China and by National key technologies R&D program of China(NO. 2001 BA201A04)

dynamic signal of the system identified and sorts the noise out as excellent frequency property of wavelet. The theory results are showed by simulation results. Both the wavelet network and the usual feedforward neural network are compared in a simulated CSTR system with serious noise. The long-range predictions based on trained wavelet network for testing data have obviously better prediction accuracy than that of he usual feedforward neural network. The prediction is very close to true output without noise. Both theory analysis and simulation study show that the identification method based on wavelet network is a robust and reliable identification method for nonlinear system. In addition, it is also generic method and is easy to use, instead of a method based on trial and error.

For online application in adaptive predictive control strategy, a recursive algorithm is given. The properties similar to that of recursive linear least-squares algorithm can be obtained as the recursive algorithm is completely same as recursive linear least squares algorithm. In addition, the closed loop-identifiability can be guaranteed. This is because the different wavelon outputs in hidden layer are irrelevant each other as orthogonal wavelet functions are adopted.

With developed recursive algorithm, a single input – single output nonlinear adaptive predictive control strategy is implemented. A same simulated CSTR process as above illustrates the application of the control scheme. Two methods to start adaptive controller are realized. Simulation results show two methods have good control results and expected performances are attained. When the parameter of controlled system is changed, online identification algorithm can track the parameter changing rapidly and then, still give good control results. The nonlinear adaptive predictive control strategy based on wavelet network is superior to the standard PID controller.

2. APPROXIMATION PRINCIPLE OF WAVELET NEURAL NETWORKS

According to approximate theory of wavelet network(Huang, 1997), two schemes for decomposing the function f(x) in $L^2(R)$ can be obtained. They are:

$$f(x) = \sum_{m,n} \left\langle f, \psi_{m,n} \right\rangle \psi_{m,n}(x) \tag{1}$$

and

$$f(x) = \sum_{n} \left\langle f, \varphi_{m_0,n} \right\rangle \varphi_{m_0,n}(x) + \sum_{m \geq m_0, n} \left\langle f, \psi_{m,n} \right\rangle \psi_{m,n}(x) \tag{2}$$

where m_0 is an arbitrary integer and represents the lowest resolution, i.e. scale, in the decomposition. Comparing equation (2) with equation (1), the former is more useful in dynamic process modeling. This is because most dynamic processes in the process industries are low-pass systems and, therefore, using scaling function can obviously decrease wavelet function terms. Furthermore, it is noted that f(x) can be closed arbitrarily only in V_M for some integer M. As long as the wavelet basis satisfies the Frame, there exists an M sufficiently large for any ε >0 (Zhang et al., 1995), such that

$$\left\| f(x) - \sum_{n} \left\langle f, \varphi_{M,n} \right\rangle \varphi_{M,n}(x) \right\| < \varepsilon \tag{3}$$

Therefore, it is realistic that a dynamic process can be approximated only by the scale function terms $\sum_{n} \left\langle f, \varphi_{M,n} \right\rangle \varphi_{M,n}(x)$ in permitted approximating accuracy. This will decrease approximating function terms and therefore decrease network size. In addition, this will also simplify wavelet network application.

The structure of a wavelet neural network is similar to that of an RBF network. However its structure can be decided by using wavelet frames. Because only scale function is used, then

$$\begin{aligned} f(x) &= \sum_{n} \left\langle f, \varphi_{M,n} \right\rangle \varphi_{M,n}(x) = \sum_{n} \left\langle f, \varphi_{M,n} \right\rangle 2^{M/2} \varphi(2^M x - n) \\ &= \sum_{n} \theta_n \varphi(Ra(x - b_n)) \end{aligned} \tag{4}$$

For multi-input systems $\varphi_{M,n}(X) = \varphi_{M,n_1}(x_1)\varphi_{M,n_2}(x_2) \cdots \varphi_{M,n_r}(x_r)$.

When the variation domains of the network inputs are defined, the neuron centers, i.e. b_n, are fixed on grids that are divided equally between each input domain. R_a is an adjustable parameter that changes the width of the frequency band of V_M .For the wavelet network studied in this paper, we use Shanonn wavelet function because it is an analytic function and is easy to use. Its scale function form is: $\varphi(x) = \frac{\sin \pi x}{\pi x}$. It is an orthonormal wavelet function. Other wavelet functions including non-orthonormal wavelet function can also be used.

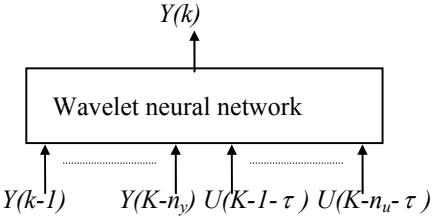

Figure 2. Wavelet network structure for dynamic system modeling

Consider a MIMO non-linear dynamic system denoted by the following equation:

$$\begin{aligned} &Y(k) = f(Y(k-1),.....,Y(k-n_y),U(k-1-\tau), \\ &.....,U(k-n_u-\tau)) \end{aligned} \tag{5}$$

where τ is the model input-output time delay, *(Y,U)* $\rightarrow$ *f(Y,U):* $R^l \times R^r \rightarrow R^l$. The network structure proposed by Narendra is adopted (Narendra and Parthasarathy, 1990). It is shown in Figure 2.

The network input and output dimensions are $\sum_{i=1}^{l} n_{yi} + \sum_{i=1}^{m} n_{ui}$ and l respectively.

The network weights are identified by linear least squares algorithm as following.

Firstly, we denote the optimum values of all $\langle f, \varphi_{M,n} \rangle$ as θ and all $\varphi_{M,n}(x)$ values at time k as *h(k)*. Then

$$Y(k) = h^T(k)\theta + n(k) \tag{6}$$

where both vector Y(k) and n(k) have dimension $1 \times l$, the dimension of h(k) is $N \times 1$ and the dimension of θ is $N \times l$. N is the number of neurons.

For *k=1,2,..., L*, the above equation constructs a linear equation group. It can be expressed in matrix form as following.

$$Y_L = H_L \theta + n_L \tag{7}$$

where

$$Y_L = [Y(1), Y(2), \cdots, Y(L)]^T$$

$$n_L = [n(1), n(2), \cdots, n(L)]^T$$

$$H_L = [H(1), H(2), \cdots, H(L)]^T$$

By linear least squares estimation, we can get the estimates of the weight parameters of the wavelet network as:

$$\hat{\theta}_{LS} = (H_L^T H_L)^{-1} H_L^T Y_L \tag{8}$$

The appropriate network structure was found through cross validation. The data for training neural network models were partitioned into the training set and validation set. A neural network was trained on the training set and tested on the validation set. A number of network structures were tried and the one giving the least error on the validation data set is adopted.

To select a proper network structure and network parameters *Ra* and *bn,* the following method is used:

(1) Determine the variation domains of the network inputs, x_{imin} and $x_{imax,}$ *i=1,...,r*;

(2) Select neuron number and centres as following: divide each input domain equally by n_i (start from a small value) and put neurons on grids. The number of neurons is: $N = n_1 . n_2 . \cdots . n_r$;

(3) Start with a small *Ra* initial value, estimate weight parameters with training set by linear least squares estimation and test the network with validation set. Increase *Ra* value until a satisfied result is obtained. Of cause, the knowledge about frequency property of process identified is helpful to estimate *Ra.*;

(4) Increase n_i and repeat steps (2) and (3) until the best network structure is obtained.

As soon as we get the network structure parameters, we can train the wavelet network. Because network structure parameters have a wide adapted ability, we do not need to search network structure parameters again in general cases. Afterward, it is only a linear least squares estimation problem. This will simplify implementation of wavelet networks and decrease training time especially in on-line model identification.

For online application in adaptive predictive control strategy, a recursive LS algorithm with exponential forgetting algorithm as following is adopted.

$$\begin{aligned}
&\hat{\theta}(t) = \hat{\theta}(t-1) + a(t)K(t)e(t) \\
&e(t) = y(t) - \varphi^T(t)\hat{\theta}(t-1) \\
&K(t) = \frac{P(t-1)\varphi(t)}{1 + \varphi^T(t)P(t-1)\varphi(t)} \\
&P(t) = \frac{P(t-1)}{\lambda} - \alpha \frac{P(t-1)\varphi(t)\varphi^T(t)P(t-1)}{I + \varphi^T(t)P(t-1)\varphi(t)} \\
&\quad + \beta I - \delta P(t-1)^2
\end{aligned} \tag{9}$$

$$K(t) = \frac{P(t-1)\varphi(t)}{\alpha + \varphi^T(t)P(t-1)\varphi(t)} \tag{10}$$

$$P(t) = \frac{1}{\alpha}[P(t-1) - \frac{P(t-1)\varphi(t)\varphi^T(t)P(t-1)}{\alpha + \varphi^T(t)P(t-1)\varphi(t)}] \tag{11}$$

Because the solid theory basis and special structure of wavelet neural network, wavelet neural network holds some advantages superior to other types of neural networks. First, its network structure is easy to specify based on its theory analysis and intuition. Secondly, network training do not rely on stochastic gradient type techniques such as the "back propagation" and avoids the problem of poor convergence or undesirable local minimum, which is more serious for other types of neural networks when training data is seriously contaminated by noise.

The properties similar to that of recursive linear least-squares algorithm can be obtained as the recursive algorithm is completely same as recursive linear least squares algorithm. In addition, the closed loop-identifiability can be guaranteed. This is because the different wavelon outputs in hidden layer are irrelevant each other as orthogonal wavelet functions are adopted

As soon as we can select appropriate value for *M*, there exists $\langle f, \varphi_{M,n} \rangle$ making $\sum_n \langle f, \varphi_{M,n} \rangle \varphi_{M,n}(X)$ approximating $f(Y_k, U_k)$ with expected accuracy. Then, we can prove the statistic properties of the weight parameter estimation of wavelet network as linear LS.

3. WAVELET NETWORK MODELING OF A MIMO NONLINEAR PROCESS

The wavelet neural network is used to model a MIMO nonlinear process as following.

$$X_{k+1} = AX_k + f(X_k)U_k \tag{12}$$

$$A = \begin{bmatrix} 0.5 & -0.35 \\ -0.15 & 0.4 \end{bmatrix} \tag{13}$$

$$f(X_k) = \begin{bmatrix} 0.15(x_k(1)+0.1) & 0.05x_k(2) \\ 0.1x_k(1) & 0.1(x_k(2)+0.03) \end{bmatrix} \tag{14}$$

The 1000 data point length's simulation data are produced by the system described by equation (12),(13) and (14). They are split into two set. The first 500 data points were used as training data while the remaining 500 data points were used as testing data.

Throughout the simulation experiment, we will follow the guidelines listed below:
The trained neural network is evaluated only by long range prediction for both the training and 'unseen' testing data. This is because both have good accuracy for one-step-ahead predictions and the dynamic model for control purpose needs to have better long-rang prediction accuracy.
We select τ = 0, n_y = [1,1], n_u = [1,1] and used 16 hidden neurons according to the experiment. The simulation results are shown in Figure 5 and Figure 6. Figure 5 is the prediction result of trained wavelet model for training data. Figure 6 is the prediction result of trained wavelet model for testing data. both prediction result for training data. and testing data is are very good. It is able to satisfy the requirement for dynamic control completely.

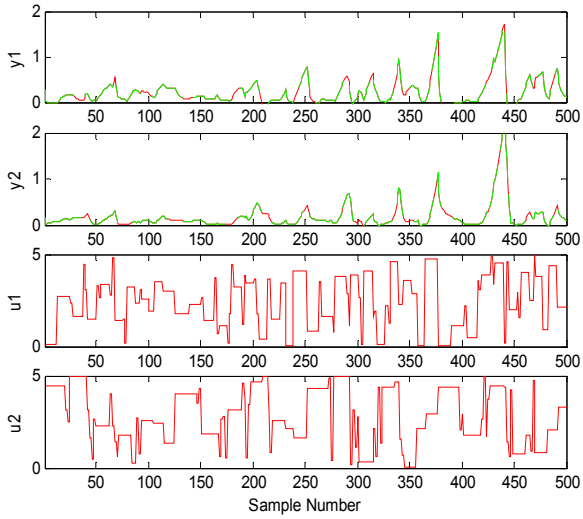

Figure 5. Predictions on training data

In the figures of output predictions, the true process output data is plotted as a solid line, the prediction output data is plotted as a dashed line.

From the simulation result, we observe that, the long range predictions based on wavelet network for training data and testing data have obviously very high prediction accuracy and the curves of both are almost superposition. Both theoretical analysis and simulation studies show that the identification method based on wavelet network is a robust and reliable identification method for non-linear systems.

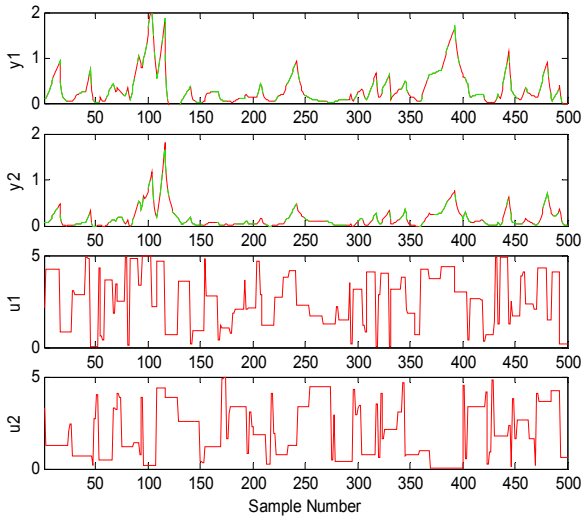

Figure 6. Predictions on testing data

4. Adaptive predictive control based wavelet network

Model predictive control is widely accepted, primarily due to its ability in real-time prediction, real-time optimisation and real-time feedback correction.

In the non-linear adaptive predictive control scheme shown in Figure 7, a process model, i.e., a wavelet network , is explicitly used to predict future process behavior. The same process model is also implicitly adopted to calculate control actions in such a way as to optimise the controller specifications at each sampling step. Furthermore, the difference between the current-time predicted output and the measured current-time process output is used to correct the model error and disturbances so as to improve its robustness. While predictive control is processed, the process model is updated by on-line recursive identification algorithm to enhance its robustness ulteriorly.

Consider MIMO non-linear dynamic system denoted by equation (5).

The selection of the control law is based on a quadratic performance index with a finite time horizon,

resulting in the following quadratic programming (QP) problem at time k

$$\min_{\Delta u(k),\Delta u(k+1),\cdots,\Delta u(k+L-1)} J(k) \quad (15)$$

where J (k) is

$$J(k)=\sum_{i=1}^{P}\left\|Y^{S}(k+i)-\hat{Y}(k+i|k)-Y(k)+\hat{Y}(k|k-P-1)\right\|_{Q}^{2} + \sum_{j=1}^{L}\left\|\Delta u(k+j-1|k)\right\|_{R}^{2} \quad (16)$$

where P is the prediction horizon, L is the control horizon, Q and R are weighting matrices.

The process model parameters, i.e. weight parameters of wavelet network, are updated by recursive identification algorithm with forgetting factor in Equation (9),(10) and (11).

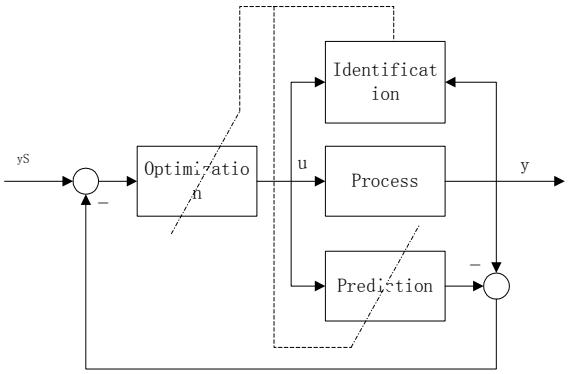

Figure 7. Adaptive Predictive Control Scheme based on Wavelet Network

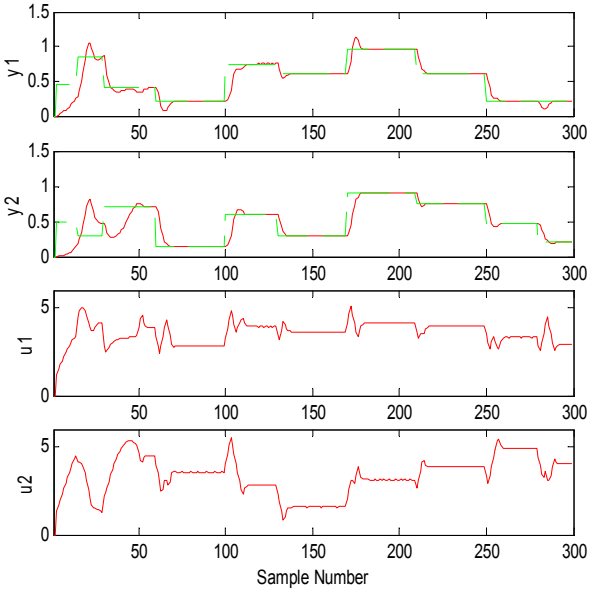

Figure 8. Adaptive Predictive Control based on Wavelet Network

A same simulated MIMO nonlinear process as above illustrates the application of the control scheme. Firstly, the control system uses PID control strategy (in this case, PID control strategy is used in first 50 steps) and then, the adaptive controller based on wavelet network model is closed after a crude model is obtained during PID control. The control result is shown in Figure 8. Simulation results show that expected performances are attained. The nonlinear adaptive predictive control strategy based on wavelet network is superior to the standard PID controller (The control result is shown in Figure 9. PID parameter is optimized by minimizing the integral squared error).

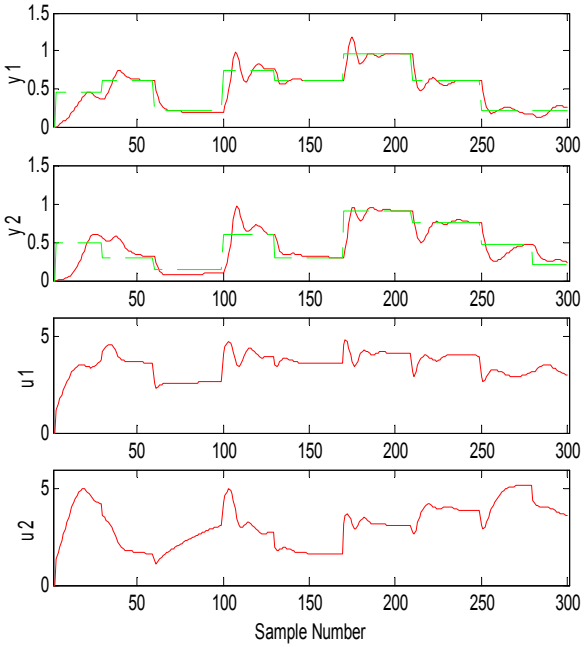

Figure 9. PID control

5. Conclusions

In this paper, a nonlinear MIMO adaptive predictive control strategy based orthogonal wavelet network model is realized. By both theory analysis and simulation study, The following conclusions can be educed.

(1) Wavelet network model only by scale function simplified wavelet network and decreased network size in online training obviously. Its weight coefficients can be estimated by a linear least-squares estimation algorithm. It is different from RBF network and other feed-forward neural networks, because its structure parameters are determined according to wavelet network reconstructing theory, instead of trial and error. In addition, its weight coefficients are estimated by a linear least-squares estimation algorithm, instead of non-linear optimization search method. Therefore, it can be proven that excellent statistic properties of its weight parameters as the

linear least-squares estimation algorithm in system identification has can be obtained (Huang, 2002). The identification method based on wavelet network is a robust and reliable identification method for nonlinear system. In addition, it is also generic method and is easy to use, instead of a method based on trial and error. The long-range predictions based on trained wavelet network for testing data with serious noise have obviously better prediction accuracy than that of the usual feed-forward neural network. The prediction is very close to true output without noise.

(2)For online application in adaptive predictive control strategy, a recursive algorithm is given. The properties similar to that of recursive linear least-squares algorithm can be obtained as the recursive algorithm is completely same as recursive linear least squares algorithm. In addition, the closed-loop identifiability can be guaranteed. This is because the different wavelon outputs in hidden layer are irrelevant each other as orthogonal wavelet functions are adopted. With developed recursive algorithm, a nonlinear MIMO adaptive predictive control strategy is implemented. A same simulated nonlinear process as above illustrates the application of the control scheme. The nonlinear MIMO adaptive predictive control strategy based on wavelet network is superior to the standard PID controller. Even if the optimal PID parameter is used, the control result for PID controller still has larger overshoot for controlled variable in high operation point and has week regulation action in low operation point as the simulated nonlinear system has a serious nonlinear character. In practice, it is difficult to get the optimal PID parameter for a large operation region. In contract, the nonlinear MIMO adaptive predictive controller can identify the control model on-line and achieve a satisfactory control effect by self. Because the controller does not need to be trained before it starts running, it is able to handle the any operating region. The nonlinear MIMO adaptive predictive control strategy is superior to nonlinear controllers in that it does not need to build non-linear control model by user and superior to the nonlinear adaptive controllers based conventional feed-forward neural networks in that it only need finite fix time to on-line updating network model in each control period because it is a recursive linear least squares problem. Besides, it is generic method for both model identification algorithm and control algorithm.

REFERENCES

I. Daubechies, “Orthonomal bases of compactly supported wavelets”, Comm. Pure Applied Math, Vol.91, pp.909-996, 1988.

D. Huang,, and Jin Y., “The application of wavelet neural networks to nonlinear predictive control”, ICNN97 IEEE, Houston, Texas, US, Vol.2, 1997.

D. Huang,, J. Wang and Y. Jin, “Application research of wavelet neural networks in process predictive control”, Journal of Tsinghua University, Vol.39, No. 1, pp. 91-94, 1999.

D. Huang, Y. Jin, J. ZHANG and A. J. Morris Nonlinear “Chemical Process Modelling and Application in Epichlorhydrine Production Plant Using Wavelet Networks”. Chinese Journal of Chemical Engineering, Vol 10, No.4, 2002.

Maner, R. B., Doyle. III, F. J., Ogunnaike, B. A. and Pearson, R. K., “ Nonlinear model predictive control of a simulated multivariable polymerization reactor using second-order volterra models” Automatica Vol.32, No.9, pp. 1285-1301, 1996

Bakshi, B. R. and Stephanopoulos, G., “Wave-net: a multiresolution, hierarchical neural network with localised learning”, AICHE J., Vol.39, No.1, pp.57-81, 1993.

T. Proll and M. N. Karim, "Real-time design of an adaptive nonlinear predictive controller", INT. J., Vol. 59, No. 3, pp. 863-889, 1994

J. Zhang,, G. Walter, G. G.,Miao, Y. and Lee, W. N. W., “Wavelet neural networks for function learning” IEEE Signal Processing, Vol.43, No.6, pp.1485-1497,1995.

INPUT-OUTPUT PAIRING OF MULTIVARIABLE PREDICTIVE CONTROL

Ling-Cong Chen[#], Pu Yuan*, Gui-Li Zhang*

**University of Petroleum, P.O. Box 902 Beijing 100083, China*
[#]*GAIN Tech Co., P.O. Box 902ext.79, Beijing 100083, China*

Abstract: Regardless of what predictive control strategy is used, the predictive horizon is the main design parameter. The stability, control performance and robustness of predictive control system are mainly depended on it. For multivariable predictive controller, selection of predictive horizon is an input-output pairing problem. In this paper, Response Index Array, Dynamic Interaction Index Array and Relative Steady-State Index Array are proposed as the criteria for the selection of predictive horizon and pairing. The design procedure for multivariable predictive controller is summed up. As an example, the pairing of a heavy oil fractionator is given. The design has been successfully implemented on several industrial fractionators. *Copyright © 2002 IFAC*

Keywords: Predictive control, Input-output pairing, MIMO System

1. INTRODUCTION

During the last two decades, model predictive control (MPC) has become an attractive control strategy within the area of process industries. MPC is a successful strategy for handling multivariable and/or constrained control problems (Garcia and Morari, 1989). Generally, the multivariable controller does not need input-output pairing, which is a main design problem in the multi-loop control, such as conventional PID control. If the predictive horizon and control horizon of MPC are determined, there is no input-output pairing problem. But, pairing problem will rise during MPC design to determine predictive horizon.

So far, the MPC presented in the literatures may be classified into two strategies:

1. MPC based on the input(manipulated variable, MV)-output (controlled variable, CV) model, such as MAC (Richalet, J et.al. 1978; Rouhani,R. and R.K. Mehra 1982), DMC (Cutler, C.R. and B.L. Remaker, 1980), GPC (Clarke, D.W. et.al. 1987,1989), IMC (Garcia and Morari ,1982,1985). Soeterboek (1992) proposed predictive control: a unified approach for such kind of MPC strategies.
2. MPC based on the state space model and state variable feedback (Yuan, 1993).

Sun and Yuan (1993, 1997) proposed Unified Predictive Control, which is based on Polynomial Matrix Description (PMD), for all kinds of the MPC strategies. Yu and Yuan (2002) proved theoretically that all kinds of MPC are equivalent, i.e., the same control performance, depends on prediction horizon P, will be achieved by different MPC strategies as long as there is no model mismatch and no disturbance. In real world, there are unknown disturbance and model mismatch. So different MPC are different in robustness and disturbance rejection. This topic will not be discussed in this paper.

For multivariable process, RGA (Bristol, 1966) is usually used to measure the interaction and the design of multi-loop control. RGA, based on steady-state gain of controlled process, is not suitable for the MPC design, which is based on the dynamic response. In the literatures, contributions on the design of MPC are presented as well as the different MPC strategies mentioned above. The main design issue is how to determine the predictive horizon. MPC has been widely used on multivariable systems, yet, by the author's knowledge, the discussion in literatures of how to determine the predictive horizon for multivariable systems is much less than that of SISO systems.

In this paper, the relationship between predictive horizon and stability, control performance and robustness of MPC system, as the basis of system design, are reviewed in second section. The design of multivariable MPC is an input-output pairing problem and dynamic response index, interaction index and relative steady-state index are proposed as pairing criteria in third section. MPC system design procedure was summed up in section IV. As an example, design of MPC for a heavy oil fractionator is illustrated.

2. PREDICTIVE HORIZON

For multivariable MPC, different CV has different

control demand and different response to MV. A reasonable design is that every CV has its own predictive horizon p_i. The predictive horizon of the system **P** is a vector:

$$\mathbf{P} = \begin{bmatrix} p_1 & p_2 & \cdots & p_r \end{bmatrix}^T \qquad (2\text{-}1)$$

where: p_i is the predictive horizon (number of discrete interval) of i^{th} controlled variable.

For illustration and without loss of gernalization, MPC with single prediction algorithm (Yuan, 1992) is used in the following discussion.

The optimal control move was deduced as:

$$\Delta u(k) = S^{-1}(P)[Y_S(k) - Y_p(k)] \qquad (2\text{-}2)$$

where:

$u \in R^m$ Manipulated variable (MV);

$Y \in R^r$ Controlled variable (CV);

$\Delta u(k) = u(k) - u(k-1)$

$$\mathbf{S[(P)]} = \begin{bmatrix} S_{11}(p_1) & S_{12}(p_1) & \cdots & S_{1r}(p_1) \\ S_{21}(p_2) & \cdots & \cdots & S_{2r}(p_2) \\ \vdots & \vdots & \vdots & \vdots \\ S_{r1}(p_r) & \cdots & \cdots & S_{rr}(p_r) \end{bmatrix} \qquad (2\text{-}3)$$

$S_{ij}(p_i)$ is i^{th} CV response at p_i^{th} interval instant after j^{th} MV unit step.

$Y_S(k) =$ Set point of controlled variable;

$Y_p(k) = Y(k) + F_X(z^{-1})\Delta X(k) + F_u(z^{-1})\Delta u(k)$

(Prediction of CV while $\Delta u(k+i) = 0, \quad i \geq 0$)

$X \in R^n$ Measurable state variable (include CV);

$\Delta X(k) = X(k) - X(k-1)$

$F(z^{-1}) = F_0 + F_1 z^{-1} + \cdots + F_q z^{-q}$

(Feedback polynomial matrix)

Xi (1993), Yuan (1992, 1993, 1994, and 1997) and others proved some theoretical results (assuming no model mismatch and *r*=*m*) for stability and control performance of MPC system related to predictive horizon:

Theorem 1: $\det[\mathbf{S(P)}] \neq 0 \qquad (2\text{-}4)$

is a necessary stability condition for MPC system.

Theorem 2: If the controlled process is stable and functionally controllable, then:

$$\frac{\det[\mathbf{S(P)}]}{\det[\mathbf{S}(\infty)]} > 0 \qquad (2\text{-}5)$$

is a necessary stability condition for MPC system, where: $[\mathbf{S}(\infty)]$ is the steady-state gain matrix of controlled process.

Theorem 3: If the controlled process is stable and $p_i (i = 1, 2, \cdots, r)$ is tuned sufficiently large, then the MPC system is stable.

Theorem 4: If: $p_i = \delta_i + 1;$ and Theorem1 and Theorem2 are satisfied, then: the i^{th} CV reaches to perfect control.

If $p_i = \delta_i + 1; \quad i = 1, 2, \cdots, r \qquad (2\text{-}6)$

And both Theorem 1 and Theorem 2 are satisfied; then: the MPC system reaches to perfect control (all CV reach to perfect control), where: $\delta_i = \delta_i^d - \delta_i^n - 1$, δ_i^d and δ_i^n are the orders of denominator and nominator of i^{th} row in impulse transfer function matrix, respectively.

Perfect Control is defined as: if CV reaches to its set-point at every control (sampling) instant after minimum time delay of set-point or disturbance step change. It is obvious that perfect control is decoupled between CV and CV to disturbance.

In real world, perfect control can be reached only for a class of controlled process with special dynamic property. In most cases, it is difficult to reach, not only limited by the above condition, but also limited by model mismatch and robustness. The control (MV) move is usually another limit. For same CV's deviation, large control move usually lead to fast response and weaker robustness. If increasing prediction horizon p_i makes smaller control move, then, the sluggish response and the better robustness; otherwise, if increasing predictive horizon leads to larger control move (may be constrained by limit), then, the contrary.

According to above analysis, Yuan (1992) proposed to use Relative Predictive Horizon (RPH) β for SISO system to select predictive horizon and trade-off the control performance and control move constraints. RPH is defined as:

$$\beta = \frac{S(p)}{S(\infty)} \qquad (2\text{-}7)$$

Where: $S(p)$ is the value of step response at predictive horizon; $S(\infty)$ is the steady-state value of step response.

$\beta = 0.3 \sim 0.8$ is recommended. Large β leads to a stronger robustness, less control move and sluggish response.

If β is specified, predictive horizon P can be calculated from eq.(2-7). Since β is a float variable and P is an integer,

If $S(\infty) \neq 0$, $\frac{S(n-1)}{S(\infty)} < \beta \leq \frac{S(n)}{S(\infty)}$, then: $p = n$;

If $S(\infty) = 0$, then: $p = \infty$. (2-8)

This result is extended to multivariable system in this paper.

3. INPUT-OUTPUT PAIRING CRITERIA

For MIMO system, every CV is related to *m*

manipulated variables, and different MV has different dynamic response. If β is specified, different MV has different predictive horizon. Which MV should be used to determine the corresponding predictive horizon? In this point, the input-output pairing is still a problem for multivariable predictive control system as well as multi-loop control system, but in different content.

For MIMO system, better control performance is desired as well as SISO system and fast response MV should be selected. The distinction is the interaction between CV and MV, and decoupling or less interaction is always required. More MV than CV or more CV than MV made the system more complicated.

The starting point of MPC design is to satisfy the required control performance, which is related to the Relative Predictive Horizon RPH as mentioned above. For MIMO system, the required control performance of i^{th} CV and corresponding RPH β_i can be specified previously. But, the predictive horizon p_i is different for different MV. If β_i is specified, to determine p_i is a problem of input (MV)-output (CV) pairing.

For input-output paring, three Index Arrays are defined.

Definition 1: Response Index Array r_{ij} (RIA)

For i^{th} CV, if β_i is specified, corresponding predictive horizon for j^{th} MV is $p_{ij}(j=1,2,\cdots,m)$,

Let: $p_{i\min}=\underset{j}{Min}\{p_{ij}\}$, $\gamma_{ij}=\dfrac{p_{i\min}}{p_{ij}}$.

$$RIA=\{\gamma_{ij}\}=\begin{bmatrix}\gamma_{11} & \gamma_{12} & \cdots & \gamma_{1m}\\ \gamma_{21} & \gamma_{22} & \ddots & \vdots\\ \vdots & \ddots & \ddots & \vdots\\ \gamma_{r1} & \cdots & \cdots & \gamma_{rm}\end{bmatrix} \qquad (3\text{-}1)$$

is defined as Response Index Array (RIA).

RIA is a criterion of response speed of different MV. The larger the p_{ij}, the faster the response of i^{th} CV to j^{th} MV. In order to make i^{th} CV has better control performance, by the knowledge of SISO system mentioned in Section 2, the prediction horizon P_i may be selected as $p_i=Min\{p_{ij}\}$ $(j=1,2,\cdots,m)$, and correspondingly $\gamma_{ij}=1$. However, for multivariable system, the interaction must be taken into account.

Definition 2: Dynamic Interaction Index Array μ_{ij} (DIA)

For i^{th} CV, if β_i is specified, it has m possible CV-MV pairing with corresponding predictive horizon p_{ij}. For every possible pairing, the corresponding Dynamic Interaction Index is defined as:

$$\mu_{ij}=\frac{\left|S_{ij}(p_{ij})\right|}{\sum_{l=1}^{m}\left|S_{il}(p_{ij})\right|} \qquad (3\text{-}2)$$

The larger the $\mu_{ij,}$ the weaker the interaction for i^{th} CV-j^{th} MV pairing. It is a possible pairing candidate.

If $\mu_{ij}=1$, it implies that i^{th} CV is affected only by the j^{th} MV and has no interaction with other MV in dynamic. It is a prior pairing candidate. However, the steady-state property must be considered also.

Definition 3: Steady-State Index Array λ_{ij} (SIA)

$$\lambda_{ij}=\frac{\left|S_{ij}(\infty)\right|}{\sum_{l=1}^{m}\left|S_{il}(\infty)\right|} \qquad (3\text{-}3)$$

If $\lambda_{ij}=1$, it implies that i^{th} CV is affected only by the j^{th} MV and has no interaction with other MV in steady-state.

Model predictive control, as showed in eq.(2-2), is a non-steady-state error control strategy for step input and decoupled in steady-state, but the control move may be too large, so, the main consideration of the SIA is the effectiveness and limit of MV.

The larger the λ_{ij}, the smaller the control move in steady-state. If λ_{ij} is near to zero, it means that this MV is ineffective.

RIA, DIA and SIA should be considered in MIMO system design. In addition, the optimization, safety and other requirements of MV should be also considered. The following pairing index $\{a_{ij}\}$ is suggested.

Definition 4: Pairing Index

$$A=\{a_{ij}\}=\begin{bmatrix}\xi_{11} & \cdots & \xi_{1m}\\ \vdots & \ddots & \vdots\\ \xi_{r1} & \cdots & \xi_{rm}\end{bmatrix}\begin{bmatrix}\delta_1 & 0 & \cdots & 0\\ 0 & \delta_2 & \ddots & \vdots\\ \vdots & \ddots & \ddots & 0\\ 0 & \cdots & 0 & \delta_m\end{bmatrix} \qquad (3\text{-}4)$$

Where: $\xi_{ij}=\gamma_{ij}+q_i\mu_{ij}+w_i\lambda_{ij}$ (3-5)

q_i = interaction weighting factor for i^{th} CV.
w_j = control move weighting factor for i^{th} CV.
δ_j = weighting factor for jth MV.

For i^{th} CV, pairing MV is:

$$MV(j):\ \{Max[a_{ij}],(j=1,2,\cdots,m)\} \qquad (3\text{-}6)$$

4. MPC DESIGN PROCEDURE

According to the above results, the design procedures for predictive horizon and input-output pairing are summed up as:

1. Give the priority of each CV and corresponding β_i according to the requirement of control performance.

β_i =0.3~0.8 is recommended. Large β leads to a stronger robustness, less control move and sluggish response. Usually, higher priority CV may have smaller β_i.

2. If the controlled process has more MV than CV, give the control priority, optimum priority and target for each MV. If the controlled process has more CV than MV, give the weighting factor of each CV. These two cases, which are beyond the scope of this paper, will not be discussed in detail.

3. Calculate p_{ij}, r_{ij}, μ_{ij}, λ_{ij}, ξ_{ij}.

4. From higher to lower priority of CV, the MV who made least value in ξ_{ij} should be selected as the pairing for control. If the selected MV has been used by higher priority CV, then in the remaining MVs, the one who made ξ_{ij} the least value is recommended in order to have stronger robustness. This procedure results a predictive horizon for each CV and predictive horizon vector $P=[p_1 \quad p_2 \quad \cdots \quad p_r]^T$ for MPC.

4. Check stability by Theorem 1, 2. If unsatisfied, tune β_i or p_i and return to step 1. According to Theorem 3, larger β_i or p_i may usually lead to a stable MPC system.

5. Check control move: MPC design should meet the requirement of control move limit. However, the control move depends on the set-point change, disturbance and status of controlled process. In order to evaluate the control move in design phase, assume all set-point has unit step and initial state equal to zero, check the control move at first sampling instant and steady-state.

The control move at first sampling instant after set-point unit step is:

$$\Delta u = S^{-1}(P) \tag{4-1}$$

The control move at steady-state after unit step is:

$$\Delta u = S^{-1}(\infty) \tag{4-2}$$

So the maximum control move is:

$$\Delta u_{j\max} = \max_i \{\overline{S}_1^j(P), \overline{S}_2^j(P), \cdots, \overline{S}_m^j(P)\} \tag{4-2}$$

$$(j = 1, 2, \cdots, m)$$

Where:

$\overline{S}_i^j(P)$ is the i^{th} element of j^{th} row of $S^{-1}(P)$ or $S^{-1}(\infty)$;

$S(P)$ = step response matrix [eq.(2-3)]

If $\Delta u_{j\max}$ violates the limit, then tune β_i or p_i and return to step 1. Large β_i or p_i usually lead to smaller control move.

6. Simulation. If unsatisfied, choose *P* again and return to step 1.

The design procedure may be extended to the case of more MV than CV or more CV than MV.

5. EXAMPLE

For illustration, consider the pairing of a heavy oil fractionator, shown in Fig.1. The fractionator has top and two side-draw products. In order to keep the product specification, top and two side-draw temperatures are main controlled variables, as CV1, CV2 and CV3 in Fig.1. Usually, it has three PID controllers TC to keep the temperatures at their set-points.

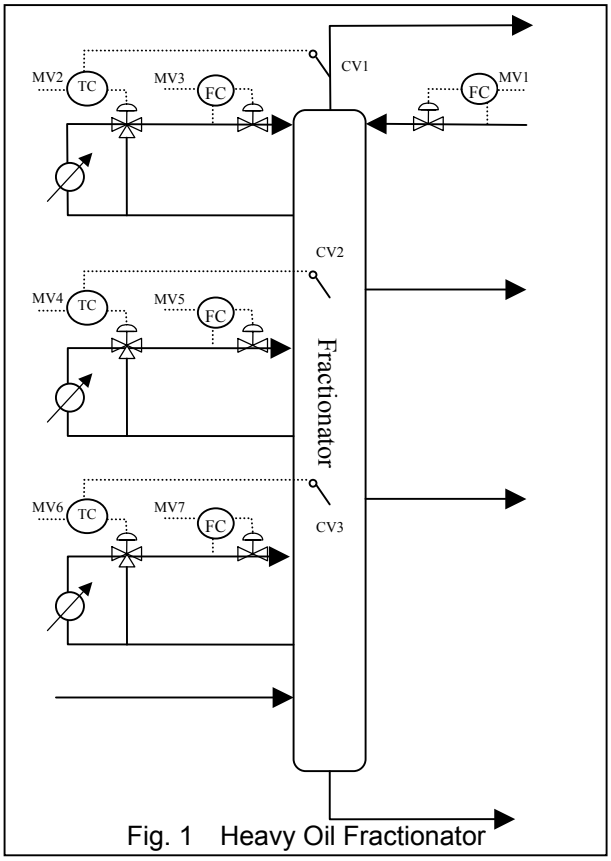

Fig. 1 Heavy Oil Fractionator

The fractionator may have seven manipulated variables:

MV1: Top Reflux Flow rate (PID set point)

MV2: Top Heat Remove Circulation Flow rate (PID set point)

MV3: Set Point of Top Temperature PID Controller (Three-way valve)

MV4: First Heat Remove Circulation Flow rate (PID set point)

MV5: Set Point of first draw Temperature PID Controller (Three-way valve)

MV6: Second Heat Remove Circulation Flow rate (PID set point)

MV7: Set Point of second draw Temperature PID Controller (Three-way valve)

All of the MV has high and low limit as well as corresponding valve opening. If one MV is limited, the controller will select other unlimited MV. So, all of the possible CV-MV pairing and corresponding predictive horizon should be given. For the 3 CV and 7 MV of a fractionator, it has 21 possible pairings. But, if the pairing has too small value of pairing index a_{ij}, it is not suitable for control, which will be illustrated below. If a CV has more suitable MV, the priority of MV should be

specified according to the value of a_{ij} and optimization requirement.

Since fractionator has more MV than CV, it is able to push some MV to its optimum value while keep the control performance by other suitable MVs. Usually the optimization targets are minimum heat remove flowrate or minimum open of by-pass (three-way) valve of heat exchanger or steam generator.

The step responses of CV1, CV2 and CV3 to the 7 MVs are given in Fig.2, Fig.3 and Fig.4 respectively.

The priority of CV is specified as: CV1, CV2 and CV3 from higher to lower. The relative predictive horizon is specified as:

$$\beta = [\beta_1\ \beta_2\ \beta_3] = [0.6 \quad 0.6 \quad 0.6]$$

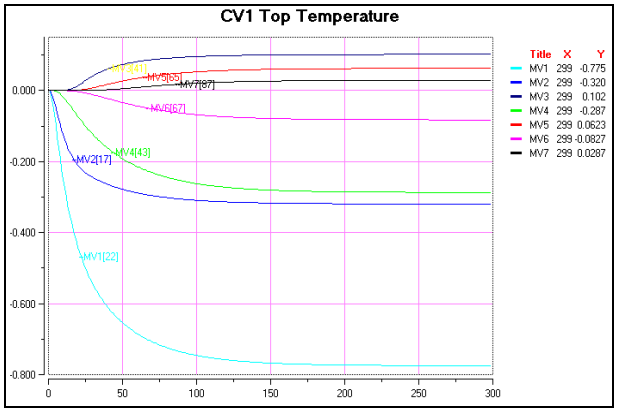

Fig. 2 CV1 Unit Step Response

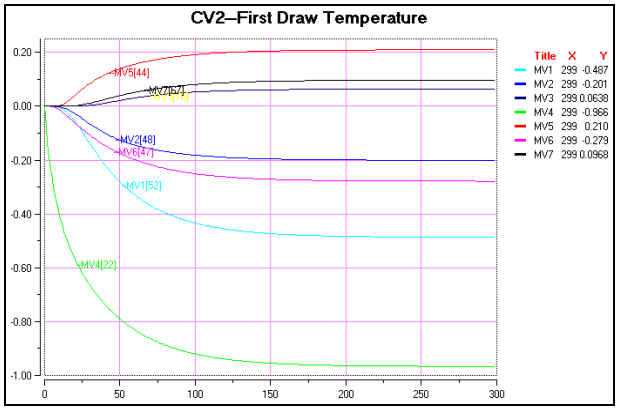

Fig. 3 CV2 Unit Step Response

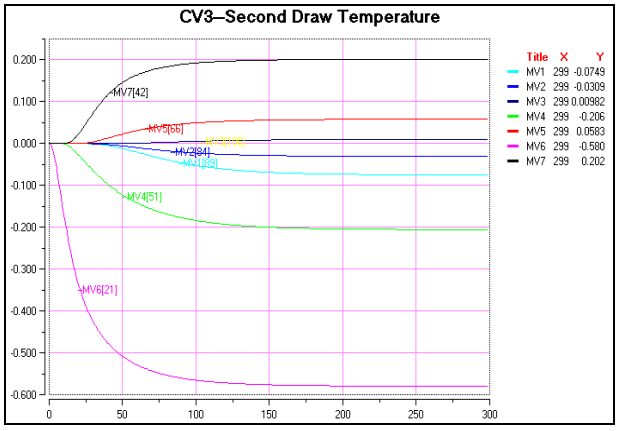

Fig. 4 CV3 Unit Step Response

According to the unit step responses, the predictive horizon, RIA, DIA and SIA are calculated as:

$$\{p_{ij}\} = \begin{bmatrix} 22 & 17 & 41 & 43 & 64 & 67 & 85 \\ 52 & 48 & 70 & 22 & 44 & 47 & 66 \\ 87 & 83 & 104 & 50 & 66 & 21 & 42 \end{bmatrix}$$

$$\{\gamma_{ij}\} = \begin{bmatrix} 0.775 & 1.0 & 0.415 & 0.395 & 0.266 & 0.254 & 0.2 \\ 0.424 & 0.459 & 0.315 & 1.0 & 0.5 & 0.467 & 0.333 \\ 0.241 & 0.253 & 0.202 & 0.42 & 0.318 & 1.00 & 0.5 \end{bmatrix}$$

$$\{\mu_{ij}\} = \begin{bmatrix} 0.568 & 0.296 & 0.06 & 0.147 & 0.027 & 0.035 & 0.009 \\ 0.181 & 0.077 & 0.02 & 0.715 & 0.085 & 0.112 & 0.032 \\ 0.044 & 0.018 & 0.005 & 0.151 & 0.038 & 0.855 & 0.169 \end{bmatrix}$$

$$\{\lambda_{ij}\} = \begin{bmatrix} 0.467 & 0.193 & 0.061 & 0.173 & 0.037 & 0.05 & 0.017 \\ 0.211 & 0.087 & 0.028 & 0.42 & 0.091 & 0.121 & 0.032 \\ 0.064 & 0.027 & 0.008 & 0.185 & 0.05 & 0.5 & 0.174 \end{bmatrix}$$

Assuming: $Q = W = diag[1] = I$

$$\delta_1 = 0.3\,,\ \delta_2 = \cdots = \delta_7 = 1.0$$

the pairing index a_{ij} is:

$$\{a_{ij}\} = \begin{bmatrix} 0.548 & 1.489 & 0.637 & 0.712 & 0.33 & 0.339 & 0.226 \\ 0.288 & 0.623 & 0.363 & 2.135 & 0.676 & 0.7 & 0.407 \\ 0.105 & 0.298 & 0.316 & 0.856 & 0.406 & 2.355 & 0.843 \end{bmatrix}$$

According to the value of ξ_{1j}, pairing is determined.

For CV1: MV1, MV2, MV3, MV4 are suitable pairings. MV5, MV6, MV7 have smaller pairing index, so they are not suitable pairings. But MV4 is a better pairing candidate to CV2, so the final pairings for CV1 are MV1, MV2 and MV3. The priority is: MV2, MV3, and MV1 from higher to lower. (MV1 has lower value of pairing index, however it is mainly required to reach its optimum value.)

For CV2: MV4 and MV5 are suitable pairings, and the priority is MV4, MV5 from higher to lower.

For CV3: MV6 and MV7 are suitable pairings, and the priority is MV4, MV5 from higher to lower.

These results show that among the 21 possible pairings only seven pairings are suitable. Each CV has fewer pairings than whole MV. Nevertheless, the control system is multivariable according to the eq.(2-2). These pairings have been applied to several industrial heavy oil fractionators.

For heavy oil fractionator, Final Boiling Point (FBP) of top product and 95% ASTM of first draw product are more important controlled variables. They are depended on the top temperature and first draw temperature respectively. They have the same step responses and use same manipulated variables of temperature control, and,

the same predictive horizon as well as pairings.

FBP and 95%ASTM should be keep on specified setpoint since they are designed as set point controlled variable. Top and first draw temperatures are designed as zone controlled variables. If the predicted temperatures do not violate their high or low limits, no control is required. The number of CV need to control and the number of available MV are depended on the operation situation. So, the structure of the fractionator as a controlled process is varied. A varied structure predictive coordinated control system based on above design and control requirements for the fractionator was implemented in several industrial plants.

The application shows that the pairing design is suitable for the multivariable control. Fig.5 is a real-time trend acquired from the industrial plant. Set-point of 95% ASTM (D) has been decreased at 9:17 and first heat remove exchanger (steam generator) by-pass valve (F) has been gradually closed to its optimum value. FBP is nearly decoupled to the set-point change of 95% ASTM. Both FBP and 95% ASTM are running with less deviation to their setpoints. MV1 is kept at its optimum value (not showed in Fig.5).

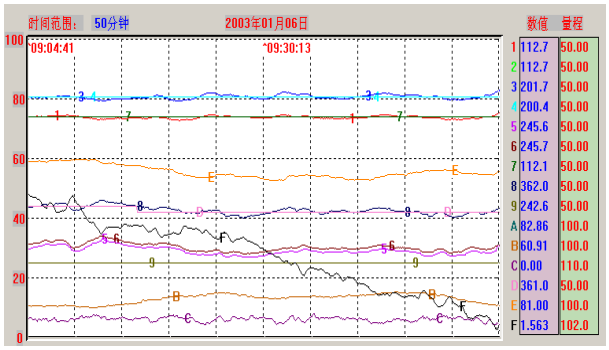

Fig.5 Real time trend of fractionatotr

1,2,7: top temperature and its set-point(CV1)
3,4: Final Boiling Point and its setpoint
5,6,9: first draw temperature and its set-point(CV2)
8,D: 95% ASTM of first draw its set-point
B: first heat remove flowrate(MV4)
C: top heat remover exchanger by-pass valve(MV3)
E: top heat remover circulation flowrate(MV2)
F: first heat remover exchanger by-pass valve(MV5)

6. CONCLUSION

Input-output pairing is a basic problem for multivariable control system design as well as the model predictive control regardless of multivariable or multi-loop structure. Pairing based on dynamics of controlled process is better than that based on steady-state gain. Response index and interaction index proposed in this paper catch on the dynamics and main control system design problems. They are effective criteria for the design of multivariable predictive control systems. The pairing problem should be developed comprehensively.

REFERENCES

Bristol, E.H. (1966). On a New Measure of Interaction for Multivariable Process Control, *IEEE. Trans. Automatic Control*, **AC-11, No.1**, pp133-134.

Clarke, D.W. , C. Mohtadi and P. S. Tuffs (1987). Generalized Predictive Control, *Automatica,* **23(2)**, pp137-160.

Clarke, D.W. and C. Mohtadi (1989). Properties of Generalized Predictive Control, *Automatica*, **25(6)**, pp859-875.

Cutler, C.R. and B.L. Remaker (1980). Dynamic Matrix Control – A Computer Control Algorithm. *Joint ACC Preprints,* Paper **WP5-B**, San Francisco.

Garcia, C.E. and M. Morari (1989). Model predictive control: theory and practice – a survey. *Automatica,* **25**, pp355-348.

Garcia C.E. and M. Morari (1982). Internal Model Control – A Unifying Review and Some New Results, *Ind. Eng. Chem. Process Des. Dev.* **21**, pp308.

Garcia C.E. and M. Morari (1985). Internal Model Control 2 – Design procedure for multivariable systems. *Ind. Eng. Chem. Process Des. Dev.* **24**, pp472-484.

Richalet, J et.al.(1978). Model predictive heuristic control.: Application to industrial processes, *Autimatica*, **14**, pp413-428.

Rouhani,R. and R.K. Mehra (1982). Model Algorithmic Control (MAC): Basic Theoretical Properties. *Automatica,* **18(4)**, pp401-414.

Soeterboek, Ronald (1992). *Predictive Control: A Unified Approach.* Prentice Hall.

Sun, D.X. and P. Yuan (1993). A Unified Predictive Control Algorithm, *Industrial Process Modeling and Control.* **6,** pp105-111.

Sun, Y.H. and P. Yuan (1994). An approach of state feedback predictive control and decoupling, *J. Da-Qing Petroleun Institute*, **18(3)**, pp73-76. (in Chinese)

Xi, Yu Geng (1993). *Predictive Control.* National Defence Publisher.

Yu Z.J. and P. Yuan (2002). Decoupling Features of Model Predictive Control. *J. University of Petroleum*, **26(3)**, pp108-112. (in Chinese)

Yuan P. (1992). Single Prediction Predictive Control, *J. of University of Petroleum,* **16(5)**, pp100-109. (in Chinese)

Yuan P., H.T. Zheng and X. Zuo (1993). State Feedback Predictive Control, *Sinica Automatica,* **19(5)**, pp569-577. (in Chinese)
Journal of Chinese Automation, **6(3)**, pp113-121, 1994 (Allerton Press Inc.)

Yuan P. (1994). *Process Dynamic Model and Its On-line Applications*. China Petro-Chemical Publisher.

Yuan P., D. X. Sun and T. Bai (1997). Unified Predictive Control, *Proceedings 2nd ASCC,* **III**, pp155-159. Seoul, Korea.

GENERALIZED PREDICTIVE CONTROL FOR A CLASS OF BILINEAR SYSTEMS

Guizhi Liu Ping Li

(School of Information Engineering, Liaoning University of Petroleum & Chemical Technology, Fushun 113001 P.R.China)

Abstract: A new generalized predictive control algorithm for a kind of input-output bilinear system is proposed in the paper (BGPC). The algorithm combines bilinear and linear terms of I/O bilinear system, and constitutes an ARIMA model analogous to linear systems. Using optimization predictive information fully, the algorithm carries out multi-step predictions by recursive approximation. The heavy computation of generic nonlinear optimization is avoided with control law of analytical form being used to the non-minimum phase bilinear systems. Simulation results show the effectiveness of the algorithm and the performance of the algorithm is better than linear generalized predictive control (LGPC).

Key words: bilinear systems; bilinear generalized predictive control (BGPC); recursive approaches; non-minimum phase systems; analytical control laws

1. INTRODUCTION

Most of practical production processes are nonlinear systems. Nonlinear systems are usually described as I/O form with the expression of polynomial and rational fraction (Korenberg, et al., 1988). Until now, the research of nonlinear system control is very effective. Bilinear system is a kind of nonlinear system with simple structure. The practical processes, such as project, social economy, zoology and biology etc, can be widely described by bilinear systems, and it can include a large class of dynamic characteristics of strong nonlinear system within a bigger area of a steady operating point. Its approximation precision is still higher than that of traditional linear model. Bilinearization provides an effective approach for the analysis and design of nonlinear systems. Therefore, the research for bilinear system (Svoronos, Stephanopoulos and Aris, 1981;Eaton and Rawlings, 1990; Hua Xiangming, 1990; Akihiro and Toru, 2001) has been largely performed since the late of 1960s.

As a new computer control algorithm, model predictive control originated directly from industrial process control in the anaphase of 1970s.It has made quite great progress in the past twenty years. More attention has been given to GPC, since GPC algorithm (Clarke, et al., 1987) was proposed by Clarke etc in 1987. Predictive control technology of linear models has been widely developed (Doyle III, 1995) and predictive control research of nonlinear model has already made great progress. When a generic nonlinear model for model predictive control is adopted, nonlinear optimization will be involved, and on-line disposal is very difficult. While bigger error is brought using linear approximate model. Therefore predictive control with bilinear model describing original nonlinear system is meaningful to practical application and academic research. Model prediction is introduced to bilinear systems (Adhemar, et. al., 2002; Liu, 1996; Yao, 1997; Jiang, 1998,1999; He, 1999), and good effect is achieved. A new approach of bilinear generalized predictive control (Adhemar, et al., 2002) is presented. Bilinear model

is handled, described as the time-step quasi-linearzed NARIMAX model and also improved, which overcomes the disadvantage that predictive error increases with the predictive horizon. Weighted adaptive predictive control is introduced to I/O discrete bilinear systems (Liu, 1996). The approach of point-by-point linearization approximation is introduced to I/O bilinear systems (Yao, et al., 1997). One-step and two-step predictive control (Jiang, 1998, 1999) are introduced to generic bilinear systems. Predictive model of generalized bilinear system based on Volterra series (Hemet al., 1999) is presented, and solving high order equation with one step prediction gains the optimal control law.

Apparently, the research on bilinear systems is inadequate by comparison to linear system predictive control. Even if there are some problems on the research mentioned above, such as it need try further to simplify Volterra series kernels identification. It needs the process's variety isn't very rapid in the approach of point-by-point linearization approximation. In conclusion, the existing result keep some distance with practicality and it need more perfect and develop. A multi-step GPC algorithm based on I/O discrete bilinear system is presented in this paper (BGPC). Bilinear and linear terms in the bilinear model are combined and the ARIMA model analogous to linear system is constituted. Making full use of optimal predictive control information, and carrying out multi-step prediction by recursive approximation, we obtain GPC algorithm with analytic form. The simulation results show the effectiveness of the algorithm.

2. REPRESENTATION OF BILINEAR SYSTEM

Consider a kind of SISO time-invariant bilinear systems

$$A(z^{-1})y(t) = B(z^{-1})u(t-1) + D(z^{-1})u(t-1)y(t-1) + C(z^{-1})e(t)/\Delta \quad (1)$$

where $A(z^{-1}) = 1 + \sum_{i=1}^{n_a} a_i z^{-i}$,

$B(z^{-1}) = \sum_{i=0}^{n_b} b_i z^{-i}$,

$C(z^{-1}) = \sum_{i=0}^{n_c} c_i z^{-i}$,

$D(z^{-1}) = \sum_{i=0}^{n_b}\sum_{j=0}^{n_a} d_{ij} z^{-i}\cdot z^{-j}$.

bilinear term

$$D(z)u(t-1)y(t-1) = \sum_{i=0}^{n_b}\sum_{j=0}^{n_a} d_{ij}u(t-1-i)y(t-1-j)$$

for the sake of simplicity, this paper will mainly discuss under the condition of $i \neq j$, $d_{ij} = 0$, here

$$D(z^{-1}) = \sum_{i=0}^{n_d} d_{ii} z^{-i}\cdot z^{-i},$$

$$D(z)u(t-1)y(t-1) = \sum_{i=1}^{n_d} d_{ii}u(t-i)y(t-i)$$

while the common condition of $i \neq j$, $d_{ij} \neq 0$ may perform analogy. $\{u(t)\}$ and $\{y(t)\}$ are the input and output sequences respectively. $\Delta = 1 - z^{-1}$ is the difference operator, $\{e(t)\}$ is a zero-mean white noise sequence. The equation (1) can be written as

$$A(z^{-1})y(t) = [B(z^{-1}) + D(z^{-1})y(t-1)]u(t-1) + C(z^{-1})e(t)/\Delta \quad (2)$$

3. GPC ALGORITHM OF BILINEAR SYSTEM

The controlled object (2) is assumed to satisfy:

(i) n_a n_b n_c and n_d are known.

(ii) $C(z^{-1})$ is stable polynomial.

The cost function has the following form

$$J = E\{\sum_{j=1}^{N}(y(t+j) - y_r(t+j))^2 + l\sum_{j=1}^{N_u}(\Delta u(t+j-1))^2 \quad (3)$$

Where N and N_u are the prediction and control horizon, whereas l is a weighting constant. In order to make the future outputs of system to track the set value y_0 as smooth as possible, the reference trajectory is:

$$y_r(t) = y(t)$$
$$y_r(t+j) = ay_r(t+j-1) + (1-a)y_0 \quad (4)$$

where a is a smoothing factor.

To obtain j -step-ahead optimizing predictions, consider the following Diophantine equations:

$$C(z^{-1}) = E_j(z^{-1})A(z^{-1})\Delta + z^{-j}F_j(z^{-1}) \quad (5)$$

$$B(z^{-1})E_j(z^{-1}) = C(z^{-1})G_{1j}(z^{-1}) + z^{-j}L_j(z^{-1}) \quad (6)$$

$$D(z^{-1})E_j(z^{-1}) = C(z^{-1})N_j(z^{-1}) + z^{-j}R_j(z^{-1}) \quad (7)$$

where $j = 1,2,\mathbf{L},N$,

$$E_j = e_{j0} + e_{j1}z^{-1} + \mathbf{L} + e_{j(j-1)}z^{-(j-1)}$$

$$F_j = f_{j0} + f_{j1}z^{-1} + \mathbf{L} + f_{jn}z^{-n}$$

$$G_{1j} = g_{1j0} + g_{1j1}z^{-1} + \mathbf{L} + g_{1j(j-1)}z^{-(j-1)}$$

$$N_j = n_{j0} + n_{j1}z^{-1} + \mathbf{L} + n_{j(j-1)}z^{-(j-1)}$$

$$L_j = l_{j0} + l_{j1}z^{-1} + \mathbf{L} + l_{jm_1}z^{-m_1}$$

$$R_j = r_{j0} + r_{j1}z^{-1} + \mathbf{L} + r_{jm_2}z^{-m_2}$$

also $\deg E_j = j-1$, $\deg F_j = n$, $\deg G_{1j} = j-1$ $\deg N_j = j-1$, $\deg L_j = m_1$, $\deg R_j = m_2$, $n = \max(n_a, n_c - j)$, $m_1 = \max(n_b - 1, n_c - 1)$ $m_2 = \max(n_d - 1, n_c - 1)$ .For the purpose of simplicity, then $A(z^{-1})$ is written as A, and $B(z^{-1})$ is written as B. Others are the same. Furthermore, the lowercases express polynomial coefficients relative to their capital letters, for example: n_{ji} is the i th coefficient of N_j.

From equation 2 and equation 5 - 7 , the j-step model predictive output can be written as

$$y_m(t+j) = (G_{1j} + G_{2j})\Delta u(t+j-1) + \frac{F_j}{C}y(t) + \frac{L_j}{C}\Delta u(t-1) + \frac{P_j}{C}\Delta u(t-1) \quad (8)$$

i.e.

$$y_m(t+j) = G_j\Delta u(t+j-1) + M_j \quad (9)$$

where

$$G_{2j} = N_j y(t+j-1) = \sum_{i=0}^{j-1} g_{2ji}z^{-i} \quad (10)$$

$$P_j = R_j y(t-1) = \sum_{i=0}^{m_2} p_{ji}z^{-i} \quad (11)$$

In equation (10)and (11),

$$g_{2ji} = n_{ji}y(t+j-i-1) \quad (12)$$

$$p_{ji} = r_{ji}y(t-i-1) \quad (13)$$

where $y(t+j-1)$ in equation (12) is unknown, it is substituted by model predictive value $y_m(t+j-1)$ after time t. The value at time t and before time t can be substituted by its true value. The equation (9) can be written in the vector form

$$\boldsymbol{Y_m} = \boldsymbol{G}\boldsymbol{U} + \boldsymbol{M} \quad (14)$$

$$\boldsymbol{M} = \frac{\boldsymbol{F}}{C}y(t) + \frac{\boldsymbol{L}}{C}\Delta u(t-1) + \frac{\boldsymbol{P}}{C}\Delta u(t-1) \quad (15)$$

where

$\boldsymbol{Y_m} = [y_m(t+1)\ \mathbf{L}\ y_m(t+N)]^T$,

$\boldsymbol{U} = [\Delta u(t)\ \mathbf{L}\ \Delta u(t+N_u-1)]^T$,

$\boldsymbol{M} = [M_1\ \mathbf{L}\ M_N]^T$,

$\boldsymbol{F} = [F_1\ \mathbf{L}\ F_N]^T$,

$\boldsymbol{L} = [L_1\ \mathbf{L}\ L_N]^T$,

$\boldsymbol{P} = [P_1\ \mathbf{L}\ P_N]^T$.

$$\boldsymbol{G} = \begin{bmatrix} g_0 & & & \\ g_1 & g_0 & & \\ \mathbf{L} & \mathbf{L} & \mathbf{L} & \mathbf{L} \\ g_{N-1} & g_{N-2} & \mathbf{L} & g_{N-N_u} \end{bmatrix}_{N\times N_u} \quad (16)$$

Define $\boldsymbol{y_r} = [y_r(t+1)\ \mathbf{L}\ y_r(t+N)]^T$

From the above definition, the cost function (3) can be written as

$$J = E\left\{(\boldsymbol{Y_m} - \boldsymbol{y_r})^T(\boldsymbol{Y_m} - \boldsymbol{y_r}) + l\boldsymbol{U}^T\boldsymbol{U}\right\} \quad (17)$$

Substituting equation (14) into equation (17), and minimize the cost function (17), we get

$$\boldsymbol{U} = (\boldsymbol{G}^T\boldsymbol{G} + l\boldsymbol{I})^{-1}\boldsymbol{G}^T(\boldsymbol{y_r} - \boldsymbol{M}) \quad (18)$$

The real-time optimal control law is given by

$$u(t) = u(t-1) + \boldsymbol{g}^T(\boldsymbol{y_r} - \boldsymbol{M}) \quad (19)$$

Where $\boldsymbol{g}^T$ is the first row of matrix $(\boldsymbol{G}^T\boldsymbol{G} + l\boldsymbol{I})^{-1}\boldsymbol{G}^T$.

4. SIMULATION RESEARCH

Consider the following bilinear system of non-minimum phase

$$y(t) - y(t-1) = u(t-1) + 1.3u(t-2) + 0.3u(t-1)y(t-1) + 0.5u(t-2)y(t-2) + e(t)/\Delta \quad \mathbf{(20)}$$

Where $e(t)$ is normal school white noise signal with covariance 0.1. The each parameter of the paper's control algorithm (BGPC) is as follows:

The parameters of model: $n_a = n_b = n_d = 1$, $n_c = 0$

The parameters of controller: $N = 5$ $N_u = 5$ $a = 0.8$ $l = 1$.

Using linear GPC (LGPC) control system, we can make linearization to work point of the object $y(t) = 8$

$$y(t) - y(t-1) = 3.4u(t-1) + 5.3u(t-2) \quad (12)$$

The parameters of controller are the same as the every parameter of BGPC.

The simulation curve of the output and control are shown in the following figures.

The output response and control curve using BGPC is shown in figure 1 and figure 2, where the solid line is system output, and the dashed line is set point.

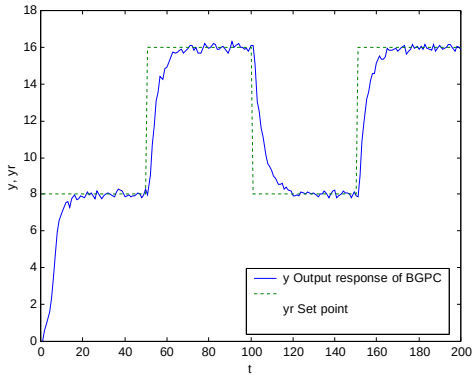

Fig. 1.Output response of the BGPC

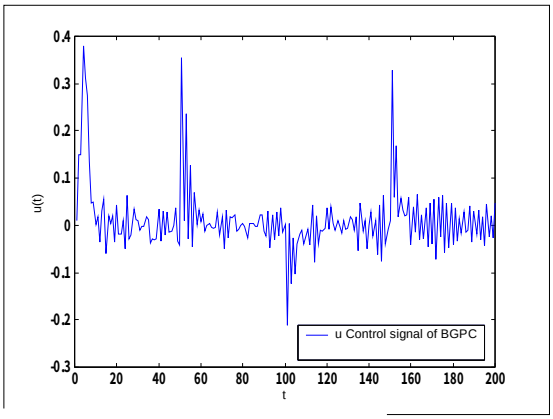

Fig. 2. Control signal of the BGPC

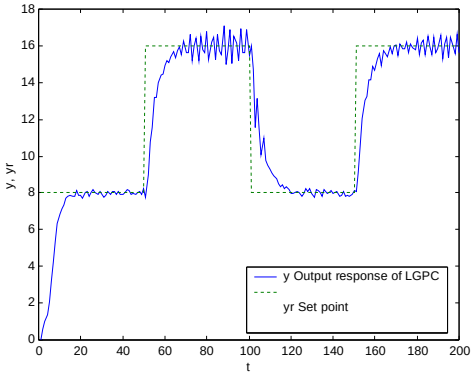

Fig.3.Output response of LGPC

The set point is changed by step amplitude 8. The output response and control curve using LGPC is shown in figure 3 and figure 4, comparing figure 1 with figure 3. It is obvious that the BGPC describes its dynamic characteristic in a biggish scope of set point because of the BGPC using nonlinear model

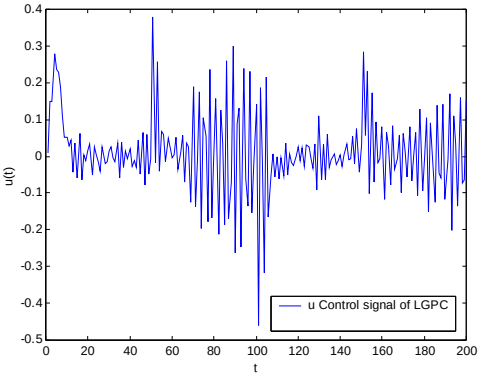

Fig.4. Control signal of LGPC

predictive, but the LGPC algorithm only makes linearization to nonlinear object's one set point, it just is stable in a baby-size scope of set point. The performance of LGPC algorithm is worse than the paper's BGPC algorithm, and the system's output can quickly track the variety of set point, BGPC algorithm's overflow in this paper is obviously more depressed than the LGPC algorithm's, and it can reject the noise well.

5. CONCLUSION

A GPC algorithm is applied to a kind of I/O bilinear systems. The analytic control law, being analogous to linear GPC, is obtained. It makes full use of optimal predictive information, and avoids the difficulty brought by generic nonlinear optimization. The simulation result proves that this algorithm is effective.

Acknowledgements---This research was supported by 863 program of China under Grant No. 2001AA413110.

REFERENCES

Akihiro S., and Toru Y (2001). A design of Generalized Minimum Variance Controllers Using a GMDH Network for Nonlinear Systems. *IEICE TRANS. Fundamentals*, **Vol. 84**, **No. 11**, pp.2901-2907

Adhemar de B F,Andre L M and Andres O S. A (2002) New Bilinear Generalized Predictive Control Approach: Algorithm and Results. *IFAC 15th Tricnnial World Congress Barcclona, Spain*

Clarke DW. Mohtadic and Tuffs Ps (1987). Generalized Predictive Control-Part Ⅰ and Ⅱ *Automatica*, **Vol.23 No. 2**, **pp.137-160**

Doyle III F, Ogunnaike B and Pearson R. (1995) Nonlinear Model-based Control Using Second Order Volterra Models. *Automatica*, **Vol. 31, No. 5**,pp. 697- 714

Eaton J and Rawlings J (1990). Feedback Control of Chemical Process Using On-line Optimization Techniques. *Computing Chemical Engineering*, **Vol.14, No. 2**, pp. 469-479

He Jianchun, Yang Maying, Yu li and Chen Guoding (1999). Predictive Control for a Class of Generic Bilinear System. *Mechanical & Electrical Engineering Magazine* **Vol.16, No. 5**, pp. 225-226

Hua Xiangming (1990). Modeling and Control of Bilinear System. *Sanghai: Press of East China Institute of Chemical Technology*

Jiang Zong (1998). One-Step Predictive Control of Bilinear System.*Journal of Anhui Institute of Architecture*, **Vol. 6, No. 2**, pp. 54-56

Jiang Zong (1999). Two-Step Predictive Control of Bilinear System. *Journal of Anhui Institute of Architecture*, **Vol.7, No. 1**, pp. 64-66

Korenberg M, Billings S A, liu Y P and Mcilroy P J (1988). Orthogonal Parameter Estimation Algorithm for Non-linear Stochastic Systems. *International Journal of Control*, **Vol. 48, No. 1**, pp.193-210

Liu Xiaohua (1996). Weighted Adaptive Predictive Control for a Class of Nonlinear Systems. *Shandong Science*, **Vol.7, No. 3**, pp. 5-8

Svoronos S, Stephanopoulos G and Aris R(1981). On Bilinear Estimation and Control. *International Journal of Control*, **Vol. 34**, pp.651-684

Yao Xinyuan and Qian Jixin (1997). Generalized Predictive Control Algorithm of Bilinear System. *Journal of Zhejiang University*, **Vol. 31, No. 2**, pp. 231-236

NONLINEAR MODEL PREDICTIVE CONTROL USING A NEURAL NETWORK

Ridong Zhang Ping Li

(School of Information Engineering, Liaoning University of Petroleum & Chemical Technology, Liaoning, Fushun 113001, P.R.China)

Abstract A neural network model-based generalized predictive control for a class of nonlinear discrete-time systems is presented with the local linearization of nonlinear activation function. The method converts the nonlinear multi-step predictions into a series of local linear multi-step predictions and uses linear GPC method to gain the control law. The method avoids the shortcomings of some past predictive algorithms , it doesn't need any assumptions and give a direct and effective multi-step predictive method. It also avoids the complicated nonlinear optimization and computation burden is not serious. A simulation result is presented in the article.

Keywords: neural-network models; generalized predictive control; nonlinearity; linearization; adaptive control.

1. INTRODUCTION

Generalized Predictive Control (Clarke D W et al.,1987) has been greatly used in the control of many industrial processes because of its excellent control performance and robustness due to its three basic features: predictive model, feedback correction and rolling optimization. However, for a nonlinear system, it is not easy to apply GPC because of the difficulty of getting an accurate nonlinear model. Since the mid-1980s, neural networks have been internationally studied to model and control nonlinear systems, and there are more and more neural network based predictive control algorithms, too. K Chao-Chee and Y L Kang(1995) presented a diagonal recurrent neural network based control strategy for dynamic systems. Among the results of nonlinear predictive control, an analytical predictive control law was presented (Furong Gao et al., 2000). A control strategy based on two assumptions was presented (Jian Guo et al., 2001). Two neural networks with an algorithm using the reverse dynamic technique was given (Qibing Jin et al., 1999), it avoids the nonlinear optimization, however, both the two networks need training and therefore its algorithm is complicated. Saint Donat J et al (1991) presented a neural net based model predictive control algorithm. A neural network predictive control strategy assuming that the process can be described as a linear part plus a nonlinear part was given (Yupu Yang et al., 1999), it uses a dynamic recurrent network to model the two parts of the system.There is also an algorithm using a global linearized model (Jun Liu et al., 2000).

The above results show that it needs to solve the following problems when applying neural networks based predictive control algorithms to nonlinear systems: (1) give a direct and effective method of multi-step prediction. (2) try to avoid the complicated nonlinear optimization. (3) reduce the sum of neural networks so as to cut down computation burden.

In this paper, using the local linearization of nonlinear activation function, a new control strategy is presented. The method converts the nonlinear multi-step predictions into a series of local linear multi-step predictions and uses linear GPC method to gain the control law. A simulation result is also given

in the paper, evidencing that the controller presents a fairly good performance.

2. NONLINEAR SYSTEMS AND THEIR REPRESENTATION

Consider the following SISO nonlinear discrete-time system described by the following model:

$$y(t) = f(y(t-1),..., y(t-n), u(t-1),..., u(t-m)) \quad (1)$$

where n, m are the orders of its output and input respectively.

The system can be described by a three-layer BP neural network as follows:

$$y(t) = g\{\sum_{i=1}^{I} w3(i) g[\sum_{j=1}^{m} w2(i, j) u(t-j) + \sum_{j=m+1}^{m+n} w2(i, j) y(t+m-j)]\} \quad (2)$$

where $w3(i), w2(i, j)\ (i = 1,..., I\ \ j = 1,..., m+n)$ are the linking weights, $n+m$ is the sum of input nodes, I the sum of hidden nodes and there is one output node. And "g" is the activation function:

$$g(x) = \frac{1}{1+e^{-x}} \quad (3)$$

In order to get a multi-step predictor, the following method is used:

Let

$$s_3(t) = \sum_{i=1}^{I} w3(i) g[\sum_{j=1}^{m} w2(i, j) u(t-j) + \sum_{j=m+1}^{m+n} w2(i, j) y(t+m-j)] \quad (4)$$

$$s_{2i}(t) = \sum_{j=1}^{m} w2(i, j) u(t-j) + \sum_{j=m+1}^{m+n} w2(i, j) y(t+m-j) \quad (5)$$

where $i = 1,..., I$ .And then $y(t) = g[s_3(t)]$ **,and** $s_3(t) = \sum_{i=1}^{I} w3(i) g[s_{2i}(t)]$ .Using the Taylor expansion technique :

$$\begin{aligned} y(t) &= g(s_{31}) + g'(s_{31})[s_3(t) - s_{31}] + F_1(\theta(t)) \\ &= g'(s_{31}) s_3(t) + g(s_{31}) - g'(s_{31}) s_{31} + F_1(\theta(t)) \\ &= g'(s_{31}) \sum_{i=1}^{I} w3(i) g[s_{2i}(t)] \\ &\quad + g(s_{31}) - g'(s_{31}) s_{31} + F_1(\theta(t)) \end{aligned} \quad (6)$$

where $\theta(t)$ refers to $[y(t-1),..., y(t-n), u(t-1),..., u(t-m)]$, F_1 is a function symbol, and s_{31} is the center of the expansion . Also define $\theta(t+i)$ as: $[y(t+i-1),..., y(t+i-n), u(t+i-1),..., u(t+i-m)]$. In general, let the center s_{31} =0. The same technique can also be employed on $s_{2i}(t)$, likewise , it derives:

$$g[s_{2i}(t)] = g(s_{2i}) + g'(s_{2i})[s_{2i}(t) - s_{2i}] + F_{2i}(\theta(t)) \quad (7)$$

where $s_{2i}\ (i = 1,..., I)$ are also the centers , also let s_{2i} =0 $(i = 1,..., I)$,and $F_{2i}\ (i = 1,..., I)$ are function symbols. Substitute eq.(7) into eq.(6) and combine the nonlinear parts $F_1(\theta(t))$ and $F_{2i}(\theta(t))\ (i = 1,..., I)$ into one nonlinear part $F_3(\theta(t))$ leads to the following:

$$\begin{aligned} y(t) &= \sum_{i=1}^{I} w3(i) g'(s_{31}) \{g(s_{2i}) + g'(s_{2i})[s_{2i}(t) - s_{2i}]\} \\ &\quad + g(s_{31}) - g'(s_{31}) s_{31} + F_3(\theta(t)) \\ &= \sum_{i=1}^{I} w3(i) g'(s_{31}) g'(s_{2i}) s_{2i}(t) \\ &\quad + \{\sum_{i=1}^{I} w3(i) g'(s_{31})[g(s_{2i}) - g'(s_{2i}) s_{2i}] \\ &\quad + g(s_{31}) - g'(s_{31}) s_{31}\} + F_3(\theta(t)) \end{aligned} \quad (8)$$

where $F_3(\theta(t))$ is the nonlinear part:

$$F_3(\theta(t)) = \sum_{i=1}^{I} w3(i) g'(s_{31}) F_{2i}(\theta(t)) + F_1(\theta(t)) \quad (9)$$

For simplicity , let $M_i = w3(i) g'(s_{31}) g'(s_{2i})\ (i = 1,..., I)$ **, and** represent the second part in eq.(8) as N , substitute eq.(5) into eq.(8) and gives:

$$y(t) = \sum_{i=1}^{I} M_i s_{2i}(t) + N + F_3(\theta(t))$$

$$= \sum_{i=1}^{I} M_i [\sum_{j=1}^{m} w2(i, j)u(t-j) \qquad (10)$$

$$+ \sum_{j=m+1}^{m+n} w2(i, j)y(t-j+m)] + N + F_3(\theta(t))$$

The discrete differential equation of $y(t)$ can be written as:

$$y(t) = a_1 y(t-1) + ... + a_n y(t-n)$$

$$+ b_0 u(t-1) + ... + b_{m-1} u(t-m) \qquad (11)$$

$$+ N + F_3(\theta(t))$$

Compare eq.(10) with eq.(11) leads to:

$$a_1 = \sum_{i=1}^{I} M_i w2(i, m+1) \quad b_0 = \sum_{i=1}^{I} M_i w2(i,1)$$

$$a_2 = \sum_{i=1}^{I} M_i w2(i, m+2) \quad b_1 = \sum_{i=1}^{I} M_i w2(i,2)$$

$$\vdots$$

$$a_n = \sum_{i=1}^{I} M_i w2(i, m+n) \quad b_{m-1} = \sum_{i=1}^{I} M_i w2(i, m) \qquad (12)$$

Now the system model has been divided into two parts: a linear part and a nonlinear part. The coefficients of the linear part are calculated by eq.(12).

3. CONTROL SYSTEM DESIGN

Note that N is a constant, eq.(11)can be written as follows:

$$y(t) = A_1 y(t-1) + ... + A_{n+1} y(t-n-1)$$

$$+ B_{1,0}\Delta u(t-1) + ... + B_{1,m-1}\Delta u(t-m) \qquad (13)$$

$$+ \Delta F_3(\theta(t))$$

where:

$$A_1 = 1 + a_1, A_i = a_i - a_{i-1} (i = 2,..., n), A_{n+1} = -a_n,$$

$B_{1,i} = b_i$ $(i = 0,..., m-1)$, and D is the differencing operator $1 - q^{-1}$.

Now, divide the optimal predictions into three parts, one is determined by past inputs and outputs, this is represented by $\boldsymbol{Y_p}$, another is determined by present and future inputs, it is represented by $\boldsymbol{GU}$, the other is the prediction error, it consists of the nonlinear error $\boldsymbol{E_1}$ and the error caused by external disturbances $\boldsymbol{E_2}$, then it derives:

$$\boldsymbol{Y} = \boldsymbol{Y_p} + \boldsymbol{GU} + \boldsymbol{E}$$

$$= \boldsymbol{Y_p} + \boldsymbol{GU} + \boldsymbol{E_1} + \boldsymbol{E_2} \qquad \textbf{(14)}$$

where:

$$\boldsymbol{Y} = [y(t+1/t), y(t+2/t),..., y(t+p/t)]^T$$
$$\boldsymbol{Y_p} = [y_p(t+1), y_p(t+2),..., y_p(t+p)]^T$$
$$\boldsymbol{U} = [\Delta u(t), \Delta u(t+1),..., \Delta u(t+p-1)]^T$$
$$\boldsymbol{E}_1 = [\varepsilon(\theta(t+1)), \varepsilon(\theta(t+2)),..., \varepsilon(\theta(t+p))]^T$$
$$\boldsymbol{E_2} = [y(t) - \hat{y}(t), y(t) - \hat{y}(t),..., y(t) - \hat{y}(t)]^T$$

$$\boldsymbol{G} = \begin{bmatrix} B_{1,0} & & & \\ B_{2,0} & B_{1,0} & 0 & \\ \cdots & \cdots & & \\ B_{p,0} & B_{p-1,0} & \cdots & B_{1,0} \end{bmatrix} \qquad (15)$$

Here the control horizon and prediction horizon are both p, $y(t)$ is the output of the system, $\overset{L}{y}(t)$ is the output of its neural network model.

Since $\boldsymbol{Y_p}$ is the "free response" of the system, it can be calculated by the neural network model. The elements in $\boldsymbol{G}$ are calculated as follows:

$$B_{1,0} = b_0$$

$$B_{k,0} = b_{k-1} + \sum_{j=1}^{k-1} A_j B_{k-j,0}, k = 2,...,p \qquad (16)$$

Moreover, let the reference trajectory be as follows:

$$y_r(t) = y(t)$$

$$y_r(t+k) = a^k y(t) + (1 - a^k) y_s \qquad \textbf{(17)}$$

where y_s is the set-point, $a \in (0,1)$.

Let the vector form of the reference trajectory and the cost function be the follows respectively:

$$\boldsymbol{Y}_r = [y_r(t+1), y_r(t+2),..., y_r(t+p)]^T \quad (18)$$

$$J = \min\{(\boldsymbol{Y}_r - \boldsymbol{Y})^T(\boldsymbol{Y}_r - \boldsymbol{Y}) + \beta^2 \boldsymbol{U}^T \boldsymbol{U}\}$$

where b^2 is the weighting factor.

Note that because the system is nonlinear and $\boldsymbol{E}_1$ is function of $\boldsymbol{\Theta}$, here $\boldsymbol{\Theta}$ refers to $[\varepsilon(\theta(t+1)),...,\varepsilon(\theta(t+p))]^T$, so $\boldsymbol{E}_1$ is not known. So the control law cannot be calculated by eq.(14).

However, the following method is used to get the control law:

First, let $\boldsymbol{E}_{10}$ =0, where $\boldsymbol{E}_{10}$ is the initial value of $\boldsymbol{E}_1$, then, from $\frac{\partial J}{\partial \boldsymbol{U}} = 0$, $\boldsymbol{U}_0$ can be calculated:

$$\boldsymbol{U}_0 = (\boldsymbol{G}^T\boldsymbol{G} + \beta^2 \boldsymbol{I})^{-1}\boldsymbol{G}^T(\boldsymbol{Y}_r - \boldsymbol{Y}_p - \boldsymbol{E}_2 - \boldsymbol{E}_{10}) \quad (19)$$

And $\boldsymbol{U}_0$ is the initial value of $\boldsymbol{U}$. Define the vector form of the multi-step predictions based on neural network model as $\boldsymbol{Y}_m$:

$$\boldsymbol{Y}_m = [y_m(t+1/t), y_m(t+2/t),..., y_m(t+p/t)]^T$$

And its value of step j is $\boldsymbol{Y}_{mj}$, the value of $\boldsymbol{Y}$ of step j is $\boldsymbol{Y}_j$, the value of $\boldsymbol{U}$ of step j is $\boldsymbol{U}_j$, the value of $\boldsymbol{E}_1$ of step j is $\boldsymbol{E}_{1j}$. Thus the optimal $\boldsymbol{U}$ can be gained by the following method:

$$\boldsymbol{Y}_j = \boldsymbol{Y}_p + \boldsymbol{G}\boldsymbol{U}_j + \boldsymbol{E}_2 + \boldsymbol{E}_{1j} \quad j = 1,2,... \quad (20)$$

Substitute $\boldsymbol{U}_j$ into its neural network model eq.(2) and $\boldsymbol{Y}_{mj}$ can be gained, then:

$$\boldsymbol{E}_{1j+1} = F(\boldsymbol{E}_{1j}) = \boldsymbol{E}_{1j} + \delta[\boldsymbol{Y}_{mj} - \boldsymbol{Y}_j] \quad (21)$$

$$\boldsymbol{U}_{j+1} = (\boldsymbol{G}^T\boldsymbol{G} + \beta^2 \boldsymbol{I})^{-1}\boldsymbol{G}^T(\boldsymbol{Y}_r - \boldsymbol{Y}_p - \boldsymbol{E}_2 - \boldsymbol{E}_{1j+1}) \quad (22)$$

where $\boldsymbol{E}_{10}$ =0, $d \in (0,1)$. Note that if the function $F(\bullet)$ is compressed mapping, the above iterative process is convergent. And when $\boldsymbol{Y}$ equals $\boldsymbol{Y}_m$, the control sequence $\boldsymbol{U}$ gained based on eq.(22) is the optimal one. However, if $\|\boldsymbol{E}_{1j+1} - \boldsymbol{E}_{1j}\| <$ a desired tolerance, $\boldsymbol{U}_{j+1}$ can be thought of as the optimal control law, define $\boldsymbol{q}^T$ as the first row of $(\boldsymbol{G}^T\boldsymbol{G} + \beta^2 \boldsymbol{I})^{-1}\boldsymbol{G}^T$, then the control law is:

$$u(t) = u(t-1) + \boldsymbol{q}^T(\boldsymbol{Y}_r - \boldsymbol{Y}_p - \boldsymbol{E}_2 - \boldsymbol{E}_{1j+1}) \quad (23)$$

Hence, the algorithm for the nonlinear predictive control method can be summarized as follows:

Step 1. Use BP algorithm to train the weights of the network and gain an initial estimate of their values.

Step 2. Pick the output $y(t)$ and give the network an on-line training so as to adjust the weights adaptively.

Step 3. Divide eq.(2) into two parts using the method of the second section.

Step 4. Compute the free response $\boldsymbol{Y}_p$ of the system.

Step 5. Get the reference trajectory using eq.(18).

Step 6. Gain the optimal $u(t)$ by using eq.(23).

Step 7. Return to step 2.

4. SIMULATION RESULT

In this section, an example is given to illustrate the above method. The system is represented by the following model:

$$y(t) = \frac{0.91y(t-1) + u(t-1)}{1 + y(t-2)u(t-2)} + e(t)/D$$

Also white noise was added to the output. Its amplitude is tenth of the set-point. The control parameters are selected as follows:

p =5, b^2 =1, $a = 0.65$, the system response can be seen in Fig.1.

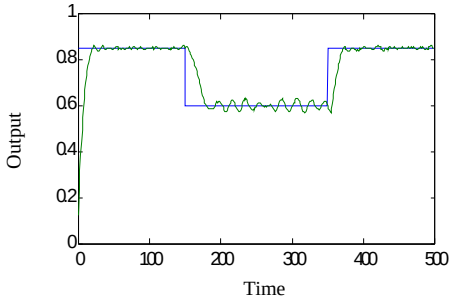

Fig. 1. Output response

5. CONCLUDING REMARKS

In this work, a new neural network based nonlinear predictive control algorithm is conducted and applied to a nonlinear system. It gives a direct and effective predictive method and avoids nonlinear optimization. In the algorithm, only one neural network is used, so the computation burden is not serious.

Acknowledgements---This research was supported by 863 program of China under Grant No. 2001AA413110.

REFERENCES

Clarke D W, Mohtadi C and Tuffs P S (1987). Generalized Predictive Control Part I. The

Basic Algorithm. *Automatica*, **Vol. 23, No. 2,** pp. 137-148

Furong Gao, Fuli Wang and Mingzhong Li (2000). An analytical predictive control law for a class of non-linear processes. *Ind.End.Chem.Res.*, **Vol. 39,** pp.2029-2034.

Jian Guo, Rijun zhu and Weili Hu (2001). Generalized Predictive Control for a Class of Nonlinear Systems. *Control and Decision*, **Vol. 16, No. 3,** pp. 358-361

Jun Liu, Xing He and Xiaoming Xu (2000). Extension of DMC Predictive Control Using Neural Network Base Nonlinear Modelsand Multi-step Operration Point Respones. *Control and Decision*, **Vol. 15, No. 3,** pp.342-344

Chao-Chee K and Kang Y L (1995). Diagonal recurrent neural networks for dynamic systems control. *IEEE trans on Neural Networks*, **Vol. 6, No. 1,** pp. 144-156

Qibing Jin, Jianhui Wang and Shusheng Gu (1999). Multi-step Prediction Cost Function based reverse-dynamic method. *Control and Decision*, **Vol. 14, No. 4,** pp.308-312

Saint Donat J, Dhat N and McAvoy T J (1991). Neural net based model predictive control. *Int J Control*, **Vol. 54, No. 6,** pp.1453-1468

Wei Wang and Jianjun Yang (1997). Generalized Predictive Control, Theory, Algorithm and Applications. *Control Theory and Applications*, **Vol. 14, No. 6,** pp.778-785

Yupu Yang, Xinmin Huang and Xiaoming Xu (1999). Nonlinear Muti-step Predictive Control Using Compound Neural Networks. *Control and Decision*, **Vol. 14, No. 4,** pp.314-318

PROCESS OPTIMIZATION AND CONTROL UNDER CHANCE CONSTRAINTS

Pu Li, Moritz Wendt, Harvey Arellano-Garcia, Günter Wozny

Institut für Prozess- und Anlagentechnik, Technische Universität Berlin, KWT 9
10623 Berlin, Germany

Abstract: We propose to use chance constrained programming for process optimization and control under uncertainty. The stochastic property of the uncertainties is included in the problem formulation. The output constraints are to be ensured with a predefined confidence level. The problem is then transformed to an equivalent deterministic NLP problem. The solution of the problem has the feature of prediction, robustness and being closed-loop. In this paper, the basic concepts and solution strategies are discussed to illustrate the potential for optimization and control under uncertainty.

Keywords: uncertainty, chance constraints, linear, nonlinear, optimization, control

1. INTRODUCTION

It is a well-known fact that uncertainties exist in every chemical process. In most previous studies on process optimization and control, the stochastic properties of uncertainties have not been taken into account. In the industrial practice, uncertainties are compensated for by using conservative operating strategies, which may lead to considerably more costs than necessary. In addition, feedback control is used to compensate for uncertainties. However, compensation without considering the uncertainty properties is in fact the wait-and-see strategy and has several drawbacks. First, it is always *a posteriori*. Second, the system propagates the disturbances to connecting systems. Third, a feedback can not ensure constraints on open-loop variables. In many cases it is impossible to on-line measure some variables which describe product properties (e.g. composition, viscosity, density). These variables have to be open-loop under the uncertainties but they should be confined to a specified region corresponding to the product specifications.

To overcome these drawbacks, we have recently proposed and studied a new framework for process optimization and control under uncertainty. The uncertainty properties are to be included in the problem formulation. These properties can be gained by statistical analysis of historical data. A stochastic programming problem under chance constraints is formulated for both optimization and control. It will be relaxed to an equivalent deterministic NLP problem. The essential challenge lies in the computation of the probabilities of holding the constraints as well as their gradients. Approaches of chance constrained programming to linear, nonlinear and dynamic problems have been developed and applied to different process engineering problems. The method of moving horizon is employed for solving dynamic optimization and control problems under uncertainty.

While chance constrained programming has been applied in many disciplines like finance and management (Prekopa, 1995; Uryasev, 2000), few applications have been made in chemical process operations (Henrion et al., 2001). It has been used for batch process planning (Petkov and Maranas, 1997). Several studies on model predictive control using chance constrained programming have been carried out for linear processes (Schwarm and Nikolaou, 1999; Li et al. 2000 and 2002a,b). Recently, a method to nonlinear chance constrained problems was introduced for process optimization under uncertainty (Wendt et al., 2002). It has been extended to nonlinear dynamic optimization problems under uncertainty (Arellano-Garcia et al., 2003). In this paper, the basic principles of chance constrained programming and its applications to process optimization and control are discussed to illustrate its potential and limitation.

2. UNCERTAINTY ANALYSIS

In process operation, there are two general types of uncertainties. *External uncertainties* are from outside but have impacts on the process. They can be the rate and/or composition of feed and recycle flows as well as flows of utilities, the temperature and pressure of the coupled operating units or market conditions. *Internal uncertainties* represent the unavailability of knowledge of the process. For a determined model structure, they are uncertain model parameters often regressed from a limited number of experimental data. We call both of these *uncertain inputs*. Due to these uncertainties, conservative or aggressive decisions may be made. While internal uncertainties have been well studied in the framework of robust control in the past (Morari and Zafiriou, 1989; Kothare et al., 1996; Bemporad et al. 2002), external uncertainties have not been much emphasized.

As shown in Fig. 1, an uncertain input ξ can be constant (e.g. model parameters) or time-dependent (e.g. atmospheric temperature) in the future horizon $t \in [t_0, t_f]$. They are undetermined before their realization. The "realization" means either the measurable uncertain variables have been measured or parameters newly estimated. The distribution of the variables may have different forms. Very often normal (Gaussian) distribution is considered as an adequate assumption for many uncertain variables in the engineering practice. The basic justification of this statement is embodied in the central limit theorem (Maybeck, 1994). The values of mean and variance are usually available. The uncertain variables may be *correlated* or *uncorrelated*.

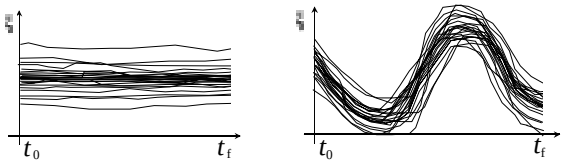

Fig. 1: Two different uncertain variables

These uncertain inputs will propagate through the process to output variables (e.g. temperature, composition). This makes the outputs also uncertain. A continuous process with constant uncertain inputs leads to a *steady-state* problem, while such a process with time-dependent uncertain inputs or a batch process is a *dynamic* problem under uncertainty. For a *nonlinear* process it is very difficult to analytically describe the distribution of the outputs. A scheme of *simulation* with sampling can address this problem. According to their distributions, random values are generated. After many runs of simulation with the sampled data, the probability distribution of the outputs can be gained. Besides Monte-Carlo, some efficient sampling strategies have been proposed (Diwekar and Kalagnanam, 1997). Obviously, the *wait-and-see* strategy can not result in satisfactory operations under these uncertainties. Thus we are confronted with making decisions *a priori* for the future operation (i.e. the *here-and-now* strategy). Under the uncertainties, a stochastic programming problem has to be defined and solved to answer these questions: 1) how to achieve an economically optimal operation? 2) how to ensure the constraints of the output variables? 3) how to prevent the propagation of the uncertainties to downstream processes? and 4) how to design a proper feedback control system?

3. CHANCE CONSTRAINED PROBLEMS

A general optimization or control problem under uncertainty can be formulated as

$$\begin{aligned} \min \quad & f(\mathbf{x},\mathbf{u},\boldsymbol{\xi}) \\ \text{s.t.} \quad & \mathbf{g}(\dot{\mathbf{x}},\mathbf{x},\mathbf{u},\boldsymbol{\xi}) = \mathbf{0}, \quad \mathbf{x}(t_0) = \mathbf{x}_0 \\ & \mathbf{h}(\dot{\mathbf{x}},\mathbf{x},\mathbf{u},\boldsymbol{\xi}) \geq \mathbf{0}, \\ & \mathbf{u}_{\min} \leq \mathbf{u} \leq \mathbf{u}_{\max}, \; t_0 \leq t \leq t_f \end{aligned} \tag{1}$$

where f is the objective function, $\mathbf{g}$ and $\mathbf{h}$ are the vectors of equality and inequality constraints. $\mathbf{x}$, $\mathbf{u}$ and $\boldsymbol{\xi}$ are the vectors of state, control and uncertain inputs, respectively. $\mathbf{x}_0$ is the known initial state. This dynamic nonlinear optimization problem has to be descretized with time intervals into a static problem so that it can be solved with the method of stochastic programming. Time-dependent uncertain inputs will be approximated as discretized uncertain variables in individual time intervals. In this work, they are assumed to have a correlated multivariate normal distribution.

There have been two general stochastic approaches (Kall and Wallace, 1994) to solve such problems. The *two-stage programming* uses recourse to deal with inequality constraints. The first-stage decision variables are determined and fixed before the realization of the uncertain variables, while the second-stage variables are decided after their realization. The violation of constraints is compensated for by some penalty functions and leads to additional costs for the second stage decisions. Since a proper penalty function is usually not available, the application of this method to operation and control may be not appropriate.

The other method is the *chance constrained programming*. Its unique feature is that the resulting solution ensures a predefined probability of satisfying the constraints. The solution will lead to an expected optimal value of the objective function by searching for the decision in a feasible region to hold a given confidence level, denoted as α $(0 \leq \alpha \leq 1)$. Since α can be defined by the user, it is possible to select different levels and make a compromise between the function value and risk of constraint violation. It should be noted that with both

solution strategies there have been, until now, no suitable approaches to nonlinear problems.

Recently, we have studied chance constrained programming for process optimization and control under uncertainty (Li et al. 2000 and 2002a,b; Henrion et al., 2001; Wendt et al., 2002). In engineering practice, a very popular form of inequality constraints is to specify or restrict some of *output variables* **y** (note **y** is part of **x**):

$$y_i^{\min} \le y_i(\mathbf{u},\xi) \le y_i^{\max} \quad i=1,\cdots,I \qquad (2)$$

$y_i^{\min}, y_i^{\max}$ are the required lower and upper bound of an output, such as a pressure or a temperature restriction of a plant. Holding these constraints is usually critical for the production and safety. For $t \in [t_0, t_f]$ a probabilistic form of (2) is

$$\Pr\left\{y_i^{\min} \le y_i(\mathbf{u},\xi) \le y_i^{\max}, i=1,\cdots,I\right\} \ge \alpha \qquad (3)$$

With this representation, all inequalities are included in the probability computation. It means that they should be satisfied simultaneously with the given probability. This is called *joint* probabilistic (chance) constraint. Another form is *single* chance constraint, where individual probabilities of ensuring each inequality will be held:

$$\Pr\left\{y_i^{\min} \le y_i(\mathbf{u},\xi) \le y_i^{\max}\right\} \ge \alpha_i, \ \ i=1,\cdots,I \qquad (4)$$

It should be noted that in deterministic approaches the expected values of the uncertain variables are usually employed. In reality, however, the uncertain variables will deviate from their expected values. Thus the implementation of the results from a deterministic approach will violate the inequality constraints with a probability of around 50%. The difference between (3) and (4) is that a joint chance constraint requires the reliability in the output feasible region as a *whole*, while single chance constraints demands the reliability in the *individual* output feasible region. If the constraints are related to the safety consideration of a process operation, a joint chance constraint may be preferred. Single chance constraints may be used when some output constraints are more critical than the other ones. The equalities in (1) are the model equations of the process. They have to be satisfied with any realization of the uncertain variables. In fact, the effect of the model equations is a projection of the space of the random variables ξ as inputs to a space of state variables **x**, with given controls **u**. Thus the equalities will be eliminated if an integration of the equations in the space of the uncertain variables is made. It implies that a sequential approach is suitable for solving stochastic problems with equality constraints. To treat the objective function in (1), minimizing the expected value and the variance of the objective function has usually been adopted (Darlington et al. 1999):

$$\min \ \mathrm{E}\left[f(\mathbf{x},\mathbf{u},\xi)\right] + \omega\, D\left[f(\mathbf{x},\mathbf{u},\xi)\right] \qquad (5)$$

E and *D* are the operators of expectation and variation, respectively. ω is a weighting factor between the two terms. In the sense of relaxation the objective function in (1) is now a deterministic function through these two operators. Now a general chance constrained problem is formulated with (5) as objective function and (3) or (4) with constraints.

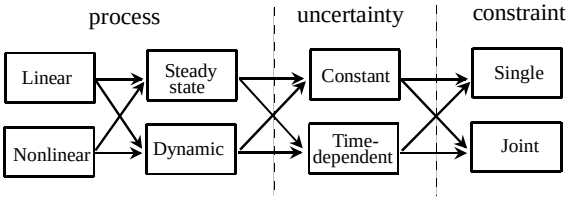

Fig. 2: Classification of chance constrained problems

As shown in Fig. 2, such problems can be classified based on the properties of processes, uncertainties and constraint forms. Thus there are 16 different formulations. We can use the initial letters to denote the problems. For example, a steady state process with constant uncertainties under single chance constraint is called an LSCS problem. It is interesting to note that LSTS and NSTS can be solved separately for each interval, while for LSTJ and NSTJ (a quasi-dynamic problem) the whole time horizon should be considered. To solve such problems with an existing optimization routine, the probability of holding the constraints has to be computed. Moreover, the gradients of the probability function to the controls are required. Different problems have different degrees of complexity for computing these values, which will be discussed in the following two sections.

4. APPROACH TO LINEAR SYSTEMS

Chance constrained linear problems can be relatively easily treated and have some nice properties. Theoretical results show that the feasible region of linear problems with quasi-concavely distributed uncertain variables is convex (Prekopa, 1995). Another merit property is that linear transformations of multivariate normally distributed variables have the same distribution. Optimization of linear steady state systems (LSCS and LSCJ) under constant uncertain variables has been well studied (see Kall and Wallace). It can be applied in process design and planning under uncertainty.

We consider *linear dynamic* systems with *time dependent* uncertain inputs (LDTS and LDTJ). The outputs in the future horizon depend on the current state, the future and past controls as well as uncertain inputs. The uncertain inputs include both uncertain parameters (e.g. step response coefficients) and disturbances. The controls in the horizon will be decided to optimize some objective function and

ensure the chance constraints for the outputs. A quadratic objective function leads to a chance constrained *model predictive control*, as shown in Fig. 3. One can easily notice that the novelty of this controller, compared with the conventional MPC, is it includes the uncertainties *explicitly* in the problem formulation. Moreover, it is worth noting that the objective function may only include the quadratic terms of controls, since the outputs are confined in the chance constraints, e.g.

$$\min \sum_j \sum_l \omega_l [u_l(t+j) - u_l(t+j-1)]^2 \qquad (5)$$

For linear MPC with *single* chance constraints (LDTS), the chance constraints can easily be transformed to linear deterministic inequalities. It leads to a QP problem and thus the solution can be derived analytically (Schwarm and Nikolaou, 1999).

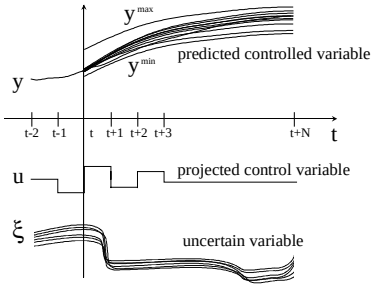

Fig. 3: Chance constrained MPC

In cases of problems with a *joint* chance constraint (LDTJ), an explicit solution cannot be obtained, since the calculation of a joint probability of multivariate uncertain variables is needed. Although one chance constraint for all outputs and all time points can be formulated, it is natural to constrain each output separately, i.e. for $i = 1, \cdots, I$

$$\Pr\left\{y_i^{\min}(t+j) \le y_i(t+j) \le y_i^{\max}(t+j),\ j = 1, \cdots, N\right\} \ge \alpha_i \qquad (6)$$

Note that even if the uncertain inputs are uncorrelated, the outputs are correlated through the linear propagation. With some linear transformation, (6) can be described as the following form

$$\Pr\{\boldsymbol{\xi}_i' \le \mathbf{A}_i \mathbf{u} + \mathbf{b}_i\} \ge \alpha_i \qquad (7)$$

$\boldsymbol{\xi}_i'$ is an *N*-dimensional uncertain vector. The joint probability makes (7) nonlinear constraints and the stochastic MPC becomes an NLP problem. Unfortunately, it is not possible to easily compute those probability values even numerically, if the dimension is larger than 3. A simulation scheme to estimate joint probabilities was proposed (Prekopa (1995). The first and second term of the inclusion-exclusion formula are computed exactly and the rest terms are evaluated by sampling. Moreover, the gradient calculation is required to solve the problem with an NLP solver, which is more difficult. We used this simulation scheme for the probability computation and proposed a reduced gradient computation strategy (Li et al., 2000, 2002a). The efficient sampling by Diwekar and Kalagnanam (1997) is used. SQP is used for the optimization and the control proceeds by moving horizon. After the control of the first time interval is implemented, together with the realization of the uncertain inputs in this interval, the system moves to the new state, and the control policy in the new horizon will be computed. The tuning parameters of this algorithm are the length *N* of the time horizon and the confidence level α. As a kind of predictive controller a large *N* is desired, but the computation time will be greater. The major computation load is due to sampling of the uncertain variables to evaluate the probabilities and their gradients. A larger *N* means more uncertain variables are included in the problem formulation.

Tuning the value of α is an issue of the relation between *feasibility* and *profitability*. Of course a high confidence level to ensure the constraints is always preferred. The solution of a defined problem, however, is only able to arrive at a maximum value $\alpha^{\max}$ which is dependent on the properties of the uncertain inputs and the restriction of the controls and outputs. The knowledge of $\alpha^{\max}$ is crucial; if a value greater than $\alpha^{\max}$ is chosen, the feasible region will be empty. An easy-to-use method was proposed to compute this maximum value for SISO systems (Li et al., 2002b) which can be extended to MIMO systems. The basic idea is to map the stochastic inputs to outputs and analyze the property of the outputs. It can be proved that the joint probability has the maximum value if the mean values of the outputs are at the middle of their restricted region $[y^{\min}, y^{\max}]$. Thus $\alpha^{\max}$ can be obtained via a simulation run. The *profitability* of the stochastic MPC means the achievability of the objective function value, which is also a function of the confidence level. They have a monotone relation: the value of objective function will be degraded if α is increased. One can analyze the profile of the function value with changing α and decide on a suitable trade-off between profitability and reliability.

5. APPROACH TO NONLINEAR SYSTEMS

The motivation to consider nonlinear chance constrained problems is to find systematic ways to compensate for uncertainties so as to avoid intuitive or empirical decisions. Recently we proposed a solution method to nonlinear *steady state* problems under *single* chance constraints (NSCS), in which direct computation of the probability of holding the output constraints is avoided (Wendt et al., 2002). The basic idea is to map the chance constrained region of the outputs back to a bounded region of the uncertain inputs. This can be done by a monotone

relationship between an input ξ_S (assuming there are *S* uncertain variables) and the constrained output y_i. Thus the output probability can be computed by integration of the density function of the uncertain inputs, e.g. if $\xi_S \uparrow \Rightarrow y_i \uparrow$, then

$$\Pr\{y_i \le y_i^{\max}\} = \Pr\{\xi_S \le \xi_S^{\max}, \forall \xi_1, \cdots \xi_{S-1}\} = \int_{-\infty}^{\infty} \cdots \int_{-\infty}^{\xi_S^{\max}} \rho(\xi_1, \cdots, \xi_S) d\xi_S \cdots d\xi_1 \quad (8)$$

For the multivariate integration, collocation on finite elements is used to discretize the bounded region of the uncertain inputs. The input boundary $\xi_S^{\max}$ is computed inversely by the Newton-Raphson method based on the output value of $y_i^{\max}$. Since this boundary depends on the realization of the uncertain variables ($\xi_1, \cdots \xi_{S-1}$), it has to be computed on each collocation point of these variables. In this way, the equality constraints (model equations) are eliminated by expressing the state variables in terms of decision and uncertain variables. Again, a sequential solution approach is used. It can principally be described with Fig. 4. Due to the uncertainty, three different controls will result in three different output distributions: 1) too conservative (e.g. resulting in great operation costs), 2) acceptable and 3) too aggressive (resulting a high probability of constraint violation). Due to the monotony, the bound values ($\xi_i^{\max(1)}, \xi_i^{\max(2)}, \xi_i^{\max(3)}$) of the uncertain variable can be determined and thus the probabilities of holding the constraint can be computed.

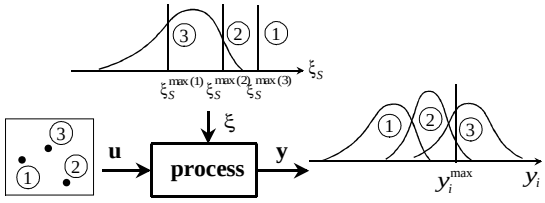

Fig. 4: Approach to nonlinear constrained problems

Principally, this approach can solve problems under uncertainties with any kind of distributions, provided the density function and a monotone relationship between the constrained variable and one of the uncertain inputs are available. A numerical integration scheme for problems with correlated Gaussian inputs is developed. It should be noted that for normal distributions the boundaries of the infinite integrals in (8) can be chosen as $[-3\sigma, 3\sigma]$. A nested computational scheme to the multivariate integration is proposed based on the fact that the *S*-dimensional integration can be computed by an (*S*-1)-dimensional integration. The gradients of the probabilities to the controls can be computed in the same way. To address the issue of feasibility, one can first define the objective function as maximization of the achievable probability. The problem is then solved for the value of $\alpha^{\max}$. For some practical processes, one may gain this value through simulation. For example, if the control is monotone with the constrained variable, then $\alpha^{\max}$ corresponds to the confidence level with the lower or upper bound of this control variable. This approach can straightforwardly be extended to multiple single probabilistic constraints. For each constraint a probability computation will be made in the form of (8). In this case, different confidence levels can be selected for different output constraints. The extension of the approach to a joint chance constrained problem (NSCJ) is not a trivial task, since it may be difficult to find an uncertain variable which is monotone with the joint probability. It may be possible to find such a variable by carefully analyzing the relations between the uncertain inputs and constrained outputs. This can be done with process simulation by perturbing the uncertain variables.

This approach has been extended to solve NDCS problems of nonlinear dynamic optimization under uncertainty (Arellano-Garcia et al., 2003). We consider dynamic problems with constrained outputs at selected time points and with constant uncertain inputs. The control policy $u(t)$ for the entire operation time will be developed to optimize the objective function subject to single chance constraints of holding the point restrictions. This is a suitable formulation to optimize batch process operations under model parameter uncertainty. Two difficulties have to be overcome in solving such dynamic problems. First, since multiple time intervals are considered, the reverse projection of the output feasible region to a region of uncertain inputs is not trivial. The method of bisection through simulation seems to be efficient to address this problem. This is because it is a one-to-one projection. Second, since the controls have different impacts on the outputs in different time intervals, the gradients of the uncertain input to the controls in each interval have to be computed and passed to the time points from interval to interval in order to compute the gradients of the probability.

6. OPEN-CLOSED FRAMEWORK

A closed-loop control requires on-line measured values of controlled variables. However, many variables in the engineering practice can not be measured on-line (e.g. concentration, viscosity, density etc.). These variables represent the qualities of products and their control is desired. To address this problem, measurable variables (temperature, pressure) are chosen as controlled variables to indirectly control the product quality. This concept can be described with Fig. 5. **y** will be controlled at their setpoints $\mathbf{y}^{SP}$ by using controls **u**. Control of $\mathbf{y}^{C}$ is desired, but due to the lack of on-line measurement it has to be open-loop. In these cases,

$\mathbf{y}^C$ needs to be constrained but **y** is not constrained. To ensure the product quality, the present solution in the industrial practice is to choose an extremely conservative setpoint value. This leads to the fact that the product quality will unnecessarily be much higher than specified and, due to the greater flow rates of the controls, the operation costs will be much higher than necessary.

Therefore, it is necessary to choose an optimal set of setpoints for the controllers. This can be gained by chance constrained optimization, i.e. the costs will be minimized and the constraints to $\mathbf{y}^C$ satisfied with a desired confidence level. This leads to a new concept of control: to control open loop processes by closed-loop control. Unlike the above problem definitions where controls are decision variables, in the closed framework the setpoints of the measurable outputs should be defined as decision variables. Moreover, controller equations have to be included in the problem formulation. It is normally a complicated NDTS or NDTJ problem. In practice, many continuous processes have constant uncertain inputs, and their impact on the controlled variables **y** can easily be compensated for by the controllers. Then the problem is reduced to a NSCS or NSCJ problem which can be solved by the approach discussed in the last section.

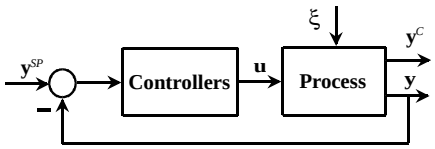

Fig. 5: The open-closed framework

The approach has been applied in a pilot distillation column to separate a methanol-water mixture with uncertain feed flow and composition as well as column pressure (Li et al. 2003). The operating energy is to be minimized subject to a rigorous model composed of component and energy balances, vapor-liquid equilibrium and tray hydraulics for each tray. The temperatures on the sensitive trays are selected as the controlled variables, while the bottom and top product purity are probabilistically constrained. The optimization results provide the profiles of the objective function value and the corresponding controller setpoints along with the confidence level to hold the product specification.

7. CONCLUSIONS

We have discussed the concepts, solution strategies and perspectives of chance constrained optimization and control. Since the uncertainty properties are taken into account, the solution of the problem is a decision *a priori*. A predefined probability to satisfy the constraints will be held under the uncertainty and thus the decision is robust. Moreover, the solution provides a comprehensive relationship between the performance criterion and the probability level of satisfying the constraints. Thus one can decide on proper actions which will result in a desired compromise between profitability and reliability. In this way, conservative or aggressive decisions, which may have been made so far, can be prevented. We have solved LDTJ, NSCS and NDCS problems and applied these approaches to several optimization and control applications. Development of more efficient methods to address high dimension NDTJ problems remains a challenge for future work.

8. REFERENCES

Arellano-Garcia, H., Martini, W., Wendt, M., Li, P., Wozny, G. (2003). Chance constrained batch distillation process optimization under uncertainty, FOCAPO2003 Proceedings, Florida, January 12-15, 2003, 609.

Bemporad, A., Morari, M., Dua, V., Pistikopoulos, E.N. (2002). The explicit linear quadratic regulator for constrained systems. *Automatica*, 38, 3.

Darlington J., Pantelides C.C., Rustem B., Tanyi, B.A. (1999). An algorithm for constrained nonlinear optimization under uncertainty. *Automatica*, 35, 217.

Diwekar, U.M., Kalagnanam, J.R. (1997). Efficient sampling technique for optimization under uncertainty. *AIChE J.* 43, 440.

Henrion, R., Li, P., Möller, A., Steinbach, M., Wendt, M., Wozny, G. (2001). Stochastic optimization for chemical processes under uncertainty, *Online Optimization of Large Scale Systems*, Grötschel et al. eds., Springer-Verlag, 455.

Kall, P., Wallace, S.W. (1994). Stochastic programming. New York: Wiley.

Kothare, M.V., Balakrishnan, V., Morari, M. (1996). Robust constrained model predictive control using linear matrix inequalities. *Automatica*, 32, 1361.

Li, P., Wendt, M., Wozny, G. (2000). Robust model predictive control under chance constraints. *Comput. & Chem. Eng.*, 24, 829.

Li, P., Wendt, M., Arellano-Garcia, H., Wozny, G. (2002a). Optimal operation of distillation processes under uncertain inflows accumulated in a feed tank. *AIChE Journal*, 48, 1198.

Li, P., Wendt, M., Wozny, G. (2002b). A probabilistically constrained model predictive controller, *Automatica*, 38, 1171.

Li, P., Wendt, M., Wozny, G. (2003). Optimal operations planning under uncertainty by using probabilistic programming. FOCAPO2003 Proceedings, Florida, January 12-15, 2003, 289.

Maybeck, P.S. (1995). Stochastic models, estimation, and control. Arlington: Navtech.

Morari, M., Zafiriou, E. (1989). Robust process control, *Prentice Hall*.

Petkov, S.B., Maranas, C. (1997). Multiperiod planning and scheduling of multiproduct batch plants under demand uncertainty. *Ind. Eng. Chem. Res.*, **36**, 4864.

Prékopa, A. (1995). Stochastic programming. Dordrecht: Kluwer.

Schwarm, A.T., Nikolaou, M. (1999). Chance-constrained model predictive control, *AIChE J.*, **45**, 1743.

Uryasev, S. (2000), Probabilistic constrained optimization: methodology and applications. Dordrecht: Kluwer.

Wendt, M., Li, P., Wozny, G. (2002). Nonlinear chance constrained process optimization under uncertainty. *Ind. Eng. Chem. Res.*, 41, 3621.

ADAPTIVE EXTREMUM SEEKING CONTROL OF NONISOTHERMAL CONTINUOUS STIRRED TANK REACTORS [1]

M. Guay [*,2] **D. Dochain** [**] **M. Perrier** [***]

[*] *Department of Chemical Engineering, Queen's University, Kingston, Ontario, Canada K7L 3N6*
[**] *CESAME, Universié Catholique de Louvain, Belgium*
[***] *Département de Genie Chimique, Ecole Polytechnique de Montréal, Montréal, PQ, Canada*

Abstract: In this paper, we present an adaptive extremum seeking control scheme for non-isothermal continuous stirred tank reactors. We assume limited knowledge of the reaction kinetics. An adaptive learning technique is introduced to construct an optimum seeking algorithm that drives the system states to optimal equilibrium concentrations of the reaction mixture. Lyapunov's stability theorem is used in the design of the extremum seeking controller structure and the development of the parameter learning laws. Under mild assumptions, the resulting controller is an output-feedback controller. the performance of the technique is demonstrated with the van de Vusse reaction.

Keywords: Extremum seeking, Lyapunov function, adaptive learning, persistence of excitation

1. INTRODUCTION

The task of extremum seeking is to find the operating set-points that maximize or minimize an objective function. Since the early research work on extremum control in the 1920's (Leblanc 1922), many successful applications of extremum control approaches have been reported (e.g., (Vasu 1957), (Astrom and Wittenmark 1995), (Sternby 1980) and (Drkunov *et al.* 1995)). Recently, Krstic et. al ((Krstic 2000), (Krstic and Deng 1998)) presented several extremum control schemes and stability analysis for extremum-seeking of linear unknown systems and a class of general nonlinear systems ((Krstic 2000) and (Krstic and Deng 1998)). An alternative Lyapunov-based adaptive extremum-seeking technique is developed in (Guay and Zhang 2002) in which the function to be optimized is not available for measurement.

In this study, we investigate an alternative extremum seeking scheme for nonisothermal continuous stirred tank reactors. Only limited knowledge of the reaction kinetics are assumed. A Lyapunov-based adaptive learning control technique is used to approximate the unknown kinetics and to steer the system to its unknown extremum. The technique ensures convergence of the system to an adjustable neighbourhood of its unknown optimum that depends on the approximation error. We also show that a certain level of persistence of excitation (PE) condition is necessary to guarantee the convergence of the extremum-seeking mechanism. The paper is organized as follows. Section 2 presents some notations and the problem for-

[1] Work support by the Natural Sciences and Engineering Council of Canada
[2] To whom correspondence should be addressed; guaym@chee.queensu.ca

mulation. Section 3 presents the adaptive extremum seeking controller and the stability and convergence of the closed-loop extremum seeking system. A numerical simulation is shown in Section 4 followed by brief conclusions in Section 5.

2. PROBLEM

We focus on a class of nonisothermal continuous stirred-tank reactor models described by

$$\dot{x} = -Dx + KC(x,T) + U_{in} \tag{1}$$
$$\dot{T} = -DT + \lambda^T C(x,T) + u \tag{2}$$

where $x \in S_x \subset \mathbb{R}^n$ denote the concentration of chemical components in the reaction mixture taking value in compact subset S_x of $\mathbb{R}^n$. The temperature is denoted by T, it takes values on a compact subset S_T of $\mathbb{R}^+$, the positive reals. $K \in R^{n\times r}$ is the $n \times r$ matrix of stoechiometric coefficients for each n components on r chemical reactions. The vector $C(x,T) \in \mathbb{R}^r$ summarizes the temperature dependent chemical kinetics for r chemical reactions of the reaction network under study. D is the CSTR dilution rate. $U_{in} \in R^n$ gives the rate of addition of each n components. The vector $\lambda \in \mathbb{R}^r$ provide the heats of reaction for each reaction. The control input u is assumed to be the rate of heating and cooling. The control objective is to design a controller, u, such that the function $y = Hx$, where $H \in \mathbb{R}^{1\times n}$, achieves its maximum at steady-state. We consider the extremum-seeking problem for the nonisothermal CSTR with unknown chemical reaction kinetics, $C(x,T)$. It is assumed that the stoechiometry of the reaction network (summarized by the matrix K) and the heats of reaction, λ, are known. The nonisothermal CSTR is initially assumed to operate at constant flowrate.

The problem is solved by first expressing the equilibrium concentrations in the reaction mixture as function of temperature, T. We assume that there exists a vector-valued function, $\pi(T)$, that solves the following equation

$$-D\pi(T) + KC(\pi(T),T) + U_{in} = 0. \tag{3}$$

The solution $\pi(T)$ is assumed to be continuous on S_T. More specifically, we require the following.

Assumption 2.1. The function $H\pi(T)$ is continuously differentiable and it admits a maximum on $\Psi_T = \{x \in S_x | x = \pi(T)\}$.

By Assumption 2.1, we consider only cases where $H\pi(T)$ is a continuously differentiable convex function of T.

We consider systems where the isothermal reaction kinetics are stable. We state this requirement as follows.

Assumption 2.2. Consider the reaction kinetics dynamics eq.(1). There exists a positive definite function $V(x) \in C^1$ such that

$$c_1\|x\|^2 \le V(x) \le c_2\|x\|^2$$

and

$$\dot{V} \le -c_3\|x - \pi(T)\| + c_4\|x\|\|\pi(T)\|$$

for positive nonzero constants c_1, c_2, c_3 and c_4.

Assumption 2.2 provides a minimum-phase property of the reaction kinetics that guarantees converge of the compositions, x, to a neighbourhood of the equilibrium $x = \pi(T)$.

The temperature dynamics eq.(2) subject to the equilibrium condition eq.(3) are written as

$$\begin{aligned}\dot{T} = &-DT + \lambda^T K^+ D\pi(T) - \lambda^T K^+ U_{in} \\ &+ u + \lambda^T (C(x,T) - C(\pi(T),T))\end{aligned} \tag{4}$$

We assume that the following holds.

Assumption 2.3. $\forall x \in S_x$ and $\forall T \in S_T$, $\exists$ a positive nonzero constant L_1 such that

$$\|C(x,T) - C(\pi(T),T)\| \le L_1\|x - \pi(T)\|. \tag{5}$$

The strategy developed in this paper consists in approximating the steady-state, or equilibrium, composition $\pi(T)$ using a linear approximation technique such as neural networks. Radial basis function (RBF) neural networks presented in (Sanner and Slotine 1992) and (Seshagiri and Khalil 2000) shall be used to approximate a continuous function $\phi : R^p \to R$ as

$$\phi(z) = W^{*T} S(z) + \mu_l(t) \tag{6}$$

with NN approximation error $\mu_l(t)$, and basis function vector

$$\begin{aligned} &S(z) = [s_1(z), s_2(z), \cdots, s_l(z)]^T \\ &s_i(z) = \exp\left[\frac{-(z-\varphi_i)^T(z-\varphi_i)}{\sigma_i^2}\right], \qquad i = 1, 2, ..l \end{aligned} \tag{7}$$

where φ_i is the center of the receptive field, and σ_i is the width of the Gaussian function. The ideal weight W^* in (6) is defined as

$$W^* := arg \min_{W\in\Omega_w} \left\{ \sup_{z\in\Omega} \left| W^T S(z) - \phi(z) \right| \right\} \quad (8)$$

where Ω is a compact subset of R^p and

$$\Omega_w = \left\{ W \;\middle|\; \|W\| \leq w_m \right\}$$

with positive constant w_m to be chosen at the design stage. Universal approximation results stated in (Funahashi 1989) (Kosmatopoulos *et al.* 1995) indicate that, if l is chosen sufficiently large, then $W^T S(z)$ can approximate any continuous function to any desired accuracy on a compact set.

We apply eq.(6) to develop an approximation of the objective function $y = H\pi(T)$ given by

$$H\pi(T) = W_p^{*T} S(T) + \mu_p(t) \quad (9)$$

where W_p^* and S are as defined in eqs.(7)-(8). Since it is assumed that the reaction kinetics are unknown, we need to approximate the term $D\lambda^T K^+ \pi(T)$. To allow for the simultaneous approximation of the objective function and the regulation of the system temperature, we breakdown the heat of reaction term as follows,

$$\lambda^T K^+ \pi(T) = \lambda^T K^+ H^T W_p^{*T} S(T) + W_o^{*T} S(T) + \mu_l(t).$$

We make the following assumption about the approximation error terms $\mu_p(t)$ and $\mu_l(t)$.

Assumption 2.4. The NN approximation errors satisfies $|\mu_p(t)| \leq \bar{\mu}_p$ and $|\mu_l(t)| \leq \bar{\mu}_l$ with constants $\bar{\mu}_p > 0$ and $\bar{\mu}_l > 0$ over the compact set $\Omega_w \times S_T$.

3. CONTROLLER DESIGN

In this section, we design a control strategy that tracts the unknown optimum of y. We first develop the parameter estimation algorithm for the unknown parameter vector W^*. Let $\hat{W}$ denote the estimate of the true parameter W^* and let $\hat{T}$ the predictions of T. Using eqs.(9)-(10) and eq.(4), the temperature dynamics are written as,

$$\begin{aligned} \dot{T} = &-DT + F(T)W^* + D\mu_l(t) - \lambda^T K^+ U_{in} + u \\ &+ \lambda \left(C(x,T) - C(\pi(T),T) \right) \end{aligned} \quad (10)$$

where $F(T) = [DS(T)^T, D\lambda^T K^+ H^T S(T)^T]$ and $W^{*T} = [W_p^{*T}, W_o^{*T}]$.

The predicted state $\hat{T}$ is generated by

$$\begin{aligned} \dot{\hat{T}} = &-DT + F(T)\hat{W} - \lambda^T K^+ U_{in} + u \\ &+ k_T(T - \hat{T}) + c_1(t)\dot{\hat{W}} \end{aligned} \quad (11)$$

with gain function $k_T > 0$ and prediction error $e_T = T - \hat{T}$. The vector-valued time-varying function $c_1(t)$ is to be assigned. It follows from (2)-(11) that

$$\begin{aligned} \dot{e}_T = &F(T)\tilde{W} + D\mu_l(t) - k_T e_T \\ &+ \lambda^T (C(x,T) - C(\pi(T),T)) - c_1(t)\dot{\hat{W}} \end{aligned} \quad (12)$$

where $\tilde{W} = W^* - \hat{W}$.

The objective of the extremum-seeking control is stabilize the closed-loop system around a point where the gradient of $y = H\pi(T)$ with respect to T vanishes while attenuating the effect of the modelling uncertainty $\mu_l(t)$.

Using the approximation eq.(9), the objective function given by

$$y = H\pi(T) = W_p^{*T} S(T) + \mu_p(t)$$

is approximated by

$$y_e = \hat{W}_p^T S(T)$$

where $\hat{W}_p$ is an estimate of the optimal weight W_p^*. The estimated gradient of y_e with respect to T is given by

$$z = \frac{\partial y_e}{\partial T} = \hat{W}_p^T dS(T) \quad (13)$$

where $dS(T) = \frac{\partial S(T)}{\partial T}$. The Hessian of y_e with respect to T is given by

$$\frac{\partial^2 y_e}{\partial T^2} = \hat{W}_p^T d^2 S(T) = \Gamma_2 \quad (14)$$

where $d^2 S(T) = \frac{\partial^2 S(T)}{\partial T^2}$

Define

$$z_s = \hat{W}_p^T dS(T) - d(t) \quad (15)$$

where $d(t) \in C^1$ is an excitation signal to be assigned. In the remainder, the dependence of the radial basis functions S on the temperature is implied and we write S, dS and $d^2 S$.

To address the controller design, we define the following auxiliary signals

$$\eta_1 = e_T - c_1(t)^T \tilde{W} \quad (16)$$

$$\eta_2 = z_s - c_2(t)^T \tilde{W} \quad (17)$$

where $c_2(t)$ is a time-varying vector valued function to be assigned in the design.

We propose the Lyapunov function candidate

$$V = \frac{1}{2}\eta_1^2 + \frac{1}{2}\eta_2^2. \tag{18}$$

The following dynamic controller is considered

$$\dot{d}(t) = c_2(t)^T \dot{\hat{W}} - k_z z_s - k_d|\Gamma_2|d(t) - \Gamma_2 a(t) \tag{19}$$

$$u = DT - F(T)\hat{W} + \lambda^T K^+ U_{in} - k_d sgn(\Gamma_2)d(t) - a(t) \tag{20}$$

where $k_z > 0$ and $k_d > 0$ are gain function to be assigned in the sequel, sgn is the sign function. The signal $a(t)$ acts as a secondary dither signal that is used to generate information about the unknown nonlinearities associated with the reaction kinetics. The dynamics of the time-varying functions $c_1(t)$ and $c_2(t)$ are assigned as follows

$$\dot{c}_1(t)^T = -k_T c_1(t)^T + F(T) \tag{21}$$

$$\dot{c}_2(t)^T = -k_z c_2(t)^T + \Gamma_2 F(T) \tag{22}$$

Taking the time derivative of V and substitution of eqs.(19)-(22) gives

$$\dot{V} = -k_T\eta_1^2 - k_z\eta_2^2 + (\eta_1 + \Gamma_2\eta_2) \times \left[D\mu_l(t) + \lambda^T \left(C(x,T) - C(\pi(T),T)\right)\right] \tag{23}$$

From Assumption 2.2 it follows that

$$\sup_{x\in S_x, T\in S_T} \|x - \pi(T)\| = C_1$$

exists and is finite. By Assumption 2.3, we get

$$\dot{V} \leq -k_T\eta_1^2 - k_z\eta_2^2 + (\eta_1 + \Gamma_2\eta_2)D\mu_l(t) + (|\eta_1| + |\Gamma_2|\|\eta_2\|)\,\|\lambda\|L_1C_1 \tag{24}$$

Completing the squares and applying the gain functions

$$k_T = k_{T0} + \frac{k_4}{2}D^2 + \frac{k_5}{2}\|\lambda\|^2, \tag{25}$$

$$k_z = k_{z0} + \frac{k_7}{2}\|\lambda\|^2\Gamma_2^2, \tag{26}$$

we obtain the following inequality

$$\dot{V} \leq -k_{T0}\eta_1^2 - k_{z0}\eta_2^2 + \left(\frac{1}{2k_4} + \frac{1}{2k_5}\right)\mu_l(t)^2 + \left(\frac{1}{2k_6} + \frac{1}{2k_7}\right)L_1^2C_1^2 \tag{27}$$

where $k_{T0} > 0$, $k_{z0} > 0$, $k_4 > 0$, $k_5 > 0$, $k_6 > 0$ and $k_7 > 0$ are constants. Eq.(27) establishes that the state, η, converges to a small neighborhood of the origin. It remains to show that the original state variables, e_T and z_s and the parameter estimation errors $\tilde{W}$ converge to a small neighborhood of the origin. To this end, we derive a persistency of excitation condition that guarantees the convergence of the parameter estimates to the ideal weights, W^*.

Consider the following matrix,

$$\Upsilon(t) = \begin{bmatrix} c_1(t)^T \\ c_2(t)^T \end{bmatrix}$$

By construction, this matrix solves the matrix differential equation

$$\dot{\Upsilon}(t) = -K(t)\Upsilon(t) + B(t) \tag{28}$$

where

$$K(t) = \begin{bmatrix} k_T & 0 \\ 0 & k_z \end{bmatrix}, \quad B(t) = \begin{bmatrix} F(T) \\ \Gamma_2 F(T) \end{bmatrix}.$$

A bound on the parameter estimates $\hat{W}$ can be ensured by choosing the following parameter update law.

$$\dot{\hat{W}} = \begin{cases} \gamma_w\Gamma & \text{if } \|\hat{W}\| \leq w_m \text{ or} \\ & \text{if} \|\hat{W}\| = w_m \text{ and } \hat{W}^T\Gamma \leq 0 \\ \gamma_w \left(I - \dfrac{\hat{W}\hat{W}^T}{\hat{W}^T\hat{W}}\right)\Gamma & \text{otherwise} \end{cases} \tag{29}$$

where $\Gamma = \Upsilon(t)^T e$ Eq.(29) is a projection algorithm which ensures that $\|\hat{W}\| \leq w_m$. The convergence of the parameter estimation scheme is considered in the sequel.

By the property of the projection algorithm and for the specific choice of basis function it is possible to show that the norm of $B(t)$ is bounded. Using the bound on $B(t)$, an explicit bound for the solution of eq.(28) can be obtained as follows,

$$\|\Upsilon(t)\| \leq C_2 e^{-\lambda_2(t-t_0)} + C_2\frac{B_M}{\lambda_2}. \tag{30}$$

where $C_2 = \|\Upsilon(t_0)\| > 0$ and $\lambda_2 > 0$ is a positive constant. Next, we want to show that the parameter estimation error $\tilde{W}$ converges to a neighborhood of the origin.

Substituting for $e = \eta + \Upsilon(t)\tilde{W}$ we obtain the perturbed dynamics

$$\dot{\tilde{W}} = -\gamma_w\Upsilon(t)^T\Upsilon(t)\tilde{W} - \gamma_w\Upsilon(t)^T\eta + \begin{cases} 0 & \text{if } \|\hat{W}\| \leq w_m \text{ or} \\ & \text{if} \|\hat{W}\| = w_m \text{ and } \hat{W}^T\Upsilon(t)^T e \leq 0 \\ \gamma_w \dfrac{\hat{W}\hat{W}^T}{\hat{W}^T\hat{W}}\left(\Upsilon(t)^T\Upsilon(t)\tilde{W} + \Upsilon(t)^T\eta\right) & \text{otherwise} \end{cases} \tag{31}$$

To establish the convergence of the parameter estimation, we make the following persistency of excitation assumption.

Assumption 3.1. The solution of eq.(28) is such that there exists positive constants $T > 0$ and $k_N > 0$ such that

$$\int_{t}^{t+T} \Upsilon(\tau)^T \Upsilon(\tau) d\tau \geq k_N I_N \tag{32}$$

where I_N is the N-dimensional identity matrix.

By a standard adaptive control argument, the persistency of excitation condition guarantees that the origin of the differential equation

$$\dot{\tilde{W}} = -\gamma_w \Upsilon(t)^T \Upsilon(t) \tilde{W} \tag{33}$$

is an exponentially stable equilibrium. Since $B(t)$ is a bounded function, it is shown that the parameter estimation error is guaranteed to decay exponentially as

$$\|\tilde{W}\| \leq \alpha_4 e^{-\lambda_4 (t-t_0)} + \frac{|\bar{\mu}_l| + L_1 C_1}{\sqrt{2kmc_3}} \tag{34}$$

Hence the parameter estimation error and the redefined state variables, η, converge exponentially fast to an adjustable neighbourhood of the origin. By definition, convergence of η and $\tilde{W}$ to a neighbourhood of the origin implies that $\|e\| \leq \|\eta\| + \|\Upsilon(t)\| \|\tilde{W}\|$. Substituting for $\|\eta\|$, $\|\Upsilon(t)\|$ and $\tilde{W}$, we obtain

$$\|e\| \leq \alpha_5 e^{-\lambda_5 (t-t_0)} + \beta_5 \tag{35}$$

where $\alpha_5 > 0$ and $\beta_5 > 0$ are computable positive constants. The convergence of the error vector, e, implies that the convergence of the prediction error, e_T and the exponential convergence of the closed-loop system to an adjustable neighbourhood of the unknown steady-state optimum. We summarize the result of the above analysis as follows.

Theorem 3.1. Consider the nonisothermal continuous stirred tank reactor model eqs.(1)-(2) in closed-loop with the state prediction eq.(11), the controller eq.(20), the dither signal eq.(19) and the adaptive learning law eq.(29). Assume that the signal $a(t)$ is such that

$$\int_{t}^{t+T} \Upsilon(\tau)^T \Upsilon(\tau) d\tau \geq k_N I_N \tag{36}$$

for positive constants $T > 0$ and $k_N > 0$ where $\Upsilon(t)$ is the solution of eq.(28). Then

- the error dynamics eq.(12) converge exponentially to a small neighbourhood of the origin
- the parameter estimation errors $\tilde{W}$ converge exponentially to a small neighbourhood of the origin
- the tracking error from the unknown steady-state, z_s, converges exponentially to a small neighbourhood of the origin.

Parameter	Value
$k_{10},\ E_1$	$1.287 \times 10^{12},\ 9758.3$
$k_{20},\ E_2$	$1.287 \times 10^{12},\ 9578.3$
$k_{30},\ E_3$	$9.043 \times 10^{9},\ 8560.0$

Table 4.1. Kinetic Parameters of the van de Vusse reactor

4. SIMULATION RESULTS

In this section, we demonstrate the effectiveness in simulation of the proposed adaptive extremum-seeking control. We consider the standard van de Vusse chemical reaction. The reaction scheme for this reactor is given by

$$A \rightarrow B$$
$$2A \rightarrow D$$

The reaction kinetics are summarized by

$$K = \begin{bmatrix} -1 & 0 & -1 \\ 1 & -1 & 0 \end{bmatrix},\ C(x,T) = \begin{bmatrix} k_{10} e^{-(\frac{E_1}{T})} x_1 \\ k_{20} e^{-(\frac{E_2}{T})} x_2 \\ k_{30} e^{-(\frac{E_3}{T})} x_1^2 \end{bmatrix}$$

where x_1 and x_2 are the concentrations of components A and B, respectively, T is the reactor temperature, k_{10}, k_{20} and k_{30} are the pre-exponential factors, E_1, E_2 and E_3 are the activation energies. The numerical values used for simulation are listed in Table 4.1.

The dilution rate, D, is 14.19 hr^{-1}. The latent heat of reaction is given by $\lambda^T = [-4.2,\ 11.0,\ -41.85]/\rho/C_p$ where $\rho = 0.9342$ and $C_p = 3.01$. The pseudo-inverse of K is given by

$$K^+ = \begin{bmatrix} -0.333 & 0.333 \\ -0.333 & -0.667 \\ -0.667 & -0.333 \end{bmatrix}$$

The objective is to steer the system to the maximum steady-state concentration of B, that is $H = [0, 1]$.

We consider the initial conditions, $x_1(0) = 1$, $x_2(0) = 0$, $T(0) = 25$. The centers of the linear approximation are evenly spaced points on the interval [75,125], $\sigma_i^2 = 10$ for $1 \leq\leq l$. The six(6) centers, ω_i, are picked evenly at spaced points on that interval. The dither signal was set to

$$a(t) = exp(-0.1t) \sum_{i=1}^{6} (sin((0.5i)t) + cos((0.5i)t))$$

The simulation results are shown in Figures 1 to 3. The concentration of component B is shown in Figure 1. Figure 2 shows the reactor temperature profile. The required control action is given in Figure 3. The true optimum concentration of B is 1.09. As shown in Figure 1, the adaptive controller recovers the unknown optimum is a relatively short time. The control profile and the temperature profile demonstrate that the control is physically realizable.

5. CONCLUSION

We have solved a class of extremum seeking control problems for continuous stirred tank reactors represented by an unknown growth kinetic model. It has been shown that when the external dither signal is designed such that a persistent of excitation condition is satisfied, the proposed adaptive extremum seeking controller guarantees the exponential convergence to an adjustable neighborhood of its optimum.

6. REFERENCES

Anderson, B.D., R.R. Bitmead, C.R.J. Johnson, P.V. Kokotovic, R.L. Kosut, I.M. Mareels, L. Praly and B.D. Riedle (1986). *Stability of Adaptive Systems: Passivity and Averaging Analysis*. MIT Press. Cambridge, MA.

Astrom, K.J. and B. Wittenmark (1995). *Adaptive Control, 2nd Edition*. Addison-Wesley. Reading, MA.

Drkunov, S., U. Ozguner, P. Dix and B. Ashrafi (1995). Abs control using optimum search via sliding modes. *IEEE Trans. Contr. Syst. Tech.* **3**, 79–85.

Funahashi, K. I. (1989). On the approximate realization of continuous mappings by neural networks. *Neural Networks* **2**, 183–192.

Guay, M. and T. Zhang (2002). Adaptive extremum seeking control of nonlineaer systems with parametric uncertainties. *Proc. IFAC World Congress, Barcelona* pp. 475–481.

Kosmatopoulos, E. B., M. M. Polycarpou, M. A. Christodoulou and P. A. Ioannou (1995). High-order neural network structures for identification of dynamical systems. *IEEE Trans. Neural Networks* **6**(2), 422–431.

Krstic, M. and H. Deng (1998). *Stabilization of Nonlinear Uncertain Systems*. Springer-Verlag.

Krstic, M. (2000). Performance improvement and limitations in extremum seeking control. *Systems & Control Letters* **5**, 313–326.

Leblanc, M. (1922). Sur l'électrification des chemins de fer au moyen de courants alternatifs de fréquence élevée. *Revue Générale de l'Electricité*.

Sanner, R. M. and J. E. Slotine (1992). Gaussian networks for direct adaptive control. *IEEE Trans. Neural Networks* **3**(6), 837–863.

Seshagiri, S. and H. K. Khalil (2000). Output feedback control of nonlinear system using rbf neural networks. *IEEE Trans. Neural Net.* **11**, 69–79.

Sternby, J. (1980). Extremum control systems: An area for adaptive control?. *Preprints of the Joint American Control Conference, San Francisco, CA*.

Vasu, G. (1957). Experiments with optimizing controls applied to rapid control of engine presses with high amplitude noise signals. *Transactions of the ASME* pp. 481–488.

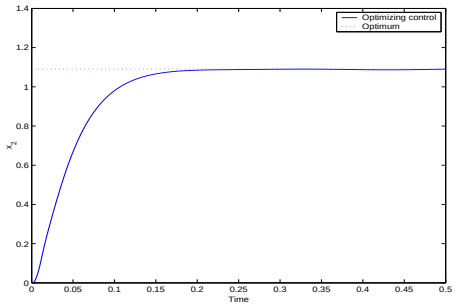

Fig. 1. Concentration of B

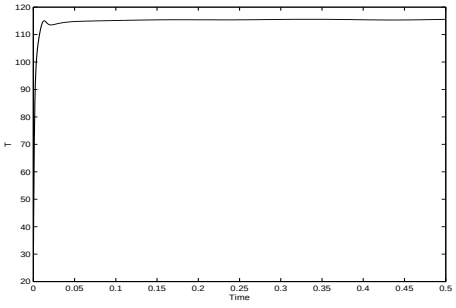

Fig. 2. Temperature Response

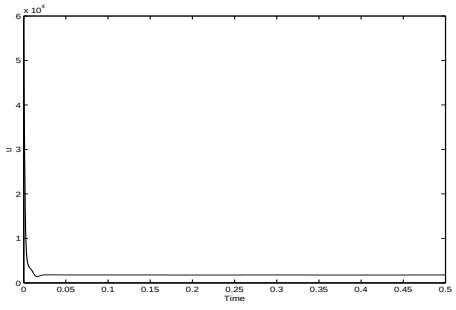

Fig. 3. Control, u

ON THE USE OF CONTROLLER PARAMETRIZATION IN THE OPTIMAL DESIGN OF DYNAMICALLY OPERABLE PLANTS

Kevin G. Dunn * **Christopher L. E. Swartz** *

* *Dept. of Chemical Engineering, McMaster University, 1280 Main Street West, Hamilton, Ontario, L8S 4L7, Canada*

Abstract: This paper explores some issues pertaining to the use of Q–parametrization in the optimal design of dynamically operable plants. An optimization–based plant design formulation in which a discrete-time implementation of the controller parametrization is embedded, is described. Its application is demonstrated through a reactor case study in which the resulting design is compared against that obtained using PI control. Differences in results obtained are discussed and related to the design problem formulation. The impact of other assumptions, such as the disturbance dynamics, is also discussed.

Keywords: integrated design and control; PI control; Q–parametrization

1. INTRODUCTION

The impact that the design of a plant can have on its ability to be satisfactorily controlled has led to a significant research effort both in the development of techniques for dynamic operability assessment and in the incorporation of dynamic operability criteria directly within plant design calculations. Reviews of work in this area include those of Walsh and Perkins [1996], van Schijndel and Pistikopoulos [2000], and Pistikopoulos and Sakizlis [2002].

Optimization-based approaches are particularly effective both for the quantitative assessment of dynamic operability, and for the design of plants that are both economically optimal and dynamically operable. This framework enables the plant-inherent control performance limitations of non-minimum phase characteristics, input constraints and uncertainty [Morari, 1983] to be simultaneously accounted for, and offers considerable flexibility in the problem formulation. Inclusion of various controller types is possible, including no control [Bahri et al., 1996], perfect control, and controllers of specified type such as multi-loop PI control [Mohideen et al., 1996; Bansal et al., 2002]. Swartz [1996] utilized Q–parametrization within an optimization-based framework to provide a controller-independent measure of operability for alternative designs; its extension to plant design formulations is described in Swartz et al. [2000].

In this paper, we outline the general optimization-based approach to integrated plant and control system design, focusing in particular on the use of Q–parametrization and PI control as the regulatory control strategy. These strategies are implemented on a comprehensive reactor case study, and the results compared. We show that the control performance metric induced by the economic objective function coupled with path constraints explains much of the similarity in the results obtained. This issue, along with other features of the optimization-based formulation, are discussed.

2. PROBLEM FORMULATION

The optimal design formulation considered here is as follows:

Maximize:	objective function
subject to:	• dynamic process model;
	• operating constraints;
	• and controller equations
	for all disturbances within a specified set
To provide:	• an optimal design;
	• an optimal operating point;
	• and optimal controller tuning.

Each aspect of this formulation will now be briefly described.

2.1 Objective function

The objectives in process design vary widely, are multifaceted and are frequently conflicting. A strategy that is widely adopted is to use an economic–based objective function, as is typically followed in steady-state design. This single measure is not likely to completely and accurately encapsulate all features of interest, such as ease of operation. These remaining features are incorporated as constraints.

The objective function in the case study that follows is formulated in terms of a physical design variable and steady-state values of certain operating variables. The optimal steady-state must be such that the operation remains feasible over a specified time horizon for all disturbances within a specified set.

2.2 The dynamic process model equations

Continuous time processes with a differential and algebraic equation (DAE) model description are considered in this formulation. As a simultaneous solution strategy is employed in this work, the differential equation elements of the model are converted to algebraic equations by using orthogonal collocation on finite elements. The complete set of algebraic, equality equations is then incorporated into the problem as constraints.

Discrete time controllers are used in this study and it is important to align their sampling time with the finite element representation of the process model. Many finite elements per sampling period are used in the model discretization strategy to capture the range of process dynamics that may occur within one sampling interval.

2.3 Operating constraints

The process operating constraints define desirable and feasible process behaviour. Collectively they define the required dynamic operability and also aide in the the solution of the optimization problem by limiting the search space.

2.4 Disturbances

Step–like disturbances will be used in this paper, going from nominal to upper or lower bound values. Combinations of disturbances are handled by using a set of parallel process models – one for each disturbance combination. All these parallel models are constrained to use the same physical design, operating point and controller tuning, thereby increasing the problem's size, but maintaining the same degrees of freedom.

2.5 Controller equations

Two feedback controller types are considered here: PI control and Q–parametrization.

2.5.1. PI control The velocity form of the digital PI controller is given by

$$\Delta u_k = K_{\mathrm{c}} \left[e_k - e_{k-1} + \frac{\Delta t}{\tau_{\mathrm{I}}} e_k \right] \quad (1)$$

where: $\Delta u_k = u_k - u_{k-1}$

Two controller tuning variables, K_{c} and τ_{I}, are introduced for every PI loop added to the process.

2.5.2. Q–parametrization is an established part of control theory and provides a convenient mechanism for representing and parameterizing all stable closed-loop maps from a set of exogenous inputs to regulated outputs in a linear feedback system [Francis, 1987; Green and Limebeer, 1995]. The IMC controller [Garcia and Morari, 1982; Morari and Zafiriou, 1989] shown in Figure 1 yields a parametrization of this type for stable plants. The feedback system is stable if Q is stable.

The significance of this representation in the present operable design application is that by including a finite dimensional approximation of Q in the decision space, a design is obtained that represents an optimum for linear control independent of controller type or tuning.

A finite impulse representation is used for Q, which for SISO systems takes the form,

$$Q(z^{-1}) = \sum_{i=0}^{L} q_i z^{-i} \qquad L = (t_f - t_0)/\Delta t \quad (2)$$

The controller decision variables are the coefficients q_i, $i = 0, 1, \ldots, L$.

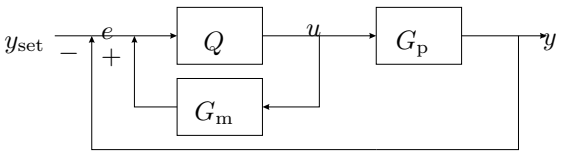

Fig. 1. The Q–parametrization structure used

Asymptotic tracking may be achieved by requiring

$$\left(\sum_{i=0}^{L} q_i\right) \overline{G}_{\text{m}} = 1$$

where $\overline{G}_{\text{m}}$ is the model gain. In addition, this condition yields an initial guess strategy for $q(z^{-1})$ by setting $q_0 = 1/\overline{G}_{\text{m}}$ and $q_i = 0$ for the remaining coefficients.

In the case study that follows, the optimization is carried out on the *nonlinear* dynamic model. The linear model required for the Q–parametrization is obtained by linearizing the nonlinear model around the current iterate of the steady-state operating variables. Upon convergence of the optimization, the Q–parametrization is consistent with the optimal steady-state operating point.

2.6 Solution Strategy

Cervantes and Biegler [2001] review solution methods for dynamic optimization problems and divide them into two major classes, Direct and Indirect methods. The Direct methods are widely used and are again divided into two categories: the *sequential* and *simultaneous* methods. In this paper a simultaneous solution strategy is used and since no integer variables are present, it results in a nonlinear programming (NLP) problem.

3. CASE STUDY

The case study presented here considers the integrated design and control of a stirred tank reactor in which an irreversible, exothermic reaction takes place. The study is based, in part, on the work of Loeblein and Perkins [1998].

The objectives of this study are to:

- find a design that is dynamically operable with respect to the given process constraints;
- determine the difference between designs using PI control and designs using a controller described by Q–parametrization;
- analyze the design by investigating the assumptions and constraints.

3.1 Process description

The process model is given by the equations in (3) with parameter values in Table 1. Values in the lower half of this table represent the values of the variables at the steady–state economic optimum, with the objective function given by Equation (3f) and constraints in Equation (4).

The disturbances are taken to be step changes from the nominal value, in parentheses, of the following two variables to their upper and lower bounds:

- $18 \leqslant C_{\text{in}}(t) \leqslant 22$ kmol/m^3 (20 kmol/m^3)
- $290 \leqslant T_{\text{in}}(t) \leqslant 310$ K (300 K)

$$\frac{dC}{dt} = \frac{F_{\text{in}}}{V}\left(C_{\text{in}} - C\right) - k_0 e^{-\frac{E}{RT}} C \tag{3a}$$

$$\frac{dT}{dt} = \frac{F_{\text{in}}}{V}\left(T_{\text{in}} - T\right) + \left(-\frac{\Delta H_{\text{R}}}{\rho C_p}\right) k_0 e^{-\frac{E}{RT}} C - \frac{Q_{\text{cool}}}{V} \tag{3b}$$

$$Q_{\text{cool}} = U_{\text{A}}(T - T_{\text{mean}}) \tag{3c}$$

$$Q_{\text{cool}} = F_{\text{c}}(T_{\text{cool}} - T_{\text{cool,in}}) \tag{3d}$$

$$T_{\text{mean}} = 0.5(T_{\text{cool}} + T_{\text{cool,in}}) \tag{3e}$$

$$\phi_{\text{econ}} = 10\overline{F}_{\text{in}}\left(C_{\text{in}} - \overline{C}\right) - 0.01\overline{Q}_{\text{cool}} - 0.1\overline{F}_{\text{in}} - 0.075V^{0.7} \tag{3f}$$

$$T(t) \leqslant 350 \text{ K} \tag{4a}$$

$$0.05 \leqslant F_{\text{in}}(t) \leqslant 0.8 \text{ m}^3/\text{s} \tag{4b}$$

$$T_{\text{cool}}(t) \leqslant 330 \text{ K} \tag{4c}$$

$$T_{\text{cool}}(t) < T(t) \tag{4d}$$

$$C(t) \leqslant 0.1 \text{ kmol/m}^3 \tag{4e}$$

$$V \leqslant 10 \text{ m}^3. \tag{4f}$$

Table 1. Nomenclature and value for the process model

Variable Name	Nominal Values	Units	Lagrange Multiplier
C_{in}	20	kmol/m^3	–
T_{in}	300	K	–
$T_{\text{cool,in}}$	300	K	–
F_{c}	0.7	m^3/s	–
k_0	2.7×10^8	s^{-1}	–
E/R	6000	K	–
U_{A}	0.35	m^3/s	–
$\frac{-\Delta H_{\text{R}}}{(\rho C_p)}$	5	m^3.K/kmol	–
C	0.1	kmol/m^3	4.6437
T	350	K	2.2603
F_{in}	0.2828	m^3/s	0
V	5.808	m^3	0
T_{cool}	320	K	0
T_{mean}	310	K	0
Q_{cool}	14	m^3.K/s	0
ϕ_{econ}	55.86	\$/hr	–

3.2 Integrated design and control

The steady–state economic optimum presented in Table 1 is not dynamically operable, even with feedback control, since a disturbance could cause

Table 2. Steady–state values for open–loop operation

Name	Value	Name	Value
$\overline{C}$	0.07146 kmol/m^3	$\overline{Q}_{\text{cool}}$	11.65 m^3.K/s
$\overline{T}$	341.6 K	$\overline{T}_{\text{mean}}$	308.3 K
$\overline{F}_{\text{in}}$	0.2007 m^3/s	$\overline{T}_{\text{cool}}$	316.6 K
V	8.803 m^3	ϕ_{econ}	39.52 \$/hr

C and/or T to violate their respective active constraints. The process operating point must be changed to achieve dynamic operability. An analysis of the design degrees of freedom shows that two independent variables may be selected in order to fix the remaining variables. Of the seven variables in the lower half of Table 1, one is a design variable, V, while the remaining are constrained operating variables, such as C, T, F_{in} and T_{cool}.

3.2.1. No feedback control: An operating point can be found for this particular example which does not require feedback control. This operating point is within the permanent feasible region, so that no constraint violation occurs when the given disturbances impact on the process either separately or together. This operating point is found by using the formulation described above without controllers where the search variables are then the tank volume and the steady state inlet flowrate, $\overline{F}_{\text{in}}$.

The design summary is given in Table 2 which shows that a sacrifice in the profit has to be made in order to operate at this point – the price to be paid to remain operable without feedback control. This design has all variability appearing in the process outputs, with the process inputs remaining constant.

3.2.2. With feedback control: The sacrifice in process profit can be reduced by implementing feedback control, but the aim of this study is to investigate how much improvement is to be had by using either PI control or Q–parametrization.

The tank temperature with a 10 second measurement delay is selected as the controlled variable; the inlet flowrate is chosen to be the manipulated variable in this study, as was done in the work of Loeblein and Perkins [1998]. The search space now consists of the process design and operating variables from the lower half of Table 1 as well as the controller tuning variables of the two controller types.

Solving the design problem with PI control results in the operating point given in Table 3. An improvement of \$ 6.62 per hour is achieved compared to the profit with open–loop operation. The integral square error (ISE) values are computed from Equation 5 with $\psi = 0$, the weighted ISE (wISE) values have $\psi = 30\ 000$ for all possible disturbance combinations, J, over a time horizon with $t_f = 500$ s.

$$w\text{ISE} = \sum_{j=1}^{J} \sum_{k=0}^{L-1} \left[\left(\overline{T} - T_{k,j} \right)^2 + \psi \left(\Delta F_{\text{in},k,j} \right)^2 \right] \Delta t \tag{5}$$

$$L = (t_f - t_0)/\Delta t \qquad J = 8 \tag{6}$$

Table 3. Design with PI control

Name	Value	Name	Value
$\overline{C}$	0.06054 kmol/m^3	$\overline{Q}_{\text{cool}}$	12.71 m^3.K/s
$\overline{T}$	345.4 K	$\overline{T}_{\text{mean}}$	309.1 K
$\overline{F}_{\text{in}}$	0.2341 m^3/s	$\overline{T}_{\text{cool}}$	318.2 K
V	10.00 m^3	ϕ_{econ}	46.14 \$/hr
K_c	0.01511	τ_I	28.50
ISE	1586	wISE	1885

Solving the same design problem using Q–parametrization yields an improvement of \$ 7.26 per hour when using 2 or more coefficients for $q(z^{-1})$. Table 4 shows the values at the nominal operating point, which do not change after two coefficients for $Q(z^{-1})$. Only the integral squared error metrics are reduced by adding further coefficients, as seen in Table 5.

Table 4. Design with Q–parametrization

Name	Value	Name	Value
$\overline{C}$	0.06034 kmol/m^3	$\overline{Q}_{\text{cool}}$	12.80 m^3.K/s
$\overline{T}$	345.7 K	$\overline{T}_{\text{mean}}$	309.1 K
$\overline{F}_{\text{in}}$	0.2372 m^3/s	$\overline{T}_{\text{cool}}$	318.3 K
V	10.00 m^3	ϕ_{econ}	46.78 \$/hr
ISE	877	wISE	1571

Table 5. Varying the number of FIR coefficients in $Q(z^{-1})$

$Q(z^{-1})$	ϕ_{econ} (\$/hr)	ISE	wISE
0.009336	45.51	3236	3306
$0.07148 - 0.06191z^{-1}$	46.78	1400	2184
$q_0 + \ldots + q_4 z^{-1}$	46.78	878	1620
$q_0 + \ldots + q_9 z^{-1}$	46.78	904	1584
$q_0 + \ldots + q_{19} z^{-1}$	46.78	877	1571

Figures 2 and 3 show trajectories for the design under PI control and for design with Q–parametrization. These trajectories represent the closed–loop response and manipulated variable inputs respectively for the case when both disturbances are stepped to their upper limits simultaneously at $t = 20$. These figures also serve to illustrate the difference between using 2 and 20 coefficients for $Q(z^{-1})$ and contrast to PI control.

3.3 Design Analysis

The above results indicate that there is not much difference, in this case study, between using PI control or the more advanced Q–parametrization strategy to maintain dynamically operable process behaviour while still remaining economically

Fig. 2. Controlled variable trajectories

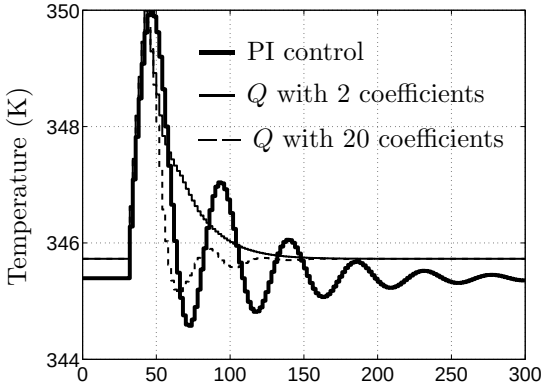

Fig. 3. Manipulated variable trajectories

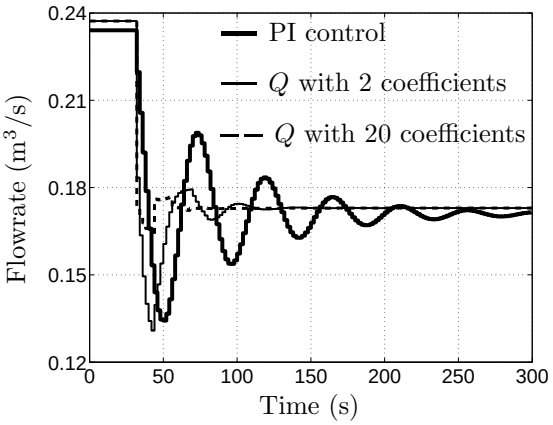

optimal. This occurs because the distance from the constraints for both controller types is approximately the same. The integral squared error is however less for the more advanced controller and unless this has a significant economic benefit the standard PI controller would be economically acceptable.

Two aspects of the study require some further analysis and discussion for completion. The first aspect is the volume constraint that is active in all of the above designs and the second is the assumption of disturbance type and its dynamics.

3.3.1. The volume constraint: Table 6 shows the result of using the formulation to relax the volume constraint in Equation 4. It is understandable that a larger tank volume would attenuate the initial deviation for the controlled variable when the disturbance impacts the process. This allows for $\overline{T}$ to be closer to the constraints of 350 K, resulting in increased profit in ϕ_{econ}.

Note that if the volume constraint is completely removed, the economically optimal tank volume is calculated as 114 m^3. Increasing the volume to such a large value may be considered as downgrading the process equipment, but it is necessary to maintain an operable system at the calculated

Table 6. Effect of the volume constraint on the process design and operation

Variable	PI Control			
	$V \leqslant 10$	$V \leqslant 20$	$V \leqslant 80$	$V \leqslant \infty$
$\overline{T}$ (K)	345.4	347.0	349.0	349.3
V (m^3)	**10.00**	**20.00**	**80.00**	**114.0**
ϕ_{econ} (\$/hr)	46.14	48.93	52.07	52.19
wISE	1885	1255	686	600

set point. A point to also note is that assumptions of perfect mixing may not be valid at such high tank residence times and the model may need to be adjusted.

3.3.2. The disturbance dynamics: The PI controller design of Table 3 was used, but the step disturbance input was replaced with the following disturbance model:

$$C_{\text{in}}(t) = 2\sin(0.01t) + 20 \qquad t \in [t_0; t_{\text{f}}]$$
$$T_{\text{in}}(t) = 10\sin(0.01t + \varphi) + 300 \qquad \varphi \in [0; 2\pi]$$

Figure 4 shows the output of the two constrained state variables at 10 equally spaced points in the range of φ. This ball of process operation can be seen to lie well within the constrained region, indicating that the nominal operating point of the current design could well be moved closer to the upper temperature and concentration constraints of 350 K and 0.1 kmol/m^3 respectively.

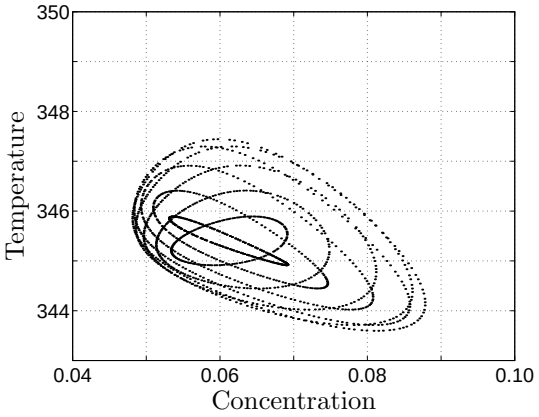

Fig. 4. The effect of sinusoidal disturbances on process variability with PI control

In summary, the effect of varying the process constraints can be understood and quantified using this formulation. It allows for more informed economic and operability trade–off when process parameters are to be investigated. Furthermore, the assumption of step–like disturbance dynamics was shown to lead to a conservative design and improved profit could be had if the disturbance dynamics were known more accurately.

4. CONCLUSIONS

An implementation of an integrated plant and control system design formulation is described,

focusing in particular on the use of PI control and a parametrization of all linear stabilizing controllers. The integrated design strategy is illustrated through an application to a reactor case study. Various scenarios are considered – steady-state optimal design; dynamic optimization without control; the inclusion of PI control; controller parametrization; relaxation of the maximum volume constraint and the effect of disturbance dynamics.

The difference between PI control and the result using controller parametrization was found to be slight. One reason for this is that the control performance metric induced by the objective function and path constraints is the distance of the steady-state operating point to active constraints, and PI control appears to be essentially as good as the best linear controller in minimizing the peak output variation in the direction of the active constraints. While the difference between the closed-loop performance as measured by the integral square error is significant, this measure is incorporated neither into the objective function nor constraints. This illustrates the importance of accurately capturing the desired design and operational objectives.

REFERENCES

P. A. Bahri, J. A. Bandoni, and J. A. Romagnoli. Effect of Disturbances in Optimizing Control: Steady-State Open-Loop Backoff Problem. *AIChE J.*, 42(4):983–994, 1996.

V. Bansal, J. D. Perkins, and E. N. Pistikopoulos. A Case Study in Simultaneous Design and Control Using Rigorous, Mixed-Integer Dynamic Optimization Models. *Ind. Eng. Chem. Res.*, 41:760–778, 2002.

A. Cervantes and L. T. Biegler. Optimization Strategies for Dynamic Systems. In C. A. Floudas and P. M. Pardalos, editors, *Encyclopedia of Optimization*, volume 4, pages 216–227. Kluwer Academic Publishers, 2001.

B. A. Francis. *A Course in $\mathcal{H}_\infty$ Control Theory*. Springer-Verlag, Berlin, 1987.

C. E. Garcia and M. Morari. Internal Model Control. 1. A Unifying Review and Some New Results. *Ind. Eng. Chem. Proc. Des. Dev.*, 21: 308–323, 1982.

M. Green and D. J. N. Limebeer. *Linear Robust Control*. Prentice-Hall, 1995.

C. Loeblein and J. D. Perkins. Economic Analysis of Different Structures of On–line Process Optimization Systems. *Comp. Chem. Eng.*, 22 (9):1257–1269, 1998.

M. J. Mohideen, J. D. Perkins, and E. N. Pistikopoulos. Optimal Design of Dynamic Systems Under Uncertainty. *AIChE J.*, 42(8):2251–2272, 1996.

M. Morari. Design of Resilient Processing Plants – III. A General Framework for the Assessment of Dynamic Resilience. *Chem. Eng. Sci.*, 38: 1881–1891, 1983.

M. Morari and E. Zafiriou. *Robust Process Control*. Prentice Hall, 1989.

E. N. Pistikopoulos and V. Sakizlis. Simultaneous Design and Control Optimization under Uncertainty in Reaction/Separation Systems. In J. B. Rawlings, B. A. Ogunnaike, and J. W. Eaton, editors, *Sixth International Conference on Chemical Process Control*, AIChE Symposium Series No. 326, Volume 98, pp. 223–238, 2002.

C. L. E. Swartz. A Computational Framework for Dynamic Operability Assessment. *Comp. Chem. Eng.*, 20(4):365–371, 1996.

C. L. E. Swartz, J. D. Perkins, and E. N. Pistikopoulos. Incorporation of Controllability in Process Design through Controller Parameterization. In *Process Control and Instrumentation*, University of Strathclyde, 2000.

J. M. G. van Schijndel and E. N. Pistikopoulos. Towards the Integration of Process Design, Process Control & Process Operability – Current Status & Future Trends. In M. F. Malone, J. A. Trainham, and B. Carnahan, editors, *Foundations of Computer-Aided Process Design*, volume 96, pages 99–112. American Institute of Chemical Engineers, 2000.

S. P. K. Walsh and J. D. Perkins. Operability and Control in Process Synthesis and Design. In *Advances in Chemical Engineering*, volume 23, pages 301–402. Academic Press, Inc., 1996.

IMPROVED PERFORMANCE OF ROBUST MPC WITH FEEDBACK MODEL UNCERTAINTY

A. L. Warren and T. E. Marlin

Department of Chemical Engineering, McMaster University, Hamilton, ON L8S 4L7 Canada

Abstract: Robust model-predictive controllers use an estimate of model uncertainty in the on-line controller calculation and can be overly conservative for some uncertainty descriptions. This paper discusses the various causes of conservative control with particular emphasis given to the concept of 'closed-loop' probabilistic predictions. A multi-input-multi-output MPC is proposed in which an off-line, non-convex calculation is used to characterize the closed-loop uncertainty a priori. This uncertainty information is incorporated into a convex, quadratic program resulting in a MPC formulation that can be efficiently solved on-line. A distillation column case study demonstrates the benefits of the proposed robust MPC.

Keywords: Robust control, Control algorithms, Closed-loop, Convex optimization.

1. INTRODUCTION

Model-predictive control (MPC) systems have found widespread success in the process industries. The vast majority of these controllers rely upon nominal models, i.e. model uncertainty is not explicitly considered in the on-line controller calculation. Extensive simulation studies and tuning are often required to ensure that these nominal-MPC systems are appropriately robust (Qin and Badgwell, 1996).

Since this situation is not desirable, techniques to create robust MPC systems have been investigated since the late 1980's (see (Badgwell, 1997) for a review). Many of the initial robust MPC systems, such as min-max MPC (Zheng and Morari, 1993), achieved robust stability at the expense of dynamic performance. There are several causes of overly conservative control in robust MPC:

1) *Min-max control strategy* - Min-max controllers are inherently conservative, because they optimize the performance for only the worst-case plant/model mismatch (Bemporad and Morari, 1999).

2) *Time-varying descriptions of process uncertainty* – Several robust MPC systems assume that the process is time-varying (Zheng and Morari, 1993). However, in the process industries many of the processes can be assumed to be time-invariant *within the prediction horizon.* A time-varying description will lead to control that is often too conservative if the actual process is time-invariant.

3) *Open-loop predictions of future system behavior* – An open-loop prediction is one in which the effect of future controller actions is not modeled. An open-loop prediction often overestimates the uncertainty in future process outputs because it does not consider that future controller actions that will respond to plant/model mismatch. This over-estimation of output uncertainty leads to conservative control when the system is near constraints (Mayne, 2000; Kothare et al., 1996).

The controller proposed in this paper addresses these issues by basing the MPC on a closed-loop, time-invariant model of future system behavior. The conservativeness inherent to min-max control is avoided by maintaining the nominal value of the process output near its setpoint while using probabilistic models to avoid output-constraint violations. In addition, the proposed controller uses engineering knowledge of the structure of the process uncertainty to avoid overly conservative uncertainty descriptions. As will be shown in case study, the resulting MPC is robust with respect to output-constraints while avoiding excess conservativeness.

In order to remain computationally feasible for on-line use, the proposed controller is implemented in two stages. In the first stage, the effect of plant/model mismatch on system behavior is captured in off-line studies involving non-convex

optimizations. In the second stage, an on-line, convex quadratic program uses the results calculated off-line to predict and to optimize the behavior of the uncertain, closed-loop system. The proposed controller is intended for processes well modeled by multi-input-multi-output (MIMO) linear, time-invariant (LTI) models with no input-constraints.

The remainder of the paper is organized as follows. In Section 2, the rationale behind the various characteristics of the proposed controller will be discussed. This section will outline the derivation of the proposed MPC. Section 3 discusses a method for using Principal Component Analysis (PCA) to improve the uncertainty description of the closed-loop system. Finally, the performance of this new MPC system is explored via a distillation column case study in Section 4.

2. ROBUST MPC UNDER CLOSED-LOOP UNCERTAINTY

2.1 Open-loop vs. Closed-loop Prediction

In unconstrained model-predictive control, the following optimization is solved at each controller execution (Garcia and Morshedi, 1986).

$$\min_{\Delta u} \left\{ (y - y_{SP})^T W (y - y_{SP}) + \Delta u^T Q \Delta u \right\} \qquad (1)$$

$$s.t. \qquad y_i = f(\Delta u, \hat{N}) \qquad \forall i = 1 \ldots n \qquad (1a)$$

Here $y, y_{sp} \in \Re^n, \Delta u \in \Re^m, W \in \Re^{n x n}$ and $Q \in \Re^{m x m}$. The process setpoint is represented by y_{sp}. The matrices, W and Q, are positive definite matrices, typically with the tuning parameters, w and q, on their respective diagonals. These tuning parameters are chosen to achieve the desired compromise between dynamic performance and robustness. Equation (1a) represents a deterministic model of the process with $\hat{N}$ a vector of the predicted value of the process disturbances. In this paper, a linear step-weight model is used and the process is assumed to be open-loop stable or a pure integrator.

The result of this optimization is a vector of input moves, Δu, of which only the first is implemented. At the next controller execution, an updated estimate of the unmeasured disturbance, $\hat{N}$, is calculated, the output prediction is updated, and the procedure begins again.

In an open-loop prediction of uncertainty, the entire vector of Δu is assumed to be known in the prediction of future output uncertainty. This is not an accurate description of a closed-loop, probabilistic system. Through the controller, uncertainty in the future outputs leads to uncertainty in future inputs as the future control actions react to plant/model mismatch. Because open-loop predictions neglect this characteristic of a closed-loop system, such predictions often overestimate the uncertainty in future process outputs and lead to robust MPC that are overly conservative.

In order to perform the required closed-loop prediction, a robust MPC needs a model of the process *and* a model of the future controller actions. In general, the structure of the future control law need not be specified. In this case, the robust MPC problem becomes a special case of the dynamic programming problem. (See Rawlings (1994) for a complete discussion of the relationship between robust MPC and dynamic programming.)

In this paper, the computational issues associated with dynamic programming problem are avoided by assuming that the future control actions are well modeled by the MPC shown in equation (1).

2.2 Overview of Control Strategy

Figure 1 illustrates the general control scheme proposed in this paper.

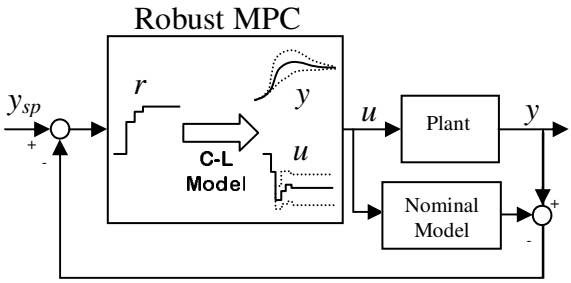

Fig. 1. Conceptual Design for Robust MPC

The controller block depicts the MPC using a closed-loop model of the system to predict the future expected value and upper and lower uncertainty bounds for the inputs, u, and outputs, y. These values are determined by an internal reference trajectory, r. The robust MPC does not directly calculate a vector of input moves as is done in nominal MPC. Instead, it calculates the vector, r. This internal reference trajectory is analogous to a setpoint and by changing this value the robust MPC predicts how a probabilistic closed-loop system will behave in response to a setpoint move. The internal reference trajectory is not a true system setpoint, but represents the desired movement in the future closed-loop system. The term internal refers to the fact that it is a variable used internally by the controller.

The proposed MPC will be implemented as an optimization of the following form.

$$\min_{r, y, \Delta u, \bar{y}, \underline{y}, \bar{u}, \underline{u}} \left\{ (y - y_{SP})^T W (y - y_{SP}) + \Delta u^T Q \Delta u \right\} \qquad (2)$$

$$s.t. \quad y = \left[A_y^{\ cl} \right]_{nominal} r, \quad \Delta u = \left[A_u^{\ cl} \right]_{nominal} r \qquad (2a)$$

$$\bar{y} \geq A_y^{cl}(\delta) r, \quad \underline{y} \leq A_y^{cl}(\delta) r, \quad \forall \delta \in \Delta \tag{2b}$$

$$\bar{u} \geq A_u^{cl}(\delta) r, \quad \underline{u} \leq A_u^{cl}(\delta) r, \quad \forall \delta \in \Delta \tag{2c}$$

$$y_{\min} \leq \bar{y}, y, \underline{y} \leq y_{\max} \tag{2d}$$

$$\delta \in \Delta \tag{2e}$$

Here $A_y^{cl}(\delta)$ and $A_u^{cl}(\delta)$ represent the closed-loop models of the system that relate r to y and u. These matrices are functions of the model-mismatch, δ. The nominal inputs and outputs as predicted by a closed-loop model with no plant-model mismatch (i.e. δ=0) are calculated in equation (2a). The upper and lower uncertainty bounds of y and u are represented by the vectors $\bar{y}$, $\underline{y}$ and by $\bar{u}$, $\underline{u}$, respectively. Equations (2b) and (2c) force these values to represent the uncertainty bounds for the worst-case mismatch, assuming $\delta \in \Delta$ where Δ represents the uncertainty set of δ. Section 3 will discuss how this uncertainty set is defined. Equation (2d) ensures that the nominal and uncertainty bounds for y do not violate the desired output constraints. The proposed controller assumes no input-constraints.

The rest of this section will discuss how the various aspects of this control strategy are implemented.

2.3 Closed-loop Predictions

The MPC shown in equation (1) is a natural choice for the model of future controller actions. The Karush-Kuhn-Tucker (KKT) conditions for this unconstrained MPC are linear and can be written as:

$$\left(A^T W^T A + Q^T\right)\Delta u - A^T W^T \left(y_{SP} - \hat{N}\right) = 0 \tag{3}$$

Here the matrix, A, represents a step-weight model of the plant. The linear process model is given by:

$$y = A\Delta u + \hat{N} \tag{4}$$

To create a closed-loop model, equations (3) and (4) are written for each time step within the prediction horizon. This linear set of equations can be combined to derive the closed-loop models, A_y^{cl} and A_u^{cl}, shown in equations (2a) through (2c).

Conceptually, these closed-loop models could be used to determine the predicted uncertainty limits of the future process inputs and outputs (equation (2b) and (2c)). For example, the upper bound in the uncertainty of y for a given r vector could be calculated as:

$$\max_{\delta} \bar{y}_k = 1_k A_y^{cl}(\delta) r \qquad \forall k = 1..n$$
$$s.t.\ \delta \in \Delta \tag{5}$$

Here 1_k is a matrix that selects the k^{th} element in the vector $\bar{y}$. This maximization would find the amount of model-mismatch, δ, that results in the largest possible y at a given time period, k, in the future.

If this optimization could be calculated on-line, the robust MPC could use the calculated uncertainty limit to determine how best to maintain the system at set point while avoiding output-constraints. However, the situation is complicated by the fact that $A_y^{cl}(\delta)$ and $A_u^{cl}(\delta)$ are highly non-linear functions of the amount of plant/model mismatch, δ. Therefore, the optimization shown in equation (5) is non-convex and impractical for on-line implementation. As will be described in the next section, this situation can be avoided if this non-convex minimization is performed off-line a priori.

2.4 Off-line Optimization

The goal of the non-convex optimization is to determine the relationship between the predicted r and the closed-loop uncertainty limits in y and u. These relationships must be summarized so that an on-line, *convex* optimization can make decisions based on this information.

Given an estimate of the model uncertainty, the off-line optimization solves the non-convex optimization problems similar to the one shown in equation (5) and uses the resulting δ to calculate the 'worst-case' $A_y^{cl}(\delta)$ and $A_u^{cl}(\delta)$. Since local optima may be found, several starting points must be used and any results must be checked against Monte-Carlo simulations.

For a MIMO system, the effect of a given δ on future system uncertainty is a function of the direction of r and the directionality of the process. Therefore, the 'worst-case' $A_y^{cl}(\delta)$ and $A_u^{cl}(\delta)$ can be different for different r-directions. Since an infinite number of r-directions exist for any MIMO system, the proposed method uses a representative sampling to estimate this set. For example, for the 2x2 system considered in this paper, 60-different r-directions were considered, each six 'degrees' from another, if one visualizes the set of all possible r-directions as a unit-circle in r_1/r_2 space.

2.5 On-Line Optimization

Naturally, the desired direction of the internal reference trajectory, r, is not known beforehand. Therefore, the on-line optimization must be able to determine the 'worst-case' $A_y^{cl}(\delta)$ and $A_u^{cl}(\delta)$ for any possible r-direction.

The information given in the sampled $A_y^{cl}(\delta)$ and $A_u^{cl}(\delta)$ matrices can be included in the constraints of

a convex optimization using the following technique. Assuming a single step change in r at time k=0, the minimization shown in equation (6) can be used to find the largest uncertainty bound for y at given time, regardless of the direction of r.

$$\min_{\bar{y}} \bar{y} \tag{6}$$

$$\begin{aligned} \bar{y} &\geq A_y^{cl}(\delta)_1 \, r(0) \\ \bar{y} &\geq A_y^{cl}(\delta)_2 \, r(0) \\ &\vdots \\ \bar{y} &\geq A_y^{cl}(\delta)_m \, r(0) \end{aligned} \tag{6a}$$

Here $A_y^{cl}(\delta)_m$ relates r to the largest uncertainty bound of y for a given r-direction. The constraints given in (6a) account for m different directions of r. Each direction could result in a different $A_y^{cl}(\delta)_m$. For a system with 60 different sampled r-directions, m could be as large as 60. However, this is usually not the case, because the $A_y^{cl}(\delta)_m$ are identical for many r-directions. For example, it is very unlikely that the worst-case plant/model mismatch will be different for a change in r of [0 1] and a change of [0.03 0.99]. In case study discussed in Section 4, fewer than 20 different $A_y^{cl}(\delta)_m$ captured the uncertainty limits for all of the tested r-directions.

Within the prediction horizon, the desired direction of r may change several times. Equation (6) can be used to calculate the upper uncertainty bound on y at a given time for a single change in r. In order to calculate the uncertainty bounds for y for a sequence of r-moves, this type of equation must be repeated for each change in the direction of r and the resulting partial uncertainty bounds must be added to give the actual uncertainty bounds. For a system with an input and output horizon of two, these equations would have the following form:

$$\begin{aligned} \bar{y}_0 &\geq A_y^{cl}(\delta)_1 \, r(0) \\ &\vdots \\ \bar{y}_0 &\geq A_y^{cl}(\delta)_m \, r(0) \\ \bar{y}_1 &\geq A_y^{cl}(\delta)_1 \, r(1) \\ &\vdots \\ \bar{y}_1 &\geq A_y^{cl}(\delta)_m \, r(1) \\ \bar{y} &\geq \bar{y}_0 + \bar{y}_1 \end{aligned} \tag{7}$$

Here $r(0)$ represents the change in r at time, t=0, and $\bar{y}_0$ is a vector representing the upper uncertainty bound for y due to the change in $r(0)$. The true upper limit on the uncertainty of y must be greater than the sum of $\bar{y}_0$ and $\bar{y}_1$ as is shown in the final inequality constraint.

With these linear inequalities, equation (2) can be rewritten as a convex quadratic program.

$$\min_{\substack{r, y, \Delta u, \bar{y}, \bar{u}, \underline{y}, \underline{u} \\ \bar{y}_1 .. \bar{y}_n, \underline{y}_1 .. \underline{y}_n \\ \bar{u}_1 .. \bar{u}_m, \underline{u}_1 .. \underline{u}_m}} \left\{ (y - y_{SP})^T W (y - y_{SP}) + \Delta u^T Q \Delta u \right\} \tag{8}$$

s.t. Equation (7) and similar equations for $\underline{y}, \bar{u}$, and $\underline{u}$ (8a)

$$y = \left[A_y^{cl} \right]_{nominal} r, \quad \Delta u = \left[A_u^{cl} \right]_{nominal} r \tag{8b}$$

$$y_{\min} \leq \bar{y}, y, \underline{y} \leq y_{\max} \tag{8c}$$

All output constraints are 'softened' to avoid feasibility and stability issues (Zafiriou, 1990). This quadratic program is solved at each controller execution. The first input move is then applied in a rolling-horizon fashion.

Implementation issues: This optimization is convex, but the size of the problem can create some computational issues. For the 2x2 case study discussed in Section 4, the problem has 1134 decision variables and 3317 inequality constraints.

The size of this QP poses a problem for active set method such as the quadprog program found in Matlab (Coleman et al., 1999). Fortunately, recent progress in the field of interior-point (IP) methods provides a solution. While the theoretical worst-case number of iterations for IP methods is bounded by $O(n^3)$ (Lobo et al., 1998), these methods have been shown to be much more efficient in practice (Andersen and Ye, 1999). Using Andersen's MOSEK interior-point algorithm, the average solution time for our quadratic program averaged only 1.35 seconds on a Pentium IV, 1.8 GHz.

As the number of inputs, outputs, and length of the prediction horizon grows, the set of equations represented by constraint (8a) will reach a point where even interior-point methods will require excessive computing time. Future work will explore how the dimensionality of this problem can be reduced.

3. CLOSED-LOOP UNCERTIANTY DESCRIPTION

The performance of the robust MPC described above depends strongly on the uncertainty description used by the controller. A poor description of the system uncertainty may lead to conservative control.

For example, consider a typical non-linear, binary distillation column from Marlin (2000). This process can be modeled by the following linear system, where X_D and X_B represent the distillate and bottoms compositions of the light key. These variables are

controlled by the reflux rate, F_R, and the amount vaporized in the reboiler, F_V.

$$\begin{bmatrix} X_D \\ X_B \end{bmatrix} = \begin{bmatrix} \dfrac{Kp_{11}e^{-\theta_{11}}}{\tau_{11}s+1} & \dfrac{Kp_{12}e^{-\theta_{12}}}{\tau_{12}s+1} \\ \dfrac{Kp_{21}e^{-\theta_{21}}}{\tau_{21}s+1} & \dfrac{Kp_{22}e^{-\theta_{22}}}{\tau_{22}s+1} \end{bmatrix} \begin{bmatrix} F_R \\ F_V \end{bmatrix} \qquad (9)$$

Assume that this linear model is used to represent a non-linear distillation column in which the feed rate, F_f, is unmeasured and not constant. Changes in the feed rate will affect the model parameters and uncertainty in the feed rate leads to uncertainty in these parameters. The feed rate has a nominal value of 10 kmol/min and varies very slowly (with respect to the closed-loop settling time) between 8.5 and 11 kmol/min. Table 1 summarizes the coefficients of the linear model fit at various feed rates with a sampling rate of 2 min^{-1}.

Table 1: Effect of Feed Rate Changes on Model

F_f (kmol/min)	Kp (%/kmol min^{-1})	τ (min)	θ (min)
8.5	$\begin{bmatrix} 0.088 & -0.079 \\ 0.14 & -0.15 \end{bmatrix}$	$\begin{bmatrix} 20.8 & 22.0 \\ 21.6 & 21.2 \end{bmatrix}$	$\begin{bmatrix} 2.60 & 3.76 \\ 3.10 & 2.34 \end{bmatrix}$
10.0	$\begin{bmatrix} 0.075 & -0.067 \\ 0.12 & -0.13 \end{bmatrix}$	$\begin{bmatrix} 17.7 & 18.7 \\ 18.3 & 18.0 \end{bmatrix}$	$\begin{bmatrix} 2.50 & 3.49 \\ 2.97 & 2.33 \end{bmatrix}$
11.5	$\begin{bmatrix} 0.065 & -0.058 \\ 0.10 & -0.11 \end{bmatrix}$	$\begin{bmatrix} 15.3 & 16.1 \\ 15.9 & 15.6 \end{bmatrix}$	$\begin{bmatrix} 2.42 & 3.33 \\ 2.89 & 2.32 \end{bmatrix}$
13.0	$\begin{bmatrix} 0.057 & -0.051 \\ 0.09 & -0.10 \end{bmatrix}$	$\begin{bmatrix} 13.5 & 14.2 \\ 14.0 & 13.7 \end{bmatrix}$	$\begin{bmatrix} 2.35 & 3.18 \\ 2.83 & 2.31 \end{bmatrix}$

One possible uncertainty description for this process is a set of equation such as:

$$\begin{aligned} &0.057 \le Kp_{11} \le 0.088, \ldots, -0.15 \le Kp_{22} \le -0.10 \\ &13.5 \le \tau_{11} \le 20.8, \quad \ldots \quad , 14.2 \le \tau_{22} \le 22.0 \\ &2.35 \le \theta_{11} \le 2.60, \quad \ldots \quad , 2.31 \le \theta_{22} \le 2.34 \end{aligned} \qquad (10)$$

However, these box-type uncertainty descriptions are inappropriate. No linear controller will be able to stabilize all of the plants described by equations (10) because the systems do not meet the integral stabilizability test of Grosdidier et al. (1985).

Even if integral stabilizability is not an issue for a given system, the box-type description is unsatisfactory because it ignores the steady-state and dynamic relationships set by the physics of the system. For example, a process uncertainty that affects the process dead-time often also affects the process time-constant and gain. Likewise, there usually exists a relationship between steady-state gains of a MIMO system.

3.1 PCA Uncertainty Description

These structured uncertainty relationships can be captured using the Principal Component Analysis (PCA) technique. PCA is a multivariate statistical method that summarizes the variation within a data set, X, in the fewest possible dimensions, d (Wold, 1987). A score vector, t, a loading vector, p, and a residual matrix, ε, summarize the data as shown in equation (11), where X_{mean} is the column-wise mean of the data.

$$X = X_{mean} + \sum_{i-1}^{d} tp' + \varepsilon \qquad (11)$$

If the information in Table 1 is summarized using PCA where each row of the data matrix represents a different flow rate and each column one of the 12 model coefficients, the majority of the variability can be summarized using a single t-variable. This illustrates the fact that there is one main source of variability within the data set (i.e. the column feed rate.) Using this PCA description, the uncertainty in the process can be summarized as:

$$X = tp' + X_{mean}, \qquad -13 \le t \le 13 \qquad (12)$$

Here p is a 12x1 constant loading vector and the inequality represents a component-wise 95%-confidence interval for t. The uncertainty in this example is summarized in a single score space, but higher dimensional descriptions are possible. In such cases, the inequality constraint shown in equation (12) expands to a multi-dimensional ellipsoid.

This PCA description of uncertainty has several advantages. The dimensionality of the non-convex optimization discussed in section 2.4 is greatly reduced. In addition, the loading and score vectors can be helpful in deciding which sources of uncertainty are important and which can be eliminated from the model.

4. CASE STUDY

The following case study illustrates the ability of the proposed MPC to robustly avoid output-constraint violations while maintaining acceptable dynamic performance. The distillation column discussed above is to be controlled by the proposed robust MPC found in equations (8). The case studies assume that uncertainty is caused by plant/model mismatch only and no disturbances are affecting the plant. This assumption can be relaxed by applying the techniques discussed in Warren (2003).

Figure 2 below shows the performance of the unconstrained system responding to a setpoint change of [1 0] mole percent at time, t=1, from an initial condition of [98 2]. The nominal plant model is given by F_f of 10 kmol/min in Table 1 and the MPC shown in equation (1) is used in the closed-loop model with the following tuning parameters; n=20, m=5, w=[1 1], q=[0.02 0.02].

The thick solid lines in Figure 2 represent the uncertainty limits of the inputs and outputs predicted from time, t=0, using equations similar to equation (7). The dashed lines in Figure 1 represent the closed-loop response of the distillation column at

feed rates of 7, 8, 9, 11, 12, 13, and 14 kmol/min. Even though some of these feed flow rates fall outside of the original range for which the robust MPC was designed, the predicted uncertainty bounds are quite accurate. Notice that the closed-loop uncertainty predictions accurately predict that the uncertainty in *y* will approach zero due to the integral action of the controller and the fact that the closed-loop system is stable.

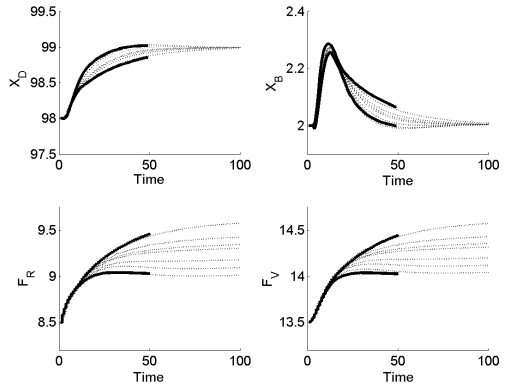

Fig. 2. Closed-Loop Uncertainty Prediction

The proposed robust MPC is able to use these uncertainty predictions to avoid output-constraints. For example, consider the case where the bottoms composition must remain below 2.5 mole percent light key. Figure 3 compares the performance of proposed robust MPC to that of a nominal MPC with softened output-constraints. In this example, the process model used by the controllers is given by F_f of 10 kmol/min in Table 1 while the true process is operating at F_f of 8.5 kmol/min. The robust system successfully avoids the output constraint without becoming overly conservative.

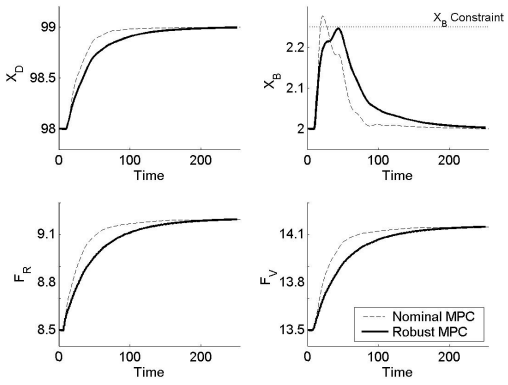

Fig 3. Comparison of Robust and Nominal MPC

5. CONCLUSIONS

This paper has discussed the importance of using an accurate closed-loop description of system uncertainty in robust MPC. A robust MPC system based on a closed-loop system description has been proposed and shown to outperform nominal MPC systems when plant/model mismatch is present.

REFERENCES

Andersen, E. D. and Y. Ye (1999). On a homogeneous algorithm for the monotone complementarity problem, *Mathematical Programming*, **84**(2), pp. 375-399.

Badgwell, T. A. (1997). Robust model predictive control of stable linear systems, *International Journal of Control*, **68**(4), pp. 797-818.

Bemporad, A. and M. Morari (1999). Robust Model Predictive Control: A Survey. *Lecture Notes in Control and Information Sciences,* **245,** Springer-Verlag, pp. 207-226.

Coleman, T., M. A. Branch, and A. Grace (1999). *Matlab Optimization Toolbox: User's Guide*, The Mathworks, Inc., Natick, MA.

Garcia, C. E. and A. M. Morshedi (1986). Quadratic Programming Solution of Dynamic Matrix Control (QDMC), *Chemical Engineering Communications*, **46**, pp. 73-86.

Grosdidier, P., M. Morari, and B. R. Holt (1985). Closed-loop Properties from Steady-State Information, *Industrial and Engineering Chemistry Fundamentals*, **24**, pp. 221-235.

Kothare, M. V., V. Balakrishnan, and M. Morari (1996). Robust Constrained Model Predictive Control using Linear Matrix Inequalities, Automatica, **32**(10), pp. 1361-1379.

Lobo, M. S., L. Vandenberghe, S. Boyd, and H. Lebret (1998). Applications of Second-order Cone Programming, *Linear Algebra & Its Applications*, **284**, pp. 193-228.

Marlin, T. E. (2000). *Process Control: Designing Processes and Control Systems for Dynamic Performance*, Chapter 20, McGraw-Hill, New York, NY.

Mayne, D. (2000). Nonlinear Model Predictive Control: Challenges and Opportunities, *Progress in Systems and Control Theory*, **26**, pp. 23-44.

Qin, S. J. and T. A. Badgwell (1996). An Overview of Industrial Model Predictive Control Technology, Proceedings of Chemical Process Control V, pp. 232-256.

Rawlings, J. B., E. S. Meadows, and K. R. Muske (1994). Nonlinear Model Predictive Control: A Tutorial and Survey, ADCHEM 1994, Kyoto, Japan, pp. 203-214.

Warren, A. L. (2003). Improved Output Constraint-Handling for MPC with Disturbance Uncertainty, *To appear in ACC 2003*, Denver, Colorado.

Wold, S., K. Esbensen, and P. Geladi (1987). Principal Component Analysis, *Chemometrics and Intelligent Laboratory Systems*, **2**, pp. 37-52.

Zafiriou, E. (1990). Robust model predictive control of processes with hard constraints, *Computers and Chemical Engineering*, **14**(4/5), pp. 359-371.

Zheng, A. and M. Morari (1993). Robust control of Constrained Model Predictive Control. Proceedings of American Control Conference, San Francisco, California, pp. 379-383.

ADAPTIVE EXTREMUM SEEKING OUTPUT FEEDBACK CONTROL FOR A CONTINUOUS STIRRED TANK BIOREACTOR

Natalia I. Marcos [*,1] **Martin Guay** [*]
Denis Dochain [**]

[*] *Chemical Engineering, Queen's University, Canada*
[**] *Universit Catholique de Louvain, Belgium*

Abstract: An adaptive extremum seeking controller is presented for the optimization of the production rate of a continuous stirred tank bioreactor. This controller is saturated outside a domain of interest and a reduced-order high-gain observer is designed to estimate the substrate concentration of the bioreactor. Semiglobal asymptotic stability is proved and recovery of the performance achieved under state feedback is shown when the speed of the high gain observer is sufficiently high. Simulation experiment is given to illustrate the proposed approach.

Keywords: Adaptive extremum seeking, parameter estimation, persistence of excitation, output feedback, separation principle.

1. INTRODUCTION

Adaptive extremum seeking control of nonlinear systems has received the attention of many researchers. The potential benefits of extremum seeking techniques in the maximization of the production rate in a continuous stirred tank bioreactor has been demonstrated by (Wang *et al.*, 1999) and (Zhang *et al.*, 2001). Practical implementation of the controller scheme designed in (Zhang *et al.*, 2001) requires the measurement of substrate concentration and production rate. However, knowledge of the substrate concentration is not always possible. The extension of these results to the output feedback requires the construction of an observer to estimate the unmeasured state of the system from its output.

Owing to nonlinearity (Lee and Khalil, 1997), a separation principle cannot be applied in the design of output feedback control as in linear control theory, but a certain degree of separation can be achieved by designing high-gain observers. High-gain observers, however, exhibit peaking in their transient behavior (Esfandiari and Khalil, 1992). Fortunately, this peaking phenomenon in certain classes of systems.

In this work, an adaptive extremum-seeking output feedback controller is designed by the application of a similar separation principle. The design is achieved in two steps. First, we saturate the controller scheme and the right hand side of the adaptation rules designed in (Zhang *et al.*, 2001) for the continuous stirred tank bioreactor. Second, we use an high-gain observer to estimate the substrate concentration, based on the measurement of the production rate. Using Lyapunov theory, we prove that the output feedback controller recovers the performance achieved under state feedback when the gain of the observer is large enough. The rest of the paper is organized as follows. Section 2 presents some notation and the problem formulation for the state feedback case. In Section 3, the reduced order high gain observer is designed. The performance recovery is shown in Section 4,

[1] Supported by Ontario Graduate Scholarships (OGS).

followed by simulation results in Section 5 and a brief conclusion in Section 6.

2. STATE FEEDBACK CONTROL

We consider the following microbial growth models for a continuous stirred tank bioreactor (Zhang *et al.*, 2001)

$$\dot{y} = -uy + \frac{\theta_\mu s^2 y - \theta_k y^2 + (s_0 - s)uy}{s(1 + \theta_s s)} \quad (1)$$

$$\dot{s} = -\theta_k y + u(s_0 - s) \quad (2)$$

where the states $s > 0$ and $y > 0$ denote the substrate concentration, and the production rate of the reaction product, respectively. The input of the system is the dilution rate $u \geq 0$, and s_0 denotes the concentration of the substrate in the feed.

The constant parameter θ_k is known, while the constant parameters θ_s, θ_μ are unknown. However, the vector $\theta = [\theta_s \quad \theta_\mu]^T$ belongs to Ω, a known compact convex subset of R^2. Let $\hat{\Omega}$ be a convex subset of R^2 which contains Ω in its interior.

The adaptive extremum seeking controller and the adaptation rules for the parameters of the system are designed in (Zhang *et al.*, 2001) for the state feedback case. The state feedback controller is

$$u = \frac{1}{(s_0 - s)}(\theta_k y - a(t) + d - k_z z_s) \quad (3)$$

where $a(t)$ and z_s corresponds to the dither signal (to be designed later) and the error in the set-point s^*, respectively

$$z_s = s - s^* + d, \quad s^* = \frac{1}{\hat{\theta}_s}\left(\sqrt{1 + s_0\hat{\theta}_s} - 1\right) \quad (4)$$

Let $\hat{\theta}$ denote the estimate of the true parameter θ and let $\hat{y}$ be the prediction of the state y by using the estimated parameters $\hat{\theta}_s$ and $\hat{\theta}_\mu$. The predicted state $\hat{y}$ and d are generated by

$$\dot{\hat{y}} = -uy + \frac{\hat{\theta}_\mu s^2 y - \theta_k y^2 + (s_0 - s)uy}{s(1 + \hat{\theta}_s s)} + k_y e_y \quad (5)$$

$$\dot{d} = -\dot{\hat{\theta}}_s \beta(\hat{\theta}_s) + a(t) - d \quad (6)$$

where $e_y = y - \hat{y}$.

We suppose Ω_s and Ω_μ are convex hypercubes, (see (Khalil, 1996)) $Omega_i = \{\theta \mid a_i \leq \theta_i \leq b_i\}$ for $i = s, \ \mu$. Let

$$\Omega_{\delta - i} = \{\theta \mid a_i - \delta_i \leq \theta_i \leq b_i + \delta_i\} \qquad for \ i = s \ \mu$$

where $\delta_s > 0$ and $\delta_\mu > 0$ are chosen such that $\Omega_{\delta - s} \subset \hat{\Omega}_s$ and $\Omega_{\delta - \mu} \subset \hat{\Omega}_\mu$.

The parameter adaptation rule for $\hat{\theta}_i$ with $i = s, \ \mu$, is taken as

$$\dot{\hat{\theta}}_i = \begin{cases} \Gamma_i & \text{if } a_i \leq \hat{\theta}_i \leq b_i \text{ or} \\ & \text{if } \hat{\theta}_i > b_i \text{ and } \Gamma_i \leq 0 \text{ or} \\ & \text{if } \hat{\theta}_i < a_i \text{ and } \Gamma_i \geq 0 \\ (1 - c_i(\hat{\theta}_i))\Gamma_i & \text{if } \hat{\theta}_i > b_i \text{ and } \Gamma_i > 0 \text{ or} \\ & \text{if } \hat{\theta}_i < a_i \text{ and } \Gamma_i < 0 \end{cases} \quad (7)$$

for $\hat{\theta}_i > b_i$ and $\Gamma_i > 0$

$$c_i(\hat{\theta}_i) = \left(\frac{\hat{\theta}_i - b_i}{\delta_i}\right) sign(\Gamma_i) \quad (8)$$

and for $\hat{\theta}_i < a_i$ and $\Gamma_i < 0$

$$c_i(\hat{\theta}_i) = \left(\frac{\hat{\theta}_i - a_i}{\delta_i}\right) sign(\Gamma_i) \quad (9)$$

Equation (7) is a smooth projection algorithm (Pomet and Praly, 1992).

The nominal value for $\dot{\hat{\theta}}_i$ is Γ_i where

$$\Gamma_s = \frac{\gamma_s \phi_s y e_y}{(1 + \hat{\theta}_s s)}, \ \Gamma_\mu = \frac{\gamma_\mu \phi_\mu y e_y}{(1 + \hat{\theta}_s s)} \quad (10)$$

with $\phi_s = -u(s_0 - s) - \hat{\theta}_\mu s^2 + \theta_k y$ and $\phi_\mu = (1 + \hat{\theta}_s s)s$. It can be seen from equations (8) and (9) that $0 \leq c_i(\hat{\theta}_i) \leq 1$ and $c_i(\hat{\theta}_i) = 0$ for $\dot{\hat{\theta}}_i = \Gamma_i$.

Equations (1)-(10) represent the system under state feedback. Let the vector $\psi = [s \ y \ d \ \hat{y} \ \hat{\theta}_s \ \hat{\theta}_\mu]^T$ represent the trajectories of the closed loop system. Then considering $\chi = [z_s \quad \tilde{\theta}_s \quad \tilde{\theta}_\mu \quad e_y]^T$, we have

$$\dot{\chi} = \begin{bmatrix} \dot{z}_s \\ \dot{\tilde{\theta}}_s \\ \dot{\tilde{\theta}}_\mu \\ \dot{e}_y \end{bmatrix} = \begin{bmatrix} \dot{s} - \dot{s}^* + \dot{d} \\ -\dot{\hat{\theta}}_s \\ -\dot{\hat{\theta}}_\mu \\ \dot{y} - \dot{\hat{y}} \end{bmatrix} = \begin{bmatrix} f_1(\psi) \\ f_2(\psi) \\ f_3(\psi) \\ f_4(\psi) \end{bmatrix} \quad (11)$$

For simplicity, we can define

$$f_r(\psi) = [f_1(\psi) \ f_2(\psi) \ f_3(\psi) \ f_4(\psi)]^T$$

and express equation (11) as

$$\dot{\chi} = f_r(\psi) \quad (12)$$

For the system (12) we consider the following Lyapunov function

$$V(\chi, t) = \frac{1}{2}\left[z_s^2 + \frac{\tilde{\theta}_s^2}{\gamma_s} + \frac{\tilde{\theta}_\mu^2}{\gamma_\mu} + (1 + \theta_s s)e_y^2\right] \quad (13)$$

The rate of change of the Lyapunov function (13) is

$$\dot{V} = \frac{\partial V}{\partial \chi} f_r(\psi) + \frac{\partial V}{\partial s}\dot{s} \leq -U_3(\chi) \quad (14)$$

where $U_3(\chi) = k_z z_s^2 + k_{y0} e_y^2$.

Remark 1. The functions $f_1(\psi), f_2(\psi), f_3(\psi)$, and $f_4(\psi)$ are locally Lipschitz in their arguments over the domain of interest.

Remark 2. Assuming that the persistency of excitation condition developed in (Zhang *et al.*, 2001) is met, the origin $(z = 0, \tilde{\theta}_s = 0, \tilde{\theta}_\mu = 0, e_y = 0)$ is an equilibrium point of the closed loop system. The asymptotic stability of the origin for the state feedback system (12) was proved in (Zhang *et al.*, 2001).

3. OUTPUT FEEDBACK CONTROL

We consider the case where only y is measurable, the substrate concentration s is not available for feedback control. By the locally observability condition (Marino and Tomei, 1995), the system is observable for $y > 0$. To implement the state feedback adaptive controller (3), we need to estimate the unmeasured state s. The estimation of the states y and s are given by $\hat{y}_{obs}$ and $\hat{s}_{obs}$. We use the reduced-order high-gain observer $\hat{x} = [\hat{y}_{obs} \quad \hat{s}_{obs}]^T$

$$\dot{\hat{y}}_{obs} = -uy + \frac{\hat{\theta}_\mu \hat{s}_{obs}^2 y - \theta_k y^2 + (s_0 - \hat{s}_{obs})uy}{\hat{s}_{obs}(1 + \hat{\theta}_s \hat{s}_{obs})} + \frac{\alpha_y}{\epsilon}\tilde{y} \quad (15)$$

$$\dot{\hat{s}}_{obs} = -\theta_k y + u(s_0 - \hat{s}_{obs}) + \frac{\alpha_s}{\epsilon^2}\tilde{y} \quad (16)$$

where $\tilde{y}$, $\tilde{s}$ are defined as $\tilde{y} = y - \hat{y}_{obs}$ and $\tilde{s} = s - \hat{s}_{obs}$ and $\alpha_s, \alpha_y, \epsilon$ are positive constants.
For the output feedback, the dynamics for the production rate is represented by (1) and the dynamics of the substrate concentration is represented by (2). The controller for the output feedback system is

$$u = \frac{1}{(s_0 - \hat{s}_{obs})}(\theta_k y - a(t) + d - k_z z_s) \quad (17)$$

In order to avoid the singularity that may happen in the controller when the estimation of the substrate concentration increases, we bound the state $\hat{s}_{obs}$ below and above by the positive bounds $\hat{s}_{obs-min}$ and $0.99 s_0$ respectively.
To overcome the peaking phenomenon associated with the high gain observer, we saturate the controller and the rate of change of $\hat{y}$, d, $\hat{\theta_s}$, and $\hat{\theta_\mu}$ outside the domain of interest. The rate of change of $\hat{y}$ and d are

$$\dot{d} = -\dot{\hat{\theta}}_s \beta(\hat{\theta}_s) + a(t) - d \quad (18)$$

$$\dot{\hat{y}} = -uy + \frac{\hat{\theta}_\mu \hat{s}_{obs}^2 y - \theta_k y^2 + (s_0 - \hat{s}_{obs})uy}{\hat{s}_{obs}(1 + \hat{\theta}_s \hat{s}_{obs})} + k_y e_y \quad (19)$$

The parameter adaptation rule for the output feedback case is the same as that for the state feedback case. However, the nominal updating laws for $\dot{\hat{\theta}}_s$ and $\dot{\hat{\theta}}_\mu$ are

$$\Gamma_s = \frac{\gamma_s \phi_s y e_y}{(1 + \hat{\theta}_s \hat{s}_{obs})}, \Gamma_\mu = \frac{\gamma_\mu \phi_\mu y e_y}{(1 + \hat{\theta}_\mu \hat{s}_{obs})} \quad (20)$$

with

$$\phi_s = -u(s_0 - \hat{s}_{obs}) - \hat{\theta}_\mu \hat{s}_{obs}^2 + \theta_k y \quad (21)$$

$$\phi_\mu = (1 + \hat{\theta}_s \hat{s}_{obs})\hat{s}_{obs} \quad (22)$$

The error dynamics for the observer are

$$\dot{\tilde{e}} = \begin{bmatrix} \dot{\tilde{y}} \\ \dot{\tilde{s}} \end{bmatrix} = \begin{bmatrix} -\frac{\alpha_y}{\epsilon} & F_1 \\ -\frac{\alpha_s}{\epsilon^2} & -u \end{bmatrix} \begin{bmatrix} \tilde{y} \\ \tilde{s} \end{bmatrix} + \begin{bmatrix} 1 \\ 0 \end{bmatrix} G \quad (23)$$

where $F_1 = \frac{y}{(1+\theta_s s)(1+\hat{\theta}_s \hat{s}_{obs})}\theta_\mu$ and G is defined as $G = \frac{y}{(1+\theta_s s)(1+\hat{\theta}_s \hat{s}_{obs})}[\theta_\mu \hat{\theta}_s \hat{s}_{obs} s + \tilde{\theta}_\mu \hat{s}_{obs} - \hat{\theta}_\mu \theta_s \hat{s}_{obs} s] + \frac{-\theta_k y^2 + (s_0 - s)uy}{s(1+\theta_s s)} - \frac{-\theta_k y^2 + (s_0 - \hat{s}_{obs})uy}{\hat{s}_{obs}(1+\hat{\theta}_s \hat{s}_{obs})}$.
We scale the observer dynamics as $\tilde{y} = \xi_1$ and $\tilde{s} = \frac{\xi_2}{\epsilon}$. Replacing equation (23) by its scaled equivalent, we get

$$\epsilon \dot{\xi} = A(t)\xi + \epsilon B G \quad (24)$$

where $\xi = [\xi_1 \quad \xi_2]^T$, $A(t) = \begin{bmatrix} -\alpha_y & F_1 \\ -\alpha_s & -u\epsilon \end{bmatrix}$ and $B = [1 \quad 0]^T$.

4. PERFORMANCE RECOVERY

In this section, we follow the procedure used in (Atassi and Khalil, 1999) and (Khalil, 1996) to show semi-global asymptotic stability of the origin.

1. BOUNDEDNESS

Considering the equations (1), (2), (18), (19) and the parameter updating laws (7) with nominal updating laws (20), the rate of change of the vector χ for the output feedback becomes

$$\dot{\chi} = \begin{bmatrix} \dot{z_s} \\ \dot{\tilde{\theta}}_s \\ \dot{\tilde{\theta}}_\mu \\ \dot{e}_y \end{bmatrix} = \begin{bmatrix} \dot{s} - \dot{s}^* + \dot{d} \\ -\dot{\hat{\theta}}_s \\ -\dot{\hat{\theta}}_\mu \\ \dot{y} - \dot{\hat{y}} \end{bmatrix} = f_r(\psi, D(\epsilon)) \quad (25)$$

and also

$$\dot{s} = h_r(\psi, D(\epsilon)) \quad (26)$$

The initial conditions for equation (25) are $\chi(0) = (z_s(0), \tilde{\theta}_s(0), \tilde{\theta}_\mu(0), e_y(0)) = (z_{s0}, \tilde{\theta}_{s0}, \tilde{\theta}_{\mu 0}, e_{y0}) \in \mathcal{U}$. Related to the set $\mathcal{U}$ there is $\mathcal{U}'$ which is the set of initial conditions for the states ψ. In other

words, $\psi(0) = (s(0), y(0), d(0), \hat{y}(0), \hat{\theta}_s(0), \hat{\theta}_\mu(0)) \in \mathcal{U}'$. The initial states for the estimated parameters are $\hat{x}(0) = (\hat{y}_{obs}(0), \hat{s}_{obs}(0)) = \hat{x}_0 \in \mathcal{Q}$.
The system (24), (25) and (26) is a standard singularly perturbed one. It can be noticed that $\xi = 0$ is the unique solution of (24) when $\epsilon = 0$. If we substitute $\epsilon = 0$ in (25) we get the closed-loop system under state feedback, equation (12). Then, the reduced system is given by

$$\dot{\chi} = f_r(\psi, 0) \tag{27}$$

The boundary-layer system obtained by applying to (24) the change of time variable $\tau = t/\epsilon$ then setting $\epsilon = 0$, is given by

$$\frac{d\xi}{d\tau} = A(t)\xi \tag{28}$$

We denote $(\chi(t,\epsilon), \xi(t,\epsilon))$ the trajectory of system (24) and (25) starting from $(\chi(0), \xi(0))$. The recovery of the boundedness of trajectories is summarized in the following theorem.

Theorem 3. Let *Remark 1* and *Remark 2* hold, then there exists $\epsilon_1^* > 0$ such that, for every $0 < \epsilon \leq \epsilon_1^*$, the trajectories (χ, ξ) of system (25) and (24), starting in $\mathcal{U} \times \mathcal{Q}$ are bounded for all $t \geq 0$.

PROOF. The origin of (12) is asymptotically stable with a region of attraction $\mathcal{R}$. Based on equations (13), and (14) there are three positive functions $U_1(\chi)$, $U_2(\chi)$ and $U_3(\chi)$, all defined and continuous on $\mathcal{R}$ such that

$$U_1(\chi) \leq V(\chi, t) \leq U_2(\chi) \tag{29}$$

$$\lim_{\chi \to \partial\mathcal{R}} U_1(\chi) = \infty \tag{30}$$

$$\dot{V} = \frac{\partial V}{\partial \chi} f_r(\psi) + \frac{\partial V}{\partial s}\dot{s} \leq -U_3(\chi) \tag{31}$$

where $U_3(\chi)$ is defined above. The functions $U_1(\chi)$ and $U_2(\chi)$ are

$$U_1(\chi) = k_{u1}\left[z_s^2 + \frac{\tilde{\theta}_s^2}{\gamma_s} + \frac{\tilde{\theta}_\mu^2}{\gamma_\mu} + e_y^2\right]$$

$$U_2(\chi) = k_{u2}\left[z_s^2 + \frac{\tilde{\theta}_s^2}{\gamma_s} + \frac{\tilde{\theta}_\mu^2}{\gamma_\mu} + (1 + \theta_s s_0)e_y^2\right]$$

with $0 < k_{u1} < 1/2$ and $1/2 < k_{u2}$. Equations (29), (30) and (31) are satisfied for all $\chi \in \mathcal{R}$. The properness of $V(\chi, t)$ in $\mathcal{R}$ guarantees that with any finite $c > max_{\chi \in \mathcal{U},\ s \in \mathcal{U}'} V(\chi, t)$, the set $\Sigma = \{\chi \in \mathcal{R} : V(\chi, t) \leq c\}$ is a compact subset of $\mathcal{R}$ and $\mathcal{U}$ is in the interior of Σ. Similarly, we can prove that there exists a compact set Σ' which is a subset of $\mathcal{R}$ and $\mathcal{U}'$ is in the interior of Σ'.

For the boundary layer system we define the Lyapunov function

$$W(\xi) = \xi^T P_0 \xi \tag{32}$$

where $P_0 = P_0^T$ is the positive definite solution of the Lyapunov equation $P_0 A(t) + A(t)^T P_0 = -Q(t)$. The matrix $Q(t)$ is symmetric and positive definite. This function satisfies

$$\lambda_{min}(P_0)\|\xi\|^2 \leq W(\xi) \leq \lambda_{max}(P_0)\|\xi\|^2 \tag{33}$$

$$\frac{\partial W}{\partial \tau} = -\xi Q(t)\xi \leq -\lambda_{min}(Q(t))\|\xi\|^2 \tag{34}$$

Let $\Lambda = \Sigma \times \{W(\xi) \leq \rho\epsilon^2\}$. Due to Remarks 1-2 we have, for all $\chi \in \Sigma$, all $\psi \in \Sigma'$ and all $\xi \in \mathcal{R}^2$

$$\|f_r(\psi, D(\epsilon)\xi)\| \leq k_1 \tag{35}$$

$$\|G(\psi, D(\epsilon)\xi)\| \leq k_2 \tag{36}$$

$$\|h_r(\psi, D(\epsilon)\xi)\| \leq k_3 \tag{37}$$

where k_1, k_2 and k_3 are positive constants independent of ϵ. Moreover, for any $0 < \tilde{\epsilon} < 1$, there is L_1, independent of ϵ, such that, for all $(\chi, \xi) \in \Lambda$ and every $0 < \epsilon \leq \tilde{\epsilon}$, we have

$$\|f_r(\psi, D(\epsilon)\xi) - f_r(\psi, 0)\| \leq L_1\|\xi\| \tag{38}$$

$$\|h_r(\psi, D(\epsilon)\xi) - h_r(\psi, 0)\| \leq L_2\|\xi\| \tag{39}$$

Proceeding as in (Atassi and Khalil, 1999), we show that there exists $0 \leq \epsilon \leq \epsilon_1^*$ such that the trajectory $(\chi(t,\epsilon), \xi(t,\epsilon))$ enters Λ during the interval $[0, T(\epsilon)]$ and remains there for all $t \geq T(\epsilon)$ where

$$T(\epsilon) = \frac{\epsilon}{\sigma_1} ln\Big(\frac{\sigma_2}{\rho\epsilon^4}\Big) \leq T_0. \tag{40}$$

Thus the trajectory is bounded for all $t \geq T(\epsilon)$. On the other hand, for $t \in [0, T(\epsilon)]$, the trajectory $(\chi(t,\epsilon), \xi(t,\epsilon))$ is bounded.

2. ULTIMATE BOUNDEDNESS

Next, we show that the trajectories of system (25) and (24), starting in $\mathcal{U} \times \mathcal{Q}$, come arbitrarily close to the origin as time progresses. This is summarized in the following theorem.

Theorem 4. Under the conditions of *Theorem 1*, given any $\eta > 0$, there exists $\epsilon_2^* = \epsilon_2^*(\eta) > 0$ and $T_1 = T_1(\eta)$ such that, for every $0 < \epsilon \leq \epsilon_2^*$, we have

$$\|\chi(t,\epsilon)\| + \|\xi(t,\epsilon)\| \leq \eta, \qquad \forall \ \ t \geq T_1. \tag{41}$$

PROOF. Due to space restrictions we omit the proof which proceeds as in (Atassi and Khalil, 1999).

3. TRAJECTORY CONVERGENCE

Let $\chi_r(t)$ be the solution of (27) starting from $\chi(0)$. In this section we follow the procedure used in (Atassi and Khalil, 1999) to prove that $\chi(t,\epsilon)$ converges to $\chi_r(t)$ as $\epsilon \to 0$ uniformly in t, for all $t \geq 0$. As in (Atassi and Khalil, 1999), we divide the interval $[0,\infty]$ into three intervals $[0,T(\epsilon)]$, $[T(\epsilon),T_2]$ and $[T_2,\infty]$, and based on *Theorem 1* and *Theorem 2*, we show $\|\chi(t,\epsilon)-\chi_r(t)\| \leq \eta$ for each interval.

4. ASYMPTOTIC STABILITY

We define $F_2^T = \left[\frac{\Phi^T(\hat{s}_{obs},y,\hat{\theta})y}{(1+\theta_s s)(1+\hat{\theta}_s\hat{s}_{obs})}\right]$ where where $\Phi^T = [\phi_s \quad \phi_\mu]$, $\tilde{\theta} = [\tilde{\theta}_s \quad \tilde{\theta}_\mu]$ and F_3 is a function ψ. From equations (1) and (19),

$$\dot{e}_y = -k_y e_y + F_{2e}^T\tilde{\theta} + (F_2 - F_{2e})^T\tilde{\theta} + F_3\tilde{s} \quad (42)$$

The subscript e indicates that the function is evaluated at steady state. From the projection algorithms (7) with the nominal updating laws (20) we define new state variables

$$\frac{\partial(F_{2e}^T\tilde{\theta})}{\partial t} = -F_{2e}^T R_e N_e e_y - F_{2e}^T(RN - R_eN_e)e_y + \left(\frac{\partial F_{2e}}{\partial t}\right)^T\tilde{\theta} \quad (43)$$

with $R = \frac{y}{(1+\hat{\theta}_s\hat{s}_{obs})}$ and $N = \begin{bmatrix}\gamma_s\phi_s(1-c_s(\hat{\theta}))\\ \gamma_\mu\phi_\mu(1-c_\mu(\hat{\theta}))\end{bmatrix}$

Re-arranging equations (42) and (43) in a matrix form, we get

$$\dot{w} = C(t)w + E(t) + F_6\tilde{s} \quad (44)$$

where $w = [e_y \quad F_{2e}^T\tilde{\theta}]^T$, $C(t) = \begin{bmatrix}-k_y & 1\\ -F_{2e}^T R_e N_e & 0\end{bmatrix}$, $E(t) = \begin{bmatrix}(F_2 - F_{2e})^T\tilde{\theta}\\ -F_{2e}^T(RN - R_eN_e)e_y + \left(\frac{\partial F_{2e}}{\partial t}\right)^T\tilde{\theta}\end{bmatrix}$ and $F_6 = [1 \quad 0]^T F_3$ Equation (44) is a linear time variant system. It can be noticed that when time$\to \infty$, $E(t) \to 0$. Matrix $C(t)$ is Hurwitz if and only if $F_{2e}^T R_e N_e > 0$.

In equation (24), the function G can be written as $G = F_4\tilde{\theta} + F_5\tilde{s}$, where F_4 and F_5 are functions of ψ. Then equation (24) becomes

$$\dot{\xi} = \frac{1}{\epsilon}A(t)\xi + BF_4\tilde{\theta} + BF_5\tilde{s} \quad (45)$$

For the system (44) and (45), we define a new Lyapunov function

$$V_T = V_w^{\frac{1}{2}} + W^{\frac{1}{2}} \quad (46)$$

where $V_w = w^T M_0 w$, and W corresponds to the Lyapunov function for the boundary layer system,equation (32). The constant matrix M_0 is positive definite and symmetric. We select the matrix $L(t)$, a positive definite and symmetric matrix such that $C(t)^T M_0 + M_0 C(t) = -L(t)$. It can be verified that the rate of change of the Lyapunov function V_T is

$$\dot{V} \leq -K_3\|w\| - K_4\|\xi\| + K_2\|2E(t)^T M_0\| \quad (47)$$

where K_3 and K_4 are positive bounds for the states over the domain of interest. Let $K_5 = min(K_3, K_4)$, and let

$$K_6 = K_5(max(\sqrt{\lambda_{max}(M_0)}, \sqrt{\lambda_{max}(P_0)}))$$

then equation (47) becomes

$$\dot{V}_T \leq -K_6 V_T + K_2\|2E(t)^T M_0\| \quad (48)$$

Integration of equation (48), yields

$$V_T(t) \leq V_T(t_0)e^{-K_6(t-t_0)} + \int_{t_0}^{t} e^{-K_6(t-\tau)}K_2\|2E(\tau)^T M_0\|d\tau \quad (49)$$

When time$\to \infty$, $E(\tau) \to 0$. Then inequality (49) vanishes as time$\to \infty$. This means that $V_T = V^{\frac{1}{2}} + W^{\frac{1}{2}} \to 0$ or

$$\|w\| = \|[e_y \quad F_{2e}^T\tilde{\theta}]^T\| \to 0 \quad (50)$$

$$\|\xi\| = D(\epsilon)^{-1}\|[\tilde{y} \quad \tilde{s}]^T\| \to 0 \quad (51)$$

where $D(\epsilon)$ is a two dimensional diagonal matrix with the first element $D(\epsilon)_{11} = 1$ and the second element $D(\epsilon)_{22} = 1/\epsilon$.

Remark 5. Equation (50) implies that $e_y \to 0$ and $F_{2e}^T\tilde{\theta} \to 0$ when time$\to \infty$. Under a Persistence of Excitation condition for the output feedback case, $\tilde{\theta} = 0$ when time $\to \infty$.

Remark 6. It can be easily proved from equations (50), and (51), that z_s under output feedback approaches z_s under state feedback as time $\to \infty$. From the asymptotic stability of the origin under state feedback, $z_s \to 0$ as time $\to \infty$. As a result, z_s under output feedback converges to zero as time $\to \infty$.

From equations (50), (51) and *Remarks 7* and *8*, the origin of $(\chi(t,\epsilon),\xi(t,\epsilon))$ is asymptotically stable.

5. SIMULATION RESULTS

A simulation study is performed using the experimental conditions provided in (Wang *et al.*, 1999). The following parameters and initial states are used in the simulation experiment.

$\epsilon = 0.01$, $\alpha_s = 1$, $\alpha_y = 50$, $K_s = 0.2$, $\mu_m = 1$, $k_1 = 2$, $k_2 = 1$, $s_0 = 10$, $s(0) = 1$, $y(0) = 0.3$, $\hat{s}_{obs}(0) = 5$, $\hat{y}_{obs}(0) = 0.1$, $\hat{y}(0) = 1.5$, $\hat{\theta}_\mu(0) = 3$,

$\hat{\theta}_s(0) = 5.5$.
The dither signal is chosen as $a(t) = 0.01(sin(0.01t)+ sin(0.05t))$. Figure 1 represents the simulation result of the substrate concentration (s), the estimation of the substrate concentration ($\hat{s}_{obs}$), the production rate (y) and the estimation of the production rate ($\hat{y}_{obs}$). Figure 2 shows that both $\hat{\theta}_s$ and $\hat{\theta}_\mu$ converge to their true value $\theta_s = \theta_\mu = 5$. From Figure 3, the trajectories under output feedback recover the trajectories under state feedback for the high gain observer with sufficiently large gain ($\epsilon = 0.01$). Furthermore, the maximum value for the production rate $y = 3.77$ is achieved under output and state feedback which confirms the effectiveness of the adaptive extremum seeking scheme.

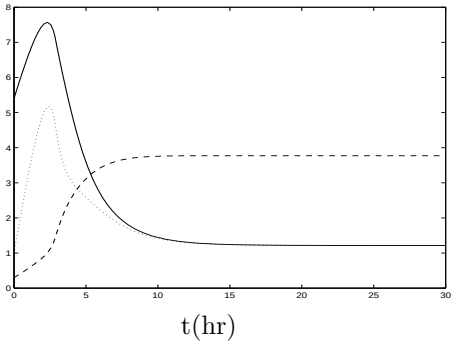

Fig. 1. Substrate concentration s("..") and its estimate $\hat{s}_{obs}$("–"), production rate y and its estimate $\hat{y}_{obs}$ ("- -")

6. CONCLUSION

An adaptive output-feedback extremum-seeking control was developed for a class of stirred tank bioreactors governed by Monod growth kinetics. The controller allows the stabilization of the system to its unknown optimal production rate.

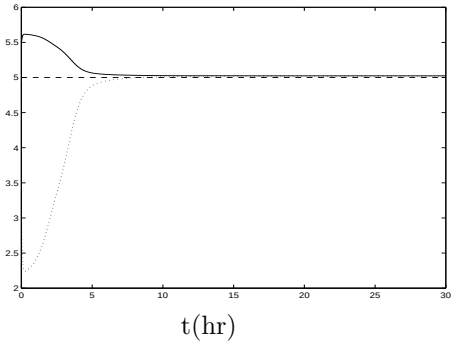

Fig. 2. Parameter θ_μ("- -") and its estimate $\hat{\theta}_\mu$("–"), parameter θ_s("- -") and its estimate $\hat{\theta}_s$("..")

REFERENCES

Atassi, A.N. and H. K. Khalil (1999). A Separation Principle for the Stabilization of a Class of Nonlinear Systems. *IEEE Transactions on Automatic Control* **44**(9), 1672–1687.

Esfandiari, F. and H. K. Khalil (1992). Output Feedback Stabilization of Fully Linearizable Systems. *International Journal of Control* **56**(5), 1007–1037.

Khalil, H. K. (1996). Adaptive Output Feedback Control of Nonlinear Systems Represented by Input-Output Models. *IEEE Transactions on Automatic Control* **41**(2), 177–188.

Lee, K. W. and H. K. Khalil (1997). Adaptive Output Feedback Control of Robot Manipulators using High-gain Observer. *International Journal of Control* **67**(6), 869–886.

Marino, R. and P. Tomei (1995). *Nonlinear Control Design*. Prentice Hall.

Pomet, J.-B. and L. Praly (1992). Adaptive Nonlinear Regulation: Estimation from the Lyapunov Equation. *IEEE Transactions on Automatic Control* **37**, 729–740.

Wang, H.H., M. Krstic and G. Bastin (1999). Optimizing Bioreactors by Extremum Seeking. *Int. Journal Adaptive Control and Signal Processing* **13**, 651–669.

Zhang, T., M. Guay and D. Dochain (2001). Adaptive Extremum Seeking Control of Continuous Stirred Tank Bioreactors. *AICHE Journal* **2**(40), 10–20.

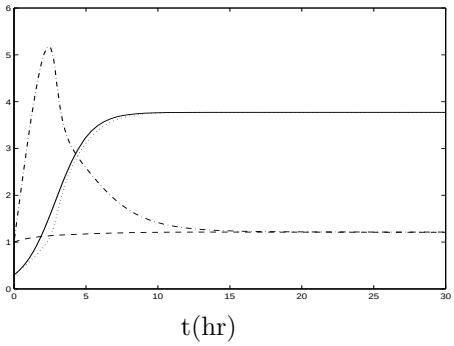

Fig. 3. y under state feedback ("–") and y under output feedback ("- -"), s under output feedback("- .") and s under state feedback ("- -")

A BMI-BASED DESIGN OF SWITCHED PID CONTROLLERS

Jun Aoyama [*] **Katsumi Konishi** [**]
Toru Yamamoto [***] **Takao Hinamoto** [*]

[*] *Department of Artificial Complex Systems Control, Graduate School of Engineering, Hiroshima University, 1-4-1 Kagamiyama, Higashi-hiroshima, Hiroshima, 739-8527, Japan*
[**] *Information Media Center, Hiroshima University, 1-4-2 Kagamiyama, Higashi-hiroshima, Hiroshima, 739-8511, Japan*
[***] *Department of Technology and Information Education, Graduate School of Education, Hiroshima University, 1-1-1 Kagamiyama, Higashi-hiroshima, Hiroshima, 739-8524, Japan*

Abstract: This paper provides a design method for two-degrees-of-freedom PID controllers including switched PD compensator based on bilinear matrix inequalities (BMIs). Two design specifications based on $\mathcal{H}_2$ norm are formulated in BMIs, and PID parameters can be exactly obtained by solving the BMI problems via branch and bound algorithms. A set of PD compensators can be obtained simultaneously using proposing design method. The most effective parameter is selected out of the set of PD compensator based on the switching criterion which obtained from estimated system conditions using recursive least square algorithms. Numerical example is also shown.

Keywords: PID controllers

1. INTRODUCTION

PID controllers play a critical role in 80-90 percent of chemical process systems [1]. They are widely used because of their simple structures which consist of only three parameters, that is, proportional parameter, integral parameter, and derivative parameter. It is, however, difficult to tune those parameters practically since the process dynamics often change due to changes in operating conditions or various disturbances. We have to design controllers such that they have both robustness for changes in conditions of the systems and good tracking properties. PID controllers with one-degree-of-freedom can not have robustness and good tracking properties since they are contrary properties. In order to design the controller with robustness and good tracking properties, this paper deals with two-degrees-of-freedom PID control systems, which have a PID control system and a PD compensator.

The design of many conventional control systems has resulted in an optimization problem, which can be solved by numerical computation based on powerful computer support. One of the most useful tools is bilinear matrix inequality (BMI), which is a flexible framework for analysis and synthesis of control systems. Although checking the solvability of BMI problems is NP hard [2], it

is not hard to obtain an exact solution of a BMI problem via branch and bound algorithms if it has a few parameters. Fortunately, a design problem of PID controller has only three parameters, so that we can design PID controller based on BMI.

This paper formulates the design problem of PID controllers with two-degrees-of-freedom as a BMI problem. The aim of the control design is to make the control system has both robustness and good tracking properties. In order to reduce the conservativeness of the control system, this paper deal with PD compensator which has switching structure. This switching structure is constructed from a system estimator using recursive least squares algorithms, the switching criterion based on stationary gain of the estimated system and a set of pre-specified PD parameters corresponding to the switching criterion.

This paper is organized as follows. The system description, problem formulations and the design method of PID controller with two-degrees-of-freedom based on BMI are given in Section 2. In Section 3, for more effective PD compensator, a switching structure based on adaptive control method is constructed. Section 4 provides branch and bound algorithms in order to obtain an exact solution of BMI problems. Finally, numerical simulation examples are presented in Section 5.

2. CONTROLLER DESIGN BESED ON BMI

2.1 System description

Consider a system described by the following continuous-time model:

$$G(s) = \frac{K_0}{1+Ts} e^{-Ls} \tag{1}$$

where K_0 expresses the system gain, T is the time-constant and L refers to the delay. By using the first order Padé approximation of the delay, the system is approximated as

$$G(s) \cong \frac{K_0}{1+Ts} \cdot \frac{1-\frac{Ls}{2}}{1+\frac{Ls}{2}} \tag{2}$$

Here, utilizing multiples of the sampling time period T_s in the equation (2), the continuous-time model is transformed to the following discrete-time model:

$$A(z^{-1})y(t) = z^{-1}B(z^{-1})u(t) + \frac{1}{\Delta}\xi(t) \tag{3}$$

where

$$\begin{aligned} A(z^{-1}) &= 1 + a_1 z^{-1} + a_2 z^{-2} \\ B(z^{-1}) &= b_0 + b_1 z^{-1} \end{aligned} \tag{4}$$

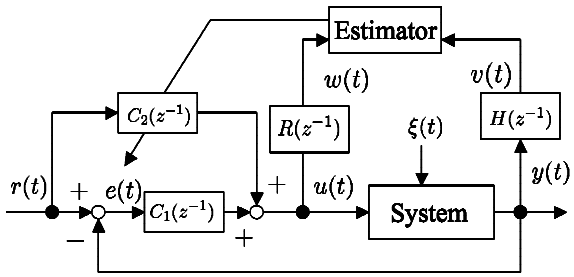

Fig. 1. Closed-loop system with two-degrees-of-freedom.

and $u(t)$, $y(t)$ and $\xi(t)$ denote the control input signal, the corresponding output signal and the stochastic noise, respectively. The operator z^{-1} denotes a backward shift, that is, $z^{-1}y(t) = y(t-1)$, and Δ denotes the differencing operator defined as $1 - z^{-1}$. This paper deals with the descrete-time model (3) as the control object instead of the continuous-model (1).

Next, consider the control system represented by the PID controller with two-degrees-of-freedom in Fig.1, where $r(t)$ and $e(t)$ refer to the reference signal and the control error, respectively. $H(z^{-1})$ and $R(z^{-1})$ denote a low pass filter, and where $C_1(z^{-1})$ and $C_2(z^{-1})$ denote the PID controller and the PD compensator, respectively. And they are given by

$$C_1(z^{-1}) = k_c + \frac{k_i}{\Delta} + \Delta k_d \tag{5}$$

$$C_2(z^{-1}) = -k_\alpha - \Delta k_\beta \tag{6}$$

The two-degrees-of-freedom PID controller in (5) and (6) includes five parameters: propotional gains k_c and k_α, integral gain k_i and derivative gains k_d and k_β. The one-degree-of-freedom PID controller $C_1(z^{-1})$ is required to satisfy the design specification for the system perturbation and the stochastic noise by using fixed PID parameters which are obtained from the BMI solution discussed in Section 4. And the PD compensator $C_2(z^{-1})$ which has a set of pre-specified PD parameters corresponding to the divided small perturbations, is required to satisfy the good tracking property by using switching structure based on the estimator discussed in Section 3.

2.2 Problem fomulation

This paper deals with the $\mathcal{H}_2$ norms which represent the integral squared errors (ISE) of the control system. They can evaluate the two design specifications which require the robustness for the control system and the tracking property for the reference signal. Moreover these evaluation measures result in the optimization problem which is represented by matrix inequalities.

First, we consider the error transfer function of the control system in Fig.1. In order to evaluate the tracking property for the step reference signal, $E_r(z^{-1})$ is defined as the transfer function from $r(t)$ to $e(t)$. Since a step input is given by $r(z^{-1}) = 1/(1-z^{-1})$ and $\xi(z^{-1}) = 0$, $E_r(z^{-1})$ can be expressed as

$$E_r(z^{-1}) = \frac{A(z^{-1}) - z^{-1}B(z^{-1})C_2(z^{-1})}{\Delta A(z^{-1}) + z^{-1}B(z^{-1})\Delta C_1(z^{-1})} \quad (7)$$

Similarly, in order to evaluate the influence of the stochastic noise $\xi(t)$, $E_d(z^{-1})$ is defined as the transfer function from $\xi(t)$ to $e(t)$. We assume that $\xi(z^{-1})$ is a white noise which is represented by $\xi(z^{-1}) = 1$ and $r(z^{-1}) = 0$, then $E_d(z^{-1})$ can be expressed as follows.

$$E_d(z^{-1}) = \frac{-1}{\Delta A(z^{-1}) + z^{-1}B(z^{-1})\Delta C_1(z^{-1})} \quad (8)$$

The ISE is described as

$$\frac{1}{2\pi}\int_{-\pi}^{\pi} E(j\omega)E(-j\omega)\, d\omega \quad (9)$$

$$= \frac{1}{2\pi}\int_{-\pi}^{\pi} |E(j\omega)|^2\, d\omega < \gamma \quad (10)$$

where $E = E_r$ or E_d and γ is positive constant. Because the $\mathcal{H}_2$-norm of $E(z^{-1})$ is defined as

$$\| E \|_2 = \left(\frac{1}{2\pi}\int_{-\pi}^{\pi} |E(j\omega)|^2\, d\omega\right)^{\frac{1}{2}} \quad (11)$$

the performance measure based on ISE results in the following two inequalities.

$$\| E_r \|_2 < \sqrt{\gamma_r} \quad (12)$$
$$\| E_d \|_2 < \sqrt{\gamma_d} \quad (13)$$

The purpose of this paper is to minimize γ_r in (12) for a given $\sqrt{\gamma_d}$.

In this paper, the error systems (7) and (8) are realized in the controllable canonical form as following equations.

$$E_r(z^{-1}) = C_{er}(zI - A_{er})^{-1}B_{er} + D_{er} \quad (14)$$
$$E_d(z^{-1}) = C_{ed}(zI - A_{ed})^{-1}B_{ed} + D_{ed} \quad (15)$$

where A_i, B_i, C_i and D_i ($i = er$ or ed) are given by the following matrices.

$$\begin{aligned} A_i &= A_{e0} + k_c A_{e1} + k_i A_{e2} + k_d A_{e3} \\ B_i &= [\,0 \quad 0 \quad 0 \quad 1\,]^T \\ C_{er} &= C_{er0} + k_c C_{er1} + k_i C_{er2} + k_d C_{er3} \\ &\quad + k_\alpha C_{er4} + k_\beta C_{er5} \quad (16) \\ C_{ed} &= C_{ed0} + k_c C_{ed1} + k_i C_{ed2} + k_d C_{ed3} \\ D_{er} &= 1 \\ D_{ed} &= -1 \end{aligned}$$

where $A_i = A_{er} = A_{ed}$, $B_i = B_{er} = B_{ed}$ and where A_{e0} thru A_{e3}, C_{er0} thru C_{er5} and C_{ed0} thru C_{ed3} are given by constant matrices.

According to papers [3], the ISE criterions which are represented by $\mathcal{H}_2$ norm in (12) and (13) equal to following matrix inequality,

$$\Phi = \begin{bmatrix} \phi_{e0}(P^{-1}, \mathbf{k}_1) & 0 & 0 \\ 0 & \phi_{ed}(P^{-1}, \mathbf{k}_1, \gamma_d) & 0 \\ 0 & 0 & \phi_{er}(P^{-1}, \mathbf{k}_2, \gamma_r) \end{bmatrix} \succ 0 \quad (17)$$

where '$\Phi \succ 0$' denotes that Φ is positive definite matrix, and where

$$\phi_{e0}(P^{-1}, \mathbf{k}_1) = \begin{bmatrix} P^{-1} & P^{-1}B_{ed} & P^{-1}A_{ed} \\ B_{ed}^T P^{-T} & 1 & 0 \\ A_{ed}^T P^{-T} & 0 & P^{-1} \end{bmatrix} \quad (18)$$

and

$$\phi_{ed}(P^{-1}, \mathbf{k}_1, \gamma_d) = \begin{bmatrix} \gamma_d & D_{ed} & C_{ed} \\ D_{ed}^T & 1 & 0 \\ C_{ed}^T & 0 & P^{-1} \end{bmatrix} \quad (19)$$

and

$$\phi_{er}(P^{-1}, \mathbf{k}_2, \gamma_r) = \begin{bmatrix} \gamma_r & D_{er} & C_{er} \\ D_{er}^T & 1 & 0 \\ C_{er}^T & 0 & P^{-1} \end{bmatrix} \quad (20)$$

and where $\mathbf{k}_1 := [k_c, k_i, k_d]$ and $\mathbf{k}_2 := [k_c, k_i, k_d, k_\alpha, k_\beta]$ are the parameter vectors of the controller and P is a 4×4 positive symmetric matrix.

Since the continuous system (1) is perturbed, the four parameters a_1, a_2, b_0 and b_1 in realized systems have perturbations. In order to treat these perturbations of the control system, we assume here that 4 parameters belong to a perturbation set Ω, and the problem is formulated as

$$\begin{array}{lll} \text{Minimize} & \gamma_r & (21) \\ \text{subject to} & \gamma_d < \tilde{\gamma}_d & (21-\text{a}) \\ & \mathbf{k}_1 \in Q_D & (21-\text{b}) \\ & \Phi \succ 0 \ \text{ for all } \begin{bmatrix} a_1 \\ a_2 \\ b_0 \\ b_1 \end{bmatrix} \in \Omega & (21-\text{c}) \end{array}$$

where $\tilde{\gamma}_d$ is a constant given in advance, Q_D is a given hyper-rectangle in $\mathcal{R}^3$, and Ω denotes the set of perturbations as following equation.

$$\Omega := \left\{ \begin{bmatrix} a_1 \\ a_2 \\ b_0 \\ b_1 \end{bmatrix} \in \mathcal{R}^4 : \begin{array}{c} a_{1min} \le a_1 \le a_{1max} \\ a_{2min} \le a_2 \le a_{2max} \\ b_{0min} \le b_0 \le b_{0max} \\ b_{1min} \le b_1 \le b_{1max} \end{array} \right\} \tag{22}$$

Because any $[a_1,\ a_2,\ b_0,\ b_1]^T$ in the set Ω can be described by linear combinations of 2^4 vertex vectors, the matrix inequalitiy (21-c) can be described by 2^4 BMIs. Although it is hard to solve BMI problems, which are NP hard in general, we can obtain the exact solution of BMI problem (21) via branch and bound algorithms discussing in Section 4 because it has only five parameters.

3. SWITCHING STRUCTURE BASED ON ADAPTIVE CONTROL METHOD

In order to reduce the conservativeness of the proposed controller, the switching structure for PD compensator is designed based on the adaptive control method in this section. This switching structure includes a system estimator, the switching criterion and a set of pre-specified PD parameters.

First, we construct the estimator in Fig1 base on recursive least square algorithms. To remove the influence of the stochastic noise $\xi(t)$ from system output $y(t)$, consider the low pass filter $H(z^{-1})$ which can effectively remove the high frequency noise. $H(z^{-1})$ is given by:

$$v(t) = H(z^{-1})y(t) \tag{23}$$

Similarly, consider the effective low pass filter $R(z^{-1})$ for the control input signal. This filter is added for more accurate estimating, that is given by the following equation.

$$w(t) = R(z^{-1})u(t) \tag{24}$$

Here, consider the following discrete-time model:

$$\tilde{A}(z^{-1})v(t) = z^{-1}\tilde{B}(z^{-1})u(t) \tag{25}$$

where

$$\begin{array}{l} \tilde{A}(z^{-1}) = 1 + \tilde{a}_1 z^{-1} + \tilde{a}_2 z^{-2} \\ \tilde{B}(z^{-1}) = \tilde{b}_0 + \tilde{b}_1 z^{-1} \end{array} \tag{26}$$

Then, the following extended least squares estimation is employed:

$$\begin{array}{l} \hat{\theta}(t) = \hat{\theta}(t-1) + \dfrac{\Gamma(t-1)\psi(t-1)\varepsilon(t)}{1+\psi^T(t-1)\Gamma(t-1)\psi(t-1)} \\ \qquad \in \mathcal{R}^4 \end{array} \tag{27}$$

$$\begin{array}{l} \Gamma(t) = \Gamma(t-1) \\ \qquad - \dfrac{\Gamma(t-1)\psi(t-1)\psi^T(t-1)\Gamma(t-1)}{1+\psi^T(t-1)\Gamma(t-1)\psi(t-1)} + \Gamma_0 \\ \qquad \in \mathcal{R}^{4\times 4} \end{array} \tag{28}$$

$$\varepsilon(t) := \Delta v(t) - \hat{\theta}^T(t-1)\psi(t-1) \quad \in \mathcal{R} \tag{29}$$

where $\varepsilon(t)$ denotes prediction errors. $\hat{\theta}(t)$ and $\psi(t-1)$ are the unknown parameter vector and the data vector of the form:

$$\hat{\theta}(t) := [\tilde{a}_1, \tilde{a}_2, \tilde{b}_0, \tilde{b}_1]^T \in \mathcal{R}^4 \tag{30}$$

$$\begin{array}{l} \psi(t-1) := [-\Delta v(t-1), -\Delta v(t-2), \\ \qquad \Delta w(t-1), \Delta w(t-2)]^T \in \mathcal{R}^4 \end{array} \tag{31}$$

By using (27) thru (31), The state of the system can be estimated recursively.

Next, we consider the switching criterion based on the estimated system condition. This paper deals with the stationary gain of the system (25) as the switching criterion. Let us define K_{sc}:

$$K_{sc} = \frac{\tilde{B}(1)}{\tilde{A}(1)} \tag{32}$$

and let PD compensator $C_2(z^{-1})$ be switched based on the following detection rule.

$$C_2(z^{-1}) = \begin{cases} C_2^{(1)}(z^{-1}) & K_{sc}^{(1)} < K_{sc} \le K_{sc}^{(2)} \\ C_2^{(2)}(z^{-1}) & K_{sc}^{(2)} < K_{sc} \le K_{sc}^{(3)} \\ \quad \vdots & \quad \vdots \\ C_2^{(p)}(z^{-1}) & K_{sc}^{(p)} < K_{sc} \le K_{sc}^{(p+1)} \end{cases} \tag{33}$$

where $K_{sc}^{(j)}$ $(j = 1 \cdots p+1)$ are given and where $C_2^{(q)}(z^{-1})$ $(q = 1 \cdots p)$ are PD compensators defined for each sector.

Here we consider the design method of $C_2^{(q)}(z^{-1})$. From (32) and (33), the gain range $K_{sc}^{(q)} < K_{sc} \le K_{sc}^{(q+1)}$ is expressed as the set of $[a_1,\ a_2,\ b_0,\ b_1]^T$ as follows.

$$\Lambda := \left\{ \begin{bmatrix} a_1 \\ a_2 \\ b_0 \\ b_1 \end{bmatrix} \in \mathcal{R}^4 : \begin{array}{c} K_{sc}^{(q)}(1+a_1+a_2) \\ -(b_0+b_1) < 0 \\ -K_{sc}^{(q+1)}(1+a_1+a_2) \\ +b_0+b_1 \le 0 \end{array} \right\} \tag{34}$$

Then the design problem of the PD compensator $C_2^{(q)}(z^{-1})$ corresponding to the pre-specified small-ranged system gain $K_{sc}^{(q)} < K_{sc} \le K_{sc}^{(q+1)}$ can be formulated as

$$\text{Minimize} \quad \gamma_r \tag{35}$$

$$\text{subject to} \quad \Phi_{PD} \succ 0 \ \text{ for all } \begin{bmatrix} a_1 \\ a_2 \\ b_0 \\ b_1 \end{bmatrix} \in \Omega \cap \Lambda \tag{35-a}$$

where Φ_{PD} is represented by the following matrix

$$\Phi_{PD} = \begin{bmatrix} \phi_{e0}(P^{-1}, \mathbf{k}_1) & 0 \\ 0 & \phi_{er}(P^{-1}, \mathbf{k}_2, \gamma_r) \end{bmatrix} \succ 0 \tag{36}$$

In the above problem, PID parameters k_c, k_i and k_d in parameter vecters of the controller $\mathbf{k}_1$ and $\mathbf{k}_2$ are given since they are already obtained by solving (21). Therefore, matrix inequality (36) can be represented by LMI, where variables are P^{-1}, k_α and k_β. The matrix inequality (35-a) can be expressed by two inequalities in (34) and 2^4 LMIs as well as the case of (21-c). Hence it is easy to obtain the optimal solution of the problem (35) because there exist polynomial algorithms based on the interior point method [4].

By using the estimator and the switching criterion as mentioned above, the most effective PD compensator which satisfies the good tracking property is selected out of the set of pre-specified PD parameters corresponding to the small divided perturbations. The switching algorithm for the proposed PID controller with two-degrees-of-freedom is summarized as follows.

【The switching algorithm for the PID controller with two-degrees-of-freedom】

[**Step 1**] Design the PID controller and the PD compensator by solving the BMI problem (21).
[**Step 2**] Design the set of PD parameters corresponding to the small divied perturbations by solving the LMI problem (35).
[**Step 3**] Estimate the system conditions using (27) thru (31).
[**Step 4**] Calculate K_{sc} from (32).
[**Step 5**] Choose the most effective PD parameter from the detection rule in (33).
[**Step 6**] Return to [**Step 3**].

4. BMI SOLUTION BY USING AN EXACT ALGORITHM

This section provides an exact algorithm for solving problem (21) based on branch and bound algorithms [5]. Branch and bound algorithms give us the lower bound Ψ_L and the upper bound Ψ_U satisfying $\Psi_L \le \inf \gamma_r \le \Psi_U$ and $(\Psi_U - \Psi_L)/\Psi_L \le \varepsilon$ for any $\varepsilon > 0$. The lower bounds are obtained using the SDP relaxation [6,7].

Let us define the function $\Psi(\cdot)$, $\Psi_L(\cdot)$ and $\Psi_U(\cdot)$ as follows.

$$\Psi(Q) \equiv \inf_{\substack{\gamma_d < \tilde{\gamma}_d, [\mathbf{k}_1, \mathbf{k}_2]^T \in Q, \\ \Phi \succ 0 \text{ for all } [a_1, a_2, b_0, b_1]^T \in \Omega}} \gamma_r, \tag{37}$$

$$\Psi_L(Q) \equiv \inf_{\substack{\gamma_d < \tilde{\gamma}_d, [\mathbf{k}_1, \mathbf{k}_2]^T \in Q, \\ \hat{\Phi} \succ 0 \text{ for all } [a_1, a_2, b_0, b_1]^T \in \Omega}} \gamma_r, \tag{38}$$

$$\Psi_U(Q, \mathbf{k}_1^*, \mathbf{k}_2^*) \equiv \inf_{\substack{\gamma_d < \tilde{\gamma}_d, \\ \Phi^* \succ 0 \text{ for all } [a_1, a_2, b_0, b_1]^T \in \Omega}} \gamma_r, \tag{39}$$

where $\hat{\Phi}$ is the SDP relaxation of Φ obtained using the method in the papers [7,8],

$$\begin{bmatrix} \mathbf{k}_1^* \\ \mathbf{k}_2^* \end{bmatrix} = \arg \inf_{\substack{\gamma_d < \tilde{\gamma}_d, [\mathbf{k}_1, \mathbf{k}_2]^T \in Q, \\ \hat{\Phi} \succ 0 \text{ for all } [a_1, a_2, b_0, b_1]^T \in \Omega}} \gamma_r,$$

and Φ^* is obtained by substituting $[\mathbf{k}_1^*, \mathbf{k}_2^*]^T$ into Φ in (17). Then $\Psi_L(Q) \le \Psi(Q) \le \Psi_U(Q)$ holds for any Q. We can obtain Ψ_L^* and Ψ_U^* such that $\Psi_L \le \inf \gamma_r \le \Psi_U$ holds for any ε using the following algorithm.

【Branch and Bound Algorithm】

[**Step 1**] Set $k \leftarrow 0, Q_0 \leftarrow Q_D, S0 \leftarrow \{Q_0\}, L_0 \leftarrow \Psi(Q_0), U_0 \leftarrow_U (Q_0)$.
[**Step 2**] Select $\bar{Q}$ from S_k such that $L_k = \Psi_L(\bar{Q})$. $S_{k+1} \leftarrow S_k \setminus \{\bar{Q}\}$.
[**Step 3**] Split $\bar{Q}$ along its longest edge into $\bar{Q}_1$ and $\bar{Q}_2$.
[**Step 4**] For $i = 1, 2$ if $\Psi_L(\bar{Q}_i) \le U_k$ then $S_{k+1} \leftarrow S_{k+1} \cup \{\bar{Q}_i\}$.
[**Step 5**] $U_{k+1} \leftarrow \min_{Q \in S_{k+1}} \Psi_U(Q)$.
[**Step 6**] Pruning: $S_{k+1} \leftarrow S_{k+1} \setminus \{Q : \Psi_L(Q) > U_{k+1}\}$.
[**Step 7**] $L_{k+1} \leftarrow \min_{Q \in S_{k+1}} \Psi_L(Q)$.
[**Step 8**] If $(U_k - L_k)/L_k \le \varepsilon$ then end else $k \leftarrow k+1$ and goto [**Step 2**].

5. NUMERICAL EXAMPLE

In order to investigate the behavior of the proposed control scheme, numerical simulation examples are illustrated in this section.

Let us consider the continuous-time model given by the following equation.

$$G(s) = \frac{K_0}{1+Ts} e^{-Ls} \quad \text{where} \quad \begin{cases} 1.0 \le K_0 \le 1.5 \\ 8 \le T \le 12 \\ L = 3 \end{cases} \tag{40}$$

From (3) and (4), the system parameters of the descrete-time model which are transformed by using sampling time period $T_s = 1$ are obtained as follows:

$$\begin{aligned} A(z^{-1}) &= 1 + a_1 z^{-1} + a_2 z^{-2} \\ B(z^{-1}) &= b_0 + b_1 z^{-1} \end{aligned} \tag{41}$$

where

$$\begin{cases} -1.4335 \le a_1 \le -1.3959 \\ 0.4531 \le a_2 \le 0.4724 \\ -0.0528 \le b_0 \le -0.0362 \\ 0.0751 \le b_1 \le 0.1100 \end{cases} \tag{42}$$

By solving the BMI problem (21), parameters of the PID controller and the PD compensator are designed as follows:

$$\begin{array}{lll} k_c = 2.7525 & k_\alpha = 0.4496 & \gamma_r = 15.4295 \\ k_i = 0.3818 & k_\beta = 0.7565 & \gamma_d = 162.6861 \\ k_d = 4.3374 & & \end{array} \tag{43}$$

We designed the pre-specified PD compensators by solving the LMI problems (35), and they are obtained as follows:

$$C_2(z^{-1}) = \begin{cases} -0.4009 - 1.9002\Delta \\ \qquad 1.0 < K_{sc} \le 1.25 \\ \qquad (\gamma_r = 6.5864) \\ -0.7843 - 2.0138\Delta \\ \qquad 1.25 < K_{sc} \le 1.5 \\ \qquad (\gamma_r = 5.9511) \end{cases} \tag{44}$$

The system parameters of the control object are given as $K_0 = 1.0$ and $T = 11.5$ in the period from 0[step] to 400[step], and $K_0 = 1.4$ and $T = 12.0$ in the period from 401[step] to 1000[step]. The reference signal is given as $r(t) = 1$ in the period from 0[step] to 200[step], $r(t) = 2$ in the period from 201[step] to 700[step] and $r(t) = 2.5$ in the period 701[step] to 1000[step]. The stochastic noise $\xi(t)$ is given as a normal distribution with $\mathcal{N}(0, 0.001^2)$. Fig.2 shows the result. We can see that the influence by the stochastic noise can be reduced, and that the system can track the reference signal well.

6. CONCLUSIONS

In this paper, a BMI based design scheme for switched PID controllers with two-degrees-of-freedom has been proposed. According to the proposed scheme, two design specification based on $\mathcal{H}_2$ norm are formulated in BMIs, and PID parameters can be exactly obtained by solving the BMI problems via branch and bound algorithms. In order to reduce the conservativeness of the control system, the proposed PD compensators have switching structure based on adaptive control method. Numerical examples have shown the effectiveness of the proposed method.

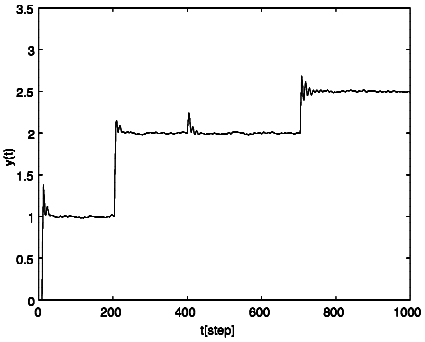

Fig. 2. Control result using the proposed PID control scheme.

REFERENCES

[1] N. Suda: PID control (System, Control and Information Library, No. 6), Asakura (1992) (in Japanese)

[2] O. Toker and H. Özbay, On the NP-hardness of solving Bilinear Matrix Inequalities and simultaneous stabilization with static output feedback, Proc. of ACC, pp. 2525–2526, 1995

[3] K. Zbou, J. C. Doyle and K. Glover: Robust and optimal control, Prentice Hall, p.561 (1996)

[4] W. F. Alizadeh, "Interior point methods in semidefinite programming with application to combinatorial optimization", SIAM Journal of Optimization, vol. 5, pp. 12–51, 1995

[5] K. C. Goh, M. G. Safonov and G. P. Papavassilopoulos, "A Global Optimization Approach for the BMI Problem", Proc. of the 33rd Conf. Decision Control, 2009-2014, 1994

[6] T. Fujita and M. Kojima, "Semidefinite relaxation for nonconvex programs", Journal of Global Optimization, Vol. 10, pp. 367–380, 1997

[7] M. Kojima and L. Tunçel, "Cones of Matrices and Successive Convex Relaxations of Nonconvex Sets", Research Reports on Mathematical and Computing Science, Series B: Operations Research, Department of Mathematical and Computing Sciences, Tokyo Institute of Technology, 1999

[8] H. Fujioka and K. Hoshijima, "Bounds for the BMI Eigenvalues Problem", Trans. of SICE, Vol. 33, No. 7, pp. 616–621, 1997

HYBRID CONTROL: IMPLEMENTING OUTPUT FEEDBACK MPC WITH GUARANTEED STABILITY REGION [1]

Prashant Mhaskar, Nael H. El-Farra and Panagiotis D. Christo des

Department of Chemical Engineering
University of California, Los Angeles, CA 90095-1592

Abstract: In this work, a hybrid control scheme that employs switching between bounded control and model predictive control (MPC) is proposed for the output feedback stabilization of linear time-invariant systems with input constraints. Initially, we design a bounded output feedback controller for which the region of constrained closed-loop stability is explicitly characterized and an MPC controller that minimizes a given performance objective subject to constraints. Switching laws are derived to orchestrate the transition between the two controllers in a way that reconciles their respective stability and optimality properties, and guarantees asymptotic closed-loop stability for all initial conditions within the stability region of the bounded controller. The hybrid scheme is shown to provide a safety net for the practical implementation of output feedback MPC by providing *a priori* knowledge, through off-line computations, of a large set of initial conditions for which closed-loop stability is guaranteed. The proposed hybrid control approach is illustrated through a simulation example.

Keywords: Hybrid control, Bounded control, MPC, State observers, Input constraints.

1. INTRODUCTION

1.1 *Classical vs. hybrid control*

The conventional, or classical", approach to control has been that of modelling the process (up to the requisite level of detail) and then designing an appropriate controller to achieve the desired control objective. The salient feature of the classical approach is the absence of a discrete component in the control structure.

In contrast, a hybrid control structure (Figure 1) involves, by design, a blend of continuous (i.e., the classical controllers) and discrete components (i.e., the logic based supervisor that switches between the controllers). The controllers within the control block could be of similar structure (but with different gains or parameters), or could be structurally different (for example, an analytic and a model predictive controller). The switching between multiple classical controllers is orchestrated by the supervisor for the purpose of either meeting an objective that cannot be achieved by the individual controllers or to reconcile the different (complementary) strengths and capabilities of different control approaches.

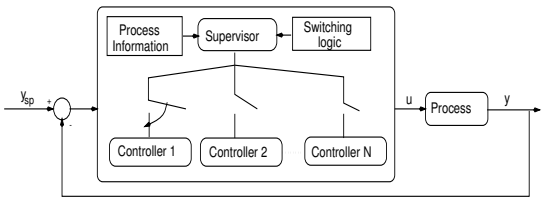

Fig. 1. A schematic representation of a hybrid control structure.

The general idea of hybrid control, manifested through switching between different controllers, has been used in the literature in a variety of contexts. Examples include gain scheduling (e.g., see (Rugh and Shamma, 2000)) as a tool for control of nonlinear systems, multiple linear models for transition control (e.g., see

[1] Financial support from NSF, CTS-0129571, is gratefully acknowledged

(Banerjee and Arkun, 1998; Sun and Hoo, 1999)) and scheduled predictive control (e.g., see (Aufderheide *et al.*, 2001)) of nonlinear processes. A recurrent theme in most of the work on hybrid control has been that of switching between different models (which results in an implicit switching between different controllers), or that of using multiple *structurally similar* controllers.

In (El-Farra *et al.*, 2002), we proposed a hybrid control structure, that employs switching between two *structurally different* controllers an MPC controller and a bounded analytical controller for the state feedback stabilization of linear systems with input constraints. The bounded controller was used to provide a safety net for the implementation of MPC within a well defined region of guaranteed stability. The proposed hybrid control structure was extended to address the problems of robust control of linear systems with uncertainties (El-Farra *et al.*, 2003*b*) and constrained stabilization of nonlinear systems (El-Farra *et al.*, 2003*a*). In this work, a hybrid control scheme, uniting bounded control with MPC, is proposed for the output feedback stabilization of linear time-invariant systems with input constraints.

1.2 *Background*

Input constraints arise as a manifestation of the physical limitations inherent in the capacity of control actuators (e.g., bounds on the magnitude of valve opening). Input constraints automatically impose limitations on our ability to steer the dynamics of the closed-loop system at will, and can cause severe deterioration in the nominal closed-loop performance and may even lead to closed-loop instability if not explicitly taken into account at the stage of controller design.

One of the key limitations imposed by input constraints is the restriction on the set of initial states of the closed-loop system that can be steered to the origin with the available control action. The absence of an *a priori* explicit characterization of this set (or an appropriate estimate thereof) can have an impact on the practical implementation of the given control policy by requiring extensive closed-loop simulations over the whole set of possible initial conditions, to check for closed-loop stability, or by limiting operation within an unnecessarily small and conservative neighborhood of the desired equilibrium point. These considerations have motivated signi cant work on the design of stabilizing bounded control laws that provide explicitly-de ned, large regions of attraction for the closed-loop system (e.g., see (Lin and Sontag, 1991; Teel, 1992; El-Farra and Christofides, 2001; El-Farra and Christo des, 2003)).

Currently, MPC, also known as receding horizon control, is a widely used control method for handling constraints within an optimal control setting. Within MPC, the control action is obtained by solving repeatedly, on-line, a nite-horizon constrained open-loop optimal control problem. The industrial success of MPC has spurred numerous research investigations into the stability properties of MPC controllers and led to a plethora of MPC formulations that focus on closed-loop stability (e.g., see (Rawlings and Muske, 1993; Allgower and Chen, 1998; Mayne *et al.*, 2000) for extensive surveys of these developments). The signi cant progress in characterizing the stability properties of MPC notwithstanding, the issue of obtaining, *a priori* (i.e. before controller implementation), an analytic characterization of the region of constrained closed-loop stability for MPC controllers remains to be adequately addressed. This dif culty can have an impact on the practical implementation of MPC by requiring extensive closed-loop simulations over the whole set of possible initial conditions to check for closed-loop stability, or by potentially limiting operation within an unnecessarily small neighborhood of the nominal equilibrium point.

In addition to the problem of input constraints, the problem of output feedback stabilization of constrained systems has been the subject of numerous research studies. Examples include scalar output feedback control of linear systems (Shamma and Tu, 1998), stability analysis of a composite system comprising of a moving horizon regulator and a moving horizon observer for control of nonlinear systems (Michalska and Mayne, 1995) and moving horizon estimation as an extension of Kalman ltering, for constrained and nonlinear processes (Rao and Rawlings, 2002). In these works, however, the stability region of the constrained closed loop system is not explicitly characterized.

Motivated by the above considerations, we propose in this paper a controller switching strategy that extends the hybrid control structure in (El-Farra *et al.*, 2002) to the case of output feedback. The guiding principle in realizing this strategy is that of using a suitable state observer design which, in conjunction with the bounded controller, yields an explicitly characterized stability region within which the operation of the MPC controller can be embedded by devising suitable switching rules (see (Mhaskar *et al.*, 2003) for a detailed analysis of the theoretical issues involved and the mathematical proofs of the results). The rest of the paper is organized as follows: in section 2, we present some preliminaries that describe the class of systems considered and review brie y the methodology of designing the state observer, and how the constrained control problem is addressed in both bounded control and model predictive control. In section 3, we formulate the controller switching problem under output feedback and propose a switching scheme that addresses the problem. Finally, in section 4, numerical simulations are presented to demonstrate the implementation of the switching scheme and test the robustness of the proposed approach with respect to measurement noise.

2. PRELIMINARIES

In this work, we consider the problem of output feedback stabilization of continuous-time linear time-

invariant (LTI) systems with input constraints, with the following state-space description:

$$\begin{aligned} \dot{x} &= Ax + Bu \\ y &= Cx \\ u(t) &\in \mathcal{U} \quad \mathbb{R}^m \end{aligned} \tag{1}$$

where $x = [x_1, \quad , x_n]' \in \mathbb{R}^n$ denotes the vector of state variables, $y = [y_1, \quad , y_k]' \in \mathbb{R}^k$ denotes the vector of output variables, $u = [u_1, \quad , u_m]'$ is the vector of manipulated inputs, taking values in a compact and convex subset, $\mathcal{U}$, of $\mathbb{R}^m$ that contains the origin in its interior. The matrices A, B and C are constant $n \quad n$, $n \quad m$ and $k \quad n$ matrices, respectively. The pairs (A, B) and (C, A) are assumed to be controllable and observable, respectively. Throughout the paper, the notation x' denotes the transpose of x.

2.1 *State observer design*

For the system of Eq.1, we use a standard Luenberger observer described by

$$\dot{\hat{x}} = A\hat{x} + Bu + L(y \quad C\hat{x}) \tag{2}$$

where $\hat{x} = [\hat{x}_1, \quad , \hat{x}_n]' \in \mathbb{R}^n$ denotes the vector of estimates of the state variables, L is a constant $n \quad k$ matrix chosen such that the eigenvalues of $A \quad LC$ are placed at $\quad a_1, \quad a_2 ... \quad a_n$ with $\quad 1$ and $a_i \neq a_j \quad 1$. In the closed loop system, the estimation error, de ned as $e = x \quad \hat{x}$, evolves independently of the controller according to $\dot{e} = (A \quad LC)e$

Note that the dynamics of the error equation can be manipulated at will by appropriate choice of the design parameters a_i and . This state estimator design guarantees convergence of the error in a way that for larger values of the parameter , the error decreases faster (i.e., given any $e_m > 0$, one can nd a T_d such that $\|e(t)\| \quad e_m \ \forall \ t \quad T_d$). However, for larger values of , the error could possibly increase to large values before eventually decaying. The design, therefore, includes the possibility of peaking of state estimates, where the observer generates incorrect estimates for short times. This, however, does not pose a problem in our design because the physical constraints on the manipulated input prevent transmission of the incorrect estimates to the plant.

2.2 *Model predictive control*

For the sake of illustration, we consider here the following nominally-stabilizing nite-horizon MPC formulation with terminal equality constraints:

$$\begin{aligned} J_s(x, t, u(\ )) &= \int_t^{t+T} (x'(s)Qx(s) + u'(s)Ru(s))ds \\ u(\ ) &= argmin\{J_s(x, t, u(\ ))|u(\ ) \in S\} \\ s.t. \quad \dot{x}(t) &= Ax(t) + Bu(t), \quad x(0) = x_0 \\ u(\ ) &\in S, \quad x(t+T) = 0 \end{aligned} \tag{3}$$

where $S = S(t, T)$ is the family of piecewise continuous functions, with period , mapping $[t, t+T]$ into the set of admissible controls, where T is the horizon length. A control $u(\ )$ in S is characterized by the sequence $\{u[k]\}$ where $u[k] := u(k \quad)$. A control $u(\ )$ in S satisfies $u(t) = u[k]$ for all $t \in [k \quad , (k+1) \quad)$. J_s is the performance index and R and Q are strictly positive de nite, symmetric matrices. Feasibility of the formulation in Eq.3 can be ensured by relaxing the terminal equality constraint; however, closed loop stability then cannot be guaranteed.

One of the issues that arise in the implementation of MPC formulations of the form of Eq.3 is the dif - culty in obtaining an explicit characterization of the stability region, which depends on a complex interplay between several factors, including the constraints, the initial condition, and the horizon length. Faced with these dif culties, the current industrial implementation of MPC relies heavily on extensive simulations to test the stability of MPC controllers.

2.3 *Bounded Lyapunov-based control*

Consider the Lyapunov function candidate $V = x'Px$, where P is a positive-de nite symmetric matrix that satis es the Riccati equation

$$A'P + PA \quad PBB'P = \quad Q \tag{4}$$

for some positive-de nite matrix Q. Using this Lyapunov function, we can construct, using a modi cation of Sontag's formula for bounded controls proposed in (Lin and Sontag, 1991) (see also (El-Farra and Christo des, 2003)), the following bounded nonlinear controller

$$u(x) = \quad 2k(x)B'Px \ := \ b(x) \tag{5}$$

where $k(x) =$

$$\left(\frac{L_f V + \sqrt{\left(L_f V\right)^2 + \left(u_{max}\|(L_g V)'\|\right)^4}}{\|(L_g V)'\|^2 \quad 1 + \sqrt{1 + \left(u_{max}\|(L_g V)'\|\right)^2}} \right)$$

with $L_f V = x'(A'P + PA)x + \quad x'Px$, $(L_g V)' = 2B'Px$, $\quad > 0$. One can show that whenever the closed-loop state trajectory evolves within the state space region described by the set:

$$(u_{max}) = \{x \in \mathbb{R}^n : L_f V \quad u_{max}\|(L_g V)'\|\} \tag{6}$$

the resulting control action respects the constraints (i.e., $\|u\| \quad u_{max}$) and asymptotically stabilizes the origin of the closed-loop system. Note that the size of the set depends on the magnitude of the constraints in a way such that the tighter the constraints, the smaller the region described by this set. Using this set, an estimate of the stability region of the controller of Eqs.5 6 can be obtained by considering an invariant subset of , preferably the largest, which we denote by (u_{max}). A common way of doing this is using the level sets of V.

Using Lyapunov arguments, one can derive bounds on the estimation errors (e_m), with respect to which

the state feedback bounded controller ensures that the closed loop state trajectory does not escape the state feedback stability region (see Figure 3). By initializing the states and the state estimates suf ciently inside (u_{max}) and choosing a consistent observer gain matrix L, one can ensure that the norm of the estimation error decays to a value less than the tolerable measurement error before the states have a chance to reach the boundary of the state feedback stability region. For a given choice of $_b$ (u_{max}), therefore, one can choose a value for the observer gain parameter that guarantees stability for all initial conditions within $_b$ under output feedback control.

3. IMPLEMENTING OUTPUT FEEDBACK MPC WITH GUARANTEED STABILITY REGION

While the bounded controller possesses a well-de ned region of initial conditions that guarantee closed-loop stability in the presence of constraints, the performance of this controller is not guaranteed to be optimal with respect to an arbitrary performance criterion. On the other hand, the MPC controller is well-suited for handling constraints within an optimal control setting; however, the analytical characterization of its set of initial conditions, for which closed loop stability is guaranteed, is a more dif cult task than it is through bounded control. The lack of state measurements introduces another level of complexity in implementing the controllers designed with the assumption of state feedback. In this section, we show how to reconcile the two control approaches by means of a switching scheme that combines the desirable properties of both approaches.

3.1 *Problem formulation and overview of solution*

Consider the linear time-invariant system of Eq.1, subject to input constraints $\|u\|$ u_{max}, and for which the observer of Eq.2, the bounded controller of Eqs.5-6 and the MPC controller of Eq.3 have been designed. We formulate the control problem as that of designing a set of switching laws that orchestrate the transition between the MPC controller and the bounded controller under output feedback in a way that guarantees asymptotic stability of the origin of the closed-loop system starting from any initial condition in an explicitly characterized set $_b$ (u_{max}), respects input constraints, and accommodates the optimality requirements whenever possible. In the remainder of this section, we present a switching scheme that addresses the problem.

3.2 *Controller switching scheme*

The four main components of the hybrid control structure include the observer, the bounded controller, the MPC controller, and a higher-level supervisor that orchestrates the switching between the two controllers. A schematic representation of this structure is shown in Figure 2. The design procedure for the hybrid control structure and the implementation of the controller switching scheme is as follows:

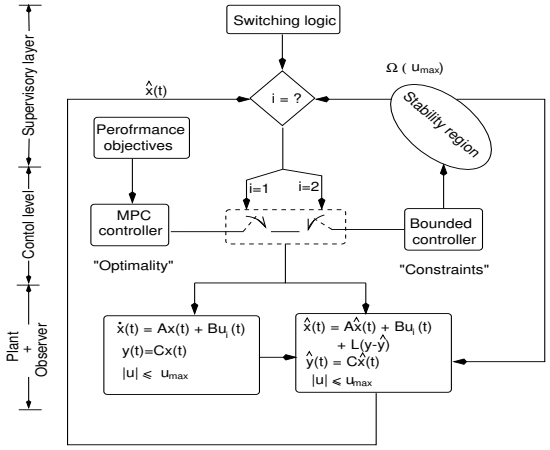

Fig. 2. A schematic representation of the hierarchical hybrid control structure merging the bounded and MPC controllers under output feedback

(1) Given the system of Eq.1 and the performance objective, design the bounded controller and the MPC controller.
(2) Compute the stability region estimate for the bounded controller under state feedback, (u_{max}), using Eq.6 and, for the state observer design, choose a consistent with the choice of the output feedback stability region $_b$.
(3) Compute the region $_s$ $_b$ and T_d such that if the norm of the error is less than a given tolerance, then $\hat{x} \in$ $_s \Rightarrow x \in$ $_b$ for all times greater than T_d.
(4) Initialize the closed loop system at an initial condition, $x(0)$ within $_b$, under the bounded controller using an initial guess for the state $\hat{x}(0)$ within $_b$.
(5) After a time T_d, once $\hat{x} \in$ $_s$, test the feasibility of the MPC controller using values of the estimates generated by the state observer.
(6) If the MPC controller is feasible, implement it for as long as $\hat{x} \in$ $_s$ and $V(\hat{x})$ keeps decaying, else switch to the bounded controller.

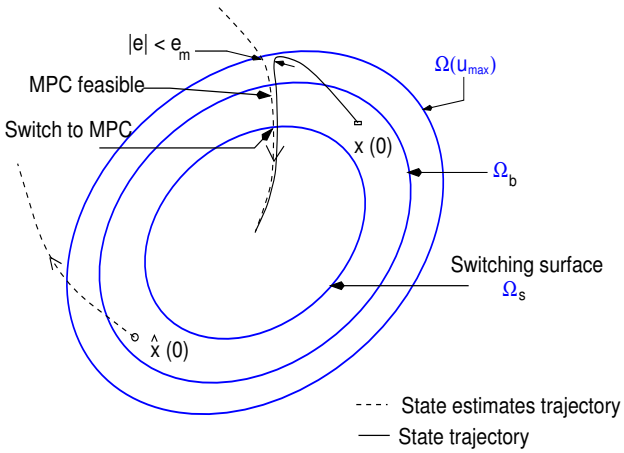

Fig. 3. A schematic representation of the implementation of the proposed controller switching scheme.

Remark 1: Figure 3 shows a representative sketch of the closed loop system under the controller switch-

ing scheme. The states are initialized at x_0 while the state estimates are initialized at $\hat{x}_0$. The state estimator design ensures that the norm of the error is under the allowable error before (and if) the state trajectory reaches the boundary of the state feedback stability region, (u_{max}). After a time T_d (by which time, the state estimator design ensures that the estimation error has gone down to a small value), the supervisor implements MPC in closed loop only if it is feasible *and* the state estimates are in $_s$, while monitoring the evolution of the Lyapunov function value. If the switching rules are satis ed, MPC is implemented in closed loop for the remaining time, else the supervisor switches back to the bounded controller to stabilize the closed loop system.

Remark 2: For a given choice of the output feedback stability region, an estimate of the necessary observer gain can be obtained; however, this estimate is typically conservative. In practice, having chosen $_s$, one can choose a 'suf ciently' large gain based on simulations or experience. The stability region under output feedback $_b$ can be made as close to the one under state feedback, as desired by increasing the gain parameter .

4. A NUMERICAL EXAMPLE

In this section, we demonstrate an application of the proposed hybrid control structure to a three dimensional linear system where only two of the states are measured. Speci cally, we consider an exponentially unstable linear system of the form of Eq.1 with $A = \begin{bmatrix} 0.55 & 0.15 & 0.05 \\ 0.15 & 0.40 & 0.20 \\ 0.10 & 0.15 & 0.45 \end{bmatrix}$, $B = \begin{bmatrix} 1 & 0 \\ 0 & 1 \\ 1 & 1 \end{bmatrix}$ and $C = \begin{matrix} 1 & 0 & 0 \\ 0 & 0 & 1 \end{matrix}$, where both inputs u_1, u_2 are constrained in the interval $[\ \ 1, 1]$. We initially used Eqs.5 to design a bounded controller and construct its stability region via Eq.6. The matrix P was chosen as:

$$P = \begin{bmatrix} 6.5843 & 4.2398 & 3.830 \\ 4.2398 & 3.6091 & 2.667 \\ 3.830 & 2.667 & 2.8033 \end{bmatrix} \qquad (7)$$

and the observer gain parameter was chosen to be $= 500$ to ensure closed loop stability for all initial conditions within $_b$. For the MPC controller, the parameters in the objective function of Eq.3 were chosen as $Q = qI$, with $q = 1$ and $R = rI$, with $r = 0.1$. We also chose a horizon length of $T = 1.5$ in implementing the MPC controller of Eq.3. The resulting quadratic program was solved using the MATLAB subroutine QuadProg, and the set of ODEs integrated using the MATLAB solver ODE45.

In the rst simulation run (solid lines in Figs.4 5), the states were initialized at $x_0 = [0.75 \quad 0.5 \quad 1.0]'$ while the observer states were initialized at $\hat{x}_0 = [0 \quad 0 \quad 0]'$ (which belong to the stability region of the bounded controller, $_b$). The supervisor employs the bounded controller, while continuously checking MPC feasibility. At $t = 5.45$, the MPC becomes feasible and is implemented in the closed-loop to stabilize the system. Note that feasibility of MPC can be achieved by increasing the horizon length to $T = 3.5$ (dashed lines in Figs.4 5). However, this conclusion could not be reached *a priori*, i.e. before running the closed-loop simulation in its entirety to check whether the choice $T = 3.5$ is appropriate. In contrast, closed loop stability starting from the given initial condition under the proposed hybrid control structure is guaranteed.

In the second set of simulation results, we demonstrate the need for a choice of observer gain consistent with the choice of $_b$. To this end, we consider now an observer design with a low gain ($= 0.5$). With the low observer gain, the estimates take a long time to converge to the true state values, resulting in the implementation of 'incorrect' control action, by which time, even though the states and state estimates are initiated within $_b$, the states have escaped (u_{max}), thereby resulting in closed loop instability (dotted lines in Figs.4 5).

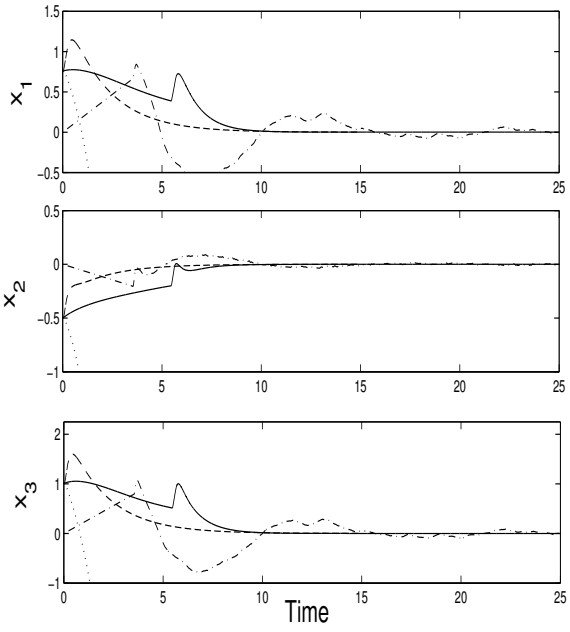

Fig. 4. Closed-loop state trajectory with $T = 1.5$ (solid line), $T = 3.5$ (dashed line), with the low observer gain (dotted line) and using observer switching (dash-dotted lines).

To recover, as closely as possible, the state feedback stability region, large values of the observer gain are needed. However, it is well known that high observer gains can amplify measurement noise and induce poor performance. This points to a fundamental tradeoff that cannot be resolved by simply changing the estimation scheme. For example, if the observer gain consistent with the choice of the output feedback stability region is abandoned, the noise problem may disappear, but then stability cannot be guaranteed. One approach to avoid this scenario in practice is to initially use an observer gain to ensure quick decay of the

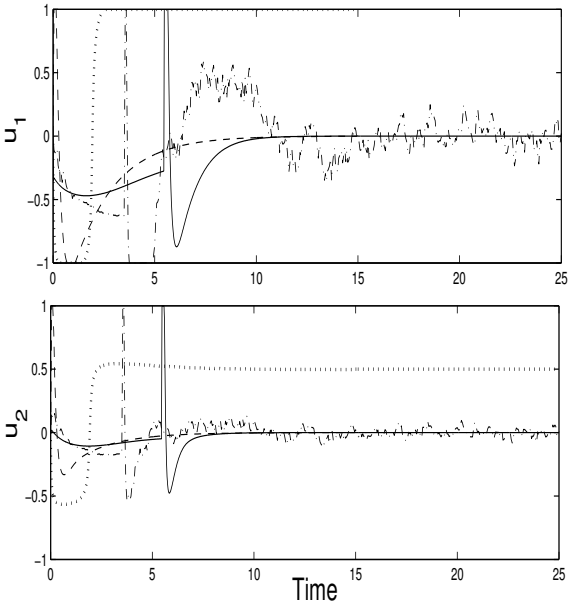

Fig. 5. Manipulated input trajectory with $T = 1.5$ (solid line), $T = 3.5$ (dashed line), with the low observer gain (dotted line) and using observer switching (dash-dotted lines).

initial estimation error, and then to switch to a low" observer gain. In the following simulation, we show how switching between an observer with a high gain and a low gain in conjunction with switching between controllers can be used to mitigate the undesirable effects of measurement noise. To illustrate the point, we use switching between the high and low observer gains used in the rst two simulation runs and demonstrate the attenuation of noise.

Speci cally, we consider the nominal system described by Eq.1, together with model uncertainty and measurement noise. The model matrix A_m is assumed to be within ve percent error of the process matrix A and the sensors are assumed to introduce noise in the measured outputs as $y(t) = Cx(t) + (t)$ where (t) is a random gaussian noise with zero mean and a variance of 0.01. As seen by the dash-dotted lines in Fig.4, starting from the initial condition, $x_0 = [0.75 \; 0.5 \; 1.0]'$, using a high observer gain followed by a switch to the low gain observer at $t = 1.0$, and a switch from bounded control to MPC at $t = 3.5$, the supervisor is still able to preserve closed loop stability, while at the same time resulting in a smooth enough control action (see Fig.5).

5. REFERENCES

Allgower, F. and H. Chen (1998). Nonlinear model predictive control schemes with guaranteed stability. In: R. Berber and C. Kravaris (Eds.), *NATO ASI on Nonlinear Model Based Process Control*. Dordrecht: Kluwer. pp. 465 494.

Aufderheide, B., V. Prasad and B. W. Bequette (2001). A comparison of fundamental model-based and multiple model predictive control. In: *Proceedings of 40th IEEE Conference on Decision and Control*. Orlando, FL. pp. 4863 4868.

Banerjee, A. and Y. Arkun (1998). Model predictive control of plant transitions using a new identification technique for interpolating nonlinear models. *J. of Process Contr.* **8**, 441 457.

El-Farra, N. H. and P. D. Christofides (2001). Integrating robustness, optimality and constraints in control of nonlinear processes. *Chem. Eng. Sci.* **56**, 1841 1868.

El-Farra, N. H. and P. D. Christo des (2003). Bounded robust control of constrained multivariabe nonlinear processes. *Chem. Eng. Sci.,* to appear.

El-Farra, N. H., P. Mhaskar and P. D. Christo des (2002). Uniting bounded control and MPC for stabilization of constrained linear systems, accepted. *Automatica*.

El-Farra, N. H., P. Mhaskar and P. D. Christo des (2003*a*). Hybrid control: A paradigm for implementing predictive control to nonlinear systems with guaranteed stability regions. In: *Proceedings of American Control Conference*. Denver, CO.

El-Farra, N. H., P. Mhaskar and P. D. Christo des (2003*b*). Hybrid control of uncertain process systems. In: *8th International Symposium on Process Systems and Engineering*. Kumming, P.R. China.

Lin, Y. and E. D. Sontag (1991). A universal formula for stabilization with bounded controls. *Syst. & Contr. Lett.* **16**, 393 397.

Mayne, D. Q., J. B. Rawlings, C. V. Rao and P. O. M. Scokaert (2000). Constrained model predictive control: Stability and optimality. *Automatica* **36**, 789 814.

Mhaskar, P., N. H. El-Farra and P. D. Christo des (2003). Hybrid predictive control of process systems, in preperation.

Michalska, H. and D. Q. Mayne (1995). Moving horizon observers and observer-based control. *IEEE Trans. Automat. Contr.* **40**, 995 1006.

Rao, C. V. and J. B. Rawlings (2002). Constrained process monitoring: Moving-horizon approach. *AIChE Journal* **48**, 97 109.

Rawlings, J. B. and K. R. Muske (1993). The stability of constrained receding horizon control. *IEEE Trans. Automat. Contr.* **38**, 1512 1516.

Rugh, W. J. and J. S. Shamma (2000). Research on gain scheduling. *Automatica* **36**, 1401 1425.

Shamma, J. S. and K. Tu (1998). Output feedback control for systems with constraints and saturations: Scalar control case. *Syst. & Contr. Lett.* **25**, 1 11.

Sun, D. and K. A. Hoo (1999). Dynamic transition control structure for a class of SISO nonlinear systems. *IEEE Trans. Contr. Syst. Tech.* **7**, 622 629.

Teel, A. (1992). Global stabilization and restricted tracking for multiple integrators with bounded controls. *Syst. & Contr. Lett.* **18**, 165 171.

AN INTERNAL MODEL CONTROL FOR MAX-PLUS LINEAR SYSTEMS WITH LINEAR PARAMETER VARYING STRUCTURE

Shiro Masuda * **Hiroyuki Goto** ** **Takashi Amemiya** *
Kazuhiro Takeyasu **

* *Dep. of Production,Information and Systems Engineering, Tokyo Metropolitan Institute of Technology,*
6-6, Asahigaoka, Hino, Tokyo, Japan, 191-0065, smasuda@cc.tmit.ac.jp
** *The Japan Research Institute, Limited; 16 Ichiban-cho, Chiyoda-ku, Tokyo 102-0082, JAPAN*

Abstract. The max-plus-linear (MPL) system is a state-space description for a certain class of discrete-event-systems, and it has remarkable analogous features to the conventional linear state-space description in the modern control theory. Hence, several control techniques in the modern control theory have been extended so that they could be applied to MPL systems. In the research context, the internal model control (IMC) for MPL systems has been proposed by Boimond et al. and it succeeds to realize feedback control techniques for discrete-event-systems described in MPL systems. In this paper, the IMC control for MPL systems is extended to the case where the controlled systems are given as MPL systems with linear parameter varying structure, which is called LPV-MPL systems. In the LPV-MPL systems, the systems parameters are explicitly represented in the systems description. Hence, the obtained IMC control law can utilize the additive information on the parameters variations effectively when the parameters are measured on-line, or the variation of the parameters are scheduled beforehand. The effectiveness of the proposed IMC is shown through a numerical example where it is applied to a two-inputs, two-outpus production system with four machines.

Keywords. max-plus-linear systems, linear parameter varying, internal model control, discrete-event-systems

1. INTRODUCTION

The researches on modeling and control of discrete-event-systems using max-plus algebra have been reported recently(Cohen *et al.*, 1989; Baccelli *et al.*, 1992). The basic operations of max-plus algebra are maximization and addition, which have a remarkable analogy with ones of conventional algebra. Especially, state-space descriptions in the max-plus algebra for a certain class of discrete-event-systems become linear representations which are similar to state-space equations in the traditional modern control theory (van den Boom and Schutter, 2001*a*). Hence, the several researches on control design for the max-plus-linear (MPL) systems have been reported from the viewpoint of the analogy (Boimond and Ferrier, 1996; van den Boom and Schutter, 2001*a*; van den Boom and Schutter, 2001*b*).

The internal model control (IMC) for MPL systems has been proposed by (Boimond and Ferrier, 1996) in the research context. It succeeds to realize feedback control techniques for discrete-event-systems described in MPL systems. In the IMC control, however, it takes much time to recover from the output delays because the input signals are modified just after the output errors are observed. Hence, it would be desirable that the information on the parameters variation would be

collected beforehand, and it could be utilized effectively.

On the other hand, the MPL systems with linear parameter varying structure, which is called LPV-MPL systems was proposed, and the design method for inverse systems of LPV-MPL systems was developed (Masuda *et al.*, 2002). In the LPV-MPL systems, the systems parameters are explicitly represented. Hence, the obtained control law can utilize the additive information on the parameters variations effectively when the parameters are measured on-line, or the variation of the parameters are scheduled beforehand.

Therefore, in this paper, the IMC control is extended so that it can be applied to the LPV-MPL systems. In the proposed control law, the information on the parameters variations in addition to the feedback signals are effectively utilized for recovery from the output delays due to large parameters variation. Furthermore, owing to the IMC control law, the proposed method has robust property even when the the information on the parameters variations has some errors.

The effectiveness of the proposed IMC is shown through a numerical example where it is applied to a two-inputs, two-outpus production system with four machines.

2. MATHEMATICAL PRELIMINARIES

The basic operations of max-plus algebra are addition denoted by $\oplus$ and mulitiplication denoted by $\otimes$, which are defined as follows.

$$x \oplus y = \max(x, y), \quad x \otimes y = x + y, \quad x, y \in \boldsymbol{R}_\varepsilon$$

where $\boldsymbol{R}_\varepsilon = \boldsymbol{R} \cup \{-\infty\}$, and $\boldsymbol{R}$ stands for the real field. Let ε be defined as $-\infty$, which is the unit element of the addition $\oplus$, and let e be defined as 0, which is the unit element of the multiplication $\otimes$. We also define the following operations.

$$x \wedge y = \min(x, y), \quad x \backslash y = -x + y \tag{1}$$

The above operations are extended to the matrices calculation whose elements belong to $\boldsymbol{R}_\varepsilon$. So, if $\boldsymbol{A}, \boldsymbol{B} \in \boldsymbol{R}_\varepsilon^{m \times n}$, $\boldsymbol{C} \in \boldsymbol{R}_\varepsilon^{n \times p}$, then

$$[\boldsymbol{A} \oplus \boldsymbol{B}]_{ij} = [\boldsymbol{A}]_{ij} \oplus [\boldsymbol{B}]_{ij} = \max\left([\boldsymbol{A}]_{ij},\ [\boldsymbol{B}]_{ij}\right) \tag{2}$$

$$[\boldsymbol{A} \wedge \boldsymbol{B}]_{ij} = [\boldsymbol{A}]_{ij} \wedge [\boldsymbol{B}]_{ij} = \min\left([\boldsymbol{A}]_{ij},\ [\boldsymbol{B}]_{ij}\right) \tag{3}$$

$$1 \le i \le n, \quad 1 \le j \le m$$

$$[\boldsymbol{A} \otimes \boldsymbol{C}]_{ij} = \bigoplus_{k=1}^{n} \left([\boldsymbol{A}]_{ik} \otimes [\boldsymbol{C}]_{kj}\right) = \max_{k=1,\cdots,n} \left([\boldsymbol{A}]_{ik} + [\boldsymbol{C}]_{kj}\right) \tag{4}$$

where $[\ \cdot\ ]_{ij}$ stands for the element in the i-th row, j-th column of the matrix, and

$$\bigoplus_{k=1}^{n} a_k = \max(a_1, a_2, \cdots, a_n)$$

. If $d \in \boldsymbol{R}_\varepsilon$, $\boldsymbol{A} \in \boldsymbol{R}_\varepsilon^{m \times n}$, then

$$[d \otimes \boldsymbol{A}]_{ij} = d \otimes [\boldsymbol{A}]_{ij} \tag{5}$$

Furthermore, we define the operator $\odot$ in the following way.

$$[\boldsymbol{A} \odot \boldsymbol{C}]_{ij} = \bigwedge_{k=1}^{n} \left([\boldsymbol{A}]_{ik} \backslash [\boldsymbol{C}]_{kj}\right) = \min_{k=1,\cdots,n} \left(-[\boldsymbol{A}]_{ik} + [\boldsymbol{C}]_{kj}\right) \tag{6}$$

where

$$\bigwedge_{k=1}^{n} a_k = \min(a_1, a_2, \cdots, a_n)$$

. In the subsequent discussions, $\boldsymbol{a} \le \boldsymbol{b}$ implies $[\boldsymbol{a}]_i \le [\boldsymbol{b}]_i$ $1 \le i \le n$ for $\boldsymbol{a},\ \boldsymbol{b} \in \boldsymbol{R}_\varepsilon^n$.

3. THE LPV-MPL SYSTEM

Consider the following MPL systems.

$$\boldsymbol{x}(k+1) = \boldsymbol{A}\boldsymbol{x}(k) \oplus \boldsymbol{B}\boldsymbol{u}(k+1) \tag{7}$$

$$\boldsymbol{y}(k) = \boldsymbol{C}\boldsymbol{x}(k) \tag{8}$$

where $\boldsymbol{A} \in \boldsymbol{R}_\varepsilon^{n \times n}$, $\boldsymbol{B} \in \boldsymbol{R}_\varepsilon^{n \times p}$, $\boldsymbol{C} \in \boldsymbol{R}_\varepsilon^{q \times n}$. And $\boldsymbol{x}(k) \in \boldsymbol{R}_\varepsilon^n$, $\boldsymbol{u}(k+1) \in \boldsymbol{R}_\varepsilon{}^p$, $\boldsymbol{y}(k) \in \boldsymbol{R}_\varepsilon^q$ are state variables, control inputs and controlled outputs respectively. These variables represent time instants at which the representing events occur at k-times. According to the custom, the operation of multiplication denoted by $\otimes$ is omitted.

In LPV-MPL systems(Masuda *et al.*, 2002), the system matrices $\boldsymbol{A}$, $\boldsymbol{B}$ and $\boldsymbol{C}$ in (7) and (8) are replaced by the parameter affine form $\boldsymbol{A}(\boldsymbol{d})$, $\boldsymbol{B}(\boldsymbol{d})$ and $\boldsymbol{C}(\boldsymbol{d})$, which are defined as

$$\boldsymbol{A}(\boldsymbol{d}) = d_0\boldsymbol{A}_0 \oplus d_1\boldsymbol{A}_1 \oplus \cdots \oplus d_l\boldsymbol{A}_l = \bigoplus_{i=0}^{l} d_i\boldsymbol{A}_i$$

$$\boldsymbol{B}(\boldsymbol{d}) = d_0\boldsymbol{B}_0 \oplus d_1\boldsymbol{B}_1 \oplus \cdots \oplus d_l\boldsymbol{B}_l = \bigoplus_{i=0}^{l} d_i\boldsymbol{B}_i$$

$$\boldsymbol{C}(\boldsymbol{d}) = d_0\boldsymbol{C}_0 \oplus d_1\boldsymbol{C}_1 \oplus \cdots \oplus d_l\boldsymbol{C}_l = \bigoplus_{i=0}^{l} d_i\boldsymbol{C}_i$$

where $\boldsymbol{A}_i$, $\boldsymbol{B}_i$ and $\boldsymbol{C}_i$,$i = 1, \cdots l$ are matrices whose elements are either ε or e and the size are the same as $\boldsymbol{A}$, $\boldsymbol{B}$ and $\boldsymbol{C}$, respectively, and $\boldsymbol{d}$ is the parameter vector whose elements are $d_0, d_1, \cdots, d_l$ as is defined in the next.

$$\boldsymbol{d} = [d_0,\ d_1,\ d_2,\ \cdots,\ d_l], \quad d_0 = e,\ \ d_i > 0,\ i = 1, \cdots l$$

Hence, the LPV-MPL system can be described as

$$\boldsymbol{x}(k+1) = \boldsymbol{A}(\boldsymbol{d})\boldsymbol{x}(k) \oplus \boldsymbol{B}(\boldsymbol{d})\boldsymbol{u}(k+1) \quad (9)$$

$$\boldsymbol{y}(k) = \boldsymbol{C}(\boldsymbol{d})\boldsymbol{x}(k) \quad (10)$$

In general, the elements of the matrices $\boldsymbol{A}$, $\boldsymbol{B}$ and $\boldsymbol{C}$ in the system representation consists of e and ε and real numbers. The elements of e and ε depend on the system structure such as the connection among the machines in the case where the production systems are modelled based on the MPL system. While parameters e and ε are expected to be unchanged even as time goes by, it should be considered that the real parameters might be the varying ones.

4. THE INTERNAL MODEL CONTROL (IMC)

The internal model control (IMC), which is a popular control technique in the field of chemical industries. The block diagram is given in Figure 1..

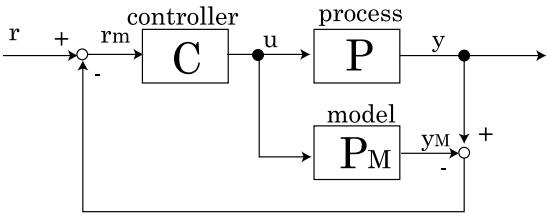

Fig. 1. The Block Diagram of IMC

In Figure 1., P stands for the real process, and P_M stands for the process model. y and y_M are the controlled process outputs and the model outputs, respectively. u and r are control input and reference signals, respectively. r_M is modified reference signals, which satisfy the following equation

$$r_M = r - (y - y_M) \quad (11)$$

Hence, if the control input is designed so that the model outputs y_M should be equal to the modified reference signals r_M, the controlled process outputs follow the given reference signals. Therefore, by using the inverse systems of the model P_M for the controller C in the IMC, we can get robust tracking of the process outputs to the reference signals even in the presence of model-plant mismatch.

Addition to the IMC control, this paper considers utilizing additive information on the parameter variation of the controlled process, depected in Figure 2.

In Figure 1., θ stands for the parameters of process model. In the conventional IMC control, it

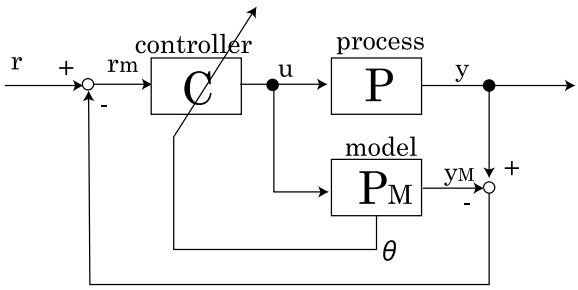

Fig. 2. The Block Diagram of the Proposed IMC

takes much time to recover from the output delays because the input signals are modified just after the output errors are observed. On the other hand, in the proposed IMC, it can be expected that we can get better performance because the information on the parameters variation would be utilized effectively.

However, the conventional controller requires recalculation of the inverse system of the MPL system according as the parameters changes because the relation between controller's parameters and the MPL system's parameters is not represented explicitly. Therefore, this paper utilizes the inverse system of LPV-MPL systems (Masuda *et al.*, 2002). Since the system's parameters are explicitly represented in the LPV-MPL systems, the additive information on the parameters variations can be utilized effectively when the parameters are measured on-line, or the variation of the parameters are scheduled beforehand.

5. THE INVERSE SYSTEM FOR LPV-MPL

As is shown in **4.**, the controller of IMC systems is designed for the model, so we will give the model equation of LPV-MPL system besides the real process model (9) and (10).

$$\boldsymbol{x}_M(k+1) = \boldsymbol{A}_M(\boldsymbol{d}_M)\boldsymbol{x}_M(k) \oplus \boldsymbol{B}_M(\boldsymbol{d}_M)\boldsymbol{u}(k+1) \quad (12)$$

$$\boldsymbol{y}_M(k) = \boldsymbol{C}_M(\boldsymbol{d}_M)\boldsymbol{x}_M(k) \quad (13)$$

This section gives the inverse system for the model equation of LPV-MPL system (Masuda *et al.*, 2002) in (12) and (13).

The first, let the predition equation be derived for the preparation of the inverse system. By using (9) and (10), we can get

$$\begin{bmatrix} y_{M1}(k+\delta_1+1) \\ \vdots \\ y_{Mq}(k+\delta_q+1) \end{bmatrix} = \boldsymbol{\Gamma}_M(\boldsymbol{d}_M)\boldsymbol{x}_M(k) \oplus \boldsymbol{\Delta}_M(\boldsymbol{d}_M)\boldsymbol{u}(k+1) \quad (14)$$

where

$$\boldsymbol{\Gamma}_M(\boldsymbol{d}_M) = \begin{bmatrix} \boldsymbol{c}_M^1(\boldsymbol{d}_M)\boldsymbol{A}_M(\boldsymbol{d}_M)^{\delta_1+1} \\ \vdots \\ \boldsymbol{c}_M^q(\boldsymbol{d}_M)\boldsymbol{A}_M(\boldsymbol{d}_M)^{\delta_q+1} \end{bmatrix}, \quad (15)$$

$$\boldsymbol{\Delta}_M(\boldsymbol{d}_M) = \begin{bmatrix} \boldsymbol{c}_M^1(\boldsymbol{d})\boldsymbol{A}_M(\boldsymbol{d}_M)^{\delta_1}\boldsymbol{B}_M(\boldsymbol{d}_M) \\ \vdots \\ \boldsymbol{c}_M^q(\boldsymbol{d}_M)\boldsymbol{A}_M(\boldsymbol{d}_M)^{\delta_q}\boldsymbol{B}_M(\boldsymbol{d}_M) \end{bmatrix} \quad (16)$$

$\boldsymbol{c}_M^h(\boldsymbol{d}_M),\ h = 1\cdots q$ is the h-th row vector of $\boldsymbol{C}_M(\boldsymbol{d}_M)$. δ_h are called the characteristic numbers (Boimond and Ferrier, 1996), which imply that δ_h-th outputs are firstly influenced after the k-th input, and they are defined as:

$$\boldsymbol{\varepsilon} = \boldsymbol{c}_M^h(\boldsymbol{d}_M)\boldsymbol{B}_M(\boldsymbol{d}_M) = \boldsymbol{c}_M^h(\boldsymbol{d}_M)\boldsymbol{A}_M(\boldsymbol{d}_M)\boldsymbol{B}_M(\boldsymbol{d}_M)$$
$$= \cdots = \boldsymbol{c}_M^h(\boldsymbol{d}_M)\boldsymbol{A}_M(\boldsymbol{d}_M)^{\delta_h-1}\boldsymbol{B}_M(\boldsymbol{d}_M) \quad (17)$$
$$\boldsymbol{\varepsilon} \neq \boldsymbol{c}_M^h(\boldsymbol{d}_M)\boldsymbol{A}_M(\boldsymbol{d}_M)^{\delta_h}\boldsymbol{B}_M(\boldsymbol{d}_M), \quad h = 1, \cdots q \quad (18)$$

$\boldsymbol{\varepsilon}$ is the vector whose elements are ε. When the desired reference signals are defined as

$$\boldsymbol{r}(k) = [r_1(k+\delta_1+1), \cdots, r_q(k+\delta_q+1)]^{\mathrm{T}},$$

it is considered that the control law for the inverse system should be satisfied with the following equation replaced the predicted output vector in (14) with the desired reference signals.

$$\boldsymbol{r}(k) = \boldsymbol{\Gamma}_M(\boldsymbol{d}_M)\boldsymbol{x}_M(k) \oplus \boldsymbol{\Delta}_M(\boldsymbol{d}_M)\boldsymbol{u}(k+1) \quad (19)$$

(19) is considered to be a linear matrix equation in max-plus algebra. Hence, let the equation be solved based on the linear equation theory in dioid(Cohen *et al.*, 1989). According to the theory, after (19) is transformed into

$$\boldsymbol{\Delta}_M(\boldsymbol{d}_M)\boldsymbol{u}(k+1) = \boldsymbol{r}(k) \oplus \boldsymbol{\Gamma}_M(\boldsymbol{d}_M)\boldsymbol{x}_M(k) \quad (20)$$

the greatest subsolution of (20) is calculated. In (Masuda *et al.*, 2002), the following control law is introuduced for the inverse systems of LPV-MPL systems.

$$\boldsymbol{u}(k+1) = \bigwedge_{i=1}^{I} \left\{ \boldsymbol{\Delta}_i^{\mathrm{T}}\boldsymbol{N}_i(\boldsymbol{d}_M) \right.$$
$$\left. \odot \left(\boldsymbol{r}(k) \oplus \bigoplus_{i=1}^{I} (\boldsymbol{M}_i(\boldsymbol{d}_M)\boldsymbol{\Gamma}_i)\boldsymbol{x}_M(k) \right) \right\} \quad (21)$$

Here,

$$\boldsymbol{\Gamma}_M(\boldsymbol{d}_M) = \bigoplus_{i=1}^{I} (\boldsymbol{M}_i(\boldsymbol{d}_M)\boldsymbol{\Gamma}_i) \quad (22)$$

$$\boldsymbol{\Delta}_M(\boldsymbol{d}_M) = \bigoplus_{i=1}^{I} (\boldsymbol{N}_i(\boldsymbol{d}_M)\boldsymbol{\Delta}_i) \quad (23)$$

where $I = (l+1)^{\bar{\delta}+2}$, $\bar{\delta} = \max_h\ \delta_h$ $\boldsymbol{\Gamma}_i$ and $\boldsymbol{\Delta}_i, i = 1, \cdots I$ are matrices whose elements are all ε and e. The size of $\boldsymbol{\Gamma}_i$ and $\boldsymbol{\Delta}_i, i = 1, \cdots I$ are the same as $\boldsymbol{\Gamma}$ and $\boldsymbol{\Delta}$, respectively. $\boldsymbol{M}_i(\boldsymbol{d})$ and $\boldsymbol{N}_i(\boldsymbol{d})$ are diagonal matrices.

Therefore, the control law for the proposed IMC can be obtained as

$$\boldsymbol{u}(k+1) = \bigwedge_{i=1}^{I} \left\{ \boldsymbol{\Delta}_i^{\mathrm{T}}\boldsymbol{N}_i(\boldsymbol{d}_M) \right.$$
$$\left. \odot \left(\boldsymbol{r}_M(k) \oplus \bigoplus_{i=1}^{I} (\boldsymbol{M}_i(\boldsymbol{d}_M)\boldsymbol{\Gamma}_i)\boldsymbol{x}_M(k) \right) \right\} \quad (24)$$

$$\boldsymbol{r}_M(k) = \boldsymbol{r}(k) - (\boldsymbol{y}(k) - \boldsymbol{y}_M(k)) \quad (25)$$

where $\boldsymbol{r}_M(k)$ is the modified reference signals.

The main feature of the control law (24) is that it explicitly includes the parameters of controlled MPL systems as free parameters. Hence, when the parameters are measured on-line, or the variation of the parameters are scheduled beforehand, the proposed control law can utilize the additive information on the parameters variations effectively.

6. A SIMULATION EXAMPLE

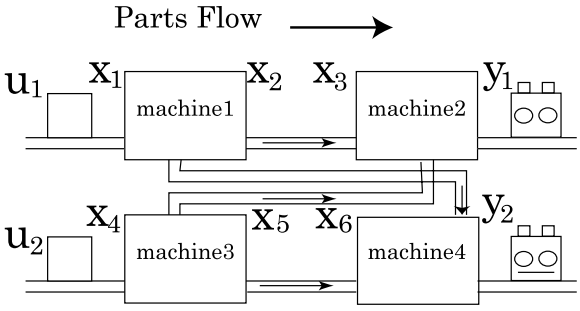

Fig. 3. Two-Inputs and Two-Outputs Production System

Consider a two-inputs, two-outpus production system with four machines depicted in Figure 3.. The inputs $u_i(k+1), i = 1, 2$ are defined as time instants at which the $k+1$-th manufactured parts are fed into the input stock in the line i. The outputs $y_i(k), i = 1, 2$ are time instants at which k-th finished products leaves the output stock in the line i. The state variables $x_1(k), x_3(k), x_4(k), x_6(k)$ are time instants at which k-th processing unit starts working in the machine 1, 2, 3 and 4, respectively. The state variables $x_2(k)$ and $x_5(k)$ are time instants at which k-th processing unit finished working in the machine 1 and 3, respectively. $d_i, i = 1, \cdots, 4$ are the working time in the machine 1, 2, 3 and 4, respectively.

The working times for each machine are $d_1 = 0.7$, $d_2 = 0.4$, $d_3 = 0.3$, $d_4 = 0.6$ for the first 15 parts, but the working times are changed into $d_1 = 1.0$,

$d_2 = 0.9$, $d_3 = 1.2$, $d_4 = 1.2$ after 16-th parts. It is assumed that the information on the parameter variations are given beforehand. Namely, the model parameter $d_{Mi} = d_i, \quad i = 1, \cdots, 4$. However, after 16-th parts, the information on d_3 has error, so the model parameter d_{M3} is assumed to be set to $d_{M3} = 0.8$.

The reference signal is given as follows

$$\begin{aligned} r_1(i+1) &= r_1(i) + 1.6, \quad r_2(i+1) = r_2(i) + 1.4 \\ & \qquad 0 \le i \le 9 \\ r_1(i+1) &= r_1(i) + 1.5, \quad r_2(i+1) = r_2(i) + 1.5 \\ & \qquad 10 \le i \le 30 \end{aligned}$$

Then, the proposed control law is applied to the production system. The following control law can be derived as is designed in section 4.

$$\boldsymbol{u}(k+1) = \bigwedge_{i=1}^{2} \left\{ \boldsymbol{\Delta}_i^{\mathrm{T}} \boldsymbol{N}_i(\boldsymbol{d}_M) \odot \left(\boldsymbol{r}_M(k) \oplus \bigoplus_{i=1}^{4} (\boldsymbol{M}_i(\boldsymbol{d}_M)\boldsymbol{\Gamma}_i)\boldsymbol{x}_M(k) \right) \right\} \tag{26}$$

$$\boldsymbol{r}_M(k) = \boldsymbol{r}(k) - (\boldsymbol{y}(k) - \boldsymbol{y}_M(k)) \tag{27}$$

where

$$\boldsymbol{N}_1(\boldsymbol{d}_M) = \begin{bmatrix} d_{M1} + d_{M2} & \varepsilon \\ \varepsilon & d_{M3} + d_{M4} \end{bmatrix},$$

$$\boldsymbol{N}_2(\boldsymbol{d}_M) = \begin{bmatrix} d_{M2} + d_{M3} & \varepsilon \\ \varepsilon & d_{M1} + d_{M4} \end{bmatrix},$$

$$\boldsymbol{M}_1(\boldsymbol{d}_M) = \begin{bmatrix} d_{M1} + d_{M2} & \varepsilon \\ \varepsilon & d_{M1} + d_{M4} \end{bmatrix}$$

$$\boldsymbol{M}_2(\boldsymbol{d}_M) = \begin{bmatrix} 2d_{M2} & \varepsilon \\ \varepsilon & \varepsilon \end{bmatrix}$$

$$\boldsymbol{M}_3(\boldsymbol{d}_M) = \begin{bmatrix} d_{M2} + d_{M3} & \varepsilon \\ \varepsilon & d_{M3} + d_{M4} \end{bmatrix}$$

$$\boldsymbol{M}_4(\boldsymbol{d}_M) = \begin{bmatrix} \varepsilon & \varepsilon \\ \varepsilon & 2d_{M4} \end{bmatrix}$$

$$\boldsymbol{\Delta}_1 = \begin{bmatrix} e & \varepsilon \\ \varepsilon & e \end{bmatrix}, \quad \boldsymbol{\Delta}_2 = \begin{bmatrix} \varepsilon & e \\ e & \varepsilon \end{bmatrix}$$

$$\boldsymbol{\Gamma}_1 = \begin{bmatrix} \varepsilon & e & \varepsilon & \varepsilon & \varepsilon & \varepsilon \\ \varepsilon & e & \varepsilon & \varepsilon & \varepsilon & \varepsilon \end{bmatrix}, \quad \boldsymbol{\Gamma}_2 = \begin{bmatrix} \varepsilon & \varepsilon & e & \varepsilon & \varepsilon & \varepsilon \\ \varepsilon & \varepsilon & \varepsilon & \varepsilon & \varepsilon & \varepsilon \end{bmatrix}$$

$$\boldsymbol{\Gamma}_3 = \begin{bmatrix} \varepsilon & \varepsilon & \varepsilon & \varepsilon & e & \varepsilon \\ \varepsilon & \varepsilon & \varepsilon & \varepsilon & e & \varepsilon \end{bmatrix}, \quad \boldsymbol{\Gamma}_4 = \begin{bmatrix} \varepsilon & \varepsilon & \varepsilon & \varepsilon & \varepsilon & \varepsilon \\ \varepsilon & \varepsilon & \varepsilon & \varepsilon & \varepsilon & e \end{bmatrix}$$

The simulation results are shown in Figure 4..

In Figure 4., the output errors, which imply $\boldsymbol{e}(k) = \boldsymbol{y}(k) - \boldsymbol{r}(k)$ with using both IMC control law and the information on the parameter variation are shown.

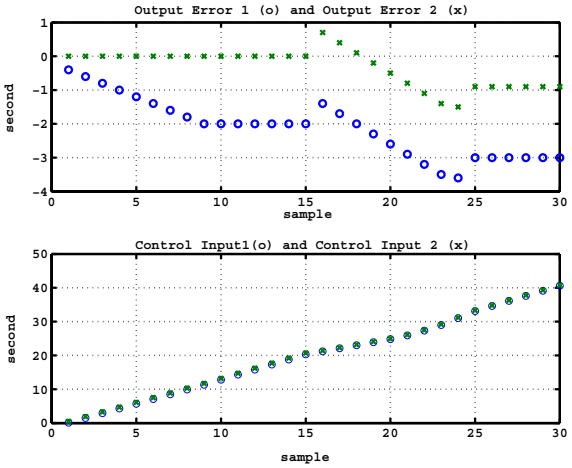

Fig. 4. Plots of the 1st output error (o) and the 2nd output error (x) with using both IMC control law and the information on the parameter variations (above) and the plots of the control input (below)

For the comparison, the output errors with only using the information on the parameter variation are shown in .

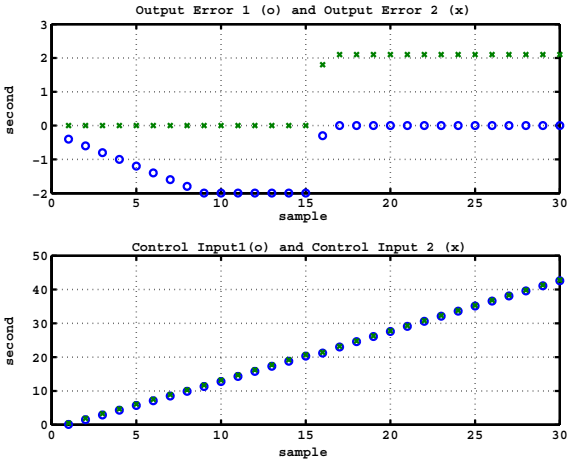

Fig. 5. Plots of the 1st output error (o) and the 2nd output error (x) with only using IMC control law (without using the information on the parameter variations) (above) and the plots of the control input (below)

From Figure 4., in the case with using both IMC control law and the information on the parameter variation, the output delays, which mean the output errors are positive value, does not occur except during 3 samples after 16-th sample at which the working time is changed. From Figure 5. and Figure 6., however, the output delays occur after the 16-th sample due to the change of the working time when either IMC control law or the information on the parameter variation is not utilized.

Therefore, it follows from the simulation result that the utilization of both IMC control law and the information on the parameter variations improves the performance of the control system.

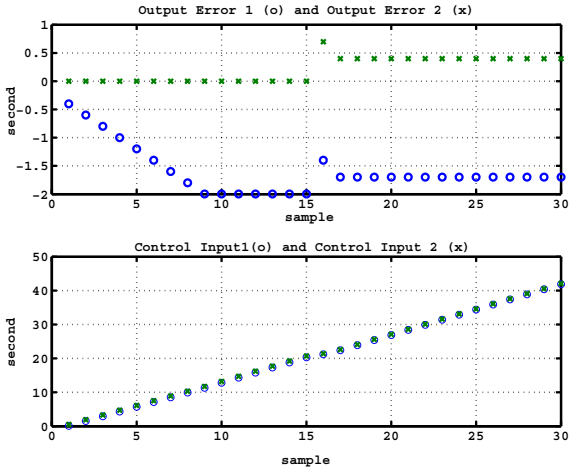

Fig. 6. Plots of the 1st output error (o) and the 2nd output error (x) with only using the information on the parameter variations (without using both IMC control law) (above) and the plots of the control input (below)

Therefore, we can see that the proposed control law shows better performance than the conventional IMC control law and the inverse systems for LPV-MPL systems with using the information on the parameter variations.

7. CONCLUDING REMARKS

This paper proposed the IMC control for MPL systems in the case where the controlled systems are given as MPL systems with linear parameter varying structure, which is called LPV-MPL systems. In the LPV-MPL systems, the systems parameters are explicitly represented in the systems description. Hence, the obtained IMC control law can utilize the additive information on the parameters variations effectively when the parameters are measured on-line, or the variation of the parameters are scheduled beforehand.

Furthermore, owing to the IMC control law, the proposed method has robust property even when the the information on the parameters variations has some errors.

The effectiveness of the proposed IMC is shown through a numerical example where it is applied to a two-inputs, two-outpus production system with four machines.

8. REFERENCES

Baccelli, F., G. Cohen, G. J. Olsder and J. P. Quadrat (1992). *Synchronization and Linearity*. New York: Jhon Wiley & Son.

Boimond, J. L. and J. L. Ferrier (1996). Internal model control and max-algebra: controller design. *IEEE Trans. on Automatic Control* **AC-41**(3), 457–461.

Cohen, G., P. Moller, J. P. Quadrat and M. Viot (1989). Algebraic tools for the performance evaluation of discrete event systems. *Proceedings of the IEEE* **77**(1), 39–58.

Masuda, S., H. Goto, T. Amemiya and K. Takeyasu (2002). An inverse system for linear parameter-varying max-plus-linear systems. In: *Proceedings of IEEE 2002 Conference on Decision and Control*.

van den Boom, T. and B. De Schutter (2001*a*). Model predictive control for max-plus-linear systems. *Automatica* **37**(7), 1049–1056.

van den Boom, T. and B. De Schutter (2001*b*). Mpc for perturbed max-plus-linear systems. In: *Proceedings of the European Control Conference 2001*. pp. 3783–3788.